The Influence of Heteroatom Substitution on Heterocyclic Carbenes and their Complexes

by

David C. Graham (BSc. Hons.)

David Carl

Submitted in fulfillment of the requirements for the Degree of
Doctor of Philosophy

UNIVERSITY
OF TASMANIA

School of Chemistry
Hobart, Australia
November 2003

Declaration of Originality

This thesis contains no material which has been accepted for a degree or diploma by the University or any other institution, except by way of background information and duly acknowledged in the thesis, and to the best of the candidate's knowledge and belief no material previously published or written by another person except where due acknowledgement is made in the text of the thesis.

David C. Graham
November, 2003

Statement of Authority of Access

This thesis may be made available for loan and limited copying in accordance with the *Copyright Act* 1968.

David C. Graham
November, 2003

Abstract

This thesis describes the influence of heteroatom substitution on heterocyclic carbenes and their corresponding complexes, using both density functional theory (DFT) and synthetic methods.

The substitution of oxygen, sulfur or phosphorus for nitrogen in imidazol-2-ylidenes gives rise to a set of ten heterocyclic carbenes that were investigated using DFT. These replacements were found to have implications for both the structure and reactivity of the free carbene, which extended to complexes bearing ligands of this type. The balance between the σ-donation and π-withdrawal conferred by the heteroatoms onto the carbene centre was found to be a key factor influencing the reactivity at the carbenic carbon. Additional thermodynamic stability was observed for those carbenes that exhibited extensive π-delocalisation (aromaticity). The self-dimerisation of heteroatom-substituted carbenes is accelerated in the presence of protons. The activation barrier for dimerisation shows little correlation with the enthalpy of reaction, indicating that the estimation of carbene stability based purely on the enthalpy of reaction is not always appropriate.

A number of novel palladium complexes bearing thiazol-2-ylidene ligands were prepared in the laboratory and their catalytic activity for Heck and Suzuki coupling assessed. While the catalysts were moderately active for both reactions, their

performance was impeded by their insoluble nature and the lack of a second exocyclic ring substituent.

DFT studies on the oxidative addition of imidazolium, thiazolium and oxazolium salts to zerovalent group-10 metals indicated that activation of C-C bonds resulting in the generation of hydrocarbyl-carbene complexes is likely to be achieved experimentally. Thiazolium salts and azoliums bearing 2-phenyl substituents show increased barriers to activation due to additional stabilizing interactions with the metal centre.

The engineering of hydrocarbyl palladium carbene complexes that show enhanced stability to reductive elimination was undertaken using DFT. Complexes bearing imidazole-based ligands showed enhanced stability over imidazoline, thiazole and oxazole as a consequence of both their superior σ-donating ability and significant occupation of the carbene p_π-orbital. Widening of the auxiliary ligand bite-angle conferred a dramatic reduction in the barrier to reductive elimination, while the dihedral twist of the carbene relative to the PdL_2 plane had little effect. Incorporation of increased steric bulk on nitrogen had little influence on the barrier to reductive elimination given its location distant from the active-site. More important were the σ-donating and π-withdrawing properties of the substituents, which conferred changes on the Pd-C bonding interaction resulting in an influence on the reductive elimination behaviour.

Acknowledgements

My sincere thanks go to:

Professor Kingsley Cavell for his insight and enthusiasm concerning the project and the opportunity to conduct my research in Cardiff for 12 months.

Dr Brian Yates for his trust and flexibility toward the project. I am very grateful for the support he has shown for the duration of my candidature.

Dr David McGuinness for his continual guidance in both the theoretical and synthetic work concerned with the project.

The completion of this project would not have been possible without the assistance of the following people, and they are gratefully acknowledged:

Dr Graham Rowbottom, Dr Noel Davies and Mr Marshall Hughes of the Central Science Laboratory, University of Tasmania, for their analysis of sometimes less than perfect samples.

David Nielsen, Kirsty Hawkes and Jeremy Rackham for their friendship and guidance on all aspects of my research.

Abbreviations

ASE	aromatic stabilisation energy
BDE	bond dissociation energy
BI	bird index
Bu	butyl
Bz	benzyl
CDA	charge decomposition analysis
COD	cyclooctadiene
CTA	carbene twist angle
Cy	cyclohexyl
DCM	dichloromethane
DFT	density functional theory
DMA	dimethylacetamide
DMSO	dimethylsulfoxide
E_{act}	activation energy
ECP	effective core potential
EN	electronegativity
^{i}Pr	isopropyl
LDA	lithium diisopropylamide
LSIMS	liquid secondary ion mass spectroscopy
Me	methyl
MNDO	moderate neglect of differential overlap
MS	mass spectroscopy
NHC	N-heterocyclic carbene
NICS	nucleus independent chemical shift
NMR	nuclear magnetic resonance
NPA	natural population analysis
OAc	acetate
PA	proton affinity
PC	precursor complex
Ph	phenyl
SBA(X)	sum of bond angles around x
TBAB	tetrabutylammonium bromide
^{t}Bu	*tertiary*-butyl
THF	tetrahydrofuran
tmiy	1,3,4,5-tetramethylimidazol-2-ylidene
TMS	tetramethylsilane
TON	turn-over number
TS	transition structure
ZPVE	zero point vibrational energy

Table of Contents

Chapter Eight

Influence of *N*-Substituents on the Stability of Palladium Carbene Complexes

Table of Contents (Appendices)

(note: these appendices are located on the supplementary CD)

Appendix D

Cartesian Coordinates of Structures from Chapter Six

Appendix E

Cartesian Coordinates of Structures from Chapter Seven

Appendix F

Cartesian Coordinates of Structures from Chapter Eight

• Chapter One •

A Review of the Relevant Literature

1.1 Impetus for Research

The term catalyst refers to any substance that alters the rate of a chemical reaction but is itself unchanged by the reaction.[1] Two types of catalyst are generally recognised: heterogeneous, in which one or more of the constituents are in different phases, and homogeneous, in which all the constituents of the reaction are present in the same phase.[2] Homogeneous catalysts, which are often found to be more active and selective than their heterogeneous counterparts,[2] comprise around 15% of all industrial catalytic processes carried out today.[3]

The activity of homogeneous catalysts stems not only from the metal reaction centre, but also the peripheral ligands attached to it. The use of ubiquitous phosphine-based ligands in homogeneous catalysis arises as a consequence of their ability to stabilise low-valent metal intermediates and their characteristic dissociation to form vacant sites at the metal centre, which promotes catalysis.[3]

Unfortunately, phosphine ligands are expensive, toxic, unrecoverable and are susceptible to bond-cleavage at high temperatures which reduces their cost effectiveness.[4]

New developments focusing on the incorporation of N-heterocyclic carbene (NHC) ligands into catalysts as a replacement for phosphines in homogeneous catalytic processes have dominated recent literature.[5-9] Despite this, little attention has been devoted to heterocyclic carbenes and their associated complexes that deviate from the original imidazol-2-ylidene template.[10]

It was the aim of this project to investigate in detail the consequences of heteroatom exchange on the nature of heterocyclic carbenes and their corresponding catalytically useful complexes. In addition to this, through application of theoretical methods, attempts were made to further engineer catalysts based on NHC complexes in order to enhance their stability in a catalytic environment.

1.2 Heterocyclic Carbenes

1.2.1 Carbene Electronic States

Carbenes are defined as species of the type :CR$_2$, in which the divalent carbon contains two unshared electrons (Figure 1.1).[1] The existence of the simplest carbene, methylene (:CH$_2$), was proposed as early as the late 1800s by Nef, who suggested that the decomposition of
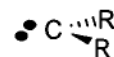
Figure 1.1 – Basic carbene structure

diazomethane (CH$_2$N$_2$) might generate this reactive species.[11] The existence of methylene was not firmly established however, until 1959, and it has since been found to be a common intermediate in many organic reactions.[12]

Although not strictly axiomatic, carbenes tend to adopt a bent conformation in an attempt to lower the energy of the n$_\sigma$ molecular orbital that is destabilised in the linear conformation.[13] Bending the molecule breaks orbital degeneracy, resulting in two frontier orbitals based around the carbene sp^2 hybridised centre, commonly referred to as σ and p$_\pi$ (Figure 1.2).[9]

p_π

$$\sigma \quad \text{(orbital diagram)} \quad \substack{\backslash\backslash R \\ R}$$
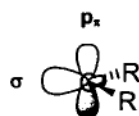
Figure 1.2 – Orbital configuration of a carbene

Consequently, this orbital structure gives rise to four possible electronic states dependent on the placement of the two valence electrons (Figure 1.3). In methylene, the closeness in energy of the σ and p_π orbitals results in a T_1 ($\sigma^1 p_\pi^1$) ground state, as electron promotion is more energetically favourable than the alternate spin pairing for the singlet ground state.[13]

p_π p_π p_π p_π

$$\sigma \quad \quad \quad \sigma \quad \quad \quad \sigma \quad \quad \quad \sigma$$

$T_1 (\sigma^1 p_\pi^1)$ $S_0 (\sigma^2)$ $S_1 (\sigma^1 p_\pi^1)$ $S_2 (p_\pi^2)$
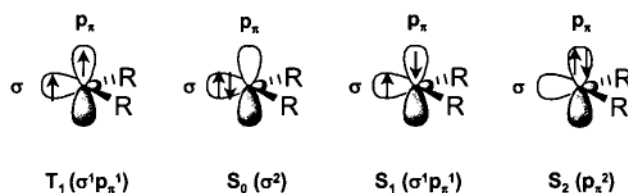
Figure 1.3 – Possible electronic states for a carbene

Carbene substituents that destabilise the p_π orbital act to confer a singlet S_0 (σ^2) ground state upon the carbene.[9] The resulting singlet carbene exhibits properties far removed from that of its highly reactive triplet relative. For this reason, the notion of singlet-triplet splitting has become an important concept for singlet carbenes as it provides information pertaining to the accessibility of the higher energy states and can thus be correlated with reactivity.[14-19]

1.2.2 Heterocyclic Carbenes Defined

One group of carbenes that are well known for exhibiting a singlet ground state are the heterocyclic carbenes. Heterocyclic carbenes have heteroatoms (e.g. N, S, O and

P) adjacent to the carbene centre usually (but not always, as the name would suggest) contained in a ring system.

Early studies by Wanzlick demonstrated that the incorporation of nitrogen atoms adjacent to the carbene centre might result in a singlet carbene with a degree of stability that would permit isolation.[20] Using an imidazoline system, Wanzlick attempted to isolate the corresponding imidazolin-2-ylidene in the 1960s (Figure 1.4). Although he was unsuccessful in isolating the carbene itself, he identified its existence through a number of trapping experiments.[20]
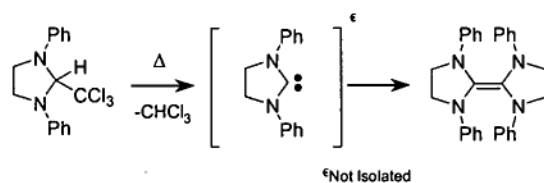
Figure 1.4 – Attempted heterocyclic carbene isolation by Wanzlick

It was not until 1991 that Arduengo *et al.* succeeded in isolating an imidazol-2-ylidene (Figure 1.5 **A**) as a stable crystalline carbene.[21]
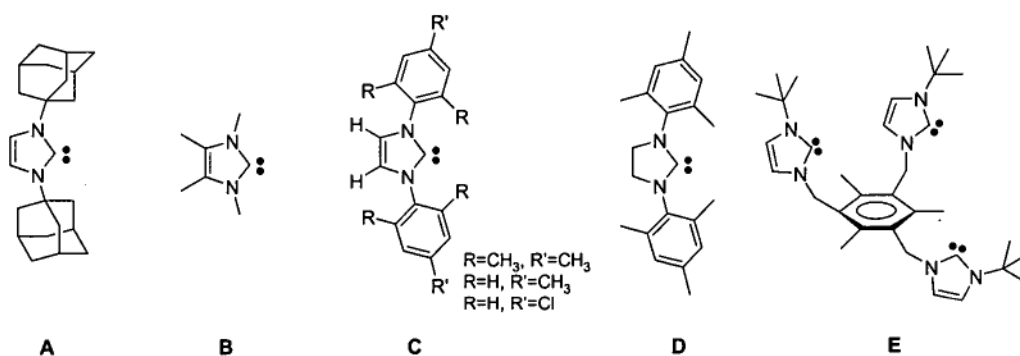
Figure 1.5 – Stable imidazole-based heterocyclic carbenes

1.2.3 Stable *N*-Heterocyclic Carbenes

Arduengo's free carbene 1,3-diadamantylimidazol-2-ylidene (Figure 1.5 **A**) was based on the diamino-substituted system proposed by Wanzlick. After Arduengo's initial finding, the field of stable heterocyclic carbenes expanded rapidly to furnish a range of stable congeners based on imidazole.[21-26]

Subsequent work by Arduengo[24] resulted in the isolation of four further imidazole-based carbenes, including the sterically unencumbered 1,3,4,5-tetramethylimidazol-2-ylidene (tmiy) (Figure 1.5 **B-C**). In 1995, the range of isolable *N*-heterocyclic carbenes (NHC's) was expanded to include a saturated imidazolin-2-ylidene (Figure 1.5 **D**).[23]

More recently, the area of imidazole based carbenes has diverged further to yield bis and tris-chelating carbenes (Figure 1.5 **E**).[27]

1.2.4 Beyond the Imidazole Ring System

Inciting a move toward 'second-generation' heterocyclic carbenes, the first diversification from the imidazol(in)e ring system was published by Enders.[28] Alpha elimination of methanol from 5-methoxytriazole in the solid state furnished an isolable carbene based on the triazole ring system (Figure 1.6 **A**).

While several combinations of heteroatoms adjacent to the carbene carbon are conceivable, it is interesting to note that all structures reported up until 1996 possessed the common structural feature of two nitrogen atoms.
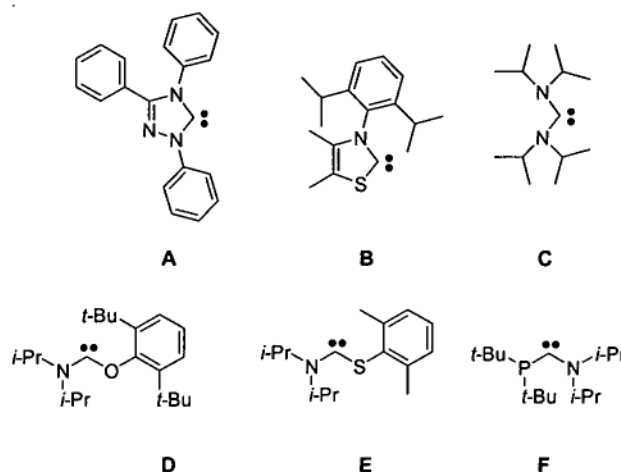
Figure 1.6 – Stable 'second-generation' heterocyclic carbenes

The substitution of one of the ring nitrogens with sulphur afforded a stable thiazol-2-ylidene (3-(2,6-diisopropylphenyl)-4,5-dimethylthiazol-2-ylidene) (Figure 1.6 **B**).[29] Although steric bulk had been disregarded as an important stabilising feature for imidazol-2-ylidenes after the isolation of tmiy,[30] the observation that only thiazol-2-ylidenes incorporating bulky *N*-substituents were isolable highlighted the differences between the two classes of compounds. Attempted isolation of thiazole-based carbenes where the *N*-substituent was small resulted in the formation of a dimer product.[29]

Alder successfully isolated the first stable acyclic carbene by deprotonation of *N,N,N',N'*-tetraisopropylformamindium chloride with lithium diisopropylamine (LDA) in THF.[31] The isolation of this carbene was aided by considerable steric bulk on nitrogen which acts to protect the reactive carbene centre (Figure 1.6 **C**). Later, Alder furthered the range of stable acyclic carbenes with the isolation of amino-thio and amino-oxy carbenes that relied heavily on steric bulk for protection of the carbene centre (Figure 1.6 **D** and **E**).[32]

Although Bertrand reported the isolation of a phosphinoamino-carbene as early as 1986, its tendency to react in a manner similar to a phosphaacetylene raised doubts concerning the extent of its carbenic character. Subsequent theoretical work confirmed this premise through observation of a small singlet-triplet splitting and significant charge separation (Figure 1.7).[33]
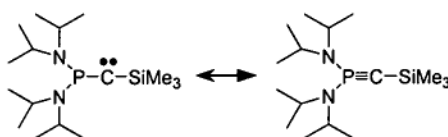
Figure 1.7 – The two-faced nature of Bertrand's original 'aminophosphinocarbene'

Recently, however, Betrand has succeeded in isolating an aminophosphino-carbene (Figure 1.6 **F**) that exhibits carbenic reactivity and the appropriate spectroscopic shifts.[34]

Further divergence in the field of carbene research to include systems in which both nitrogens are replaced by other heteroatoms has proved fruitless. For example, attempts to isolate dialkoxycarbenes as stable compounds have resulted in decomposition products,[35-37] while deprotonation of dithiolium perchlorates to form dithiocarbenes resulted in a dimeric product.[38]

Substitution of the carbene carbon with the higher group homologues has resulted in stable silylenes[39] and germylenes[40] that exhibit characteristics similar to those of their carbene counterparts (Figure 1.8).[41-43]
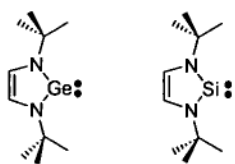
Figure 1.8 – Heavier germylene and silylene analogues

1.2.5 Synthesis of Heterocyclic Carbenes

Stable heterocyclic carbenes may be isolated through a number of synthetic routes (Scheme 1.1). Imidazolium salts represent the most convenient precursor for free carbene synthesis as they can be prepared via a number of reliable routes.[7]
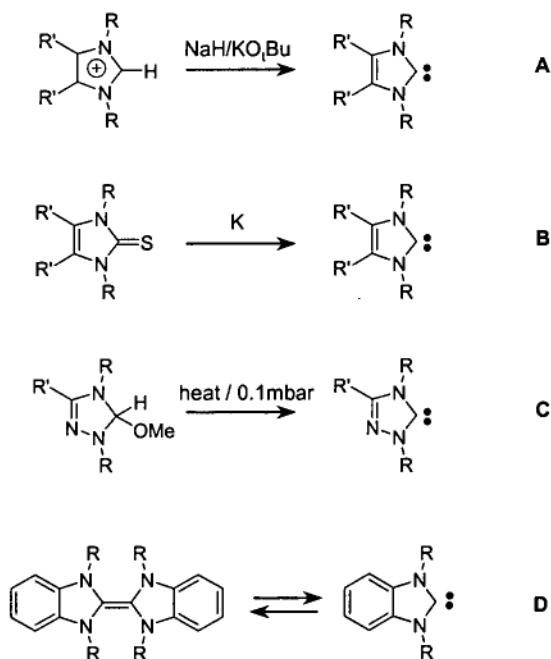
Scheme 1.1 – Synthesis methods for free heterocyclic carbenes

Deprotonation of imidazolium salts represents the most common method of free carbene isolation (Scheme 1.1 **A**).[21-26,29] This method was employed by Arduengo[21] to isolate the first stable crystalline carbene. Specifically, the imidazolium salt was suspended in THF and deprotonated with a metal hydride. The efficacy of this method is hampered by the fact that both the hydride and imidazolium salt are usually sparingly soluble in the reaction media, resulting in long reaction times. To obtain reasonable rates of reaction, catalytic amounts of either KO^{t}Bu or the DMSO anion must be added. Complete replacement of the hydride base with KO^{t}Bu has been successful, but is hampered by the low volatility of ^{t}BuOH and has thus far proved unsuitable for imidazolinium salts.[44]

Low temperature (−50°C), homogeneous phase synthesis of free carbenes (via salt deprotonation) can be carried out with short reaction times in liquid NH_3/THF.[45,46] This allows for the isolation of less temperature-stable carbenes. Some problems may occur when deprotonating imidazolium salts as a result of undesired deprotonation of other acidic protons within the molecule,[47] but this can usually be avoided by using milder bases such LDA.[48]

The reduction of an imidazole-2(3H)-thione with metallic potassium in boiling THF, as reported by Kuhn,[30] furnishes the corresponding carbene in excellent yields (Scheme 1.1 **B**). This preparative method is also applicable to imidazol-2-ylidenes that contain minimal bulk at nitrogen.[30] Less widely used methods for NHC generation have involved thermolysis of methanol adducts[28] and the scission of electron-rich double bonds in tetraaminoethylenes to yield benzimidazol-2-ylidenes (Scheme 1.1 **C** and **D**).[49]

1.2.6 Theoretical Work Pertaining to Heterocyclic Carbenes

Theoretical research flourished after the isolation of 1,3-bisadamantylimidazol-2-ylidene (Figure 1.4 A), with a number of groups publishing theories attempting to explain the remarkable stability of this carbene.[22,41,43,50-54] Arduengo initially attributed the stability of the carbene to both the N–C=C–N donor system affording a large singlet-triplet splitting and the kinetic stability provided by the bulk of the two adamantyl nitrogen substituents.[21,51] The early controversy concerning the stabilising features centred on the importance of π-delocalisation within the imidazol-2-ylidene ring system. While the importance of ylidic resonance structures was initially thought to be minor, the publication of two concurrent, independent theoretical research reports in 1996 questioned this assumption.[41,43] Both suggested that while complete π-delocalisation was not a requirement for stability, the ylidic resonance forms resulting from donation of π-density from the adjacent nitrogens were of paramount importance in providing sufficient stability to facilitate isolation. After these concurrent reports by Heinemann[41] and Frenking,[43] theoretical research on imidazol-2-ylidenes lay relatively dormant until 2002, when Herrmann published theoretical research based on AIM methods that suggested the imidazole-based carbenes exhibited hindered π-electron delocalisation with localised lone pairs on the nitrogen atoms.[55]

It is evident that the factors bringing about the stabilisation of heterocyclic carbenes isolated more than ten years ago still remain controversial and hard evidence remains elusive.

1.2.7 Theoretical Studies on Non-Imidazole Heterocyclic Carbenes

The extension of theoretical work to heterocyclic carbenes other than those based on imidazole has been limited. A theoretical MNDO study on the nucleophilicity of cyclic aminooxy-, dioxo-, diamino-, aminothio- and dithio-2-ylidenes was carried out by Geijo,[56] while Sauers calculated their proton affinities and aromatic stabilization energies.[26] More recently, Nyulaszi covered a range of both five and six-membered heterocyclic carbenes incorporating phosphorus, and reported their potential as candidates for experimental isolation.[57-59]

1.2.8 Reactivity of Heterocyclic Carbenes

While the simplest carbene, methylene, shows reactivity born from its triplet electronic state, the corresponding singlet heterocyclic carbenes exhibit quite different reactivity.

Singlet carbenes are capable of demonstrating both nucleophilic and electrophilic reactivity as a consequence of their σ-lone pair and vacant p_π orbital. The literature is filled with both experimental observations[60,61] and theoretical calculations[50,53,62-66] on the basic reactions of heterocyclic carbenes.

The most widespread decomposition reaction of NHCs, and possibly the most synthetically important, is self-dimerisation (Scheme 1.2).[50,53,63,64] The original search for stable imidazolin-2-ylidenes by Wanzlick resulted in dimerisation leading to electron-rich tetraaminoethenes.[20] Although it was proposed that the resultant tetraaminoethene

was in equilibrium with its corresponding carbene, recent reinvestigations through

crossover experiments by two different groups have provided conflicting results.[49,67]
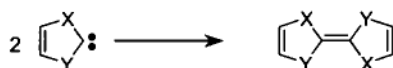
Scheme 1.2 – Free carbene dimerisation

Dimerisation continues to hamper attempts to isolate non-imidazole based free-

carbenes, with thiazol-2-ylidenes,[29] imidazolin-2-ylidenes,[68,69] acyclic diaminocarbenes,[63]

benzimidazol-2-ylidenes[70] and benzothiazol-2-ylidenes[71] all exhibiting dimerisation

behaviour under certain conditions. The stability of imidazol-2-ylidenes is influenced by

a number of factors, including aromaticity, singlet-triplet splitting and σ-withdrawing

effects.[50,53,58,63,64] There have been few attempts to determine these parameters for

carbenes with differing heteroatoms, and thus their relative stabilities remain unknown.

Imidazol-2-ylidenes show no tendency to dimerise, although altering the reaction

conditions significantly through tethering imidazolium salts in a manner described by

Taton and Chen[72] can change this.

There are several known instances in which heterocyclic carbenes are capable of

acting as catalysts. In particular, the catalytically active form of vitamin B_1 (thiamin)

(Figure 1.9) that catalyses the decarboxylation of pyruvic acid is believed to be a thiazol-

2-ylidene.[71] Additionally, thiazol-2-ylidenes are also active catalysts for benzoin

condensation, although this claim has been more recently disputed in favour of the

bis(thiazol-2-ylidene) dimer.[73-75]
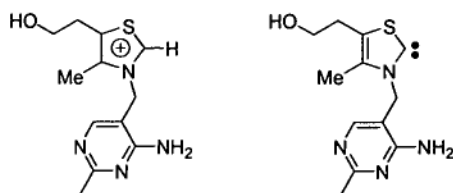
Figure 1.9 – Vitamin B$_1$ (thiamin) (left) and its proposed catalytically active form (right)

1.3 Complexes of Heterocyclic Carbenes

1.3.1 Bonding Characteristics of Heterocyclic Carbenes

The bonding modes of carbenes are historically divided according to the nature of the metal-carbon bond. The metal-carbene bond of Fischer-type complexes involves a ligand-to-metal σ-donation and metal-to-ligand π-back-donation (a donor-acceptor bond). Stable Fischer-type carbene complexes commonly have a π-donor group attached to the carbene carbon and involve a transition metal in a low oxidation state (Figure 1.10). In contrast, Schrock-type carbene complexes have nucleophilic carbene ligands, typically with hydrogen, alkyl, or aryl groups, but no π-donor substituents at the carbene carbon atom. Schrock-type complexes typically involve transition metals in a high oxidation state (Figure 1.10).[76-78]
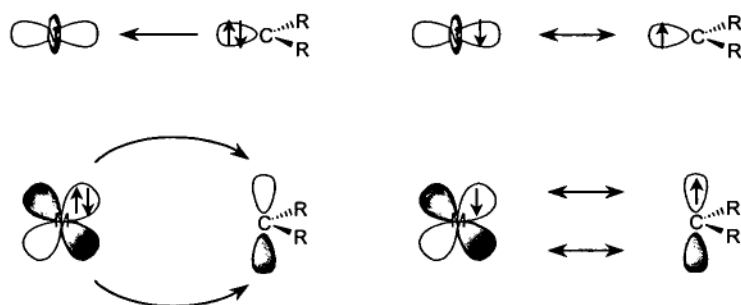
Figure 1.10 – Fischer (left) and Schrock (right) type bonding

Although many types of carbene complexes can be described as either Fischer or Schrock, some do not fit comfortably into either category. Complexes of *N*-Heterocyclic carbenes show strong σ-donor bonding to metal centres, yet negligible back-donation normally associated with Fischer type complexes (Figure 1.11).[78-80]

back-donation does not occur
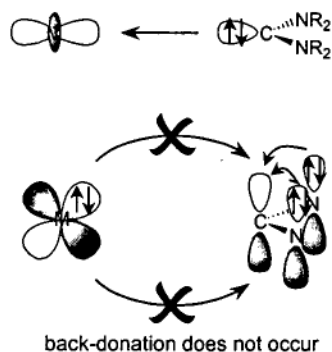
Figure 1.11 – NHC complex type bonding

It is likely that the stabilizing π-back-donation observed for Fischer carbene complexes is not required for NHC complexes because the carbene p_π orbital is already significantly occupied as a result of donation from the adjacent nitrogen heteroatoms.[78]

DFT calculations on group-10 metals have demonstrated that bonding occurs primarily through σ-donation from the carbene lone pair.[79] This premise has been confirmed through photoelectron spectroscopy.[79] In addition, single crystal x-ray data shows the metal-carbene bonds to be of a similar length to single bonds rather than double bonds, [10] with metal-carbene bonds being long (> 210 pm), while in Fischer and Schrock-type complexes they are significantly shorter (around 200 pm) due to pronounced backbonding.[7] N-heterocyclic carbenes are observed to behave like typical σ-donor ligands and can substitute typical 2e⁻ donors such as amines and phosphines. For this reason, NHCs have been compared to electron-rich phosphines and hence have made the transition to catalysis where phosphines are ubiquitous. Nolan remarked that with the exception of the sterically demanding adamantyl carbene, NHC's behave as better donors than the best phosphine donor ligands.[81]

The basicity of donor ligands such as carbenes often gives a good indication of their ability to donate σ-electrons to a metal. The conjugate acid pK_a of a heterocyclic carbene has been estimated as 24, which is stronger than many proton sponges.[82]

1.3.2 Synthetic Pathways to Heterocyclic Carbene Complexes

Transition-metal complexes containing NHC's have received increasing attention, largely due to their favourable application in homogeneous catalysis.[8] The first complexes of NHCs came via separate reports from Öfele[83] and Wanzlick[84] in 1968, who synthesized chromium and mercury complexes via metallic salt deprotonation (Figure 1.12).
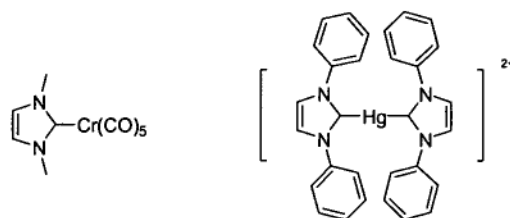
Figure 1.12 – Öfele (left) and Wanzlick's (right) heterocyclic carbene complexes

The generation of heterocyclic carbene complexes may be undertaken via a number of well-established synthetic routes,[6-8] including *in situ* deprotonation of ligand precursors by basic metal salts, scission of electron-rich olefins, reaction with metal-carbon precursors, metal-transfer routes, complexation via displacement of labile ligands by the free carbene, and oxidative addition-type reactions (Scheme 1.3).

Synthesis via Basic Metal Deprotonation

The most common synthetic route involves deprotonation of an appropriate azolium salt by a basic metal salt, thus generating the carbene complex (Scheme 1.3 **A**). The first observed heterocyclic carbene complex was prepared in this manner by reaction of mercury acetate with 1,3-diphenylimidazolium perchlorate.[84] This pathway has several advantages, most notably that handling of the free carbene is unnecessary, and thus it is often used when the carbene is unstable or difficult to handle. The metal precursor has a dual function in that it acts as the deprotonating agent as well as the

ligand acceptor. This route has been extended to prepare complexes from benzimidazolium, pyrazolium, triazolium and tetrazolium salts.[85-87]
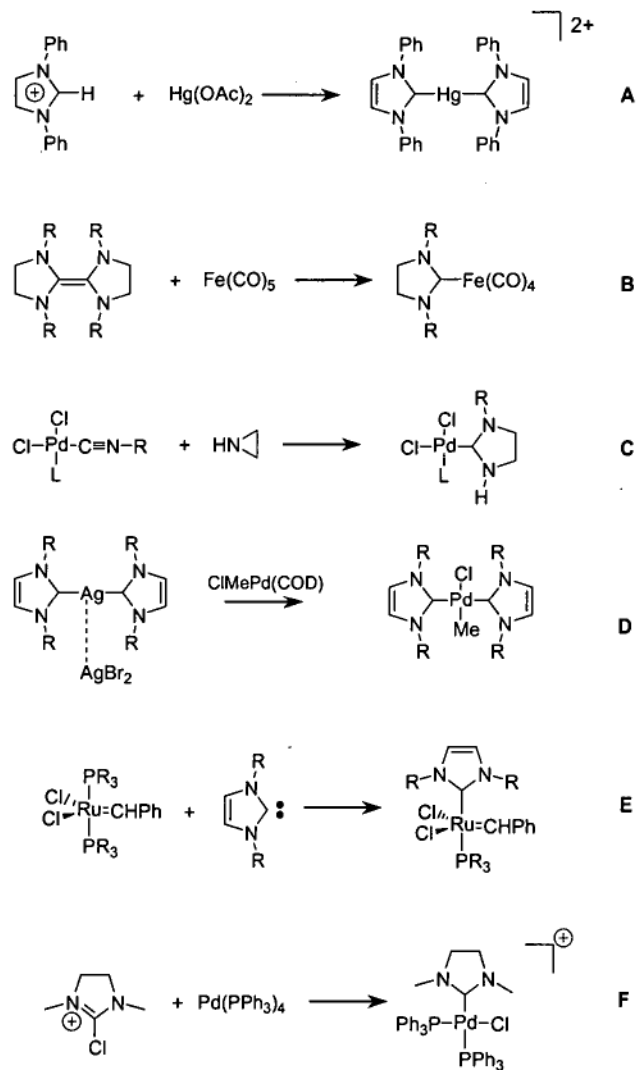
Scheme 1.3 – Synthetic routes for heterocyclic carbene complexes

Synthesis by Scission of Electron Rich Olefins

Bond breaking of tetraaminoethylenes also represents a common methodology for complex generation (Scheme 1.3 **B**). Here tetraaminoethylene carbene dimers are broken by reaction with electrophilic metal centres (including metal carbonyls of iron, ruthenium and nickel). This method is used commonly with dimers of benzimidazoles and saturated imidazolines. Lappert *et al.* have developed a general synthesis of metal-carbene complexes that involves treatment of these electron-rich olefins with transition-metal complexes such as chlorotris(triphenylphosphine)rhodium(I).[88]

Synthesis by Reaction of Organometallic Compounds

A method less commonly applied for NHC complex generation involves the generation of the carbene heterocycle from a precursor complex already containing the required metal-carbon bond. Saturated *N*-heterocyclic carbenes can be generated at a metal centre by transforming other C-bound ligands. For example, reaction of metal-isocyanides with thiirane and aziridine furnishes complexes with thiazolin-2-ylidene and imidazolin-2-ylidene ligands, respectively (Scheme 1.3 **C**).[89,90]

Carbene Transfer

Carbene transfer methods have recently become popular,[47,91-94] due in particular to the development of a silver-transfer method by Wang and Lin.[91] This involves the generation of a silver-carbene complex by reaction of an azolium salt with a silver base (Ag$_2$O or Ag$_2$CO$_3$) and subsequent transfer to a metal with readily displaceable ligands

(Scheme 1.3 **D**). This method has been successfully applied within our research group to afford carbene complexes of palladium via the corresponding silver carbene complexes.[47,94]

Synthesis via the Complexation of Free Carbenes

With the isolation of stable heterocyclic carbenes[21] came the availability of new pathways that could access complexes that were previously thought unavailable. The main advantage of this pathway stems from the larger number metal precursors that may be used. The free carbene may be used to displace weakly coordinating ligands such as acetonitrile or 1,5-cyclooctadiene (COD) to afford heterocyclic carbene complexes (Scheme 1.3 **E**). Generation of the free carbene can be carried out using the methods discussed previously (Section **1.2.5**). This synthetic approach is limited to those carbenes that are stable in solution, particularly imidazol-2-ylidenes and some imidazolin-2-ylidenes.

Synthesis via Oxidative Addition Pathways

The application of oxidative addition methods for the synthesis of heterocyclic carbene complexes has regained attention over the past two years. Earlier work in 1974 by Stone and coworkers[95] furnished a range of heterocyclic carbene complexes through oxidative addition of 2-chloroazolium salts to zero-valent group-10 metal complexes. Their work with thiazole and benzoxazole has only very recently been extended to include oxidative addition of both imidazolium[96,97] and imidazolinium salts[98] to generate a number of hydrido-platinum carbene complexes.

1.3.3 Diversity of Heterocyclic Carbene Complexes

The range of known heterocyclic carbene complexes has grown rapidly in recent times. Imidazol-2-ylidene-based complexes bearing one, two, three or four carbene ligands are known,[99] as are chelating,[100] hemilabile,[47,94] donor-carbene-donor,[101] carbene-donor-carbene[101-103] and cyclophane-type complexes.[94,104,105] Complexes that deviate from the basic imidazole backbone are less well investigated.

1.4 NHC Complexes in Catalysis

Instances of rhodium-based heterocyclic carbene catalysis performed by Lappert and others may be found throughout the 1970s and 80s.[106-108] This pioneering work was followed by more recent studies concerning palladium-based NHC catalysis by Herrmann.[10]

1.4.1 Advantages of NHC-Based Catalysis over Traditional Phosphine Catalysis

Reports citing the superiority of NHCs over the ubiquitous phosphines in catalysis have continually mounted over time.[10] In addition, NHC-based catalysts are continually being applied to new systems.

The strong metal-carbene bonds in NHC complexes result in catalysts with high thermal and hydrolytic durability.[10] DFT calculations have found the metal-carbene bond to be significantly stronger than that of metal-phosphine bonds.[109,110] Additionally,

NHCs do not suffer from the inherent P-C bond cleavage that has proven problematic with phosphine catalytic systems.[111] The lability of the metal-phosphine bond often requires that a significant excess of phosphine ligand be present in the catalytic system. This increases cost significantly, and on an industrial scale this can far outweigh the cost of the catalysts itself.[6,7] In addition, many heterocyclic carbene complexes are stable with respect to heat, oxygen and moisture,[10] an important attribute as many industrial catalytic process are carried out at high temperatures. Herrmann's palladium-biscarbene Heck catalyst[10] melted without decomposition at 299 °C, and catalytic processes using NHC complexes have been carried out in air at up to 184 °C.[112]

Catalysis based on NHCs now reaches into many areas where phosphines were once considered dominant.[6,7,9] Palladium-based Heck and Suzuki coupling,[113-115] ruthenium-based olefin metathesis[116,117] and palladium-based telomerisation[118,119] have all shown improved turnover numbers and rates of reaction when NHC-based catalysts are utilised.

With the continual extension of NHC-based catalysts into a range of catalytic fields, it has become apparent that they have shed their phosphine-mimic tag and in many cases surpassed their phosphine analogues in both activity and scope of application.

1.4.2 Divergence from Conventional NHC Systems

Variations on standard palladium(imidazol-2-ylidene) homogeneous catalysts have recently been applied with successful results. For example, polymer-supported catalysts for the Heck reaction have resulted in good catalytic turnovers with minimal catalyst leaching.[110]

The Calo group have employed various catalytic processes in ionic liquids[120] using a benzothiazol-2-ylidene palladium catalyst for the Heck reaction.[121,122] The use of ionic liquids as solvents has been extended by Beller[123] and applied to telomerisation by Chauvin.[124] The reportedly advantageous nature of azolium-based ionic liquids may stem from the fact that they are easily converted to metal-carbene complexes which may themselves act as the catalyst.[125]

Nolan has taken a tangential approach to catalysis by NHC complexes by generating the carbene *in situ* in the presence of an appropriate palladium-zero precursor.[126] This method has proven advantageous for the Suzuki reaction and avoids the handling of air- and moisture-sensitive carbenes.[127,128] The indirect formation of the active catalyst is expected through *in situ* deprotonation of the imidazolium salt by a base and subsequent complexation with the palladium-zero precursor.

1.4.3 Heck-type C-C Coupling Reactions

Widespread and successful use of palladium-NHC catalysts has been reported for such carbon-carbon coupling processes as the Heck[4,10,101,102,123,129] and Suzuki reactions.[47,94,113,114,129-131] The Heck reaction is mainly applied in the synthesis of specialist chemicals that are used for dyes, UV screens and pharmaceuticals (Scheme 1.4).[4]
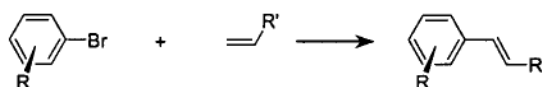
Scheme 1.4 – Heck reaction

The success of palladium catalysts lies in the ability of zero-valent palladium to activate carbon-halogen bonds via oxidative addition, and the subsequent addition of newly formed RPdX intermediates to unsaturated bonds [4,132]

The traditional mechanism for the Heck reaction proposes a 14-electron PdL$_2$ active species that through the process of oxidative addition and reductive elimination affords the required C–C coupled product (Scheme 1.5).[133] Alternative mechanisms have been suggested by Amatore and Jutand,[132] who have proposed a palladium(0) anionic catalytic cycle involving a pentacoordinate palladium, and Shaw who has suggested a Pd^{II}/Pd^{IV} cycle.[134,135]
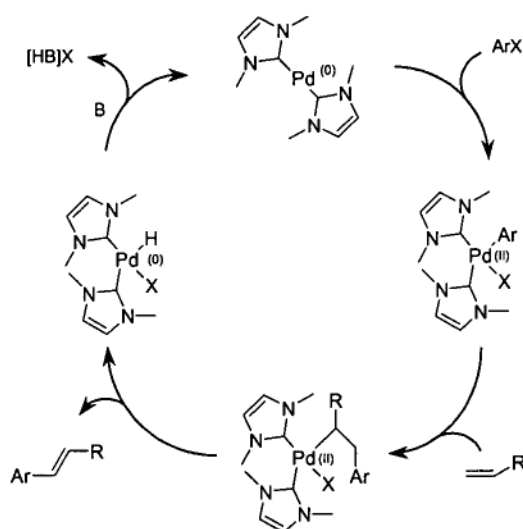
Scheme 1.5 – Heck catalytic cycle

If the traditional mechanism for Heck catalysis is adhered to, then the success of the catalytic process is dependent on the generation of the active palladium(0) catalyst. This statement is true also if an anionic catalytic cycle is in operation. In a phosphine-free system, the olefin is thought to carry out the reduction of the pre-catalyst to form the

palladium(0) active species.[4] The addition of external reducing agents such as sodium

formate and hydrazine, aid in the immediate generation of the active catalyst and has

been observed to result in an instantaneous increases in turn-over.[10] If the catalysis is

performed in the ionic liquid tetrabutylammonium bromide, this too can act as a reducing

agent to furnish the active catalyst (Scheme 1.6).[10]

(pre-catalyst)   (proposed active catalyst)
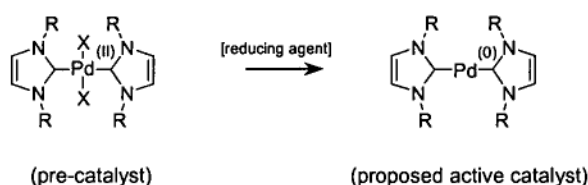
Scheme 1.6 – Generation of the palladium(0) active catalyst

1.4.4 Applications of Alkyl-Palladium Carbene Complexes

Work by the Cavell group has centred on the incorporation of a metal-alkyl bond

in the pre-catalyst.[47,94,130,136-138] It was envisioned that generation of the active catalyst

may occur much faster and thus would eliminate the need for external reducing agents.[138]

While this methodology met with substantial success, it was noted that a side-reaction

resulting in the formation of 2-alkylimidazolium salts and subsequent catalyst

deactivation occurred occasionally (Scheme 1.7).[94,130,137-139]
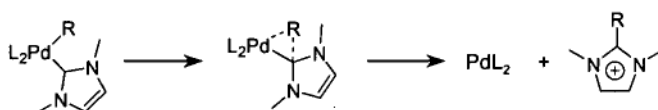
Scheme 1.7 – Decomposition mode for hydrocarbyl-palladium carbene complexes

A theoretical investigation demonstrated that facile decomposition occurred from a three-centred intermediate in a manner akin to reductive elimination, with the pπ orbital of the carbene intimately involved in the reaction.[139]   As hydrocarbyl-metal species are proposed as intermediates in many catalytic transformations, this reaction may represent an important route to catalyst deactivation.   Further theoretical information pertaining to the decomposition noted that features of the catalyst including chelation of the spectator ligands and chelating carbene-based ligands may help to impede this unwanted route.[139]

1.5 Aims and Thesis Overview

The broad aim of this project was to investigate the influence of heteroatom substitution on heterocyclic carbenes and their corresponding complexes. The theoretical work contained in this project covers a wide range of heterocyclic carbenes (containing N, S, O and P) and complexes. The synthetic component concentrated on the synthesis of novel palladium bis(thiazol-2-ylidene) complexes and their catalytic activity in the Heck and Suzuki reactions.

The general aims of this project were to:

- Investigate the ramifications of heteroatom exchange on the nature of heterocyclic carbenes.

- Establish general synthetic routes to palladium catalysts bearing thiazol-2-ylidene ligands.

- Investigate the possibility of generating group-10 metal carbene complexes via oxidative addition.

- Employ theoretical methods to engineer methyl-palladium carbene complexes for enhanced stability.

This thesis is divided into three main parts; investigations into the nature of heterocyclic carbenes that diversify from imidazol-2-ylidene; routes for the synthesis of group-10 (especially palladium) carbene complexes and their properties; and methods to enhance the stability of methyl-palladium carbene complexes.

The influence that heteroatom exchange has on the geometric and electronic properties of heterocyclic carbenes is discussed in Chapter 2 using results obtained via density functional theory (DFT). Substitution of phosphorus, oxygen and sulphur for nitrogen in the ring system leads to dramatic changes in geometry, electronics and simple reactivity. Phosphorus-containing heterocycles are found to adopt non-planar geometries and show decreased thermodynamic stability in comparison to their nitrogen analogues.

Dimerisation presents the primary problem in isolating carbenes with substituted heteroatoms. In Chapter 3, the range of heterocyclic carbenes investigated in Chapter 2 is evaluated with respect to their activation barrier and exothermicity in dimerisation reactions. Additionally, a subset of these carbenes is evaluated in proton-catalysed dimerisation. Imidazol-2-ylidene proves to be the most stable with respect to either mode of decomposition. Indirect theoretical methods to assess the barrier to decomposition are found to be generally poor over the set of carbenes evaluated.

Preparation of a number of novel thiazolium salts and their corresponding palladium complexes is the focus of Chapter 4. Their characteristics are similar to their analogous benzimidazole and imidazole counterparts. Additionally, Heck and Suzuki carbon-carbon coupling activity for these complexes is assessed. All complexes prove to be active in both processes, even more so with the addition of specific reducing agents.

The formation of group-10 metal carbene complexes via oxidative addition is investigated using DFT in Chapter 5. Using a chelated metal zero precursor, all pathways show a preference for the product, with 2-hydridoazoliums adding with little or no barrier. The possibility of complexation via carbon-carbon bond activation seems likely for a number of pathways.

The final three chapters detail a DFT study on the engineering of methyl-palladium carbene complexes to achieve enhanced stability with respect to reductive elimination. Chapter 6 deals with the reductive elimination of carbenes with differing ring systems. Imidazole-based complexes exhibit enhanced stability over imidazoline, thiazole and oxazole as a consequence of their σ-donating ability and occupation of the carbene p_π-orbital. Chapter 7 looks at the geometric influences on reductive elimination. Widening the auxiliary bite-angle is found to have a dramatic influence on the reductive elimination, while twisting the carbene's dihedral angle has only minor effects. Chapter 8 deals with the influence of N-substituents on the reductive elimination of imidazol-2-ylidenes. The steric bulk appears to play only a minor role due to its orientation in the complex. More important are the σ-donating and π-withdrawing properties of the substituents, which confer changes on the Pd-C bonding interaction.

1.6 References

(1)   *A Concise Dictionary of Chemistry*; Oxford University Press: Oxford, 1990.

(2)   Masters, C. *Homogeneous Transition-metal Catalysis - a gentle art*; Chapman and Hall: New York, 1981.

(3)   Cornils, B., Herrmann, W. A. *Applied Homogeneous Catalysis with Organometallic Compounds*; VCH: Verlag, 1996; Vol. 2.

(4)   Beletskaya, I. P., Cheprakov, A. V., *Chem. Rev.* **2000**, *100*, 3009.

(5)   Regitz, M., *Angew. Chem., Int. Ed. Engl.* **1991**, *30*, 674.

(6)   Herrmann, W. A., Kocher, C., *Angew. Chem., Int. Ed. Engl.* **1997**, *36*, 2163.

(7)   Herrmann, W. A., *Angew. Chem., Int. Ed. Engl.* **2002**, *41*, 1291.

(8)   Weskamp, T., Bohm, V. P. W., Herrmann, W. A., *J. Organomet. Chem.* **2000**, *600*, 12.

(9)   Bourissou, D., Guerret, O., Gabbai, F. P., Bertrand, G., *Chem. Rev.* **2000**, *100*, 39.

(10)   Herrmann, W. A., Elison, M., Fischer, J., Kocher, C., Artus, G. R. J., *Angew. Chem., Int. Ed. Engl.* **1995**, *34*, 2371.

(11)   Gilchrist, T. L., Rees, C. W. *Carbenes, Nitrenes and Arynes*; The Pitman Press: Bath, U.K., 1969.

(12)   Morrison, R. T., Boyd, R. N. *Organic Chemistry*; Sixth ed.; Prentice Hall: New Jersey, 1992.

(13)   Rauk, A. *Orbital Interaction Theory of Organic Chemistry*; John Wiley and Sons: New York, 1994.

(14)   Su, M. D., *Inorg. Chem.* **1995**, *34*, 3829.

(15)   Hu, C. H., *Chem. Phys. Lett.* **1999**, *309*, 81.

(16)   Cramer, C. J., Truhlar, D. G., Falvey, D. E., *J. Am. Chem. Soc.* **1997**, *119*, 12338.

(17)   Matzinger, S., Fulscher, M. P., *J. Phys. Chem.* **1995**, *99*, 10747.

(18)   Carter, E. A., Goddard, W. A., III, *J. Phys. Chem.* **1986**, *90*, 998.

(19)   Worthington, S. E., Cramer, C. J., *J. Phys. Org. Chem.* **1997**, *10*, 755.

(20)   Wanzlick, H.-W., Schikora, E., *Chem. Ber.* **1961**, *94*, 2389.

(21)   Arduengo, A. J., Harlow, R. L., Kline, M., *J. Am. Chem. Soc.* **1991**, *113*, 361.

(22)   Arduengo, A. J., Dias, H. V. R., Dixon, D. A., Harlow, R. L., Klooster, W. T., Koetzle, T. F., *J. Am. Chem. Soc.* **1994**, *116*, 6812.

(23)   Arduengo, A. J., Goerlich, J. R., Marshall, W. J., *J. Am. Chem. Soc.* **1995**, *117*, 11027.

(24)   Arduengo, A. J., Dias, H. V. R., Harlow, R. L., Kline, M., *J. Am. Chem. Soc.* **1992**, *114*, 5530.

(25)   Arduengo, A. J., Goerlich, J. R., Krafczyk, R., Marshall, W. J., *Angew. Chem., Int. Ed. Engl.* **1998**, *37*, 1963.

(26)   Arduengo, A. J., Davidson, F., Dias, H. V. R., Goerlich, J. R., Khasnis, D.,

Marshall, W. J., Prakasha, T. K., *J. Am. Chem. Soc.* **1997**, *119*, 12742..

(27)   Dias, H. V. R., *Tetrahedron Lett.* **1994**, *35*, 1365.

(28)   Enders, D., Breuer, K., Raabe, G., Runsink, J., Teles, J. H., Melder, J. P.,

Ebel, K., Brode, S., *Angew. Chem., Int. Ed. Engl.* **1995**, *34*, 1021.

(29)   Arduengo, A. J., Goerlich, J. R., Marshall, W. J., *Liebigs Ann.-Recl.* **1997**,

365.

(30)   Kuhn, N., Kratz, T., *Synthesis* **1993**, 561.

(31)   Alder, R. W., Allen, P. R., Murray, M., Orpen, G., *Angew. Chem., Int. Ed.

Engl.* **1996**, *25*, 1121.

(32)   Alder, R. W., Butts, C. P., Orpen, A. G., *J. Am. Chem. Soc.* **1998**, *120*,

11526.

(33)   Dixon, D. A., Dobbs, K. D., Arduengo, A. J., Bertrand, G., *J. Am. Chem.

Soc.* **1991**, *113*, 8782.

(34)   Merceron, N., Miqueu, K., Baceiredo, A., Bertrand, G., *J. Am. Chem. Soc.*

2002, *124*, 6807.

(35)   Corey, E. J., Winter, R. A. E., *J. Am. Chem. Soc.* **1963**, *85*, 2677.

(36)   Corey, E. J., Winter, R. A. E., *J. Am. Chem. Soc.* **1965**, *87*, 934.

(37)   Sauers, R. R., *Tetrahedron Lett.* **1994**, *35*, 7213.

(38)   Buza, D., Gradowska, W., *Pol. J. Chem.* **1980**, *54*, 717.

(39)   Denk, M., Lennon, R., Hayashi, R., West, R., Belyakov, A. V., Verne, H.

P., Haaland, A., Wagner, M., Metzler, N., *J. Am. Chem. Soc.* **1994**, *116*, 2691.

(40)   Herrmann, W. A., Denk, M., Behm, J., Scherer, W., Klingan, F. R., Bock, H., Solouki, B., Wagner, M., *Angew. Chem., Int. Ed. Engl.* **1992**, *31*, 1485.

(41)   Heinemann, C., Muller, T., Apeloig, Y., Schwarz, H., *J. Am. Chem. Soc.* **1996**, *118*, 2023.

(42)   Heinemann, C., Herrmann, W. A., Thiel, W., *J. Organomet. Chem.* **1994**, *475*, 73.

(43)   Boehme, C., Frenking, G., *J. Am. Chem. Soc.* **1996**, *118*, 2039.

(44)   Arduengo, A. J., Krafczyk, R., Schmutzler, R., Craig, H. A., Goerlich, J. R., Marshall, W. J., Unverzagt, M., *Tetrahedron* **1999**, *55*, 14523.

(45)   Herrmann, W. A., Kocher, C., Goossen, L. J., Artus, G. R. J., *Chem.-Eur. J.* **1996**, *2*, 1627.

(46)   Herrmann, W. A., Elison, M., Fischer, J., Kocher, C., Artus, G. R. J., *Chem.-Eur. J.* **1996**, *2*, 772.

(47)   McGuinness, D. S., Cavell, K. J., *Organometallics* **2000**, *19*, 741.

(48)   Tulloch, A. A. D., Danopoulos, A. A., Tooze, R. P., Cafferkey, S. M., Kleinhenz, S., Hursthouse, M. B., *Chem. Commun.* **2000**, 1247.

(49)   Liu, Y. F., Lindner, P. E., Lemal, D. M., *J. Am. Chem. Soc.* **1999**, *121*, 10626.

(50)   Cheng, M. J., Hu, C. H., *Chem. Phys. Lett.* **2000**, *322*, 83.

(51)   Dixon, D. A., Arduengo, A. J., *J. Phys. Chem.* **1991**, *95*, 4180.

(52)   Heinemann, C., Thiel, W., *Chem. Phys. Lett.* **1994**, *217*, 11.

(53)   Cheng, M. J., Hu, C. H., *Chem. Phys. Lett.* **2001**, *349*, 477.

(54)   Cioslowski, J., *Int. J. Quantum Chem.* **1993**, 309.

(55)   Tafipolsky, M., Scherer, W., Ofele, K., Artus, G., Pedersen, B., Herrmann, W. A., McGrady, G. S., *J. Am. Chem. Soc.* **2002**, *124*, 5865.

(56)   Geijo, F., LopezCalahorra, F., Olivella, S., *J. Heterocycl. Chem.* **1984**, *21*, 1785.

(57)   Nyulaszi, L., *Chem. Rev.* **2001**, *101*, 1229.

(58)   Nyulaszi, L., Veszpremi, T., Forro, A., *PCCP Phys. Chem. Chem. Phys.* **2000**, *2*, 3127.

(59)   Fekete, A., Nyulaszi, L., *J. Organomet. Chem.* **2002**, *643-644*, 278.

(60)   Arduengo, A. J., Calabrese, J. C., Davidson, F., Dias, H. V. R., Goerlich, J. R., Krafczyk, R., Marshall, W. J., Tamm, M., Schmutzler, R., *Helv. Chim. Acta* **1999**, *82*, 2348.

(61)   Chen, Y. T., Jordan, F., *J. Org. Chem.* **1991**, *56*, 5029.

(62)   Su, M. D., Chu, S. Y., *Inorg. Chem.* **1999**, *38*, 4819.

(63)   Alder, R. W., Blake, M. E., Oliva, J. M., *J. Phys. Chem. A* **1999**, *103*, 11200.

(64)   Oliva, J. M., *Chem. Phys. Lett.* **1999**, *302*, 35.

(65)   Jursic, B. S., *J. Chem. Soc., Perkin Trans. 2* **1999**, 1805.

(66)   Su, M. D., Chu, S. Y., *Chem. Phys. Lett.* **1999**, *308*, 283.

(67)   Liu, Y. F., Lemal, D. M., *Tetrahedron Lett.* **2000**, *41*, 599.

(68)   Cetinkaya, E., Hitchcock, P. B., Jasim, H. A., Lappert, M. F., Spyropoulos, K., *J. Chem. Soc., Perkin Trans. 1* **1992**, 561.

(69)   Cetinkaya, B., Gurbuz, N., Seckin, T., Ozdemir, B., *J. Mol. Catal. A: Chem.* **2002**, *184*, 31.

(70)   Cetinkaya, E., Hitchcock, P. B., Kuecuekbay, H., Lappert, M. F., Al-Juaid, S., *J. Organomet. Chem.* **1994**, *481*, 89.

(71)   Bordwell, F. G., Satish, A. V., *J. Am. Chem. Soc.* **1991**, *113*, 985.

(72)   Taton, T. A., Chen, P., *Angew. Chem., Int. Ed. Engl.* **1996**, *35*, 1011.

(73)   Castells, J., Domingo, L., Lopezcalahorra, F., Marti, J., *Tetrahedron Lett.* **1993**, *34*, 517.

(74)   LopezCalahorra, F., Castro, E., Ochoa, A., Marti, J., *Tetrahedron Lett.* **1996**, *37*, 5019.

(75)   Castells, J., LopezCalahorra, F., Geijo, F., Perez-Dolz, R., Bassedas, M., *J. Heterocycl. Chem.* **1986**, *23*, 715.

(76)   Frenking, G., Frohlich, N., *Chem. Rev.* **2000**, *100*, 717.

(77)   Vyboishchikov, S. F., Frenking, G., *Chem.-Eur. J.* **1998**, *4*, 1428.

(78)   Boehme, C., Frenking, G., *Organometallics* **1998**, *17*, 5801.

(79)   Green, J. C., Scurr, R. G., Arnold, P. L., Cloke, F. G. N., *Chem. Commun.* **1997**, 1963.

(80)   Frohlich, N., Pidun, U., Stahl, M., Frenking, G., *Organometallics* **1997**, *16*, 442.

(81)   Huang, J. K., Schanz, H. J., Stevens, E. D., Nolan, S. P., *Organometallics* **1999**, *18*, 2370.

(82)   Alder, R. W., Allen, P. R., Williams, S. J., *Chem. Commun.* **1995**, 1267.

(83)   Oefele, K., *J. Organomet. Chem.* **1968**, *12*, 42.

(84)   Wanzlick, H.-W., Schoenerr, H. J., *Angew. Chem., Int. Ed. Engl.* **1968**, *7*, 141.

(85)   Oefele, K., Kreiter, C. G., *Chem. Ber.* **1972**, *105*, 529.

(86)   Oefele, K., *Angew. Chem., Int. Ed. Engl.* **1969**, *8*, 515.

(87)   Oefele, K., Roos, E., Herberhold, M., *Z. Naturforsch.* **1976**, *Teil B 31*, 1070.

(88)   Trost, B. M., Fleming, I., Eds. *Thiazoles and their Benzo Derivatives (Part 6)* in Comprehensive Organic Synthesis; Pergamon Press:, 1991.

(89)   Bertani, R., Mozzon, M., Michelin, R. A., *Inorg. Chem.* **1988**, *27*, 2809.

(90)   Belluco, U., Michelin, R. A., Ros, R., Bertani, R., Facchin, G., Mozzon, M., Zanotto, L., *Inorg. Chim. Acta* **1992**, *189-200*, 883.

(91)   Wang, H. M. J., Lin, I. J. B., *Organometallics* **1998**, *17*, 972.

(92)   Liu, S. T., Reddy, K. R., *Chem. Soc. Rev.* **1999**, *28*, 315.

(93)   Liu, S. T., Hsieh, T. Y., Lee, G. H., Peng, S. M., *Organometallics* **1998**, *17*, 993.

(94)   Magill, A. M., McGuinness, D. S., Cavell, K. J., Britovsek, G. J. P., Gibson, V. C., White, A. J. P., Williams, D. J., White, A. H., Skelton, B. W., *J. Organomet. Chem.* **2001**, *617*, 546.

(95)   Fraser, P. J., Roper, W. R., Stone, F. G. A., *J. Chem. Soc., Dalton Trans.* **1974**, 102.

(96)   McGuinness, D. S., Cavell, K. J., Yates, B. F., Skelton, B. W., White, A. H., *J. Am. Chem. Soc.* **2001**, *123*, 8317.

(97)   McGuinness, D. S., Cavell, K. J., Yates, B. F., *Chem. Commun.* **2001**, 355.

(98)   Furstner, A., Seidel, G., Kremzow, D., Lehmann, C. W., *Organometallics* **2003**, *22*, 907.

(99)   Herrmann, W. A., Schwarz, J., Gardiner, M. G., Spiegler, M., *J. Organomet. Chem.* **1999**, *575*, 80.

(100)   Herrmann, W. A., Schwarz, J., Gardiner, M. G., *Organometallics* **1999**, *18*, 4082.

(101)   Grundemann, S., Albrecht, M., Loch, J. A., Faller, J. W., Crabtree, R. H., *Organometallics* **2001**, *20*, 5485.

(102)   Nielsen, D. J., Cavell, K. J., Skelton, B. W., White, A. H., *Inorg. Chim. Acta* **2002**, *327*, 116.

(103)   Nielsen, D. J., Magill, A. M., Yates, B. F., Cavell, K. J., Skelton, B. W., White, A. H., *Chem. Commun.* **2002**, 2500.

(104)   Baker, M. V., Skelton, B. W., White, A. H., Williams, C. C., *Organometallics* **2002**, *21*, 2674.

(105)   Baker, M. V., Skelton, B. W., White, A. H., Williams, C. C., *J. Chem. Soc., Dalton Trans.* **2001**, 111.

(106)   Cardin, D. J., Doyle, M. J., Lappert, M. F., *Chem. Commun.* **1972**, 927.

(107)   Hill, J. E., Nile, T. A., *J. Organomet. Chem.* **1977**, *137*, 293.

(108)   Lappert, M. F., Maskell, R. K., *J. Organomet. Chem.* **1984**, *264*, 217.

(109)   Albert, K., Gisdakis, P., Rosch, N., *Organometallics* **1998**, *17*, 1608.

(110)   Schwarz, J., Bohm, V. P. W., Gardiner, M. G., Grosche, M., Herrmann, W. A., Hieringer, W., Raudaschl-Sieber, G., *Chem.-Eur. J.* **2000**, *6*, 1773.

(111)   Garrou, P. E., *Chem. Rev.* **1985**, *85*, 171.

(112)   Peris, E., Loch, J. A., Mata, J., Crabtree, R. H., *Chem. Commun.* **2001**, 201.

(113) Gstottmayr, C. W. K., Bohm, V. P. W., Herdtweck, E., Grosche, M., Herrmann, W. A., *Angew. Chem., Int. Ed. Engl.* **2002**, *41*, 1363.

(114) Herrmann, W. A., Reisinger, C. P., Spiegler, M., *J. Organomet. Chem.* **1998**, *557*, 93.

(115) Weskamp, T., Bohm, V. P. W., Herrmann, W. A., *J. Organomet. Chem.* **1999**, *585*, 348.

(116) Weskamp, T., Kohl, F. J., Hieringer, W., Gleich, D., Herrmann, W. A., *Angew. Chem., Int. Ed. Engl.* **1999**, *38*, 2416.

(117) Frenzel, U., Weskamp, T., Kohl, F. J., Schattenman, W. C., Nuyken, O., Herrmann, W. A., *J. Organomet. Chem.* **1999**, *586*, 263.

(118) Jackstell, R., Andreu, M. G., Frisch, A., Selvakumar, K., Zapf, A., Klein, H., Spannenberg, A., Rottger, D., Briel, O., Karch, R., Beller, M., *Angew. Chem., Int. Ed. Engl.* **2002**, *41*, 986.

(119) Jackstell, R., Frisch, A., Beller, M., Rottger, D., Malaun, M., Bildstein, B., *J. Mol. Catal. A: Chem.* **2002**, *185*, 105.

(120) Wasserscheid, P., Keim, W., *Angew. Chem., Int. Ed. Engl.* **2000**, *39*, 3773.

(121) Calo, V., Del Sole, R., Nacci, A., Schingaro, E., Scordari, F., *Eur. J. Org. Chem.* **2000**, 869.

(122) Calo, V., Nacci, A., Lopez, L., Mannarini, N., *Tetrahedron Lett.* **2000**, *41*, 8973.

(123) Selvakumar, K., Zapf, A., Beller, M., *Org. Lett.* **2002**, *4*, 3031.

(124) Basset, J.-M., Niccolai, G. P., Chauvin, Y., Magna, L., EP 1201634, 2002.

(125) Xu, L. J., Chen, W. P., Xiao, J. L., *Organometallics* **2000**, *19*, 1123.

(126)   Hillier, A. C., Grasa, G. A., Viciu, M. S., Lee, H. M., Yang, C. L., Nolan, S. P., *J. Organomet. Chem.* **2002**, *653*, 69.

(127)   Grasa, G. A., Viciu, M. S., Huang, J. K., Zhang, C. M., Trudell, M. L., Nolan, S. P., *Organometallics* **2002**, *21*, 2866.

(128)   Zhang, C. M., Huang, J. K., Trudell, M. L., Nolan, S. P., *J. Org. Chem.* **1999**, *64*, 3804.

(129)   Loch, J. A., Albrecht, M., Peris, E., Mata, J., Faller, J. W., Crabtree, R. H., *Organometallics* **2002**, *21*, 700.

(130)   McGuinness, D. S., Cavell, K. J., Skelton, B. W., White, A. H., *Organometallics* **1999**, *18*, 1596.

(131)   Bohm, V. P. W., Gstottmayr, C. W. K., Weskamp, T., Herrmann, W. A., *J. Organomet. Chem.* **2000**, *595*, 186.

(132)   Amatore, C., Jutand, A., *Acc. Chem. Res.* **2000**, *33*, 314.

(133)   Heck, R. F., *J. Am. Chem. Soc.* **1968**, *90*, 5518.

(134)   Shaw, B. L., Perera, S. D., Staley, E. A., *Chem. Commun.* **1998**, 1361.

(135)   Shaw, B. L., *New J. Chem.* **1998**, *22*, 77.

(136)   Green, M. J., Cavell, K. J., Skelton, B. W., White, A. H., *J. Organomet. Chem.* **1998**, *554*, 175.

(137)   McGuinness, D. S., Cavell, K. J., *Organometallics* **2000**, *19*, 4918.

(138)   McGuinness, D. S., Green, M. J., Cavell, K. J., Skelton, B. W., White, A. H., *J. Organomet. Chem.* **1998**, *565*, 165.

(139)   McGuinness, D. S., Saendig, N., Yates, B. F., Cavell, K. J., *J. Am. Chem. Soc.* **2001**, *123*, 4029.

• Chapter Two •

Properties of X,Y Heterocyclic Carbenes (X,Y = N, S, O and P)

2.1 Introduction

The isolation of Arduengo's free carbene ten years ago[1] resulted in a proliferation of research in the area of heterocyclic carbenes.[2-7] Utilising evidence that isolable carbenes may be achieved by stabilising the carbene center through a π-donation, σ-withdrawing electronic scheme,[8-14] the backbone structure of free carbenes has diversified from the original imidazole template to include heterocyclic[15] (1) and acyclic NCS[16] (2), acyclic NCO[16] (3) and more recently acyclic NCP[17] carbenes (4) (Figure 2.1).
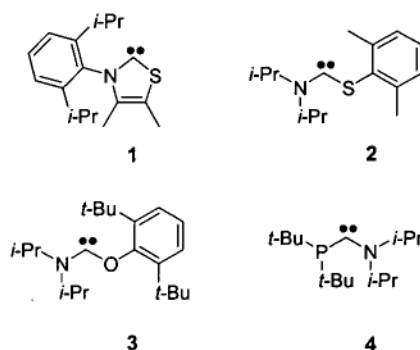
Figure 2.1 - Isolated carbenes showing diversification from diamino substitution

The factors that contribute to the considerable stability of the imidazole-based carbenes have been heavily debated.[8,14,18] Structure, π-donation and σ-withdrawal from adjacent atoms, electron delocalisation (aromaticity), singlet-triplet splittings, stability with respect to dimerisation and the nucleophilic and electrophilic reactivity of the carbenic center are all thought to influence the overall stability of imidazol-2-ylidenes.

Many of these attributes have also been assessed for the saturated imidazolin-2-ylidene,[8,10,19-22] with little extension to other five-membered heterocyclic carbenes.[22-27]

This chapter comprehensively assesses the factors that contribute to carbene stability for a range of five-membered heterocycles (Figure 2.2). Conclusions are then drawn regarding the influence of the heteroatoms on the carbenic centre. The selected heteroatoms (specifically N, S, O and P) are all known to stabilise isolable carbenes (Figure 2.1), and exhibit remarkable differences in electronegativities, hybridisation and their ability to donate π-electron density to the carbenic centre. The varying properties of the heteroatoms give rise to wide variations in both the geometric and electronic structure of the carbenes.

$X, Y = N\text{-}CH_3, P\text{-}CH_3, O, S$

5
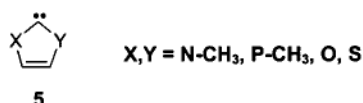
Figure 2.2. The set of heterocyclic carbenes that are the focus of this study

Presented in this chapter are results from DFT calculations of the geometries, singlet-triplet splittings and enthalpies of reaction for protonation, hydrogenation and indirectly, dimerisation. In addition, a quantitative description of the aromaticity of the heterocyclic carbenes is provided using physical and geometric methods. Where appropriate the influences of the adjacent heteroatoms on the geometric and electronic nature of the carbene are explained and related to overall stability.

2.2 Computational Methods

All geometry optimisations were carried out with the B3LYP[28-30] density functional level of theory employing a 6-31G(d)[31] basis set. Single-point energy calculations on these optimized structures were carried out for all molecules at the B3LYP level using a 6-311+G(2d,p)[32-34] basis set and include zero point vibrational energy (ZPVE) corrections from frequency calculations at the lower level of theory (giving ΔH_0). Energies are discussed at the B3LYP/6-311+G(2d,p)//B3LYP/6-31G(d) + ZPVE level unless otherwise noted.

Singlet-triplet splittings were calculated using coupled cluster methods[35,36] at the CCSD(T)/6-311G(d,p)//B3LYP/6-31G(d) + ZPVE level using optimized geometries for both the singlet and triplet species. $<S^2>$ values for all the triplet species were acceptable with the highest value being 2.13 for the carbene containing P and S.

A combination of literature methods was utilized to quantitatively assess aromaticity and by comparing these different approaches, the applicability of each method to the species involved in the current study was assessed.

Specifically, the magnetic shieldings required for the NICS method were calculated using the HF-GIAO/6-31+G(d)//B3LYP/6-31G(d) method as recommended by the original authors.[37] These values were computed at the center (NICS(0)) and one Ångstrøm above the center (NICS(1)) of the five-membered ring. The homodesmic reaction previously described by Sauers[25] was used to evaluate the aromatic stabilisation

energies (ASE).   The Bird index[38,39] (BI) was computed to evaluate the electronic

delocalisation in each of the five membered rings.   The required constants for Gordy's

formula were taken from Bird's original evaluation.[38]

The nature of the stationary points was determined by evaluating the Hessian

matrix. All calculations were carried out with the Gaussian 98 suite of programs.[40]

2.3 Results and Discussion

2.3.1 Geometries

The calculated geometries of the singlet carbenes are shown in Figure 2.3. A subset of the molecules has been published previously at both the MNDO[41] and MP2[25] levels, and the results shown are in satisfactory agreement. Experimental structures are available for **NS** and **NN** carbenes and the geometrical parameters observed[15,42] for the central cores of these heterocycles are similar to those calculated in the current work (shown in parentheses - Figure 2.3).

While the majority of the carbenes shown are planar, those heterocycles containing phosphorous are not. Phosphorus prefers a pyramidal conformation largely as a result of its high inversion barrier in comparison to nitrogen (PH$_3$ 35 kcal/mol *c.f.* NH$_3$ 6 kcal/mol).[43] The energy barriers to achieving carbene planarity (C$_s$ symmetry) are shown in Table 2.1. Note that the energy barrier for achieving planarity is relatively low for **PP** and **PS** compared to **NP** and **PO**. Also shown in Table 1 is the ΣP (sum of angles around phosphorous) parameter, which demonstrates that the **NP** and **PO** carbenes show significant sp^3 hybridisation about phosphorous, while the **PP** and **PS** carbenes adopt a less pyramidal (closer to sp^2) conformation.

While the adjacent carbene carbon should promote planarity at phosphorus, it is known that electron-withdrawing substituents (eg N, O) near phosphorus will impede it from achieving planarity. In contrast, lack of significant electronegative substituents will

enable phosphorus to adopt a more planar configuration as in the **PS** and **PP** heterocycles.[44] It is for this reason then that a divide in seen between the **PS/PP** and **NO/NP** carbene groups.
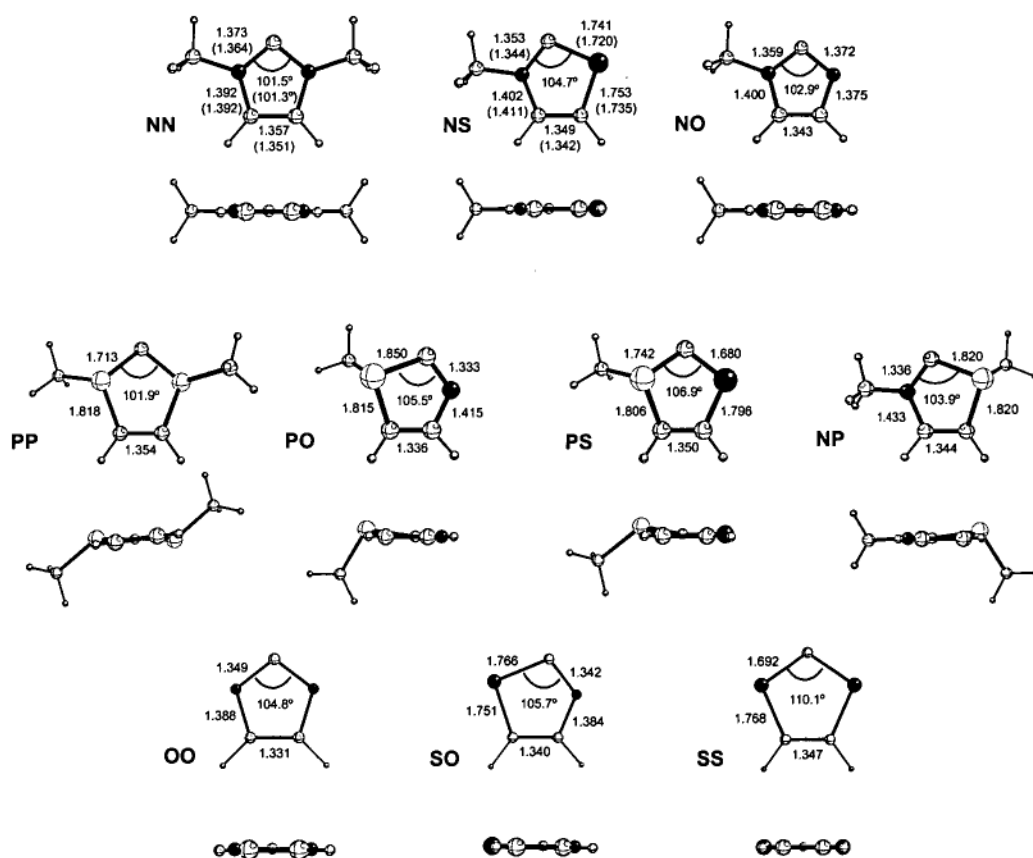
Figure 2.3. Optimised singlet geometries of the **XY** heterocyclic carbenes (Å and °). Each molecule is shown from two perspectives (top and back). Numbers shown in parentheses correspond to experimental structures: 3-diisopropylphenyl-4,5-dimethylthiazol-2-ylidene[15] and 1,3,4,5-tetramethylimidazol-2-ylidene[42]

Table 2.1. Degree of pyramidalisation of phosphorus in singlet carbenes

carbene	ΣP^a	$\Delta H(Planarity)^b$
NP	305.7°	8.59
PO	303.2°	5.97
PP	338.3°, 338.3°	3.18
PS	328.3°	0.62

$^a\Sigma P$ is the sum of bond angles around phosphorus;
^{b}Energy requirement to force ring system to C_s symmetry (kcal/mol/phosphorus)

The degree of double bond character exhibited by the heteroatom-C(2) bond depends strongly on the heteroatom. Bond lengths are shown in Table 2.2 and Figure 2.3.

Table 2.2. Properties of heterocyclic carbenes at the carbenic centre

carbene (XY)	bond C-X		bond C-Y		properties at C(2)		
	R (Å)	WBI^a	R (Å)	WBI^a	Mulliken charge	natural charge	p_π (NPA)^b
NN	1.373	1.2	1.373	1.2	0.098	0.117	0.652
NO	1.359	1.3	1.372	1.1	0.159	0.291	0.593
NP	1.336	1.4	1.820	1.1	-0.141	-0.265	0.567
NS	1.353	1.3	1.741	1.4	-0.122	-0.194	0.671
OO	1.349	1.1	1.349	1.1	0.243	0.471	0.518
PO	1.850	1.2	1.333	1.2	-0.048	-0.050	0.459
PP	1.713	1.5	1.713	1.5	-0.364	-0.986	0.845
PS	1.742	1.4	1.680	1.5	-0.364	-0.758	0.715
SO	1.766	1.4	1.342	1.2	-0.032	0.004	0.591
SS	1.692	1.5	1.692	1.5	-0.360	-0.626	0.744

^{a}WBI = Wiberg Bond Index, ^{b}NPA = Natural Population Analysis of p_π orbital

For example, the limited π-donating ability of oxygen[39,45] is well illustrated by the low WBI values of oxygen-containing heterocycles. In addition, the more planar phosphorus-containing heterocycles (**PP, PS**) show enhanced double bond character when compared to the more pyramidal phosphorous carbenes (**NP, PO**).

Generous p_π-donation by adjacent heteroatoms leads to a moderation of electrophilic activity of the heterocyclic carbene.[4,13] Imidazole-based carbenes are thought to be devoid of electrophilic activity due to considerable donation by both nitrogen substituents.[9] This is reflected in the large occupation (0.652 e) of the carbene p_π orbital (Table 2.2) and the substantial double bond character shown by the Wiberg bond indices (1.2 and 1.2). Those heterocycles containing the larger sulphur and phosphorus atoms also show a significantly filled p_π orbital and are likewise expected to exhibit reduced electrophilic reactivity. The poor σ-withdrawing ability of phosphorus and sulfur is likely to result in a high-energy in-plane lone pair, which will act to destabilise these heterocyclic carbenes.[11,13]
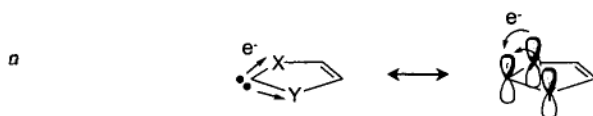
Figure 2.4. 'Push-pull' electronic stabilization scheme of heterocyclic carbenes

The Mulliken[46] and natural charges at the carbene carbon (C(2)) are shown in Table 2.2. The observed charges at C(2) can be rationalised on the basis of the electronegativity of the adjacent heteroatoms. The higher electronegativity of nitrogen (*c.f.* carbon) effectively removes excess σ-electron density from C(2) resulting in enhanced electronic stability due to a lowering in energy of the carbene in-plane sp^2 orbital.[1,11,14] Conversely, electropositive phosphorus can not alleviate the excess electron

density on C(2) and thus a less stable carbene is expected. Consequently, near neutral charges at C(2) are observed for those carbenes including nitrogen (e.g. Mulliken Charge(**NN**) = 0.098) and large negative charges from those carbenes including phosphorus (e.g. Mulliken Charge (**PP**) = –0.364).

In summary, it seems that an ideal mix of 'push-pull' characteristics for the adjacent heteroatoms is favourable for stabilising the carbene centre.[8] Heteroatoms that 'push' electrons in to the formally empty carbene p_{π} orbital, but balance this with σ-withdrawal ('pull') along the bond result in an approximate net charge of zero on C(2) (Figure 4). Consequently, these carbenes are expected to show enhanced stability over those carbenes that lack charge balance at the C(2) centre.

2.3.2 Singlet-triplet splittings

Singlet-triplet splittings ($\Delta E_{st} = E_t - E_s$) are shown in Table 2.3. Calculated splittings for **NN** and **PP** carbenes are in good agreement with previous results calculated at similar levels of theory (see table). The low energy triplet states found for the **NN** carbene are presented in Figure 2.5.

1(C_2)   2(C_1)   3(C_2)
ΔE= +1.3 kcal/mole   ΔE= +0.6 kcal/mole   ΔE= 0.0 kcal/mole
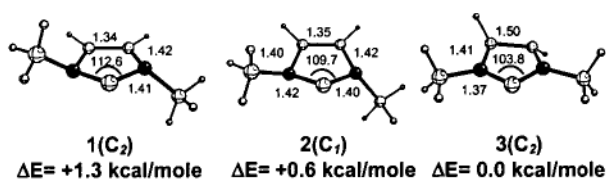
Figure 2.5. Optimised geometries located for the imidazol-2-ylidene triplet

Previous workers have described the C_2 symmetric (Figure 2.5 (**1**)) and C_1 (Figure 2.5 (**2**)) triplet states, but an additional lower energy C_2 triplet state (Figure 2.5(**3**)) was

located on the potential energy surface at the B3LYP/6-31G(d) level of theory. This triplet state exhibits a narrow valence angle (103.8°) but an elongated C-C bond (1.504Å) where the spin density was found to reside. The geometry of this low energy C_2 **NN** triplet state (Figure 2.5 **(3)**) was used for the high-level single-point calculations. Similar triplet geometries for the remaining nine carbenes were not located on the potential energy surface.

Table 2.3. Singlet-Triplet Splittings

carbene	valence bond angle		ΔE_{s-t}[a]
	singlet	triplet	(kcal/mol)
NN	101.5	103.8	83.7 (83.0)[b]
NO	102.9	112.5	79.8
NP	103.9	115.5	36.3
NS	104.7	113.0	67.8
OO	104.8	111.5	76.7
PO	105.5	116.6	26.3
PP	101.9	121.8	18.8 (20.1)[c]
PS	106.9	121.4	30.4
SO	105.7	113.2	57.1
SS	110.1	116.9	52.6

[a]ΔE_{st} = E(triplet)-E(singlet); [b]Literature value[15]; [c]Literature value[24]

Appreciable correlation between the singlet-triplet splitting values and the electronegativity (EN) of the adjacent heteroatoms (EN: O > N > S > P) is observed. Previous studies have indicated that σ electron withdrawing substituents favour the singlet over the triplet state by increasing the s-character of the sigma non-bonding

orbital, therefore making the sigma-electrons more difficult to promote.[3,4,23,47] Heterocycles containing highly electronegative heteroatoms show the largest singlet-triplet splittings (ΔE_{s-t}(**NN**)= 83.7, (**NO**) = 79.8, (**OO**) = 76.7 kcal/mol) while those that contain the electropositive phosphorus exhibit splittings between 15-40 kcal/mole. Low splitting values observed for phosphorus-containing heterocycles suggest a higher reactivity as a result of the more attainable reactive triplet state.

Geometrically, the carbene valence angle opens on going from the singlet to the triplet state (Figure 2.5, Table 2.3, *c.f.* Figure 2.3). This opening is more pronounced for the rings containing the larger sulfur and phosphorus heteroatoms.
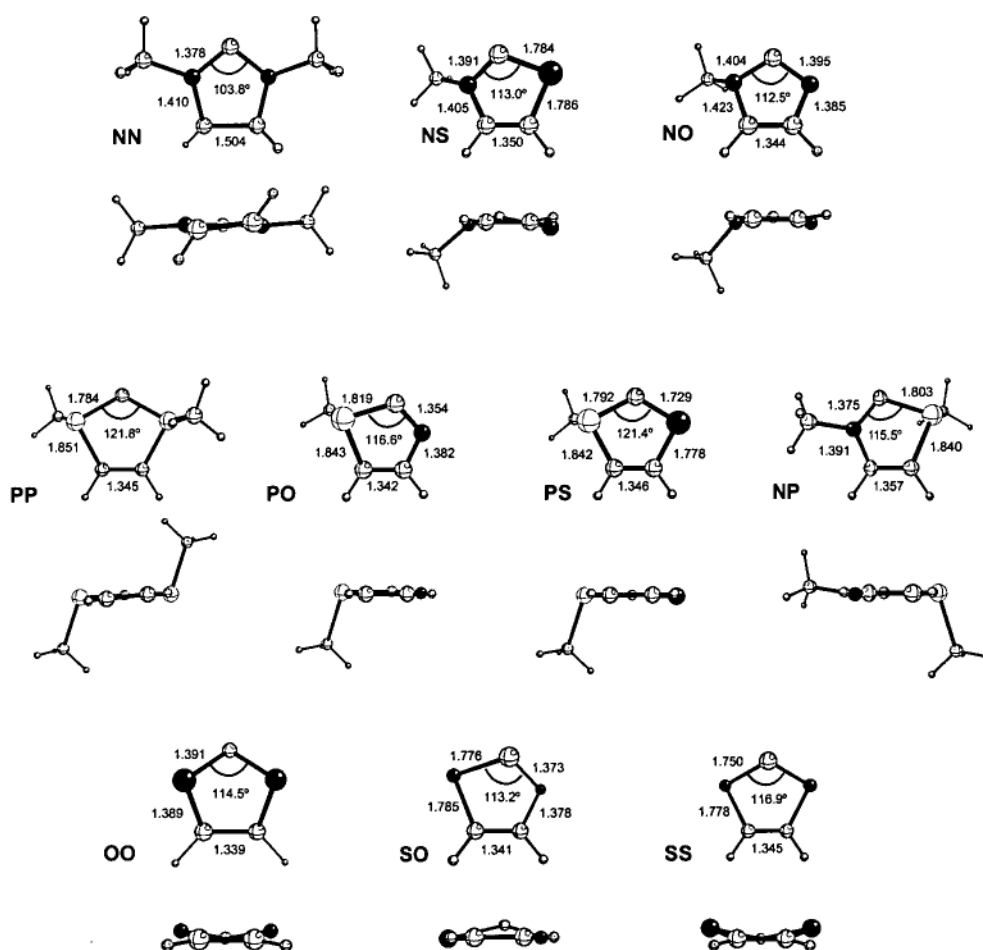
Figure 2.5. Optimised triplet geometries of the **XY** heterocyclic carbenes (Å and °). Each molecule is shown from two perspectives (top and back).

In general, triplet geometries exhibit elongated C-X and C-Y bond lengths and a buckled core in comparison to their corresponding singlets. In all the carbenes except for **NN**, the spin density is located on the carbene carbon. As expected, this corresponds to one electron in an sp^2 orbital and one electron in a (delocalised) p orbital on carbon.

The presence of an extra electron in the p_π orbital breaks down the aromatic system and the heteroatom adopts a tetrahedral (sp^3) orientation, as it can no longer regain the sp^2 promotional energy through aromaticity. The exception is **NN** where, as already noted, the unpaired electrons exist in the π and π^* obitals of the C=C bond.

2.3.3 Proton Affinity

As the majority of free carbenes are made via deprotonation of azolium salts, the proton affinity (Scheme 2.1) is an interesting characteristic to explore.[12]

Scheme 2.1 Proton Affinity

X,Y = N-CH$_3$, P-CH$_3$, O, S
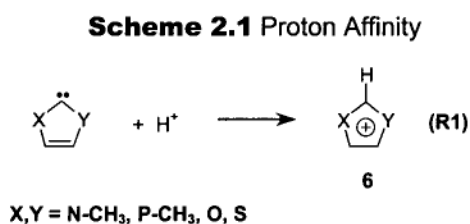
The proton affinities (Table 2.4) show a trend in that the carbenes containing group-15 elements are stronger Lewis-bases than those containing group-16 elements (**NN**, **NP** and **PP** *ca.* 260 kcal/mol; **NO**, **NS**, **PO** and **PS** *ca.* 240-250 kcal/mol; **SO**, **SS** and **OO** 220-235 kcal/mol). The fact that the proton affinity changes little within each group on going down the periodic table is remarkable and indicates that the affect on the carbene proton affinity of exchanging P for N, for example, is negligible.

Overall, the high values obtained for the proton affinities indicate that heterocyclic carbenes are among some of the most powerful neutral Lewis-bases known.[4]

The geometries of the protonated carbenes in Figure 2.7 show similarities to their singlet carbene counterparts. The five-membered core is planar with nitrogen adopting an sp^2 hybridised geometry. Valence angles relax slightly due to the lack of repulsion by the lone pair in the singlet carbene and there is a significant increase in aromaticity[1,11] (see Section 2.3.4) (Table 2.4).

Table 2.4. Proton affinity and aromaticity of protonated carbenes

carbene	proton affinity[a]	salt aromaticity (I_5)[b]
NN	259.5 (257.3, 228.2, 258.4)[c,d,e]	63.0
NO	243.7 (247.2)[d]	45.0
NP	260.3	43.0
NS	248.8 (254.7)[d]	58.8
OO	220.9 (228.2)[d]	31.5
PO	249.9	47.6
PP	258.6	52.1
PS	248.9	63.0
SO	233.1	46.9
SS	234.9 (247.7)[d]	60.2

[a]kcal/mol; [b]Bird Aromaticity Index (refer to text)[38,39]; [c]mp2 (corrected)[11]; [d]mp2 (FC)[25]; [e]b3lyp[12]
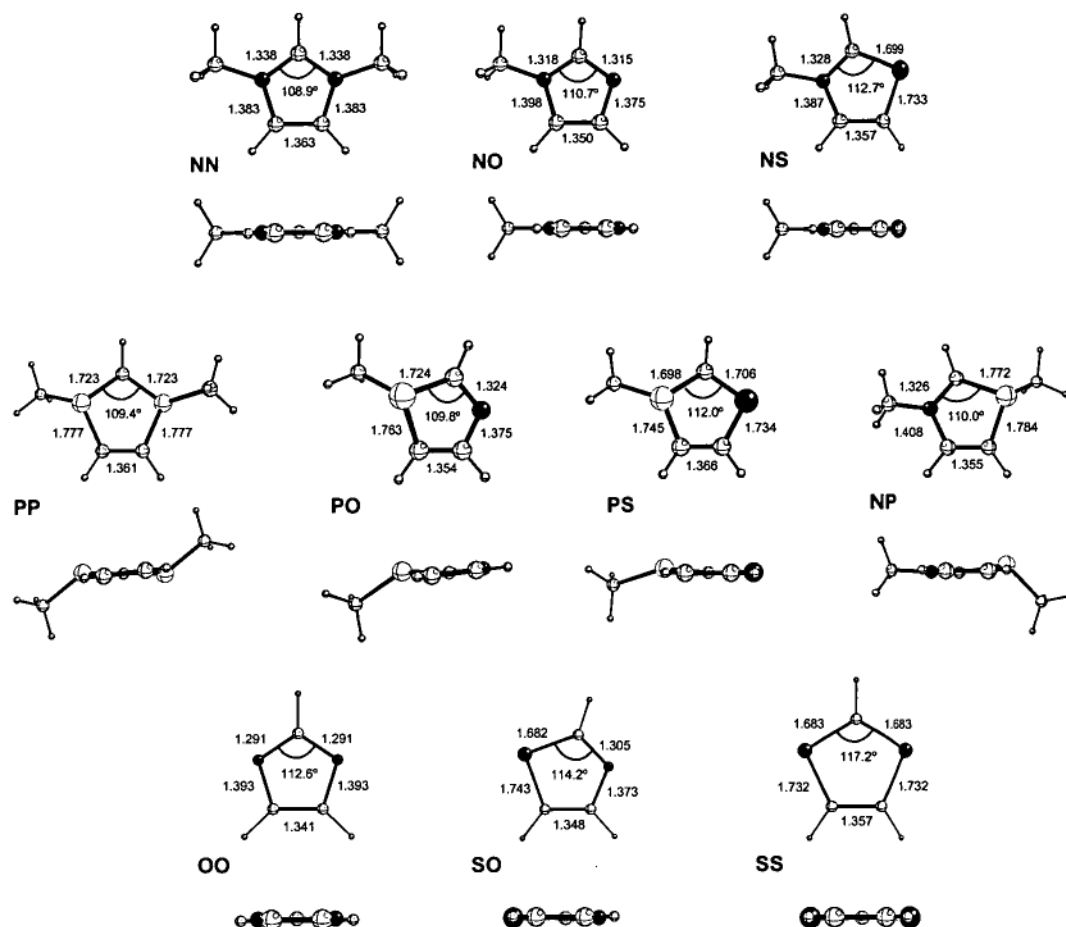
Figure 2.7. Optimised protonated geometries of the **XY** heterocyclic carbenes (Å and °). Each molecule is shown from two perspectives (top and back).

2.3.4 Aromaticity

Although electron delocalisation into the p_π carbene orbital provides appreciable stability, complete aromaticity provides an additional thermodynamic benefit for the carbene.[8]

X,Y = N-CH$_3$, P-CH$_3$, O, S
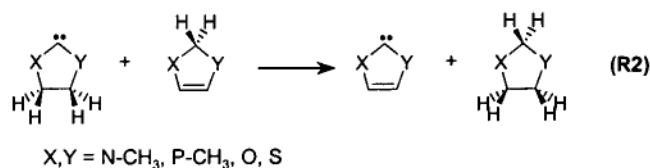
Scheme 2.2. Aromatic stabilisation energy (ASE) isodesmic reaction

Isodesmic reaction schemes are commonly used to assess the degree of aromaticity in heterocycles.[21,22,25,27] The results for the isodesmic reaction[25] (Scheme 2.2 **R2**) are shown in Table 2.5. The **NN** carbene clearly obtains the greatest thermodynamic benefit from aromaticity (ASE = 10.8 kcal/mol). The order of thermodynamic stability (**NN > NS > SS > NO > OO**) parallels previous findings.[25] The heterocyclic carbenes containing highly pyramidalised phosphorus (**NP** and **PO**) gain no (in fact negative!) thermodynamic benefit from cyclic delocalisation, which is a consequence of the unavailability of a significant proportion of the p_π orbital on the phosphorus to participate in aromaticity (*vide supra*). Aromaticity has been associated with the planarity of phosphorus,[44] although the actual correlation is still subject to debate.[48]

Table 2.5. Aromaticity measurements of the heterocyclic carbenes

carbene	ASE[a]	Bird Index (I_5)[b]	NICS(0)[c]	NICS(1)[c]
NN	10.8	54.5	-11.69	-9.45
NO	7.6	36.4	-10.44	-8.67
NP	-1.9	20.1	-4.85	-6.21
NS	9.4	46.4	-11.49	-9.88
OO	3.3	24.4	-10.33	-8.15
PO	-5.2	7.2	-2.97	-6.20
PP	1.0	31.5	-11.30	-9.04
PS	1.3	32.6	-9.30	-9.03
SO	6.3	32.3	-10.04	-9.11
SS	8.3	43.1	-12.63	-10.92

[a]ASE = Aromatic Stabilisation Energy from Scheme 2.2 (kcal/mol); [b]Bird's Aromaticity Index for Five-Membered Heterocycles[39]; [c]NICS(X) = Nucleus Independent Chemical Shift at X Angstroms above the ring centre.[37]

The Bird aromaticity index[38,39] (BI (I_5), Table 2.5) shows excellent correlation with the results obtained using the previous method. Employed here, the Bird Index (BI) is for five-membered rings (I_5) where 0 signifies a non-delocalised Kekulé-type structure, while 100 denotes complete delocalisation. The **NN**, **NS**, **SS** and **NO** carbenes all show significant aromaticity ($I_5 > 35$) while **NP** ($I_5 = 20.1$) and **PO** ($I_5 = 7.2$) exhibit little delocalisation. A trend similar to the ASE values described above is observed. The BI has previously been shown to correlate well with experimental data and works well in heterocycles provided the number of carbon atoms is greater than the number of heteroatoms.[49]

The magnetic criteria measurement (NICS)[37] results are collected in Table 2.5. This method has proven to be an effective theoretical measure of ring current by using a nuclear independent probe.[37,50] There is not a great deal of discrimination between the NICS(0) values, with the majority exhibiting a value which indicates that the heterocyclic carbenes studied are more aromatic than benzene (–9.7).[37] The **NP** and **PO** carbenes show meagre cyclic delocalisation in comparison to the rest of the carbene set (NICS(0)(**NP** = –4.85, **PO** = -2.97)).

NICS(0) has been shown to have problems dealing with small ring systems[51] as the value is affected by sigma-bond shielding. Use of the new DNICS[51] method (which has not yet been implemented in Gaussian98), which partitions contributions to the magnetic moment into σ and π contributions, could alleviate this problem in the future. It is likely that the NICS(0) values may also be affected through shielding of groups that lie above or below the ring.[48] This could occur in the situations where the P-Me group extends in to the space above the ring (ie **NP**, **PP**, **PO** and **PS**). Moving to NICS(1)

appears to provide no real benefit, as the height of the delocalised system is likely to shift as we change heteroatoms.[52] In the cases where NICS measurements present difficulties the geometrical indexes of aromaticity may be more effective.

In general, the three measures of aromaticity show good correlation (Figure 2.8). **NN, NS, NO** and **SS** all show a significant degree of thermodynamic stability attributed to aromaticity. **NP** and **PO** appear to show little aromaticity in comparison to the rest of the carbene set and the inherent lack of thermodynamic stability is likely to make them more susceptible to all types of decomposition reactions. Although the phosphorus-containing carbenes in general show little electron delocalisation, a planar phosphorus system may result in a significant increase in thermodynamic stability resulting from aromaticity. In fact, theoretical studies have shown aromaticity to increase markedly in the **PP** carbene by constraining the system to be planar (at minimal energy cost (Table 2.1)).[44]
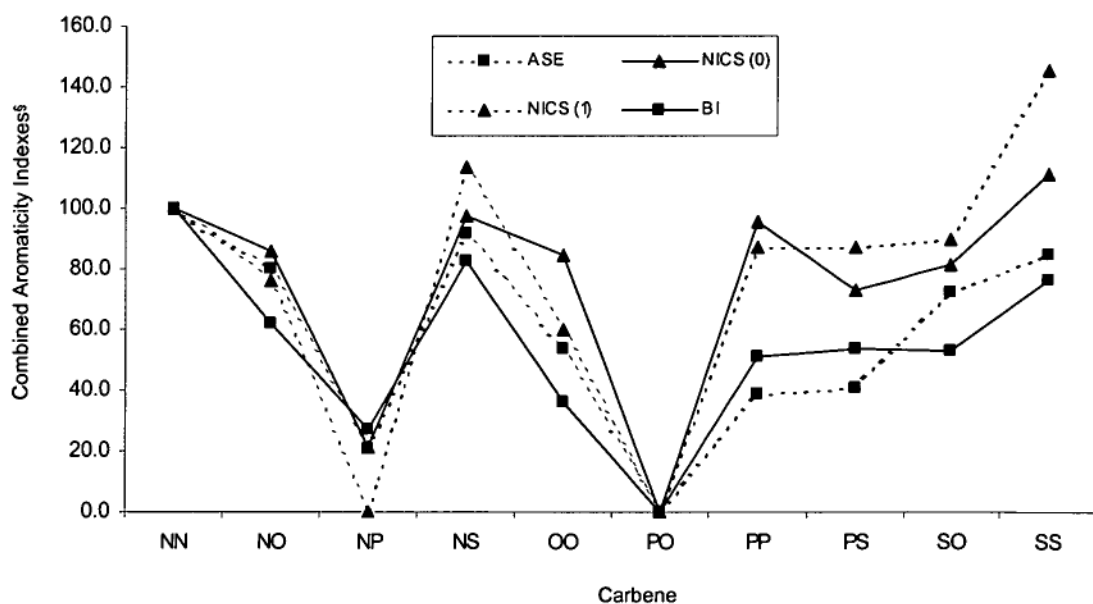
Figure 2.8. Correlation of the various methods of aromaticity.

§Combined Aromaticity Index = [Index(**XY**)-Index(**NN**)]/[Index(**XY**)-Index(**PO**)]

2.3.5 Reactivity

It is an imperative feature that carbenes that are to be experimentally isolable show good thermodynamic and kinetic stability. The carbenic carbon can show elements of electrophilic reactivity through its formally empty p_π orbital and nucleophilic reactivity via its in-plane σ-sp^2 lone pair. The general effects on the electrophilic and nucleophilic reactivity of the carbene centre based on the diversity of the adjacent heteroatoms was discussed previously. Focus is now shifted to specific reactions of heterocyclic carbenes to further assess their thermodynamic stability.

Dimerisation has been described as the most important decomposition reaction of N-heterocyclic carbenes.[21] Two schemes have recently shown the ability to indirectly predict the stability of heterocyclic carbenes to dimerisation. These are the isodesmic reaction **(R3)**[22,27] and the bond dissociation energy (BDE)[53] **(R4)** (Scheme 2.4). In the literature, **R3** has also been used as an alternative measure of aromatic stabilization energy.[22,27] The results of these calculations are shown in Table 2.6.

Scheme 2.3. Indirect methods to assess the tendency toward dimerisation

$$BDE(XYC=CXY) = 172 - 2^*\Delta E_{s-t}(XYC:) \quad \textbf{(R4)}$$

$$X,Y = \text{N-CH}_3, \text{P-CH}_3, \text{O, S}$$
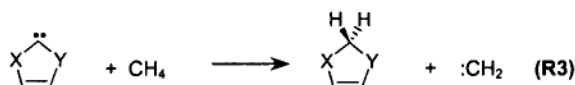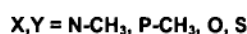
Very good correlation (Figure 2.9, $R^2 = 0.9162$) is observed between the two sets of results (Table 2.6), with the **NN** carbene clearly the most stable (ΔH(**R3**) =

106.0 kcal/mol, ΔH(R4) = 4.6 kcal/mol) to dimerisation using these indirect methods. The phosphorus containing heterocycles show poor tolerance to dimerisation (ΔH(R3) < 73 kcal/mol, ΔH(R4) > 99 kcal/mol) while the NS and NO carbenes show excellent tolerance.

Table 2.6. Stability toward dimerisation reactions[a]

carbene	ΔH(R3)[b]	BDE(R4)[c]	ΔH(R5)[d]
NN	106.0	4.6	-14.3
NO	96.5	12.5	-23.8
NP	72.5	99.3	-47.8
NS	94.1	36.4	-26.2
OO	86.1	18.5	-34.2
PO	53.0	119.4	-67.3
PP	53.5	134.3	-66.8
PS	63.0	111.2	-57.3
SO	78.8	57.7	-41.5
SS	82.6	66.9	-37.7

[a]Energies in kcal/mol, [b]Isodesmic reaction with methane, [c]Bond Dissociation Energy, [c]Enthalpy of Hydrogenation

Nyulaszi[27] proposed that any heterocycle that was more stable than 90 kcal/mol in the isodesmic reaction (R3) (Scheme 2.3) should be isolable as the free carbene. If this relation holds then NN, NS and NO carbenes should all be capable of isolation. (Figure 2.9)
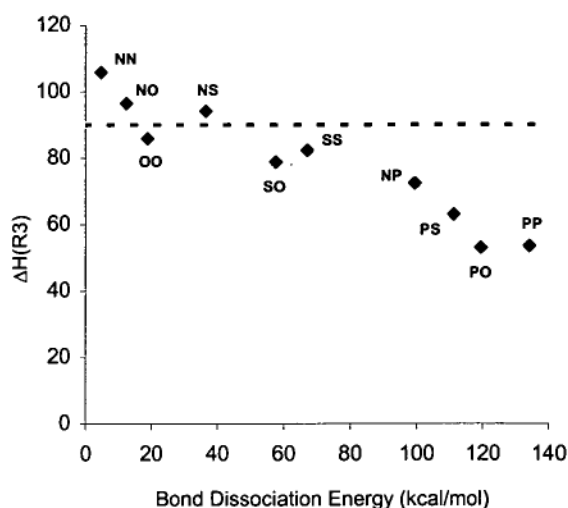
Figure 2.9. Correlation of methods in order to assess dimerisation tendency.
The dashed line represents the 90 kcal/mol free carbene limit (see text)

The heat of hydrogenation (Scheme 2.4, Table 2.6) provides a further indication of the thermodynamic stability of the heterocyclic carbene. Values are commonly referenced against that of the hydrogenation enthalpy of the simplest carbene, methylene (-130.9 kcal/mol).

Scheme 2.4. Hydrogenation

$X,Y = N\text{-}CH_3, P\text{-}CH_3, O, S$
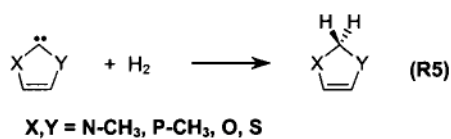
The phosphorus containing heterocycles are least stable to hydrogenation ($\Delta H(\textbf{R5}) < -47$ kcal/mol), while **NN** ($\Delta H(\textbf{R5}) = -14.3$ kcal/mol), **NO** ($\Delta H(\textbf{R5}) = -23.8$ kcal/mol) and **NS** ($\Delta H(\textbf{R5}) = -26.2$ kcal/mol) are the most stable. Frenking[8] has correlated the occupation of the p_π orbital with enthalpy of hydrogenation for imidazol(in)-2-ylidenes but little correlation is seen here. Hydrogenation enthalpies have

been found[21] to provide little information on the stability when applied to a wide range of

imidazole-based carbenes so its usefulness is still under debate.

2.4 Conclusions

A series of five-membered heterocyclic carbenes has been investigated to assess their underlying properties.

NN, **NS** and **NO** (imidazol-2-ylidene, thiazol-2-ylidene and oxazol-2-ylidene) carbenes show excellent thermodynamic stability. It is not surprising then that **NN** (cyclic and acyclic), **NS** (cyclic and acyclic) and **NO** (acyclic) carbenes have been observed experimentally. Cyclic **NO** carbenes are yet to be observed and this may be due to their instability with respect to a base or the instability of the oxazolium salt precursor.[54]

Steric protection can certainly aid kinetic stability, so it is likely that the lack of thermodynamic stability of some of the carbenes surveyed here can be compensated for by intuitive placement of auxiliary groups to aid kinetic stability. This methodology has been employed experimentally to allow isolation of saturated **NN** heterocyclic carbenes as well as **NS** heterocyclic carbenes.

SS, **SO** and **OO** carbenes show attributes favourable for isolation (high singlet-triplet splittings, appreciable thermodynamic stability to dimerisation and hydrogenation) but lack the flexibility of the group 15 elements (N and P) to add exocyclic substituents for steric protection enhancing kinetic stability. The synthesis of these and other heterocyclic carbenes await methodologies to overcome the inherent lack of

thermodynamic stability due to heteroatoms that are unable to fully stabilize the carbenic

centre.

2.5 References

(1)　　Arduengo, A. J., Harlow, R. L., Kline, M., *J. Am. Chem. Soc.* **1991**, *113*, 361.

(2)　　Herrmann, W. A., *Angew. Chem., Int. Ed. Engl.* **2002**, *41*, 1291.

(3)　　Bourissou, D., Guerret, O., Gabbai, F. P., Bertrand, G., *Chem. Rev.* **2000**, *100*, 39.

(4)　　Herrmann, W. A., Kocher, C., *Angew. Chem., Int. Ed. Engl.* **1997**, *36*, 2163.

(5)　　Regitz, M., *Angew. Chem., Int. Ed. Engl.* **1991**, *30*, 674.

(6)　　Weskamp, T., Bohm, V. P. W., Herrmann, W. A., *J. Organomet. Chem.* **2000**, *600*, 12.

(7)　　Arduengo, A. J., *Acc. Chem. Res.* **1999**, *32*, 913.

(8)　　Boehme, C., Frenking, G., *J. Am. Chem. Soc.* **1996**, *118*, 2039.

(9)　　Arduengo, A. J., Dias, H. V. R., Dixon, D. A., Harlow, R. L., Klooster, W. T., Koetzle, T. F., *J. Am. Chem. Soc.* **1994**, *116*, 6812.

(10)　　Heinemann, C., Thiel, W., *Chem. Phys. Lett.* **1994**, *217*, 11.

(11)　　Dixon, D. A., Arduengo, A. J., *J. Phys. Chem.* **1991**, *95*, 4180.

(12)　　Alder, R. W., Blake, M. E., Oliva, J. M., *J. Phys. Chem. A* **1999**, *103*, 11200.

(13)   Arduengo, A. J., Dias, H. V. R., Harlow, R. L., Kline, M., *J. Am. Chem. Soc.* **1992**, *114*, 5530.

(14)   Heinemann, C., Muller, T., Apeloig, Y., Schwarz, H., *J. Am. Chem. Soc.* **1996**, *118*, 2023.

(15)   Arduengo, A. J., Goerlich, J. R., Marshall, W. J., *Liebigs Ann.-Recl.* **1997**, 365.

(16)   Alder, R. W., Butts, C. P., Orpen, A. G., *J. Am. Chem. Soc.* **1998**, *120*, 11526.

(17)   Merceron, N., Miqueu, K., Baceiredo, A., Bertrand, G., *J. Am. Chem. Soc.* **2002**, *124*, 6807.

(18)   Tafipolsky, M., Scherer, W., Ofele, K., Artus, G., Pedersen, B., Herrmann, W. A., McGrady, G. S., *J. Am. Chem. Soc.* **2002**, *124*, 5865.

(19)   Jursic, B. S., *J. Chem. Soc., Perkin Trans. 2* **1999**, 1805.

(20)   Arduengo, A. J., Goerlich, J. R., Marshall, W. J., *J. Am. Chem. Soc.* **1995**, *117*, 11027.

(21)   Cheng, M. J., Hu, C. H., *Chem. Phys. Lett.* **2001**, *349*, 477.

(22)   Nyulaszi, L., Veszpremi, T., Forro, A., *PCCP Phys. Chem. Chem. Phys.* **2000**, *2*, 3127.

(23)   Su, M. D., Chu, S. Y., *Chem. Phys. Lett.* **1999**, *308*, 283.

(24)   Schoeller, W. W., *Eur. J. Inorg. Chem.* **2000**, 369.

(25)   Sauers, R. R., *Tetrahedron Lett.* **1996**, *37*, 149.

(26)   Sauers, R. R., *Tetrahedron Lett.* **1994**, *35*, 7213.

(27)   Fekete, A., Nyulaszi, L., *J. Organomet. Chem.* **2002**, *643-644*, 278.

(28)   Becke, A. D., *J. Chem. Phys.* **1993**, *98*, 5648.

(29)   Becke, A. D., *Phys. Rev. A.* **1988**, *38*, 3098.

(30)   Lee, C., Yang, W., Parr, R. G., *Phys. Rev. B.* **1988**, *37*, 785.

(31)   Hariharan, P. C., Pople, J. A., *Theor. Chim. Acta* **1973**, *28*, 213.

(32)   Krishnan, R., Binkley, J. S., Seeger, R., Pople, J. A., *J. Chem. Phys.* **1980**, *72*, 650.

(33)   McLean, A. D., Chandler, G. S., *J. Chem. Phys.* **1980**, *72*, 5639.

(34)   Frisch, M. J., Pople, J. A., Binkley, J. S., *J. Chem. Phys.* **1984**, *80*, 3265.

(35)   Cizek, J., *Adv. Chem. Phys.* **1969**, *14*, 35.

(36)   Purvis, G. D., Bartlett, R. J., *J. Chem. Phys.* **1982**, *76*, 1910.

(37)   Schleyer, P. V., Maerker, C., Dransfeld, A., Jiao, H. J., Hommes, N., *J. Am. Chem. Soc.* **1996**, *118*, 6317.

(38)   Bird, C. W., *Tetrahedron* **1992**, *48*, 335.

(39)   Bird, C. W., *Tetrahedron* **1985**, *41*, 1409.

(40)   Gaussian 98, Revision A.7, Frisch, M. J., Trucks, G. W., Schlegel, H. B., Scuseria, G. E., Robb, M. A., Cheeseman, J. R., Zakrzewski, V. G., Montgomery, J. A., Jr., Stratmann, R. E., Burant, J. C., Dapprich, S., Millam, J. M., Daniels, A. D., Kudin, K. N., Strain, M. C., Farkas, O., Tomasi, J., Barone, V., Cossi, M., Cammi, R., Mennucci, B., Pomelli, C., Adamo, C., Clifford, S., Ochterski, J., Petersson, G. A., Ayala, P. Y., Cui, Q., Morokuma, K., Malick, D. K., Rabuck, A. D., Raghavachari, K., Foresman, J. B., Cioslowski, J., Ortiz, J. V., Baboul, A. G., Stefanov, B. B., Liu, G., Liashenko, A., Piskorz, P., Komaromi, I., Gomperts, R., Martin, R. L., Fox, D. J., Keith, T., Al-Laham, M. A., Peng, C. Y., Nanayakkara, A., Gonzalez, C., Challacombe, M., Gill, P. M. W.,

Johnson, B., Chen, W., Wong, M. W., Andres, J. L., Gonzalez, C., Head-Gordon, M., Replogle, E. S., Pople, J. A., Gaussian Inc, Pittsburgh, PA, 1998

(41)   Geijo, F., LopezCalahorra, F., Olivella, S., *J. Heterocycl. Chem.* **1984**, *21*, 1785.

(42)   Kuhn, N., Kratz, T., *Synthesis* **1993**, 561.

(43)   Schwerdtfeger, P., Laakkonen, L., Pyykko, P., *J. Chem. Phys.* **1992**, *96*, 6807.

(44)   Nyulaszi, L., *Chem. Rev.* **2001**, *101*, 1229.

(45)   Kapp, J., Schade, C., ElNahasa, A. M., Schleyer, P. V., *Angew. Chem., Int. Ed. Engl.* **1996**, *35*, 2236.

(46)   Mulliken, R. S., *J. Chem. Phys.* **1955**, *23*, 1833.

(47)   Worthington, S. E., Cramer, C. J., *J. Phys. Org. Chem.* **1997**, *10*, 755.

(48)   Mattmann, E., Mathey, F., Sevin, A., Frison, G., *J. Org. Chem.* **2002**, *67*, 1208.

(49)   Katritzky, A. R., Jug, K., Oniciu, D. C., *Chem. Rev.* **2001**, *101*, 1421.

(50)   Schleyer, P. V., Jiao, H. J., Hommes, N., Malkin, V. G., Malkina, O. L., *J. Am. Chem. Soc.* **1997**, *119*, 12669.

(51)   Schleyer, P. V., Manoharan, M., Wang, Z. X., Kiran, B., Jiao, H. J., Puchta, R., Hommes, N., *Org. Lett.* **2001**, *3*, 2465.

(52)   Baldridge, K. K., Uzan, O., Martin, J. M. L., *Organometallics* **2000**, *19*, 1477.

(53)   Carter, E. A., Goddard, W. A., III, *J. Phys. Chem.* **1986**, *90*, 998.

(54)   Turchi, I. J., Dewar, M. J. S., *Chem. Rev.* **1975**, *75*, 389.

• Chapter Three •

Dimerisation Mechanisms of X,Y Heterocyclic Carbenes (X,Y = N, S, O and P)

3.1 Introduction

The problems associated with the isolation of free *N*-heterocyclic carbenes were evident as early as the 1960s when attempts were made by Wanzlick to isolate 1,3-diphenylimidazolin-2-ylidene. Although the existence of the carbene was established via trapping experiments, repeated attempts to isolate the stable free carbene afforded the corresponding dimer (Scheme 3.1).[1]
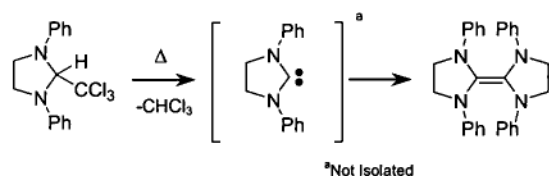
Scheme 3.1 - Wanzlick's attempted carbene isolation

Resurgence in the heterocyclic carbene field sparked by Arduengo's successful isolation of 1,3-diadamantylimidazol-2-ylidene[2] led to a number of carbenes stabilised by adjacent heteroatoms other than nitrogen (see Chapter 2). These 'second-generation' carbenes exhibit considerable thermodynamic instability (see Chapter 2) and thus are prone to dimerisation. This may be overcome by sequestering the carbenic centre with steric bulk in order to provide sufficient kinetic stability for isolation.[3-5] Only through appropriate protection it seems, can carbene systems other than diamino be isolated as 'bottle-able' species.

The stability of *N*-heterocyclic carbenes to decomposition has been comprehensively studied and dimerisation found to be the favoured course of decomposition.[6-8] The alternate 1,2-methyl-[7] and hydrogen-shifts[7,9] and alkyl C-H insertion[10] have been found to be less thermodynamically or kinetically favourable.

Investigations attempting to establish the active catalytic species in the benzoin condensation led to three proposed pathways for carbene dimerisation.[11-17] The direct dimerisation and indirect proton catalysed dimerisation (addition and insertion) are illustrated in Scheme 3.2.
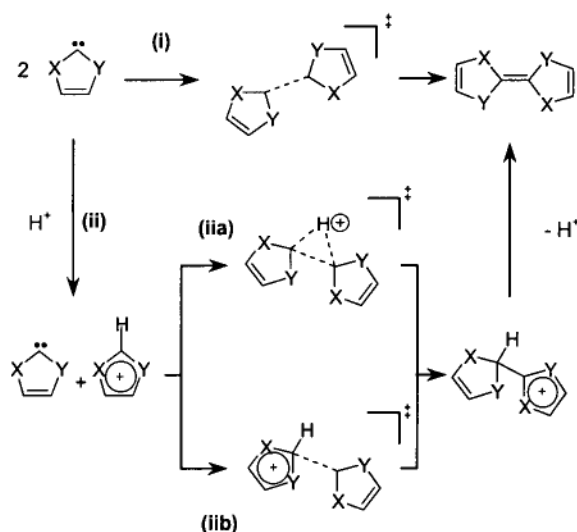
Scheme 3.2. Dimerisation pathways for free carbenes
(i) direct carbene + carbene dimerisation, (ii) proton catalysed dimerisation
(a) Insertion mechanism, (b) Addition mechanism

Jordan and Chen[16] demonstrated via NMR crossover experiments with thiazol-2-ylidenes the existence of an "unsymmetrical dimer" resulting from a proton catalysed addition pathway (Scheme 3.2 (iib)). Arduengo noted[3] that dimerisation of his 'bottle-able' 3-diisopropylphenyl-4,5-dimethylthiazol-2-ylidene proceeded smoothly in the

presence of trace amounts of protic acids, while under aprotic conditions dimeric products could not be detected on a time scale of weeks. Further evidence for rate changes of dimerisation reactions in the presence of protons is also available for diaminocarbenes.[8,18] Despite evidence that thiazol-2-ylidenes decompose via a proton catalysed mechanism and subsequent information implying acid catalysis of some diaminocarbene dimerisations, theoretical studies have ignored this alternate pathway opting only to study the direct carbene decomposition route.

Past theoretical work on dimerisation of NHCs involved attempts to correlate various factors to the enthalpy of reaction. Singlet-triplet splittings,[6] isodesmic reaction schemes[19,20] and aromaticity[6,7] have all shown a degree of correlation to both ΔH and E_{act}. The absence of a significant kinetic barrier to dimerisation or a barrier in accordance with Hammond's postulate[21] is usually assumed.

In general, rigorous dimerisation studies for heterocyclic carbenes have been lacking.[7] Studies have been performed on simple acyclic diaminocarbenes[22,23] with little extension to cyclic systems. Cheng and Hu[6] have performed the only complete theoretical investigation on the direct dimerisation of imidazol-2-ylidene, reporting a barrier of 19.4 kcal/mol and a reaction enthalpy of +1.1 kcal/mol. The Nyulaszi group[19] have investigated the dimerisation of thiazol-2-ylidene and dithiol-2-ylidene using theoretical methods, though no activation barriers were calculated.

In this chapter the susceptibility to dimerisation of a series of five-membered heterocyclic carbenes (Figure 3.2) with neighbouring atoms akin to those that have recently been identified as stable species (Chapter 2, Figure 2.1) is comprehensively

investigated. Additionally, a subset of these carbenes $(X,Y = N, S$ and $O)$ are analysed with respect to proton catalysed decomposition and results are compared to the direct carbene dimerisation route.

X,Y = N-CH$_3$, P-CH$_3$, O, S
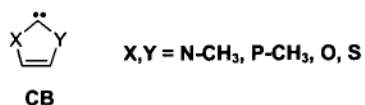
Figure 3.2. The set of heterocyclic carbenes that are the focus of this study

An assessment of the barriers and enthalpies of dimerisation via the two mechanisms is carried out using density functional theory. The applicability of indirect methods utilised in the recent literature to estimate the susceptibility to dimerisation is assessed with mixed results.

3.2 Computational Methods

All geometry optimizations were carried out with the use of the B3LYP[24-26] density functional level of theory employing a 6-31G(d)[27] basis set. High-level energy calculations on these optimised geometries were carried out at the B3LYP level using a 6-311+G(2d,p)[28-30] basis set and include unscaled zero point vibrational energy (ZPVE) corrections from frequency calculations at the lower level of theory. Energies are discussed at the B3LYP/6-311+G(2d,p)//B3LYP/6-31G(d) + ZPVE level unless otherwise noted.

The nature of the stationary points was determined by evaluating the Hessian matrix. All calculations were carried out with the Gaussian 98 suite of programs.[31]

3.3 Results and Discussion

3.3.1 Direct Carbene + Carbene Dimerisation. The energies for the structures on this decomposition pathway (Scheme 3.2 (**i**)) are collected in Table 3.1 and are shown graphically in Figure 3.2.

Table 3.1. Relative energies on pathway (**i**)[a] (Direct Dimerisation) (Scheme 3.2)

carbene	reactants (RCT-DD)	precursor complex (PC-DD)	transition structure (TS-DD)	product (dimer) (PRD)
NN	0.0	-0.8	22.6	-0.7
NO	0.0	-3.1	9.1	-19.8
NP	0.0	-0.4	3.8	-67.0
NS	0.0	-1.3	13.7	-25.7
OO	0.0	0.3	3.2	-32.5
PO	0.0	-2.7	-1.1	-105.8
PP	0.0	-2.1	8.3	-97.0
PS	0.0	-2.7	5.0	-82.4
SO	0.0	1.0	2.4	-55.4
SS	0.0	0.4	9.4	-48.3

[a]All values are in kcal/mol and are relative to reactants
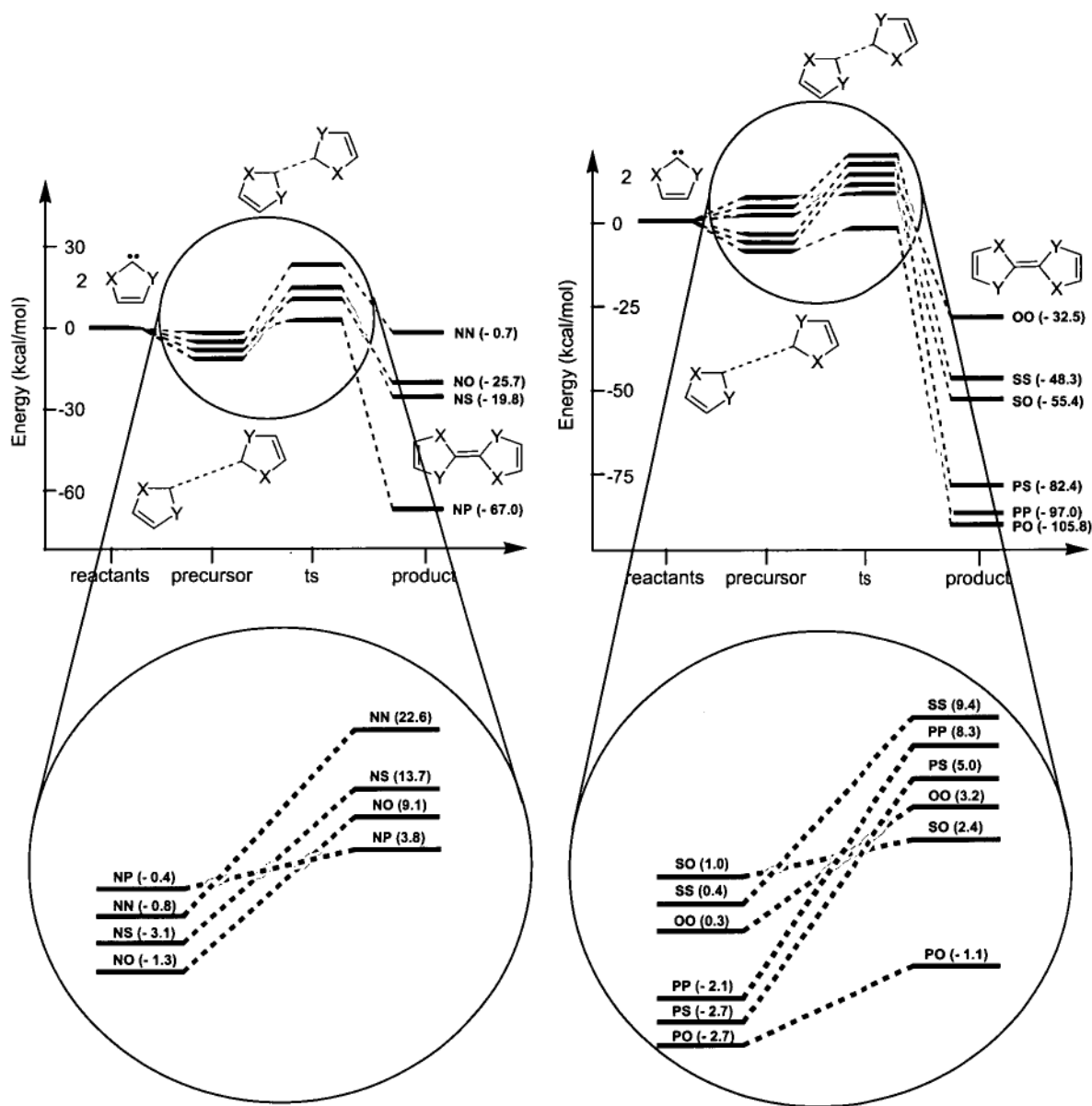
Figure 3.2. Potential energy surface for direct dimerisation (pathway **(i)**)
(Divided into two separate diagrams for the purpose of clarity)

The dimerisation of all **XY** carbenes is an exothermic reaction. The enthalpy of
dimerisation for the **NN** carbene (**CB**, X=Y=N) is similar to values that have been
previously predicted using both direct[6,7] and indirect[9,19] computational methods. **NN,
NO, NS** and **OO** carbenes show the greatest thermodynamic stability to dimerisation (ΔH

< -32.5 kcal/mol). Entropy considerations are expected to disfavour dimerisation by an additional 10 kcal/mol based on previous ΔH and ΔG calculations.[7,19] The phosphorus containing heterocyclic carbenes show the greatest tendency to dimerise via this route, with those showing reduced aromaticity (see Chapter 2) (**NP** and **PO**) being the least thermodynamically stable. This is in agreement with a number of reports that correlate ΔH (dimerisation) with aromaticity.[6,7,9,19,32,33]

The isodesmic reaction scheme used by Nyulaszi[19] (Scheme 3.3, **R1**) and the bond dissociation energy[20] (BDE) (Scheme 3.3, **R2**) which is based on the carbene singlet-triplet splitting (Table 3.2, see also Chapter 2) show excellent correlation with the enthalpy of dimerisation (Table 3.2 and Figure 3.4) with R^2 values of 0.99 and 0.93 respectively. This shows that the indirect methods used to estimate the enthalpy of dimerisation extend well across the series of heterocyclic carbenes in this work.

Scheme 3.3. Reaction schemes for indirect determination of dimerisation susceptibility
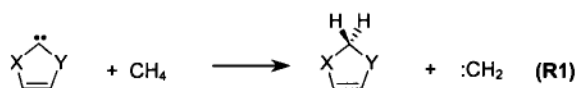
$$BDE(XYC=CXY) = 172 - 2^*\Delta E_{s-t}(XYC:) \quad \textbf{(R2)}$$

$$X,Y = N\text{-}CH_3, P\text{-}CH_3, O, S$$
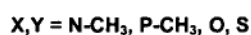
Table 3.2. Various properties of heterocyclic carbenes (kcal/mol)

carbene	$\Delta H(R1)^a$	$BDE(R2)^b$	$\Delta E_{s\text{-}t}{}^c$	ΔH(dimerisation)	E_{ac}(dimerisation)
NN	106.0	4.6	83.7	-0.7	23.4
NO	96.5	12.5	79.8	-19.8	12.2
NP	72.5	99.3	36.3	-67.0	4.2
NS	94.1	36.4	67.8	-25.7	15.0
OO	86.1	18.5	76.7	-32.5	2.8
PO	53.0	119.4	26.3	-105.8	1.6
PP	53.5	134.3	18.8	-97.0	10.4
PS	63.0	111.2	30.4	-82.4	7.7
SO	78.8	57.7	57.1	-55.4	1.4
SS	82.6	66.9	52.6	-48.3	9.0

[a]Nyulaszi's Isodesmic Reaction Enthalpy[19], [b]Bond Dissociation Energy[20], [c]Singlet-Triplet Splitting (= $E_{triplet} - E_{singlet}$)
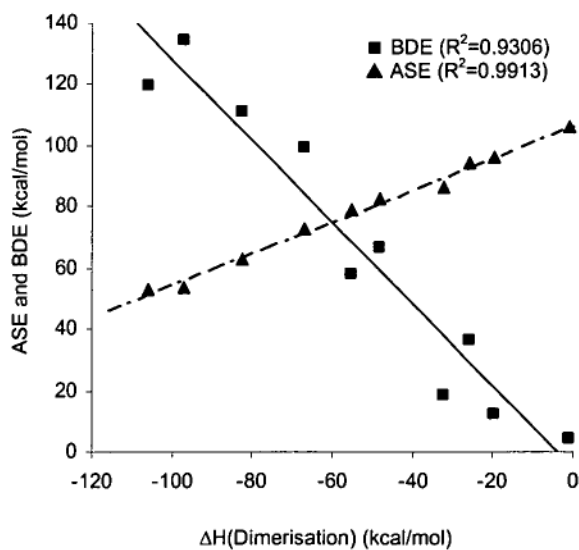
Figure 3.4. Correlation of ASE(R1) and BDE with enthalpy of dimerisation

In the cases where more than one geometrical isomer could exist, calculations were performed on all isomers to ascertain the lowest energy conformer.
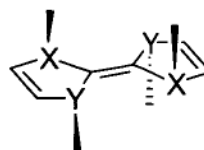
Figure 3.5 – Lowest energy dimer geometry

The lowest energy isomers all adopt similar geometries, with the heteroatoms in opposing carbene units *trans* to one another, R groups *trans* in the same carbene unit, and R groups *cis* on the same heteroatom across carbene units (Figure 3.5).

All conformations of this type exhibit zero imaginary frequencies implying true minima, while in most cases dimers of other conformations exhibit one or more imaginary frequencies. The geometrical data for the higher energy conformations can be found in the appendices (on the supplementary CD).

The dimer geometries (Figure 3.6) all show comparable C(2)-C'(2) bond lengths of 1.35 ± 0.02 Å. Deviation in the bond lengths appears to be attributed to steric strain, with those carbene units bearing two exocyclic ring substituents (**NN**, **NP** and **PP**) having elongated C-C bonds in comparison to those bearing one or no exocyclic substituents. Nitrogen and phosphorus prefer to adopt non-planar orientations in the dimer which has been shown both experimentally[3] and theoretically[9] for similar systems, presumably in an attempt to reduce steric repulsion.
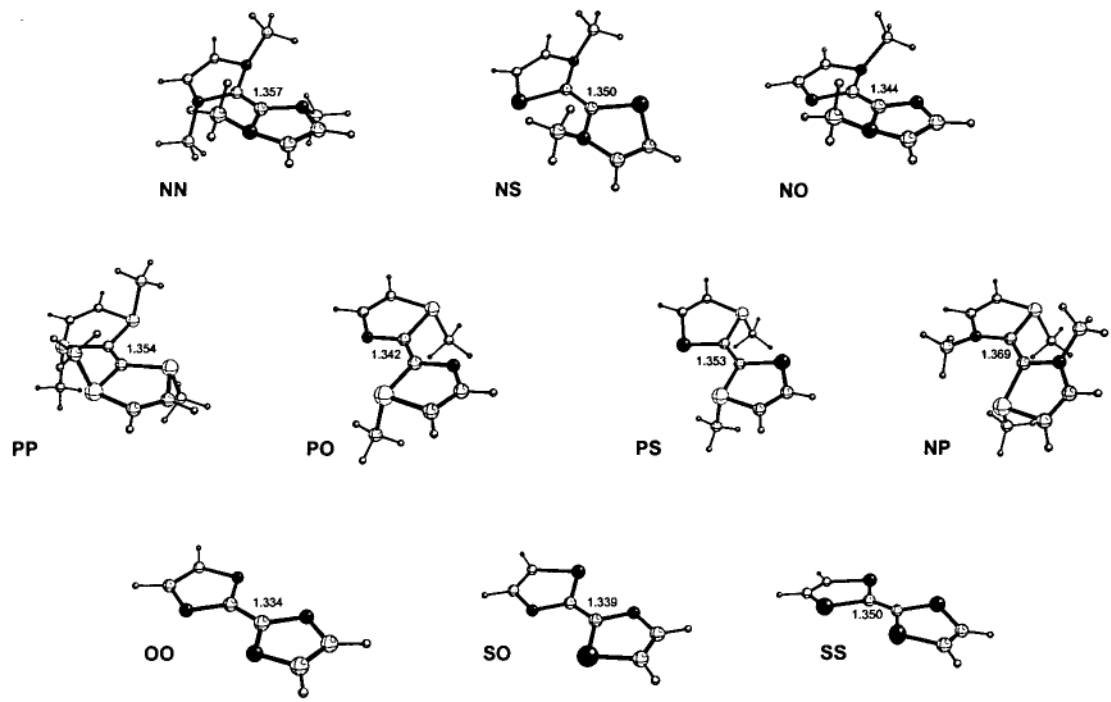
Figure 3.6 – Optimised dimer geometries (PRD-DD)
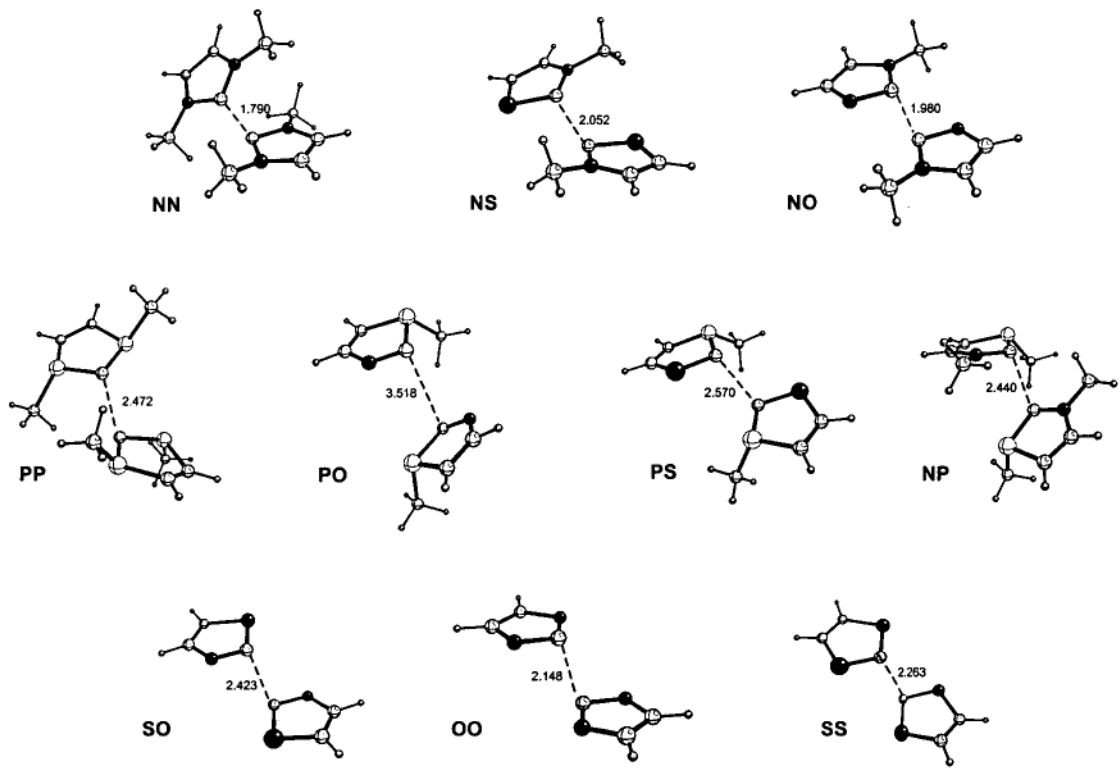
Figure 3.7 – Optimised transition structure geometries (TS-DD)

The transition state geometries (Figure 3.7) support the non-least motion pathway (Figure 3.8) approach of the two carbenes.[34] The repulsion of lone pairs implicit in the least motion (direct) approach is avoided in this method and is replaced by a bonding electrophilic-nucleophilic interaction.

The C-C bond lengths in the TS vary from 1.79-3.52 Å with **NN**, **NO** and **NS** exhibiting 'late' transition states. In accordance with Hammond's postulate,[21] these three
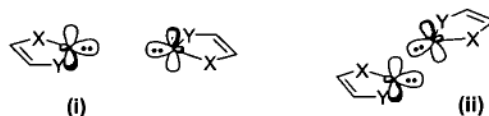
Figure 3.8 – Carbene approach methods
(i) least motion; (ii) non-least motion

carbenes also show the least exothermic reactions as well as high barriers to dimerisation (23.4, 12.2 and 15.0 kcal/mol, respectively). Despite this correlation, Hammond's postulate is not strictly adhered to across the series of carbenes investigated. This is not unexpected given that the steric bulk across the series of carbenes varies markedly as we move from the non-substituted (**OO**, **SO** and **SS**) to mono-substituted (**NS**, **NO**, **PS** and **PO**) and di-substituted (**PP**, **NP** and **NN**) carbenes. Large changes in the sterics of the carbene[6] along with significantly dissimilar transition states[35] have resulted in a non-conformity of Hammond's postulate in the past. Previous work[6,7] where ΔH and E_{act} *have* shown good correlation exhibit very little variation of the structures in the sample set. In fact, Cheng and Hu[6] only achieved good correlation with E_{act} after "outliers" that contained considerable bulk were excluded from the sample set. Lack of correlation between ΔH and E_{act} (Figure 3.9) in this case shows that the assumption of kinetic stability of carbenes (E_{act}) purely based on their thermodynamic stability to dimerisation (ΔH) is not always appropriate.

A case in point is dioxol-2-ylidene (**OO**), which shows excellent thermodynamic stability but only a small barrier to dimerisation (2.8 kcal/mol), presumably due to the lack of steric protection of the carbene carbon.
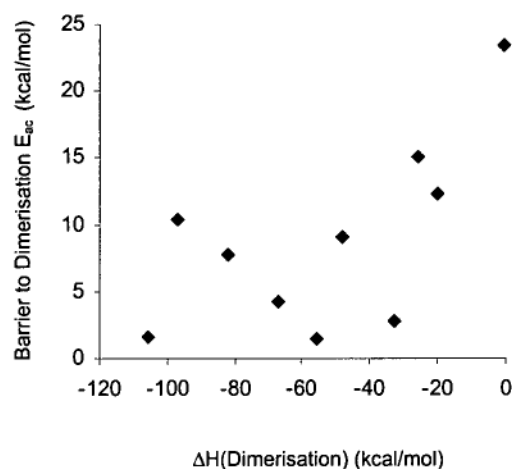
Figure 3.9 – Non-adherence to Hammond's postulate

Monitoring the change in the C-X and C-Y bond lengths can provide information about the aromaticity of the XY carbene (Table 3.3). Participation of the p_π orbital of the carbene carbon in the transition structure (as previously mentioned) breaks any aromaticity that the free carbene may have possessed. Elongation of the C–N bonds (0.026 Å) in the **NN** transition structure suggests that the aromaticity initially held by the **NN** carbene was appreciable and this is consistent with the fact that the thermodynamic cost of attaining the transition structure is high (23.4 kcal/mol).

Those carbenes that show little bond elongation (C-X and C-Y < 0.006 Å) (*i.e.* **OO**, **PO** and **SO)** are unlikely to possess significant aromaticity and therefore the

transition state barrier is more easily attained (E_{act} 2.8, 1.6 and 1.4 kcal/mol, respectively).

Table 3.3. Change in carbene-heteroatom bond lengths[a]

carbene	transition structure		product (dimer)	
	ΔL^a (Å)		ΔL^a (Å)	
	C-X	C-Y	C-X	C-Y
NN	0.026	0.026	0.060	0.060
NO	0.015	0.010	0.064	0.029
NP	0.009	0.011	0.082	0.053
NS	0.016	0.029	0.069	0.065
OO	0.006	0.006	0.039	0.039
PO	-0.006	-0.001	0.001	0.063
PP	0.029	0.029	0.151	0.151
PS	0.030	0.009	0.111	0.114
SO	0.006	0.001	0.022	0.048
SS	0.025	0.025	0.096	0.096

[a]The change in bond length relative to the corresponding free carbene geometry

Recent studies[6,7] comparing imidazol-2-ylidenes with the less aromatic imidazolin-2-ylidenes have supported the argument that high barriers to dimerisation are as a result of the aromatic character of the carbene. Additionally, this correlation may be influenced by the change in p_π occupation of the carbenic carbon as greater electron delocalisation is achieved from the neighbouring heteroatoms. Appreciable donation

from adjacent groups into the formally empty p_π orbital reduces the electrophilic nature

of the carbene, which is a critical component in the dimerisation pathway.[32,36]

In summary, while ΔH(dimerisation) can be estimated reasonably well based on

the properties of the carbene itself (eg ΔE_{s-t}), the E_{act}(dimerisation) appears to be a

function of not only the aromatic nature but the steric protection provided by the

exocyclic groups, making estimation of this quantity via indirect methods more difficult.

3.3.2 Proton Catalysed Dimerisation

The alternate dimerisation pathway proposed by Metzger[11] (Scheme 3.2 **(ii)**)

contains an intermediate that can be formed through C-H insertion (Scheme 3.2 **(iia)**) or

via nucleophilic attack on the carbene carbon (Scheme 3.2 **(iib)**)[16]. Despite rigorous

searching of the potential energy surface, no transition structures for the insertion

mechanism could be located. Although insertion of heterocyclic carbenes in to acidic C–

H bonds is commonly observed,[37] the strongly basic nature of the carbene[38] means that

formation of the intermediate through C-H insertion is unlikely. The conclusion that the

intermediate is formed via addition rather than insertion has been reinforced by

experimental evidence for thiazol-2-ylidenes and is generally accepted.[16]

Problems associated with the chirality of phosphorus would greatly complicate

the potential energy surfaces for these carbenes. In addition, experimentally the

phosphorous containing heterocycles exhibit thermodynamic and kinetic instability. For

these reasons the alternate dimerisation pathway for phosphorus based carbenes was

omitted.

The energies of the structures for the proton-catalysed dimerisation (PCD) pathway are presented in Table 3.4 and are represented graphically in Figure 3.10.

Table 3.4. Relative energies for pathway **(iib)**[a] (Proton Catalysed Dimerisation) (Scheme 3.2)

carbene	reactants	carbene plus salt	precursor complex (PC-PCD)	ts (rel)[b] (TS-PCD)	Intermediate (INT-PCD)	Dimer (PRD)
NN	0	-259.5	-275.4	-259.4 (15.9)	-271.2	-0.7
NO	0	-243.7	-260.0	-258.2 (1.8)	-266.9	-19.8
NS	0	-248.8	-265.1	-256.0 (9.1)	-272.9	-25.7
OO	0	-220.9	-	- (-)	-253.6	-32.5
SO	0	-233.1	-251.2	-248.8 (2.4)	-274.9	-55.4
SS	0	-234.9	-250.5	-245.0 (5.5)	-266.7	-48.3

[a]Energies are in kcal/mol and are referenced to the reactants; [b]Energy of transition structure relative to precursor complex

The initial step involves the protonation of one carbene to form an -olium salt. Given the strongly basic nature of heterocyclic carbenes, this proceeds with a large enthalpy of reaction ($\Delta H < -220$ kcal/mol). The next stage of the reaction involves nucleophilic attack of the carbene on the p_π orbital of its conjugate acid, resulting in an intermediate formally described by Jordan and Chen.[16]
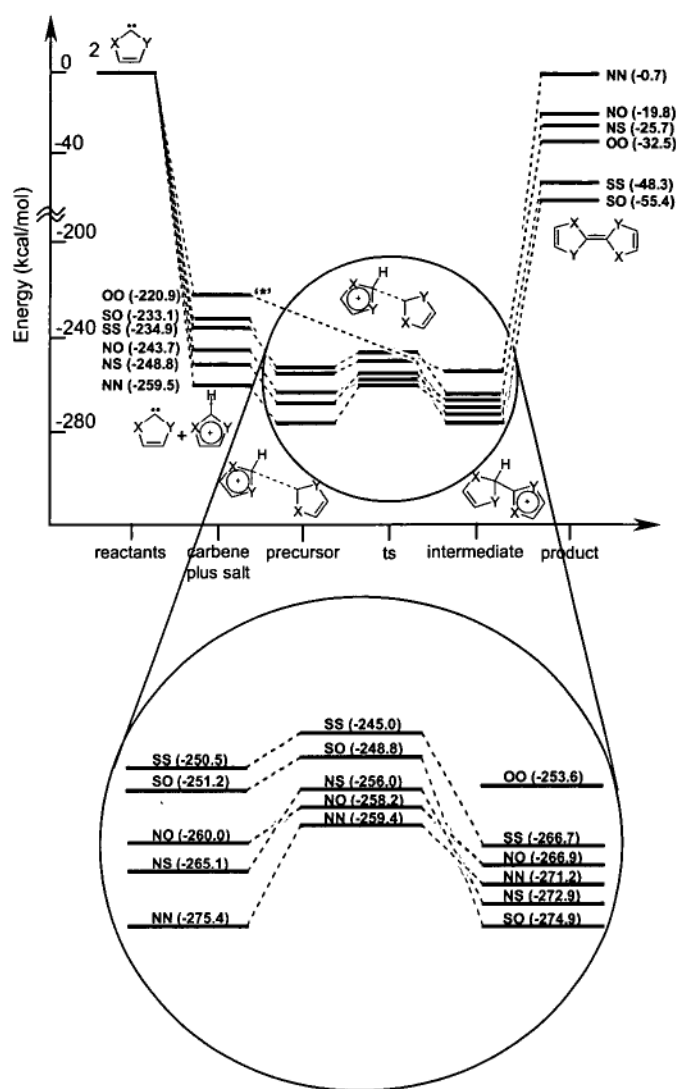
Figure 3.10. Graphical representation of decomposition energies on pathway **(iib)**
*No transition structure was found for the **OO** pathway (refer to text)

The geometries of the transition structures and intermediates are collectively shown in Figure 3.11, together with selected bond lengths in Table 3.5. The transition structures are similar and are what might be expected from the attack of the carbene lone pair on the p_π orbital of the C(2) carbon of the salt (Scheme 3.5).

Scheme 3.5 – Carbene approach on corresponding salt showing the change from sp^2 to sp^3 hybridisation of the azolium C(2)

Table 3.5. Selected bond lengths for optimised structures on pathway (iib)[a]

carbene	C-C$_{pc}$	C-C$_{ts}$	C-C$_{int}$
NN	3.176	1.941	1.513
NO	2.646	2.153	1.543
NS	3.166	2.225	1.509
OO	-	-	1.572
SO	3.062	2.940	1.502
SS	3.087	2.562	1.519

[a]All bond lengths are in Ångstrøms (Å)
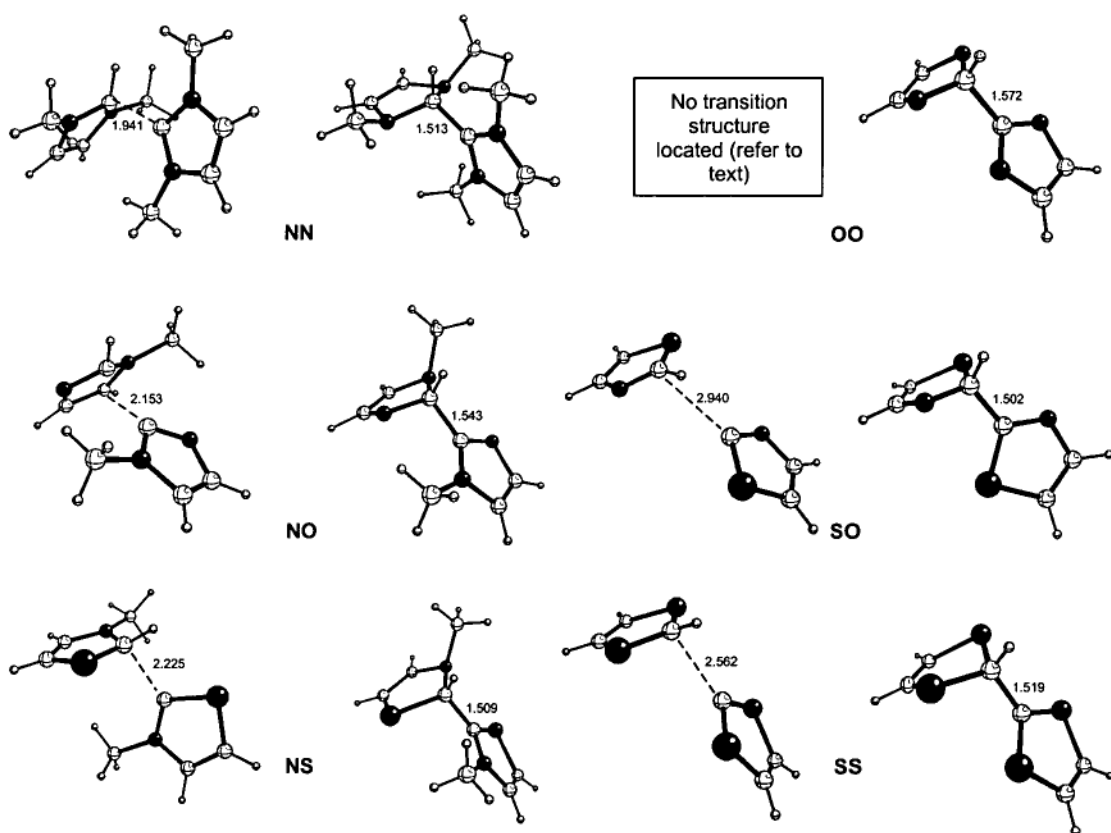
Figure 3.11. Transition structure (left) **(TS-PCD)** and intermediate geometries (right) **(INT-PCD)** on pathway **(iib)** (proton catalysed dimerisation)

The intermediates (Figure 3.11) clearly show the C(2) carbon is sp^3 hybridised as a result of this attack and salt's nitrogen atoms in the intermediate adopt a non-planar configuration.

All the carbenes show a thermodynamic tendency to form the intermediate from the carbene and salt. No transition structure for **OO** was found and a potential energy scan from the reactants to the intermediate showed no barrier.

Based on the C-C bond lengths in the transition structures the **NN** transition structure is late in comparison to the others and shows the greatest barrier to forming the intermediate (15.9 kcal/mol) and the lowest enthalpy (-11.7 kcal/mol when referenced to 'carbene + salt'). Only **NN** and **NS** (9.1 kcal/mol) show a significant barrier to decomposition via this method.

The considerable stability possessed by the intermediates (see Figure 3.10, Table 3.4) means that they require the action of a strong base in order to abstract the final proton to form the dimer. Any carbene present can act as the base (Scheme 3.4), making the requirement of an external base unnecessary.
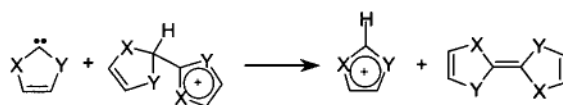
Scheme 3.4 – Deprotonation of intermediate
by its corresponding carbene

Table 3.6. Enthalpy of proton abstraction from intermediate
relative to proton affinity of the carbene[a] (Scheme 3.4)

carbene	$\Delta H_{abstraction}$
NN	10.9
NO	3.3
NS	-1.6
OO	0.1
SO	-13.6
SS	-16.5

[a]All Energy values are in kcal/mol

The enthalpy of proton abstraction by a free carbene is shown in Table 3.6. As well as being related to the strength of the C–H bond in the intermediate, this energy is also dependent on the proton affinity of the corresponding carbene (see Chapter 2). It demonstrates clearly that the **SO** and **SS** intermediates coupled with their analogous carbenes have a thermodynamic driving force which prefers the dimer ($\Delta H = -13.6$ and -16.5 kcal/mol respectively). Final proton abstraction in the **NN** carbene case is unlikely ($\Delta H = 10.9$ kcal/mol) and the significant barrier required to initially attain the dimer (15.9 kcal/mol) would be likely to prevent the intermediate from being formed. Both these factors reinforce to make formation of the neutral **NN** dimer unlikely.

3.3.3 Comparison of Pathways

The carbenes that show considerable kinetic stability to dimerisation via the self-condensation pathway (*i.e.* **NN**, **NS** and **NO**) all exhibit lower activation in the presence of a proton (Table 3.6).

Table 3.6. Comparison of activation energies for both pathways[a]

carbene	$E_{ac}(1)$[b]	$E_{ac}(2)$[c]	$\Delta H_{dimerisation}$
NN	23.4	15.9	-0.7
NO	12.2	1.8	-19.8
NP	4.2	-	-67.0
NS	15.0	9.1	-25.7
OO	2.8	0.0[d]	-32.5
PO	1.6	-	-105.8
PP	10.4	-	-97.0
PS	7.7	-	-82.4
SO	1.4	2.4	-55.4
SS	9.0	5.5	-48.3

[a]All energy values are in kcal/mol; [b]Free carbene dimerisation activation energy (Pathway **(i)**); [c]Proton induced carbene dimerisation (Pathway **(iib)**); [d]No barrier could be found for this dimerisation reaction (see text)

In the presence of a proton catalyst, the activation energy for dimerisation of the **NN** carbene is reduced from 23.4 to 15.9 kcal/mol. These values suggest that **NN** carbenes are kinetically and thermodynamically stable to both dimerisation mechanisms. Experimental observations confirm this postulate. One observer reported the formation of a carbene-H-carbene adduct in the presence of hydrogen ions,[39] however there are no recorded observations of dimer formation.

The presence of protons lowers the activation energy of **NS** dimerisation by 5.9 kcal/mol to 9.1 kcal/mol. It is possible, then, that otherwise stable **NS** carbenes may form dimers in the presence of protons. Indeed, this phenomenon has been demonstrated experimentally by Arduengo (Scheme 3.6).[3]
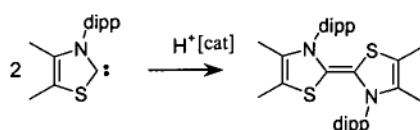
Scheme 3.6. Arduengo's proton catalysed dimerisation[3]

It is not surprising that heterocyclic **NO** carbenes are yet to be observed given the low barrier to dimerisation (12.2 kcal/mol), in particular proton-catalysed dimerisation (1.8 kcal/mol), calculated herein. Additionally, **SS**, **SO** and **OO** carbenes all exhibit a lack of kinetic stability with respect to both dimerisation mechanisms and have an increased thermodynamic driving force for dimerisation.

Steric protection of the carbene centre via the introduction of large exocyclic substituents at nitrogen may increase the kinetic stability of a nitrogen containing heterocycle. This approach has allowed the successful isolation of a number of carbenes that may otherwise have dimerised.[3,4,8] It is unlikely that we will ever observe **SS**, **SO** and **OO** heterocyclic carbenes due to the inherent lack of kinetic and thermodynamic stability unless elaborate steric protection for the carbene carbon is incorporated at the 4 and 5 positions of the ring.

3.4 Conclusions

The dimerisation pathways for X,Y heterocyclic carbenes have been investigated using density functional theory. Imidazole-based (**NN**) carbenes show thermodynamic stability and a kinetic barrier to dimerisation in both of the pathways investigated. Thiazole-based (**NS**) carbenes show stability in aprotic conditions but dimerisation becomes more likely in the presence of hydrogen ions. Phosphorus-containing carbenes are predicted to have low barriers to dimerisation and have an increased thermodynamic tendency to form the dimer product. Those carbenes that lack exocyclic ring substituents (**SO**, **OO** and **SS**) show low barriers to dimerisation via both pathways, with **OO** showing no barrier to proton catalysed dimerisation.

Proton catalysed dimerisation is predicted to go through an addition rather than insertion mechanism, in agreement with previous investigations.[16]

Proposed methods for indirectly predicting the dimerisation enthalpy extend well across the series of heterocyclic carbenes studied here. Caution must be exercised however, when suggesting the kinetic stability of the carbene to dimerisation can be assessed using indirect methods such as isodesmic reaction schemes and aromaticity. Due to steric differences in the range of carbenes considered, the Hammond postulate is not strictly adhered to and as a consequence, the barrier to dimerisation cannot be adequately estimated.

As dimerisation is more facile in the presence of protons, it may be beneficial to isolate less stable free carbenes in aprotic media through routes that do not require the presence of protons or protonated salts. The isolation pathway devised by Kuhn[40] (see Chapter 1) may provide a safer route to as-yet unisolable free carbenes.

3.5 References

(1)   Wanzlick, H.-W., Schikora, E., *Chem. Ber.* **1961**, *94*, 2389.

(2)   Arduengo, A. J., Harlow, R. L., Kline, M., *J. Am. Chem. Soc.* **1991**, *113*, 361.

(3)   Arduengo, A. J., Goerlich, J. R., Marshall, W. J., *Liebigs Ann.-Recl.* **1997**, 365.

(4)   Alder, R. W., Butts, C. P., Orpen, A. G., *J. Am. Chem. Soc.* **1998**, *120*, 11526.

(5)   Merceron, N., Miqueu, K., Baceiredo, A., Bertrand, G., *J. Am. Chem. Soc.* **2002**, *124*, 6807.

(6)   Cheng, M. J., Hu, C. H., *Chem. Phys. Lett.* **2001**, *349*, 477.

(7)   Cheng, M. J., Hu, C. H., *Chem. Phys. Lett.* **2000**, *322*, 83.

(8)   Denk, M. K., Thadani, A., Hatano, K., Lough, A. J., *Angew. Chem., Int. Ed. Engl.* **1997**, *36*, 2607.

(9)   Heinemann, C., Thiel, W., *Chem. Phys. Lett.* **1994**, *217*, 11.

(10)   Su, M. D., Chu, S. Y., *Inorg. Chem.* **1999**, *38*, 4819.

(11)   Metzger, J., Larive, H., Dennilauler, R., Baralle, R., Gaurat, C., *Bull. Soc. Chim.* **1964**, 2857.

(12)   Castells, J., LopezCalahorra, F., Geijo, F., Perez-Dolz, R., Bassedas, M., *J. Heterocycl. Chem.* **1986**, *23*, 715.

(13)   Chen, Y. T., Barletta, G. L., Haghjoo, K., Cheng, J. T., Jordan, F., *J. Org. Chem.* **1994**, *59*, 7714.

(14)   Bordwell, F. G., Satish, A. V., *J. Am. Chem. Soc.* **1991**, *113*, 985.

(15)   Castells, J., Domingo, L., Lopezcalahorra, F., Marti, J., *Tetrahedron Lett.* **1993**, *34*, 517.

(16)   Chen, Y. T., Jordan, F., *J. Org. Chem.* **1991**, *56*, 5029.

(17)   LopezCalahorra, F., Castro, E., Ochoa, A., Marti, J., *Tetrahedron Lett.* **1996**, *37*, 5019.

(18)   Alder, R. W., Blake, M. E., *Chem. Commun.* **1997**, 1513.

(19)   Nyulaszi, L., Veszpremi, T., Forro, A., *PCCP Phys. Chem. Chem. Phys.* **2000**, *2*, 3127.

(20)   Carter, E. A., Goddard, W. A., III, *J. Phys. Chem.* **1986**, *90*, 998.

(21)   Hammond, G. S., *J. Am. Chem. Soc.* **1955**, *77*, 334.

(22)   Alder, R. W., Blake, M. E., Oliva, J. M., *J. Phys. Chem. A* **1999**, *103*, 11200.

(23)   Oliva, J. M., *Chem. Phys. Lett.* **1999**, *302*, 35.

(24)   Becke, A. D., *J. Chem. Phys.* **1993**, *98*, 5648.

(25)   Becke, A. D., *Phys. Rev. A.* **1988**, *38*, 3098.

(26)   Lee, C., Yang, W., Parr, R. G., *Phys. Rev. B.* **1988**, *37*, 785.

(27)   Hariharan, P. C., Pople, J. A., *Theor. Chim. Acta* **1973**, *28*, 213.

(28)   Krishnan, R., Binkley, J. S., Seeger, R., Pople, J. A., *J. Chem. Phys.* **1980**, *72*, 650.

(29)   McLean, A. D., Chandler, G. S., *J. Chem. Phys.* **1980**, *72*, 5639.

(30)   Frisch, M. J., Pople, J. A., Binkley, J. S., *J. Chem. Phys.* **1984**, *80*, 3265.

(31)   Gaussian 98, Revision A.7, Frisch, M. J., Trucks, G. W., Schlegel, H. B., Scuseria, G. E., Robb, M. A., Cheeseman, J. R., Zakrzewski, V. G., Montgomery, J. A., Jr., Stratmann, R. E., Burant, J. C., Dapprich, S., Millam, J. M., Daniels, A. D., Kudin, K. N., Strain, M. C., Farkas, O., Tomasi, J., Barone, V., Cossi, M., Cammi, R., Mennucci, B., Pomelli, C., Adamo, C., Clifford, S., Ochterski, J., Petersson, G. A., Ayala, P. Y., Cui, Q., Morokuma, K., Malick, D. K., Rabuck, A. D., Raghavachari, K., Foresman, J. B., Cioslowski, J., Ortiz, J. V., Baboul, A. G., Stefanov, B. B., Liu, G., Liashenko, A., Piskorz, P., Komaromi, I., Gomperts, R., Martin, R. L., Fox, D. J., Keith, T., Al-Laham, M. A., Peng, C. Y., Nanayakkara, A., Gonzalez, C., Challacombe, M., Gill, P. M. W., Johnson, B., Chen, W., Wong, M. W., Andres, J. L., Gonzalez, C., Head-Gordon, M., Replogle, E. S., Pople, J. A., Gaussian Inc, Pittsburgh, PA, 1998

(32)   Bourissou, D., Guerret, O., Gabbai, F. P., Bertrand, G., *Chem. Rev.* **2000**, *100*, 39.

(33)   Fekete, A., Nyulaszi, L., *J. Organomet. Chem.* **2002**, *643-644*, 278.

(34)   Hoffmann, R., Gleiter, R., Mallory, F. B., *J. Am. Chem. Soc.* **1970**, *92*, 1460.

(35)   Jursic, B. S., *J. Chem. Soc., Perkin Trans. 2* **1999**, 1805.

(36)   Arduengo, A. J., Dias, H. V. R., Dixon, D. A., Harlow, R. L., Klooster, W. T., Koetzle, T. F., *J. Am. Chem. Soc.* **1994**, *116*, 6812.

(37)   Arduengo, A. J., Calabrese, J. C., Davidson, F., Dias, H. V. R., Goerlich, J. R., Krafczyk, R., Marshall, W. J., Tamm, M., Schmutzler, R., *Helv. Chim. Acta* **1999**, *82*, 2348.

(38)   Herrmann, W. A., Kocher, C., *Angew. Chem., Int. Ed. Engl.* **1997**, *36*, 2163.

(39)   Arduengo, A. J., Gamper, S. F., Tamm, M., Calabrese, J. C., Davidson, F., Craig, H. A., *J. Am. Chem. Soc.* **1995**, *117*, 572.

(40)   Kuhn, N., Kratz, T., *Synthesis* **1993**, 561.

• Chapter Four •

Synthesis and Catalytic Applications of Palladium Thiazol-2-ylidene Complexes

4.1 Introduction

Although preliminary catalytic testing with NHC complexes of ruthenium was undertaken by Lappert and others in the 1970s and 80s,[1-3] Herrmann established the general catalytic importance of complexes bearing *N*-heterocyclic ligands during the 1990s.[4] Despite the increased attention stemming from Herrmann's bis-carbene catalyst (Figure 4.1 **A**), little research focused on the diversification of the original imidazole template to other potential heterocyclic carbene complexes.

A   B   C   D   E
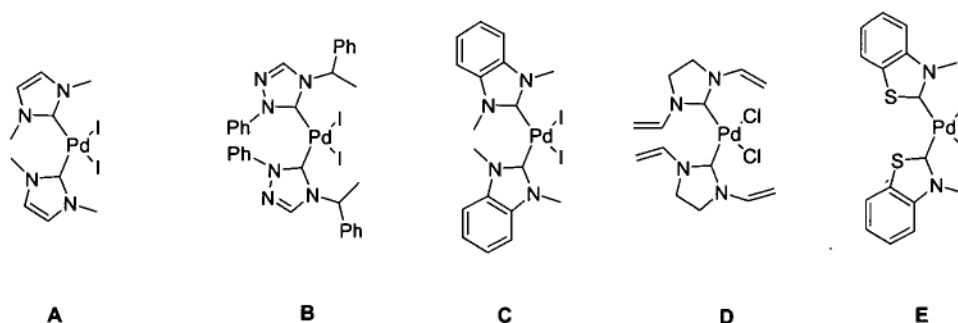
Figure 4.1 – Heterocycle diversity in palladium carbene complexes

In the period following Herrmann's discovery, Enders *et. al*[5] succeeded in the isolation of a free carbene based on the triazolinylidene heterocycle. The same group, at a later date, also synthesized the corresponding palladium diiodide complex[6] (Figure 4.1 **B**). Extensions to the heterocyclic carbene family have also been afforded through

alterations to the carbon-carbon backbone of imidazole. This resulted in complexes based on both the benzimidazole[7] and imidazoline[8] ring systems (Figure 4.1 **C** and **D**).

It was 1997 before a free carbene was characterized that diverged from the nitrogen donors common to all previously isolated carbenes. Arduengo's stable thiazol-2-ylidene[9] (Figure 4.2) was based on a thiazole template and benefited from the push-pull donation capacities of nitrogen as well as sulfur atoms (see Chapter 2). In the following five years, no novel palladium complexes bearing ligands based on the thiazole heterocycle have been synthesized or tested for catalytic activity.
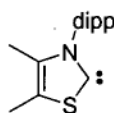
Figure 4.2 – Arduengo's stable
thiazol-2-ylidene

A variation on the thiazol-2-ylidene ligand, benzothiazol-2-ylidene, has been successfully incorporated into a palladium complex[10] (Figure 4.1 **E**) and has shown catalytic activity.[10-15] Despite this, no effort has been made to extend and optimise this range of complexes by varying substitution at nitrogen.

Palladium complexes bearing thiazol-2-ylidene ligands are known, but little is known about their properties and a general synthetic route has been largely unexplored.

Work performed by Fraser and Stone[16] in 1974 resulted in two complexes formed via oxidative addition of a 2-chlorothiazolium salt to a suitable palladium zero complex (Scheme 4.1). Further to this, in 1987 Fehlhammer[17] reacted carbon disulfide with an

isocyanide ligand resulting in a tungsten carbene complex that was used as a transfer

agent to produce the resulting palladium complex (Scheme 4.2).
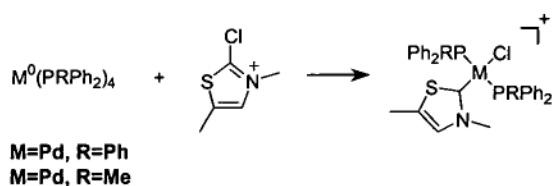
Scheme 4.1 – Synthesis of palladium thiazol-2-ylidene complexes – 1

Scheme 4.2 – Synthesis of palladium thiazol-2-ylidene complexes - 2

Thiazole-based carbene complexes of other transition metals are more abundant in

the literature. A considerable amount of work by Raubenheimer with lithiated thiazoles

has resulted in complexes with Mo, W, Cr,[18] Au[19,20] and Cu[21] metal centres.

Azolium salts are the most versatile precursors in the main synthetic routes
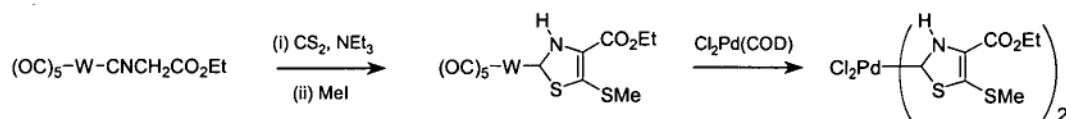
utilised to generate palladium carbene complexes. Conveniently, the role of thiazolium

salts in benzoin condensation[22-24] as well as their similarity to vitamin B$_1$[25] have resulted

in a plethora of research focusing on their synthesis.[26]

The high potential of NHCs as ligands in catalytic systems has been realised in

recent years with their application in carbon-carbon coupling,[27-29] telomerisation,[30,31]

olefin metathesis[32,33] and copolymerisation.[34] Despite this, the catalytic activity of

palladium complexes bearing other NHCs such as thiazol-2-ylidenes has been largely

unexplored. The complexes prepared by Stone and Fraser in 1974[16] (Scheme 4.1) have only recently been patented, suggesting that they may be suitable for catalysis.

Although not strictly a thiazol-2-ylidene ligand, the complex prepared by Calo bearing benzothiazole-based ligands (Figure 4.1 **E**) has been the subject of a variety of catalytic testing.[10-15] The turnover numbers (TONs) shown by **E** in the Heck reaction reached up to 93,000 when formic acid was used as a reducing agent.[10] Through substitution of standard organic solvents by the ionic liquid tetrabutylammonium bromide (TBAB), the performance of **E** in the Heck reaction gave 95% yield after 1 hour for the coupling of activated arylchlorides.[15] Further research on **E** showed Heck coupling of substituted reactants as well as catalytic carbonylation.[11-14]

This chapter deals with the synthesis and characterization of a number of palladium-based thiazol-2-ylidene complexes along with their catalytic behaviour in both the Heck and Suzuki carbon-carbon coupling reactions. The isolation of Arduengo's thiazol-2-ylidene in 1997 provided much of the impetus for this research.[9] The stability associated with the isolated carbene was akin to that found for a series of stable imidazol-2-ylidenes. Consequently it was envisioned that their ability to act as ligands for homogeneous catalysis may also be transferable, resulting in complexes that are catalytically active.

In the work described here, novel alkyl and aryl-substituted thiazolium salts were prepared via quaternisation and Hantzsch condensation, respectively. Their subsequent reaction with palladium acetate afforded six new palladium dihalide complexes bearing thiazol-2-ylidene ligands. The synthetic methods and characteristics of the resulting

compounds are discussed. These complexes are the first of their type in the ever-increasing field of palladium complexes bearing non-imidazole type heterocyclic carbene ligands. All the complexes surveyed are active to some degree in both the Heck and the Suzuki reactions. With concentrations of 0.01 mol% catalyst, conversions greater than 75% were achieved in the Heck reaction. In the first examples of catalytic Suzuki coupling using complexes bearing thiazol-2-ylidene ligands, conversions were similar to those obtained in the Heck reaction with no formation of side products.

4.2 Results and Discussion

4.2.1 Preparation of Thiazolium Salts

Thiazolium salts **3a-d** were prepared by reacting an alkyl halide with 4,5-dimethylthiazole according to Scheme 4.3.
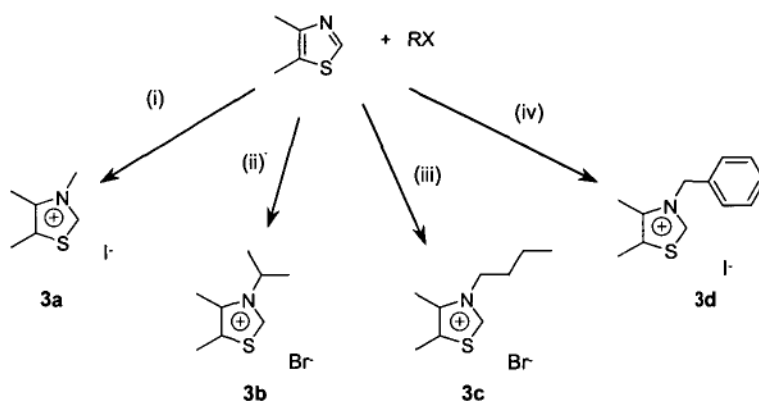
Scheme 4.3 – Synthesis of alkyl substituted thiazolium salts **3a-d**
(i) excess MeI, r.t. 24 h; (ii) ^{i}PrBr, acetone, 110°, overnight in bomb;
(iii) excess ^{n}BuBr, Δ, 48 h; (iv) BzI, acetone, Δ, 20 h

Simple quaternisation is unsuitable for aryl-substituted thiazolium salts (**3e-g**) due to the unreactive nature of aryl halides with respect to the heterocyclic ring nitrogen.[35] As a result of this, a number of other routes were investigated to generate *N*-aryl-substituted thiazolium salts.

Ultimately, *N*-aryl-substituted thiazolium salts were prepared via Hantzsch condensation[36] of the corresponding *N*-substituted thioformamide with 3-chloro-2-butanone, followed by halide exchange to produce the iodide salt (Scheme 4.4). *N*-

substituted thioformamides were prepared via established routes (Scheme 4.5) the full

details of which are given in the experimental section (Section **4.3**).
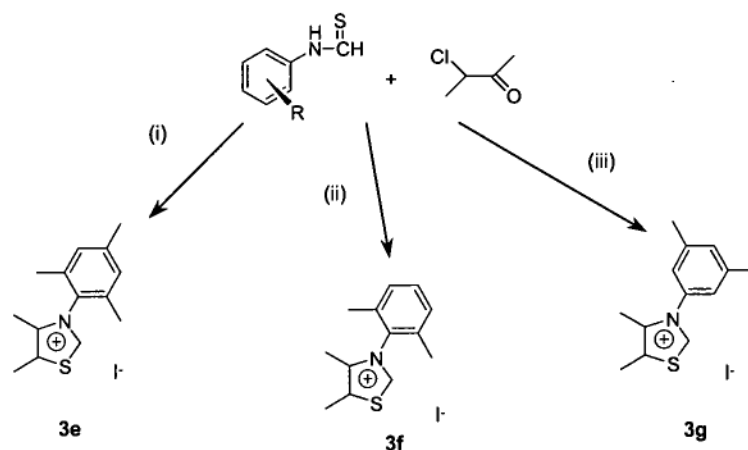
Scheme 4.4 – Synthesis of aryl substituted thiazolium salts **3e-g**
(i) 100°C for 2h; NaI/acetone; (ii) 100°C for 2h; NaI/acetone; (iii) 100°C for 2h; NaI/acetone
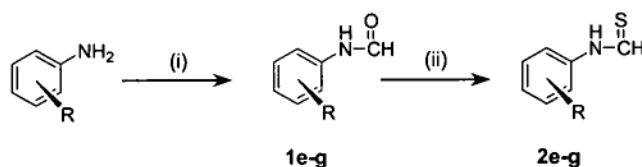
Scheme 4.5 – Synthesis of N-aryl thioformamides
(i) formic acid reflux; (ii) P$_2$S$_5$/NaHCO$_3$ in THF

The thiazolium salts bearing isopropyl, *n*-butyl, 2,6-dimethylphenyl and 3,5-

dimethylphenyl substituents at nitrogen are all novel compounds. A detailed synthetic

procedure for the preparation of Arduengo's[9] *N*-aryl-thiazolium salts is unavailable. The

patent referenced in the literature[37] refers to a general 'one-pot' synthetic procedure in

which no *N*-aryl substituted thioformamides are involved, and attempts to synthesise the

salts via these methods led to yields of less than 5%. Yields of 40 to 70%, which were

obtained for the synthetic method employed here represent a significant improvement on

the 'one-pot' method alluded to by Arduengo. An improved experimental procedure for the synthesis of Arduengo's thiazolium salt is provided in the experimental section.

4.2.2 Attempted Synthesis of 'Bulky' *N*-Alkyl Thiazolium Salts

It is clear from the work of Arduengo that steric bulk on the ring nitrogen is paramount for isolation of the free carbene.[9] The prepared thiazolium salts (**3e-g**) lack the steric bulk required for free carbene isolation, so attempts were made to synthesize salts with significantly more bulk on the exocyclic ring substituent with the aim of counteracting the dimerisation reaction preventing isolation (see previous chapters). Both *tertiary*-butyl and adamantyl groups were expected to have the appropriate bulk to allow isolation of the free carbene. Attempts to quaternise the ring nitrogen using the appropriate alkyl halides proved unsuccessful. The tertiary substitution at the alpha carbon coupled with the fact that thiazole is notoriously difficult to alkylate (60 times more difficult than 1-methylimidazole[38]), makes this result unsurprising. Consequently, the Hantzsch condensation method[36] was employed in an attempt to synthesize the required compounds (Scheme 4.6).
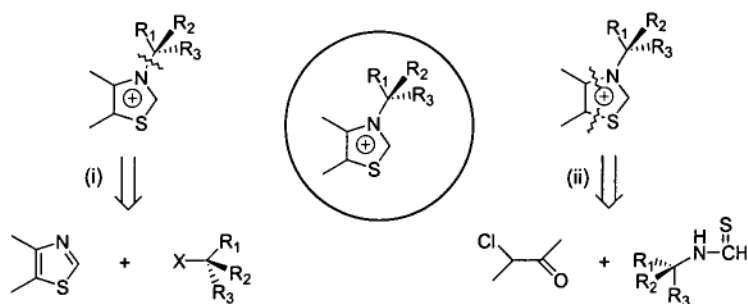
Scheme 4.6 – Retrosynthetic strategies for *N*-bulky thiazolium salts

Synthesis of the required *N-tertiary*-butyl and *N*-adamantyl thioformamides (**2h** and **2i**, respectively) was straightforward using the previously described route, though condensation with 3-chloro-2-butanone (or 3-bromo-2-butanone) afforded none of the required product. On analysis of the reaction mixture neither of the reactants were present and a significant amount of the original amine was observed as a decomposition product. The difficulty in condensation was thought to occur during the cyclisation step in which the increased steric bulk of the *N*-substituent may prevent the approach of the carbonyl group within close enough proximity to allow the reaction to take place (Scheme 4.7 step 3).
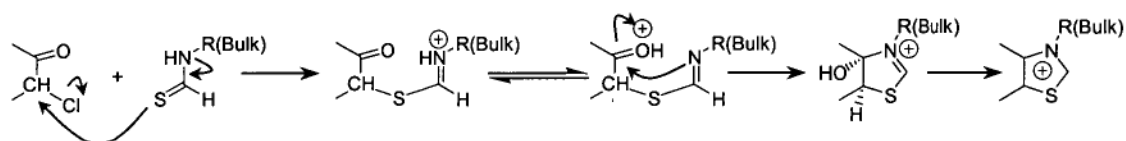
Scheme 4.7 – Mechanism for Hantzsch condensation[39]

4.2.3 Characterisation of Thiazolium Salts

The nature of the thiazolium salts is highly dependent on both the *N*-substituent and the corresponding halide counter-ion. The hydrophobic nature of the *n*-butyl group resulted in a thiazolium salt that was a sticky tar at room temperature and a liquid at higher temperatures. It is not surprising that a similarly substituted salt has been utilized as a green-solvent for catalysis,[40] a title bestowed on those compounds that are ionic liquids at low temperatures.[41] The *N*-aryl substituted thiazolium chlorides formed via Hantzsch condensation were extremely hygroscopic and formed tars from which solvents

were difficult to remove. Halide exchange resulted in a manageable iodide salt that was more easily purified.

The summarised ^{13}C NMR data is collected in Table 4.1. Shifts for the carbon atoms comprising the main backbone of the thiazolium ring system are essentially constant with the only discernable change being the downfield shift of the C(2) carbon for those salts with *N*-aryl substituents (δ 158.5-159.8) compared to those bearing *N*-alkyl substituents (δ 155.9-157.0).

Table 4.1 – Chemical shifts of thiazolium salts (3a-g)[a]

thiazolium	C$_2$ (δ)	C$_4$ (δ)	C$_5$ (δ)	C$_4$-CH$_3$ (δ)	C$_5$-CH$_3$ (δ)
3a[b]	155.9	142.5	132.6	12.4	11.5
3b[c]	156.4	141.6	133.9	13.4	12.8
3c[c]	157.0	141.8	133.7	13.4	12.5
3d[c]	156.7	142.8	132.1	13.6	13.1
3e[c]	159.8	142.6	133.1	14.3	12.4
3f[c]	159.7	142.3	132.3	14.4	12.4
3g[c]	158.5	142.9	134.5	14.0	13.5

[a]Shifts are quoted in ppm, relative to TMS; [b]DMSO-d$_6$; [c]CDCl$_3$

4.2.4 Complexation Methods

The inherent instability of thiazole-based free carbenes led to a search for alternative methods for complexation to palladium. With the established route involving the displacement of COD (e.g. in PdCl$_2$(COD)) by the free carbene[42,43] being unavailable,

the recent silver transfer route proposed by Wang and Ling[44] was investigated (Scheme 4.8).
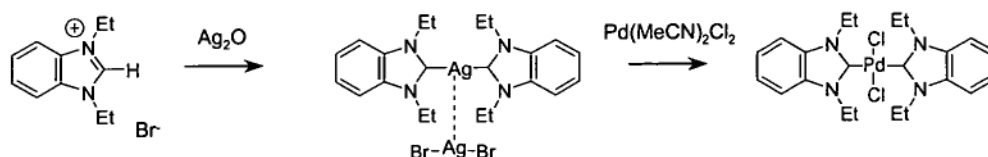
Scheme 4.8 – Palladium imidazole carbene complex synthesis via silver transfer

The researchers reported that the reaction of simple imidazolium salts with silver oxide or silver carbonate yielded Ag^I bis(carbene) complexes that could be used as transfer agents for palladium complexes. This route is now well established and is widely used for synthesis of palladium carbene complexes.[45,46]

Silver complexes of thiazol-2-ylidene ligands are not known and attempted coupling via this method yielded none of the desired product, with the high-field shifted C(2) proton of the thiazolium salt still evident via ^{1}H NMR. The inclusion of sulfur rather than substituted nitrogen in the ring may result in a silver-sulfur interaction that prevents formation of the desired complex. The sulfur lone pair additional to that involved in the aromatic system can facilitate this supplementary interaction. Imidazolium salts lack an additional lone pair and consequently no side-interaction with the metal centre is expected to take place. In fact, silver-benzothiazole complexes in which benzothiazole is bound to the metal centre via sulfur are known[47] (Figure 4.3), and therefore the incompatibility of this pathway with thiazole based reagents was not surprising.
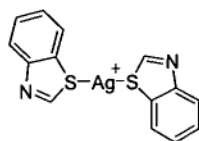
Figure 4.3 – A literature example[47] of sulfur interaction with a silver metal centre

4.2.5 Generation of Palladium Complexes

Reaction of thiazolium salts **3a-f** with palladium acetate in THF afforded the corresponding complexes **4a-f** in good yields (Scheme 4.9).
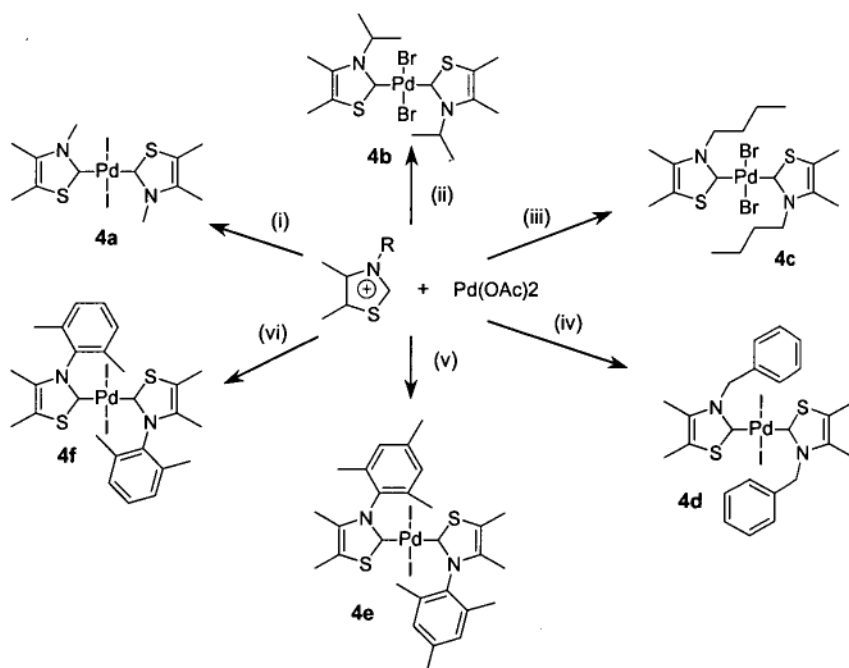
Scheme 4.9 – Synthesis of complexes **4a-f** via palladium acetate coupling
(i) **3a**, 2 days at r.t. in THF; (ii) **3b**, 2 days at r.t. in THF; (iii) **3c**, 3 days at r.t. in THF;
(iv) **3d**, 2 days at r.t. in THF; (v) **3e**, 1 day reflux, 2 days stirring at r.t. in THF;
(vi) **3f**, 1 day reflux, 2 days stirring at r.t. in THF

In general, 2.1 equivalents of the thiazolium salt were reacted with 1 equivalent of palladium acetate in THF for up to 3 days at temperatures between room temperature and reflux, followed by removal of the THF *in vacuo* and extraction of excess salt with methanol. Yields were typically good (40-70%), with the resultant complexes characterized via elemental analysis, mass spectrometry (LSIMS) and nuclear magnetic resonance (NMR) spectroscopy. Even though the reaction with **3g** appeared to proceed smoothly, an analytically pure sample of the complex could not be obtained.

4.2.6 Complex Characteristics

All complexes exhibited limited solubility in most common organic solvents. Consequently, this meant that crystals suitable for x-ray analysis could not be grown and obtaining ^{13}C NMR data was problematic. Complexes **4d** and **4f** were particularly insoluble, even in DMSO at temperatures up to 100°C.

Complex **4a**, containing thiazolium ligands with *N*-methyl substituents, exhibited isomerism observed via ^{1}H NMR, showing a 2:1 ratio of isomers. After 2 hours of heating at 65°C in DMSO-d$_6$, the major isomer initially observed had been converted to a more stable form. Given the asymmetric nature of the carbene ligand, four separate isomers can be envisaged (Figure 4.4).

*trans-anti-*4a   *trans-syn-*4a   *cis-anti-*4a   *cis-syn-*4a
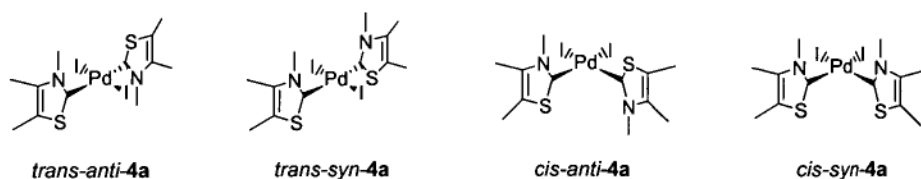
Figure 4.4 – Possible isomers for complex **4a**

Cis-trans isomerism has been observed by Calo[10] and Herrmann[4] for *N*-methylbenzothiazol-2-ylidene and *N*-methylimidazol-2-ylidene palladium diiodide complexes, respectively. Deducing the exact nature of the isomerism via NMR is hampered by the fast conversion of the less stable to the more stable isomer. The conversion is complete after 30 minutes in DMSO-d_6 at 65°C, which is insufficient time to resolve the C(2) shift of the initial isomer via ^{13}C NMR. Given the similarities between **4a** and those complexes observed as having *cis-trans* isomerism it is likely that the same case is observed here, although the existence of rotamers can not be ruled out. As the limited solubility of **4a** has resulted in the inability to grow crystals for x-ray analysis, the exact nature of the complex remains elusive. On moving to larger *N*-substituents, no isomerism was observed and literature trends would suggest that the complexes are purely the *trans-anti* form.[6,10,48]

^{13}C NMR data for the complexes is collected in Table 4.2. The observed shift of the C(2) carbon (δ 190-200 ppm) is downfield somewhat compared to the observed shifts of palladium imidazol-2-ylidene complexes (δ 165-185 ppm). This is not entirely unexpected as the C(2) shift for the thiazole-based free carbenes (δ 251-255 ppm)[9] are considerably more downfield than their imidazole-based counterparts (δ 210-230 ppm).[49]

All of the complexes exhibit appreciable tolerance to both high temperature and oxygen. Heating a solution of complex **4a** in DMSO-d_6 to temperatures in excess of 120°C for 4 hours in air resulted in no evidence of decomposition via NMR.

Table 4.2 – Chemical shifts of palladium complexes (4a-f)[a]

complex	C_2 (δ)	C_4 (δ)	C_5 (δ)	C_4-CH_3 (δ)	C_5-CH_3 (δ)
4a[b,d]	195.2	140.4	131.7	11.4	11.0
4b[b]	195.7	140.0	133.6	12.5	11.3
4c[b]	196.6	139.4	130.8	10.4	10.2
4d[e]	-	-	-	-	-
4e[c]	196.8	140.3	133.2	12.5	11.7
4f[e]	-	-	-	-	-

[a]All values are in ppm relative to TMS; [b]DMSO-d_6; [c]CDCl$_3$; [d]Most stable isomer (see text);[e]Too insoluble (see text)

4.2.7 Heck Coupling

Palladium complexes **4a-f** were used as pre-catalysts for the coupling of 4-bromoacetophenone with *n*-butyl acrylate to form *n*-butyl (*E*)-4-acetylcinnamate (Scheme 4.10). Results are collected in Tables 4.3 and 4.4.
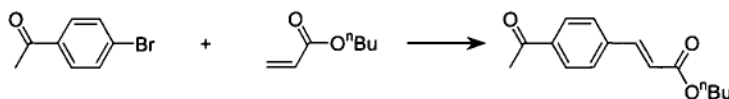
Scheme 4.10 - Heck coupling

Table 4.3 – Heck reaction catalysis results[a]

run	catalyst	conversion (%)	TON
H1	4a	41	410
H2	4b	45	450
H3	4c	21	210
H4	4d	43	430
H5	4e	36	360
H6	4f	16	160

[a]Conditions : 1.0×10^{-1} mol% catalyst; 8.0 mmol NaOAc; DMA for 20hrs @ 120°C (see experimental details at the end of chapter)

Table 4.4 – Heck reaction catalysis results 2[a]

Run	Catalyst	Amount (mol%)	Base	Additives[c]	Conversion (%)	TON
H7	4a	1.0×10^{-1}	NaOAc	TBAB	88	880
H8	4b	1.0×10^{-1}	NaOAc	TBAB	70	700
H9	4d	1.0×10^{-1}	NaOAc	TBAB	69	690
H10	4a	1.0×10^{-1}	NaOOCH	-	12	120[d]
H11	4a	1.0×10^{-1}	NaOOCH	TBAB	76	760[d]
H12	4a	1.0×10^{-1}	NaHCO$_3$	-	54	540
H13	4b[b]	1.0×10^{-2}	NaOAc	TBAB	50	5000
H14	4b[b]	1.0×10^{-2}	NaOOCH	TBAB	83	8300
H15	4a[b]	1.0×10^{-2}	NaOAc	TBAB	44	4400
H16	4a[b]	1.0×10^{-2}	NaOOCH	TBAB	74	7400
H17	4a[b]	1.0×10^{-2}	NaOAc	HZ	0	0
H18	4b[b]	1.0×10^{-2}	NaOAc	HZ	0	0

[a]Conditions : In DMA for 20hrs/[b]30hrs @ 120°C (see experimental details at the end of chapter); [c]TBAB = 2mmol of tetrabutylammonium bromide added to run; HZ = 50 μL of hydrazine hydrate added to run; [d]Palladium black observed

Using 0.1 mol% of pre-catalyst and sodium acetate as the base (Runs H1-H6), the conversion was moderate, with none of the catalysts providing conversions exceeding 50%. Pre-catalysts **4a**, **4b** and **4d** all gave conversions of between 40 and 50% corresponding to TONs of 410, 450 and 430 respectively.

The effect of altering the base in the Heck reaction, as well as the addition of reducing agents and promoters, is illustrated in Table 4.4 (Runs H7-H18).

The benefits of adding an ammonium salt such as tetrabutylammonium bromide (TBAB) to the reaction mixture has been demonstrated previously.[4,15,50] Salts of this type have long been known to improve the efficiency of Heck coupling,[51] either via its action as a phase-transfer catalyst, or through the formation of anionic Pd(0) species as the active catalysts.[52,53] Including TBAB boosted conversion to above 70% on those catalysts trialled (Runs H7–H9) resulting in TONs of up to 880 (88% conversion) for **4a**. Additionally, reducing the catalyst loading and extending the run time to 30 hrs (Run H13 and H15) resulted in an increase in TON to up to 5000 (**4a**) at the expense of conversion.

The addition of a reducing agent to dihalide palladium bis-carbene complexes has been shown to efficiently reduce the pre-catalyst to the proposed palladium(0) active catalyst resulting in the absence of a catalytic induction period and higher overall TONs (Scheme 4.11).[4] Addition of 50 μL of hydrazine hydrate to the catalytic run (H17-H18) resulted in no conversion and a number of unidentified decomposition products and palladium zero deposition.

(pre-catalyst)   (proposed active catalyst)
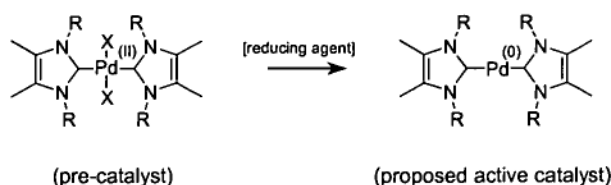
Scheme 4.11 – Reduction to active catalyst

The substitution of alternate bases for sodium acetate has resulted in improved conversions in greatly reduced time for palladium bis(benzothiazol-2-ylidene)diiodide in ionic liquids.[15] The use of sodium bicarbonate as a base (Run H12) showed little benefit over sodium acetate with conversion rising to 54% from 41% for catalyst **4a**. The replacement of sodium acetate with sodium formate led to a decrease in the conversion rate from 41% to 12% (Run H10), but in combination with the addition of a promoter (TBAB), conversion rates were boosted above 75% resulting in turn-over numbers of up to 8300 (Run H14) with catalyst **4b**. Sodium formate is known to act as both a base and a reducing agent in the catalytic process.[4] While the addition of sodium formate led to the observed deposition of palladium black in some cases (Runs H10 and H11), it appears that in combination with a promoter such as TBAB, the benefits may out-weigh the disadvantages. Sodium formate appears to be a milder reducing agent than hydrazine hydrate, which resulted in no conversion when used.

Observation of the Heck product via ^{1}H NMR revealed only the E isomeric form.

4.2.8 Suzuki Coupling

Palladium complexes **4a-f** were used as precatalysts for the coupling of 4-bromoacetophenone with phenylboronic acid to form 1-(1,1'-biphenyl-4-yl)ethanone (Scheme 4.12). Results are collected in Tables 4.5 and 4.6.
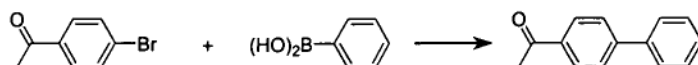
Scheme 4.12 – Suzuki Coupling

Table 4.5 – Suzuki Reaction Catalysis Results[a]

Run	Catalyst	Conversion (%)	TON
S1	**4a**	27	270
S2	**4b**	40	400
S3	**4c**	52	520
S4	**4d**	46	460
S5	**4e**	25	250
S6	**4f**	11	110

[a]Conditions : 1.0×10^{-1} mol% catalyst; 2.0 mmol K_2CO_3; Reflux in toluene for 20hrs
(see experimental details at the end of chapter)

Table 4.6 – Suzuki Reaction Catalysis Results 2

Run	Catalyst	Amount (mol%)	Salt	Additives[b]	Conversion (%)	TON
S7	**4a**	1.0×10^{-1}	K_2CO_3	TBAB	30	300
S8	**4a**	1.0×10^{-1}	K_2CO_3	TBAB, HZ	0	0
S9	**4a**	1.0×10^{-1}	Cs_2CO_3	-	25	250
S10	**4a**	1.0×10^{-1}	Cs_2CO_3	TBAB, HZ	0	0
S11	**4c**	1.0×10^{-1}	K_2CO_3	TBAB	15	150
S12	**4d**	1.0×10^{-1}	K_2CO_3	TBAB	40	400
S13	**4b**	1.0×10^{-1}	K_2CO_3	TBAB	36	360
S14	**4b**	1.0×10^{-1}	Cs_2CO_3	TBAB	17	170
S15	**4b**	1.0×10^{-2}	K_2CO_3	NaOOCH	75	7500
S16	**4b**	1.0×10^{-2}	K_2CO_3	TBAB, NaOOCH	0	0

[a]Conditions : Reflux in toluene for 20 hrs (see experimental details at the end of chapter); [b]TBAB = 2mmol of tetrabutylammonium bromide added to run; HZ = 50 μL of hydrazine hydrate added to run; NaOOCH = 2mmol of sodium formate added to run

Using 0.1 mol% of catalyst, the conversions were moderate, with **4c** providing a conversion of 52% corresponding to a TON of 520 (Run S3).

In general, the inclusion of TBAB as a promoter had a negative effect on conversion, with a new peak appearing in the GC-MS at the expense of the product; the new peak could not be identified. Calo *et al.* have previously described an undesirable effect of carbonate salts on their TBAB ionic liquids and this may well be the case here.[15]

The TON of Complex **4c** went from 520 to 150 on the inclusion of TBAB. Only in the runs where TBAB was used were undesirable side products observed.

The use of cesium carbonate in place of potassium carbonate resulted in a slight decrease in conversion under both standard conditions (**4a**, 27% (S1) to 25% (S9)) and with the inclusion of TBAB (**4b**, 36% (S13) to 17% (S14)). Cesium carbonate has been touted as the base of choice for Suzuki catalysis by the Nolan group,[54,55] but the observed increase in activity may be due to its benefits in producing the active catalyst via imidazolium salt deprotonation rather than its role in the catalytic cycle.

Using hydrazine hydrate as a reducing agent resulted in complete catalyst deactivation (S8 and S10), while using catalytic amounts of the alternate reducing agent sodium formate (0.02 mol %) resulted in the greatest conversions observed. Conversions of up to 75% and a corresponding turn-over number of 7500 (Run S15) were observed under these conditions.

4.3 Conclusions

Six novel palladium bis(thiazol-2-ylidene) complexes were utilized as pre-catalysts for the Heck and Suzuki carbon-carbon coupling reactions.

Complex **4b** exhibited turn-over numbers of up to 8300 for the Heck reaction when ionic liquids were added to the solution and sodium formate was used as a reducing agent. In the Suzuki reaction a turn-over number of 7500 was observed for complex **4b** when combined with sodium formate. The addition of an ionic liquid (TBAB) to the Suzuki reaction resulted in a reduction in yields in most cases and the formation of an unidentified side-product.

Use of the reducing agent hydrazine hydrate had a detrimental effect on the catalytic runs for both the Heck and Suzuki reactions. Addition of catalytic amounts resulted in catalyst poisoning and no turn-over was observed.

The thiazole-based catalysts tested here do not perform anywhere near as well as their imidazole counterparts. Turn-over numbers for imidazole-based catalysts for the Heck reaction conditions used here have exceeded one million.[45] The catalytic activity of the complexes tested here is most probably hampered by their lack of solubility in a range of organic solvents. Additionally, Nolan has proposed that steric bulk on nitrogen is essential for increased activity in the Suzuki reaction.[55] Lack of an exocyclic ring substituent in thiazole (c.f. imidazole) may slow the Suzuki product elimination step in the catalytic cycle and thus reduce the turn-over.

The availability of the sulfur lone-pair in the catalyst may also result in unfavourable additional interactions between the catalyst and substrates (as observed in Chapters 5 and 6). Given the difficulty in formation of silver-carbene complexes of thiazole it may not be surprising if similar interactions are occurring during the catalytic cycle and thus hampering the overall activity.

4.4 Experimental

4.4.1 General Comments

Unless otherwise stated, all reactions involving thiazolium salts were performed using standard Schlenk line techniques. Solvents were purified using standard methods[56] and distilled under nitrogen immediately prior to use, except anhydrous DMA, which was purchased from Aldrich. All other reagents were used as received. Thioformamides were synthesized based on literature methods,[57-59] while compounds **3a** and **3d** were prepared according to the method of Chen and Jordan.[60]

4.4.2 Preparation of *N*-aryl Thiazolium Salts

N-(2,4,6-trimethylphenyl)formamide (1e). 2,4,6-trimethylphenylamine (10 mL, 71.2 mmol) was refluxed in formic acid (10 mL) for 2hrs. After this time water (20 mL) was added resulting in the precipitation of an off-white solid that was filtered and washed repeatedly with water. After recrystallising from ethanol, the resulting white crystalline solid was oven dried (80°C) overnight. Yield: 11.5 g (99%). ^{1}H NMR (200 MHz, CDCl$_3$): δ 8.41 (s, 1*H*, ArylN*H*C), δ 8.09 and 8.02 (s, 1*H*, C(O)*H*), δ 6.94 (s, 1*H*, Aryl*H*), δ 6.92 (s, 1*H*, Aryl*H*), δ 2.30 (s, 3*H*, ArylC*H*$_3$), δ 2.27 (s, 3*H*, ArylC*H*$_3$), δ 2.22 (s, 3H, ArylC*H*$_3$).

N-(2,6-dimethylphenyl) formamide (1f). This compound was prepared in the same manner as **1e** using 2,6-dimethylphenylamine (10 mL, 81.2 mmol). Yield: 9 g (74%). ^{1}H NMR (200 MHz, CDCl$_3$): δ 8.42 (s, 1*H*, Aryl*NHC*), δ 8.14 and 8.08 (s, 1*H*, C(O)*H*), δ 7.14 (gr, 3*H*, Aryl*H*), δ 2.31 (s, 3*H*, ArylC*H$_3$*), δ 2.27 (s, 3*H*, ArylC*H$_3$*).

N-(3,5-dimethylphenyl) formamide (1g). This compound was prepared in the same manner as **1e** using 3,5-dimethylphenylamine (10 mL, 80.3 mmol), except that the water was extracted with DCM (40 mL). The organic layer was isolated and subsequently concentrated *in vacuo* to yield a white crystalline solid. The product was recrystallised from ethanol. Yield: 8.20 grams (68%). ^{1}H NMR (200 MHz, CDCl$_3$): δ 8.71 and 8.65 (s, 1*H*, Aryl*NHC*), δ 8.36 (s, 1*H*, C(O)*H*), δ 7.17 (s, 1*H*, Aryl*H*(para)), δ 6.8-6.7 (gr, 2*H*, Aryl*H*(ortho)), δ 2.32 (s, 3*H*, ArylC*H$_3$*), δ 2.31 (s, 3*H*, ArylC*H$_3$*).

N-adamantyl formamide (1h). This compound was prepared as per the literature procedure.[61] 1-Adamantanamine (1.6 g, 10.6 mmol) was mixed with excess ethylformate (15 mL, 0.19 mol), DMSO (5 mL) and heated (100 °C) in a sealed pressure tube for 24 hrs. After cooling, the solution was poured over cold water and the white product isolated via filtration. Yield: 0.9 g (47%).

N-(2,4,6-trimethylphenyl) thioformamide (2e). Sodium bicarbonate (1.55 g, 18.4 mmol) and phosphorus pentasulfide (4.09 g, 9.19 mmol) were dissolved in THF (30 mL) with heating (50°C) and stirred for 30 minutes. To the pale yellow solution was added **1e** (5.00 grams, 30.6 mmol) in portions over 30 minutes, during which time the

solution became colourless. After refluxing overnight, *ca.* 25 mL of the THF was removed *in vacuo* and water added (100mL) resulting in the precipitation of a white powder that was left to stir for 2 hours. The white fluffy product was air-dried after filtration and recrystallised from ether and light petroleum. Yield: 4.39 g (80%). ^{1}H NMR (200 MHz, CDCl$_3$): δ 9.67 and 9.64 (s, 1*H*, ArylN*H*C), δ 9.22 and 9.15 (s, 1*H*, C(S)*H*), δ 6.93 (s, 2*H*, Aryl*H*), δ 2.30 (s, 3H, ArylC*H*$_3$), δ 2.26 (s, 3H, ArylC*H*$_3$), δ 2.22 (s, 3H, ArylC*H*$_3$).

N-(2,6-dimethylphenyl) thioformamide (2f). This compound was prepared in the same manner as **2e** using **1f** (5.00 grams, 33.5 mmol). Yield: 4.20 grams (76%). ^{1}H NMR (200 MHz, CDCl$_3$): δ 9.64 (sb, 1*H*, ArylN*H*C), δ 9.24 (sb, 1*H*, C(S)*H*), δ 7.15 (gr, 3*H*, Aryl*H*), δ 2.31 (s, 3H, ArylC*H*$_3$), δ 2.24 (s, 3H, ArylC*H*$_3$).

N-(3,5-dimethylphenyl) thioformamide (2g). This compound was prepared in the same manner as **2e** using **1g** (7.00 grams, 46.9 mmol), except the product was recrystallised from water and acetone. Yield: 3.98 grams (52%). ^{1}H NMR (200 MHz, DMSO-d$_6$): δ 12.08 and 12.04 (s, 1*H*, ArylN*H*C), δ 9.97 and 9.90 (s, 1*H*, C(S)*H*), δ 7.03 (s, 2*H*, Aryl*H*(ortho)), δ 6.85 (s, 1*H*, Aryl*H*(para)), δ 2.27 (s, 6*H*, ArylC*H*$_3$).

N-adamantyl thioformamide (2h). This compound was prepared in the same manner as **2e** using **1h** (1.30 g, 7.26 mmol), except the product was extracted into DCM, which was dried over MgSO$_4$, filtered and the DCM stripped *in vacuo* to reveal a white powder. Yield: 0.90 g (64%). ^{1}H NMR (200 MHz, CDCl$_3$): δ 9.21 and 9.19 (s, 1*H*,

C(S)*H*), δ 7.96 (sb, 1*H*, AlkylN*H*C), δ 2.11 (s, 3*H*, C*H*), δ 1.78 (s, 6*H*, C*H*$_2$), δ 1.68–1.53 (gr, 6*H*, C*H*$_2$).

***N-tertiary*-butyl thioformamide (2i).** This compound was prepared in the same manner as **2e** using *N-tertiary*-butylformamide (3.00 g, 29.7 mmol), except the product was extracted from the water with diethylether (2 x 10 mL). The diethylether was then stripped *in vacuo* to yield a white powder, which was washed with petroleum spirits. Yield: 1.8 g (52%). ^{1}H NMR (200 MHz, DMSO-d$_6$): δ 9.31 and 9.28 (s, 1*H*, C(S)*H*), δ 8.59 (sb, 1*H*, AlkylN*H*C), δ 1.38 (s, 9*H*, C*H*$_3$).

***N*-(2,4,6-trimethylphenyl)-4,5-dimethyl thiazolium iodide (3e).** To **2e** (2.00 grams, 11.2 mmol) was added an excess of 3-chloro-2-butanone (1.3 mL, 12.9 mmol) together with acetone (2 mL) to aid initial mixing. The yellow mixture was stirred at 100°C for 2 hrs resulting in an orange-red solution, which upon cooling was washed with ether (3 x 10mL). Acetone was added (20 mL) along with sodium iodide (2.1 grams, 14.0 mmol) and the solution stirred overnight. The acetone was removed *in vacuo* and DCM added (50 mL) and the solution dried over magnesium sulfate. After filtration through celite, the DCM was stripped and the mustard coloured powder recrystallised from acetone/ether. Yield: 1.60 grams (40%). Micro Analysis. Calculated (C$_{14}$H$_{18}$NSI): C 46.80%, H 5.05%, N 3.90%, S 8.92%. Found: C 46.52%, H 5.20%, N 3.92%, S 8.79%. MS (LSIMS) m/z: 232.1 [M]$^+$ (100%). ^{1}H NMR (200 MHz, CDCl$_3$): δ 10.42 (s, 1*H*, C(2)*H*), δ 7.03 (s, 2*H*, Aryl*H*), δ 2.68 (s, 3*H*, C*H*$_3$), δ 2.33 (s, 3*H*, SCC*H*$_3$), δ 2.09 (s, 3*H*, ArylCH$_3$(para)), δ 1.94 (s, 6H, ArylCH$_3$(ortho)). ^{13}C NMR (50 MHz, CDCl$_3$): δ

159.8 (NCHS), δ 142.6 (NCCS), δ 142.4 (Aryl-C$_{para}$), δ 135.2 (Aryl-C$_{ipso}$), δ 134.0 (Aryl-C$_{ortho}$), δ 133.1 (SCCN), 130.7 (Aryl-C$_{meta}$), δ 21.7 (ArylCH$_3$(para)), δ 18.2 (ArylCH$_3$(ortho)), δ 14.3 (NCCH$_3$), δ 12.4 (SCCH$_3$).

N-(2,6-dimethylphenyl)-4,5-dimethyl thiazolium iodide (3f). This compound was prepared in the same manner as **3e** using **2f** (2.50 grams, 15.1 mmol), 3-chloro-2-butanone (1.6 mL, 15.8 mmol) and sodium iodide (2.5 grams, 16.7 mmol) resulting in a reddish brown solid. Yield: 3.65 grams (70%). Micro Analysis. Calculated (C$_{13}$H$_{16}$NSI) : C 45.23%, H 4.67%, N 4.06%, S 9.29%. Found: C 45.21%, H 4.74%, N 4.09%, S 9.19%. MS (LSIMS) m/z : 218.1 [M]$^+$ (100%). ^{1}H NMR (200 MHz, CDCl$_3$) : δ 10.64 (s, 1H, thiazoleH), δ 7.5-7.3 (gr, 3H, ArylH), δ 2.70 (s, 3H, SCCH$_3$), δ 2.12 (s, 3H, NCCH$_3$), δ 2.04 (s, 6H, ArylCH$_3$). ^{13}C NMR (50 MHz, CDCl$_3$): δ 159.7 (NCHS), δ 142.3 (NCCS), δ 135.6 (Aryl-C$_{para}$), δ 135.4 (Aryl-C$_{ipso}$), and δ 134.5 (Aryl-C$_{ortho}$), δ 132.3 (SCCN), δ 130.2 (Aryl-C$_{meta}$), δ 18.4 (ArylCH$_3$), δ 14.4 (NCCH$_3$), δ 12.4 (SCCH$_3$).

N-(3,5-dimethylphenyl)-4,5-dimethyl thiazolium iodide (3g). This compound was prepared in a similar manner as **3e** using **2g** (2.10 grams, 12.8 mmol), 3-chloro-2-butanone (1.6 mL, 15.8 mmol) and excess sodium iodide (2.5 g, 16.7 mmol), except that the product was recrystallised from DCM/ether resulting in a pale purple powder. Yield 2.0 grams (45%). Micro Analysis. Calculated (C$_{13}$H$_{16}$NSI): C 45.23%, H 4.67%, N 4.06%, S 9.29%. Found: C 45.32%, H 4.84%, N 4.11%, S 9.15%. MS (LSIMS) m/z: 218.1 [M]$^+$ (100%). ^{1}H NMR (200 MHz, CDCl$_3$): δ 10.31 (s, 1H, thiazoleH), δ 7.22 (s, 1H, ArylH), δ 7.13 (s, 2H, ArylH), δ 2.62 (s, 3H, NCCH$_3$), δ 2.39 (s, 6H, ArylCH$_3$), δ

2.27 (s, 3H, SCCH_3). ^{13}C NMR (50 MHz, CDCl$_3$) : δ 158.5 (NCHS), δ 142.9 (NCCS), δ 141.3 (Aryl-C$_{meta}$), δ 136.9 (Aryl-C$_{ipso}$), δ 134.5 (SCCN), δ 133.9 (Aryl-C$_{para}$), δ 123.7 (Aryl-C$_{ortho}$), δ 21.7 (Aryl$C$H$_3$), δ 14.0 (NCCH$_3$), δ 13.5 (SCCH$_3$).

4.4.3 Preparation of *N*-alkyl Thiazolium Salts

N-methyl-4,5-dimethyl thiazolium iodide (3a). Prepared according to literature procedure.[60] 4,5-Dimethylthiazole (2.00 mL, 18.9 mmol) and 2 equivalents of methyl iodide (2.4 mL, 38.6 mmol) were stirred at room temperature for 24 hrs with protection from light. The resultant white solid was then broken up and triturated with ethyl acetate. The solid was filtered, washed with ethyl acetate (3 x 10 mL) and air-dried. Yield: 3.70 grams (77%). Micro Analysis. Calculated (C$_6$H$_{10}$NSI): C 28.25%, H 3.95%, N 5.49%, S 12.57%. Found: C 28.34%, H 4.01%, N 5.46%, S 12.77%. MS (LSIMS) m/z: 128.0 [M]$^+$ (100%). ^{1}H NMR (200 MHz, DMSO-d$_6$): δ 10.0x (s, 1H, thiazole$H$), δ 4.1 (s, 3H, NCH_3), δ 2.5x (s, 3H, SCCH_3), δ 2.4x (s, 3H, NCCH_3). ^{13}C NMR (50MHz, DMSO-d$_6$): δ 155.9 (NCHS), δ 142.5 (NCCS), δ 132.6 (SCCN), δ 40.7 (NCH$_3$), δ 12.4 (NCCH3), δ 11.5 (SCCH3).

N-isopropyl-4,5-dimethyl thiazolium bromide (3b). 4,5-dimethylthiazole (3.40 grams, 30.0 mmol) and excess 2-bromopropane (4.10 grams, 33.3 mmol) were mixed in acetone (15 mL) and reacted overnight with stirring in a bomb at 110°C. The resulting green solution was poured in to a schlenk and the solvent removed *in vacuo*. The resulting green oil was washed with ether (2 x 15 mL) and stirred with THF (30 mL), from which precipitated a yellow-green powder. The THF was decanted and the product

dried *in vacuo*. Yield: 5.31 g (75%). Micro Analysis. Calculated ($C_8H_{14}NSBr$): C

40.69%, H 5.98%, N 5.93%. Found: C 41.02 %, H 6.05%, N 5.11%. MS (LSIMS) m/z:

156.1 $[M]^+$ (100%). ^{1}H NMR (200 MHz, CDCl$_3$): δ 11.13 (s, 1*H*, thiazole*H*), δ 4.93 (m,

1*H*, NC*H*(CH$_3$)$_2$), δ 2.55 (s, 6*H*, NCH(C*H$_3$*)$_2$), δ 1.76 (s, 3*H*, NCC*H$_3$*), δ 1.73 (s, 3*H*,

SCC*H$_3$*). ^{13}C NMR (50MHz, CDCl$_3$): δ 156.4 (N*C*HS), δ 141.6 (N*C*CS), δ 133.9

(S*C*CN), δ 57.7 (N*C*H(CH$_3$)$_2$), δ 23.6 (NCH(*C*H$_3$)$_2$), δ 13.4 (NC*C*H3), δ 12.8 (SC*C*H3).

N-butyl-4,5-dimethyl thiazolium bromide (3c). 4,5-dimethylthiazole (1.2 mL,

11.3 mmol) and *n*-butylbromide (3.0 mL, 27.9 mmol) were refluxed for 48 hrs. The

resultant brown oily product was washed with ether (2 x 10 mL), and repeatedly with

THF. The residue was dried *in vacuo* to give a brown viscous product. Yield 2.09 g

(74%). The sample was unsuitable for micro analysis. MS (LSIMS) m/z: 170.1 $[M]^+$

(100%). MS (HR-LSIMS) m/z: Calculated $[C9H16NS]^+$ 170.1003, Found 170.10103

(4.02 ppm deviation). ^{1}H NMR (200 MHz, CDCl$_3$): δ 11.02 (S, 1*H*, thiazole*H*), δ 4.60 (t,

2*H*, NC*H$_2$*), δ 2.48 (s, 3H, SCC*H$_3$*), δ 2.42 (s, 3H, NCC*H$_3$*), δ 1.77 (m, 2H, C*H$_2$*), δ 1.32

(m, 2H, C*H$_2$*), δ 0.83 (t, 3H, CH$_2$C*H$_3$*). ^{13}C NMR (50 MHz, CDCl$_3$): δ 157.0 (N*C*HS), δ

141.8 (N*C*CS), δ 133.7 (S*C*CN), δ 54.2 (N*C*H$_2$), δ 32,3 (*C*H$_2$), δ 19.9 (*C*H$_2$), δ 14.0

(CH$_2$*C*H$_3$), δ 13.4 (NC*C*H$_3$), δ 12.5 (SC*C*H$_3$).

N-benzyl-4,5-dimethyl thiazolium iodide (3d). To 1.2 equivalents of sodium

iodide (5.11 g, 34.1 mmol) were added 4,5-dimethylthiazole (3.0 mL, 28.4 mmol) and

excess benzyl chloride (5.0 mL, 43.4 mmol). Dry acetone (50 mL) was added and the

solution refluxed for 20 hrs, after which the solution was a deep orange and contained a

bright yellow precipitate. The acetone was stripped *in vacuo* and the remaining solid washed with several (10 mL) portions of ether. The resultant pale yellow powder was extracted with DCM overnight in a soxhlet apparatus. The solution was dried over magnesium sulfate, filtered through celite and the solvent stripped. The resulting honeycomb was washed repeatedly with THF to yield a pale yellow powder. Yield: 7.06 grams (75%). Micro Analysis. Calculated ($C_{12}H_{14}NSI$): C 43.52%, H 4.26%, N 4.23%, S 9.68%. Found: C 42.87 %, H 4.43%, N 4.06%, S 9.86%. MS (LSIMS) m/z: 204.1 $[M]^+$ (100%). ^{1}H NMR (200 MHz, CDCl$_3$): δ 11.05 (s, 1*H*, thiazole*H*), δ 7.26 (gr, 5*H*, Aryl*H*), δ 5.96 (s, 2*H*, C*H$_2$*), δ 2.41 (s, 3*H*, SCC*H$_3$*), δ 2.33 (s, 3*H*, NCC*H$_3$*). ^{13}C NMR (50 MHz, CDCl$_3$): δ 156.7 (N*C*HS), δ 142.8 (N*C*CS), δ 133.9 (Aryl), δ 132.1 (S*C*CN), δ 129.9, 129.8, 128.8 (Aryl), δ 57.8 (*C*H$_2$), δ 13.6 (NC*C*H$_3$), δ 13.1 (SC*C*H$_3$).

4.4.4 Alternative Preparation for Arduengo's *N*-(2,6-diisopropylphenyl)-4,5-dimethyl thiazolium chloride.

***N*-(2,6-diisopropylphenyl) formamide (1j).** This compound was prepared in the same manner as **1e** using 2,6-diisopropylphenylamine (10 mL, 53.0 mmol). Yield: 10 g (92%). ^{1}H NMR (200 MHz, CDCl$_3$): δ 8.48 (s, 1*H*, ArylN*H*C), δ 8.06 and 8.01 (s, 1*H*, C(O)*H*), δ 7.38–7.17 (gr, 3*H*, Aryl*H*), δ 3.19 (m, 2*H*, C*H*(CH$_3$)$_2$), δ 1.23 (s, 6*H*, C*H$_3$*), δ 1.20 (s, 6*H*, C*H$_3$*). Micro Analysis. Calculated ($C_{13}H_{19}NO$): C 76.06%, H 9.33%, N 6.82%. Found: C 76.16%, H 9.21%, N 6.91%.

N-(2,6-diisopropylphenyl) thioformamide (2j). This compound was prepared in the same manner as **2e** using **1j** (2.50 grams, 12.2 mmol). Yield: 2.10 grams (78%). ^{1}H NMR (200 MHz, CDCl$_3$): δ 9.81 (s, 1*H*, ArylN*H*C), δ 9.19 and 9.11 (s, 1*H*, C(S)*H*), δ 7.40–7.17 (gr, 3*H*, Aryl*H*), δ 3.14 (m, 2*H*, C*H*(CH$_3$)$_2$), δ 1.25 (s, 6*H*, C*H*$_3$), δ 1.21 (s, 6*H*, C*H*$_3$). MS (LSIMS) m/z: 222.1 [M+H]$^+$ (100%).

N-(2,6-diisopropylphenyl)-4,5-dimethyl thiazolium chloride. To **2j** (1.30 g, 5.88 mmol) was added an excess of 3-chloro-2-butanone (0.9 mL, 8.91 mmol) together with absolute ethanol (20 mL). The mixture was refluxed for 24 hrs, cooled and the ethanol removed *in vacuo*. The remaining dark-red oil was washed with ether (2 x 10 mL), taken up in water (50 mL), raised to pH 8 (NaHCO$_3$) and extracted further with ether (3 x 10 mL). The aqueous solution was reduced *in vacuo* and the product taken up in DCM and dried over MgSO$_4$. After filtration through celite, the DCM was stripped and the pale pink powder dried overnight *in vacuo* and recrystallised from DCM/ether. Yield: 1.00 grams (55%). The product may be metathesised to the iodide salt. Micro Analysis. Calculated (C$_{17}$H$_{24}$NSI): C 50.86%, H 6.03%, N 3.49%, S 7.97%. Found: C 50.82%, H 6.05%, N 3.51%, S 8.22%. MS (LSIMS) m/z: 274.1 [M]$^+$ (100%). ^{1}H NMR (200 MHz, CDCl$_3$): δ 10.59 (s, 1*H*, C(2)*H*), δ 7.70–7.50 (gr, 3*H*, Aryl*H*), δ 2.65 (s, 3*H*, NCC*H*$_3$), δ 2.08 (s, 3*H*, SCC*H*$_3$), δ 2.03 (m, 2*H*, C*H*(CH$_3$)$_2$), δ 1.19 (s, 6*H*, C*H*$_3$), δ 1.14 (s, 6*H*, C*H*$_3$). ^{13}C NMR (50 MHz, CDCl$_3$): δ 159.4 (N*C*HS), δ 142.5 (Aryl-C$_{ortho}$), δ 139.9 (N*C*CS), δ 132.9 (Aryl-C$_{ipso}$), δ 130.5 (Aryl-C$_{para}$), δ 130.1 (S*C*CN), 123.3 (Aryl-C$_{meta}$), δ 26.9 (*C*H), δ 23.1 (*C*H$_3$), δ 21.2 (*C*H$_3$), δ 11.1 (NC*C*H$_3$), δ 9.9 (SC*C*H$_3$).

4.4.5 Preparation of Palladium Bis(thiazol-2-ylidene) Diiodide Complexes

Palladium   bis(*N*-methyl-4,5-dimethylthiazol-2-ylidene)   diiodide   (**4a**).

Palladium acetate (100 mg, 0.445 mmol) and **3a** (0.24g, 1.07 mmol) were mixed in THF

(15 mL). The dark red/brown solution was stirred at room temperature. After 2 days the

solution had changed to a bright orange containing a pale yellow solid. The THF was

removed *in vacuo* and the remaining solid washed with methanol (3 x 5 mL). The

resulting pale yellow solid was dried *in vacuo*. Yield 0.25 g (91%). Micro Analysis.

Calculated ($C_{12}H_{18}N_2S_2I_2Pd$): C 23.45%, H 2.95%, N 4.56%, S 10.43%. Found: C

23.61%, H 2.88%, N 4.70%, S 10.48%. MS (LSIMS) m/z: 614.0 [M] (60%), 487.0 [M-

I]$^+$ (100%), 360.0 [M-2I]$^{2+}$ (65%). ^{1}H NMR (200MHz, DMSO-d$_6$): 2 isomers (a:b, 2:1),

δ 4.23 (s, 6H, NCH$_{3(a)}$), δ 4.14 (s, 6H, NCH$_{3(b)}$), δ 2.34 (s, 6H, SCCH$_{3(b)}$), δ 2.32 (s, 6H,

NCCH$_{3(b)}$), δ 2.29 (s, 6H, SCCH$_{3(a)}$), δ 2.28 (s, 6H, NCCH$_{3(a)}$). ^{13}C NMR (100.5 MHz,

DMSO-d$_6$ @ 65°C): most stable isomer only (b) (refer to text), δ 195.2 (N*C*HS), δ 140.4

(N*C*CS), δ 131.7 (S*C*CN), δ 43.3 (N*C*H$_3$), δ 11.4 (NC*C*H$_3$), δ 11.0 (SC*C*H$_3$).

Palladium   bis(*N*-isopropyl-4,5-dimethylthiazol-2-ylidene)   dibromide   (**4b**).

This compound was prepared in a similar manner to **4a** using **3b** (0.16 g, 0.677 mmol)

and palladium acetate (75 mg, 0.334 mmol) resulting in a pale yellow powder. Yield:

0.12 grams (62%). Micro Analysis. Calculated ($C_{16}H_{26}N_2S_2Br_2Pd$): C 33.32%, H 4.54%,

N 4.86%, S 11.12%. Found: C 33.46%, H 4.66%, N 4.91%, S 10.98%. MS (LSIMS)

m/z: 497.1 [M-Br]$^+$ (15%), 415.1 [M-2Br]$^{2+}$ (60%). ^{1}H NMR (200MHz, DMSO-d$_6$): δ

6.35 (m, 2H, NC*H*(CH$_3$)$_2$), δ 2.40 (s, 6H, NCCH$_3$), δ 2.25 (s, 6H, SCCH$_3$), δ 1.74 (d,

12H, NCH(C*H*$_3$)$_2$). ^{13}C NMR (100.5 MHz, DMSO-d$_6$ @ 65°C): δ 195.7 (N*C*HS), δ

140.0 (NCCS), δ 133.6 (SCCN), δ 61.6 (NCH), δ 20.6 (CH(CH$_3$)$_2$), δ 12.5 (NCCH$_3$), δ 11.3 (SCCH$_3$).

Palladium bis(*N*-butyl-4,5-dimethylthiazol-2-ylidene) diiodide (4c). A 2.5 mL aliquot containing **3c** (0.23 g, 0.919 mmol) in dry DCM was transferred to a Schlenk under nitrogen. The DCM was removed *in vacuo* and palladium acetate (100 mg, 0.445 mmol) added under a constant flow of nitrogen. THF (10 mL) was added and the heterogeneous solution was stirred at room temperature for 3 days. The THF was stripped *in vacuo* yielding a bright yellow precipitate that was washed with methanol (3 x 5 mL). The yellow powder was dried under vacuum. Yield: 180 mg (67%). Micro Analysis. Calculated (C$_{18}$H$_{30}$N$_2$S$_2$Br$_2$Pd): C 35.75%, H 5.00%, N 4.63%, S 10.60%. Found: C 35.96%, H 5.79%, N 3.96%, S 10.05%. MS (LSIMS) m/z: 605.0 [M+H]$^+$ (5%), 525.0 [M-Br]$^+$ (100%), 444.1 [M-2Br]$^{2+}$ (30%). ^{1}H NMR (200MHz, CDCl$_3$): δ 4.85 (bm, 4*H*, NC*H*$_2$), δ 2.30 (s, 6*H*, SCC*H*$_3$), δ 2.24 (s, 6*H*, NCC*H*$_3$), δ 2.09 (br m, 4*H*, C*H*$_2$), δ 1.59 (bm, 4*H*, C*H*$_2$), δ 1.09 (t, 6*H*, CH$_2$C*H*$_3$). ^{13}C NMR (100.5 MHz, DMSO-d$_6$ at 40°C): δ 196.6 (NCHS), δ 139.4 (NCCS), δ 130.8 (SCCN), δ 54.1 (NCH$_2$), δ 29.4 (CH$_2$), δ 18.3 (CH$_2$), δ 12.1 (CH$_3$), δ 11.6 (NCCH$_3$), δ 10.2 (SCCH$_3$).

Palladium bis(N-benzyl-4,5-dimethylthiazol-2-ylidene) diiodide (4d). This compound was prepared in a similar manner to **4a** using **3d** (0.43 g, 1.30 mmol) and palladium acetate (156 mg, 0.695 mmol) resulting in a very insoluble pale yellow powder. Yield: 300 mg (60%). Micro Analysis. Calculated (C$_{24}$H$_{26}$N$_2$S$_2$I$_2$Pd): C 37.59%, H 3.42%, N 3.65%, S 8.36%. Found: C 38.14%, H 3.66%, N 3.57%, S 9.04%.

MS (LSIMS) m/z: 639.0 [M-I]$^+$ (30%), 204.1 [ylidene]$^+$ (100%). ^{1}H NMR (200MHz, CDCl$_3$): δ 7.31-7.07 (sb, 10H, Aryl$H$), δ 6.02 (s, 4H, CH_2), δ 2.20 (s, 6H, SCCH_3), δ 1.98 (s, 6H, NCCH_3).

Palladium bis(N-(2,4,6-trimethylphenyl)-4,5-dimethylthiazol-2-ylidene) diiodide (4e). This compound was prepared in a similar manner to **4a** from **3e** (0.34 grams, 0.946 mmol) and palladium acetate (100 mg, 0.445 mmol), except the solution was refluxed for 1 day, followed by 2 days of stirring at room temperature. The pale yellow-brown powder was dried *in vacuo*. Yield: 0.23 g (63%). Micro Analysis. Calculated (C$_{28}$H$_{34}$N$_2$S$_2$I$_2$Pd): C 40.87%, H 4.16%, N 3.40%, S 7.79%. Found: C 42.48%, H 3.97%, N 3.77%, S 7.52%. MS (LSIMS) m/z: 820.9 [M-H]$^+$ (2%), 695.1 [M-I]$^+$ (30%), 232.1 [ylidene]$^+$ (100%). ^{1}H NMR (399.7 MHz, DMSO-d$_6$): δ 7.18 (s, 2H, Aryl$H$), δ 7.10 (s, 2H, Aryl$H$), δ 2.44 (s, 6H, SCCH_3), δ 2.34 (s, 6H, NCCH_3), δ 2.17 (s, 6H, ArylCH_3), δ 1.81 (s, 6H, ArylCH_3),, δ 1.35 (s, 6H, ArylCH_3). ^{13}C NMR (100.5 MHz, CDCl$_3$ at 40°C): δ 196.8 (NCHS), δ 140.7 (ArylC), δ 140.3 (NCCS), δ 138-134 (ArylC), δ 133.2 (SCCN), δ 129.7 (ArylC), δ 30.9 (ArylCH$_3$), δ 21.3 (ArylCH$_3$), δ 19.2 (ArylCH$_3$), δ 12.5 (NCCH$_3$), δ 11.7 (SCCH$_3$).

Palladium bis(N-(2,6-dimethylphenyl)-4,5-dimethylthiazol-2-ylidene) di-iodide (4f). This compound was prepared in a similar manner to **4a** from **3f** (0.34 g, 0.985 mmol) and palladium acetate (100 mg, 0.445 mmol), except the solution was refluxed for 1 day, followed by 2 days of stirring at room temperature. The pale yellow powder was dried *in vacuo*. Yield: 0.28 g (79%). Micro Analysis. Calculated

($C_{26}H_{30}N_2S_2I_2Pd$): C 39.29%, H 3.80%, N 3.52%, S 8.07%. Found: C 39.18%, H 3.76%,

N 3.64%, S 7.93%. MS (LSIMS) m/z: 794.1 [M] (2%), 667.1 [M-I]$^+$ (10%), 218.1

[ylidene]$^+$ (100%). ^{1}H NMR (399.7 MHz, DMSO-d$_6$ at 65°C): δ 7.40-7.00 (bm, 6H,

Aryl*H*), δ 2.32 (s, 6H, SCC*H$_3$*), δ 1.90 (s, 12H, ArylC*H$_3$*), δ 1.78 (s, 6H, NCC*H$_3$*),.

4.4.6 Intermolecular Heck Coupling Conditions

In a typical run, 4-bromoacetophenone (1.00 g, 5.0 mmol) and anhydrous NaOAc

(0.57 g, 8.0 mmol) were placed in a Schlenk reactor under nitrogen. To this was added *n*-

butyl acrylate (1.0 mL, 6.98 mmol), *N,N*-dimethylacetamide (5 mL) and a 200 μL

solution of the catalyst in an appropriate solvent (DCM, DMSO). The reaction vessel

was then heated by means of an oil bath to 120°C for the appropriate time. After heating,

the solution was cooled, and 200 μL of diethyleneglycol di-*n*-butyl ether (DEBE) added

for use as an internal GC standard. A 500μL aliquot of the reaction mixture was taken

and washed with 5% HCl (5 mL) and extracted in to DCM (2.5 mL) which was then

analysed by gas chromatography and GC-MS.

4.4.7 Suzuki Coupling Conditions

In a typical run, 4-bromoacetophenone (0.2 g, 1.0 mmol), phenylboronic acid

(0.13 g, 1.2 mmol) and potassium carbonate (0.28 g, 2.0 mmol) were added to a long

Schlenk tube that was placed under nitrogen. To this was added 3mL of toluene and a

200 μL solution of the catalyst in an appropriate solvent (DCM, DMSO). The solution

was brought to reflux and left for the desired time. After heating, the solution was

cooled, and 50 μL of diethyleneglycol di-*n*-butyl ether (DEBE) added for use as an

internal GC standard. A 500µL aliquot of the reaction mixture was taken and washed with 5% HCl (5 mL) and extracted in to DCM (2.5 mL) which was then analysed by gas chromatography and GC-MS.

4.5 References

(1)   Cardin, D. J., Doyle, M. J., Lappert, M. F., *Chem. Commun.* **1972**, 927.

(2)   Hill, J. E., Nile, T. A., *J. Organomet. Chem.* **1977**, *137*, 293.

(3)   Lappert, M. F., Maskell, R. K., *J. Organomet. Chem.* **1984**, *264*, 217.

(4)   Herrmann, W. A., Elison, M., Fischer, J., Kocher, C., Artus, G. R. J., *Angew. Chem., Int. Ed. Engl.* **1995**, *34*, 2371.

(5)   Enders, D., Breuer, K., Raabe, G., Runsink, J., Teles, J. H., Melder, J. P., Ebel, K., Brode, S., *Angew. Chem., Int. Ed. Engl.* **1995**, *34*, 1021.

(6)   Enders, D., Gielen, H., Raabe, G., Runsink, J., Teles, J. H., *Chem. Ber.-Recl.* **1996**, *129*, 1483.

(7)   Hahn, F. E., Foth, M., *J. Organomet. Chem.* **1999**, *585*, 241.

(8)   Chamizo, J. A., Morgado, J., Castro, M., Berens, S., *Organometallics* **2002**, *21*, 5428.

(9)   Arduengo, A. J., Goerlich, J. R., Marshall, W. J., *Liebigs Ann.-Recl.* **1997**, 365.

(10)   Calo, V., Del Sole, R., Nacci, A., Schingaro, E., Scordari, F., *Eur. J. Org. Chem.* **2000**, 869.

(11)   Calo, V., Giannoccaro, P., Nacci, A., Monopoli, A., *J. Organomet. Chem.* **2002**, *645*, 152.

(12)   Calo, V., Nacci, A., *Z. Naturforsch., A: Phys. Sci.* **2001**, *56*, 702.

(13)   Calo, V., Nacci, A., Monopoli, A., Lopez, L., di Cosmo, A., *Tetrahedron* **2001**, *57*, 6071.

(14)   Calo, V., Nacci, A., Lopez, L., Napola, A., *Tetrahedron Lett.* **2001**, *42*, 4701.

(15)   Calo, V., Nacci, A., Lopez, L., Mannarini, N., *Tetrahedron Lett.* **2000**, *41*, 8973.

(16)   Fraser, P. J., Roper, W. R., Stone, F. G. A., *J. Chem. Soc., Dalton Trans.* **1974**, 102.

(17)   Fehlhammer, W. P., Achatz, D., Plaia, U., Volkl, A., *Z. Naturforsch.* **1987**, *42b*, 720.

(18)   Raubenheimer, H. G., Stander, Y., Marais, E. K., Thompson, C., Kruger, G. J., Cronje, S., Deetlefs, M., *J. Organomet. Chem.* **1999**, *590*, 158.

(19)   Raubenheimer, H. G., Olivier, P. J., Lindeque, L., Desmet, M., Hrusak, J., Kruger, G. J., *J. Organomet. Chem.* **1997**, *544*, 91.

(20)   Raubenheimer, H. G., Scott, F., Kruger, G. J., Toerien, J. G., Otte, R., Vanzyl, W., Taljaard, I., Olivier, P., Linford, L., *J. Chem. Soc., Dalton Trans.* **1994**, 2091.

(21)   Raubenheimer, H. G., Cronje, S., Olivier, P. J., *J. Chem. Soc., Dalton Trans.* **1995**, 313.

(22)   LopezCalahorra, F., Castro, E., Ochoa, A., Marti, J., *Tetrahedron Lett.* **1996**, *37*, 5019.

(23)   Castells, J., Domingo, L., Lopezcalahorra, F., Marti, J., *Tetrahedron Lett.* **1993**, *34*, 517.

(24)   Castells, J., LopezCalahorra, F., Geijo, F., Perez-Dolz, R., Bassedas, M., *J. Heterocycl. Chem.* **1986**, *23*, 715.

(25)   Herrmann, W. A., Kocher, C., *Angew. Chem., Int. Ed. Engl.* **1997**, *36*, 2163.

(26)   Leeper, F. J., Smith, D. H. C., *J. Chem. Soc., Perkin Trans. 1* **1995**, 861.

(27)   Gstottmayr, C. W. K., Bohm, V. P. W., Herdtweck, E., Grosche, M., Herrmann, W. A., *Angew. Chem., Int. Ed. Engl.* **2002**, *41*, 1363.

(28)   Herrmann, W. A., Reisinger, C. P., Spiegler, M., *J. Organomet. Chem.* **1998**, *557*, 93.

(29)   Weskamp, T., Bohm, V. P. W., Herrmann, W. A., *J. Organomet. Chem.* **1999**, *585*, 348.

(30)   Jackstell, R., Andreu, M. G., Frisch, A., Selvakumar, K., Zapf, A., Klein, H., Spannenberg, A., Rottger, D., Briel, O., Karch, R., Beller, M., *Angew. Chem., Int. Ed. Engl.* **2002**, *41*, 986.

(31)   Jackstell, R., Frisch, A., Beller, M., Rottger, D., Malaun, M., Bildstein, B., *J. Mol. Catal. A: Chem.* **2002**, *185*, 105.

(32)   Weskamp, T., Kohl, F. J., Hieringer, W., Gleich, D., Herrmann, W. A., *Angew. Chem., Int. Ed. Engl.* **1999**, *38*, 2416.

(33)   Frenzel, U., Weskamp, T., Kohl, F. J., Schattenman, W. C., Nuyken, O., Herrmann, W. A., *J. Organomet. Chem.* **1999**, *586*, 263.

(34)   Gardiner, M. G., Herrmann, W. A., Reisinger, C. P., Schwarz, J., Spiegler, M., *J. Organomet. Chem.* **1999**, *572*, 239.

(35)   Morrison, R. T., Boyd, R. N. *Organic Chemistry*; Sixth ed.; Prentice Hall: New Jersey, 1992.

(36)   Hantzsch, *Chem. Ber.* **1887**, 3118.

(37)   Hromatka, O., US2,160,867, (Merck and Co.), 1939.

(38)   Joule, J. A., Mills, K., Smith, G. F. *Heterocyclic Chemistry*; 3rd ed.; Chapman and Hall: London, 1995.

(39)   Trost, B. M., Fleming, I., Eds. *Thiazoles and their Benzo Derivatives (Part 6)* in Comprehensive Organic Synthesis; Pergamon Press:, 1991.

(40)   Davis, J. H., Forrester, K. J., *Tetrahedron Lett.* **1999**, *40*, 1621.

(41)   Wasserscheid, P., Keim, W., *Angew. Chem., Int. Ed. Engl.* **2000**, *39*, 3773.

(42)   Green, M. J., Cavell, K. J., Skelton, B. W., White, A. H., *J. Organomet. Chem.* **1998**, *554*, 175.

(43)   McGuinness, D. S., Green, M. J., Cavell, K. J., Skelton, B. W., White, A. H., *J. Organomet. Chem.* **1998**, *565*, 165.

(44)   Wang, H. M. J., Lin, I. J. B., *Organometallics* **1998**, *17*, 972.

(45)   Magill, A. M., McGuinness, D. S., Cavell, K. J., Britovsek, G. J. P., Gibson, V. C., White, A. J. P., Williams, D. J., White, A. H., Skelton, B. W., *J. Organomet. Chem.* **2001**, *617*, 546.

(46)   McGuinness, D. S., Cavell, K. J., *Organometallics* **2000**, *19*, 741.

(47)   Dash, R. N., Rao, D. V. R., *J. Indian Chem. Soc.* **1974**, *51*, 787.

(48)   Xu, L. J., Chen, W. P., Bickley, J. F., Steiner, A., Xiao, J. L., *J. Organomet. Chem.* **2000**, *598*, 409.

(49)   Bourissou, D., Guerret, O., Gabbai, F. P., Bertrand, G., *Chem. Rev.* **2000**, *100*, 39.

(50)   Bohm, V. P. W., Herrmann, W. A., *Chem.-Eur. J.* **2000**, *6*, 1017.

(51)   Jeffrey, T., *Chem. Commun.* **1984**, 1287.

(52)   Amatore, C., Jutand, A., *Acc. Chem. Res.* **2000**, *33*, 314.

(53)   Amatore, C., Jutand, A., Suarez, A., *J. Am. Chem. Soc.* **1993**, *115*, 9531.

(54)   Grasa, G. A., Viciu, M. S., Huang, J. K., Zhang, C. M., Trudell, M. L., Nolan, S. P., *Organometallics* **2002**, *21*, 2866.

(55)   Hillier, A. C., Grasa, G. A., Viciu, M. S., Lee, H. M., Yang, C. L., Nolan, S. P., *J. Organomet. Chem.* **2002**, *653*, 69.

(56)   Armarego, W. L. F., Perrin, D. D. *Purification of Laboratory Chemicals*; 4th ed.; Butterworth-Heinemann: Oxford, U.K., 1996.

(57)   Someswara Rao, C., Murty, V. S. N., Tattu, P. K., *Indian J. Chem.* **1981**, *20B*, 1083.

(58)   Brillon, D., *Synth. Commun.* **1990**, *20*, 3085.

(59)   Scheeren, J. W., Ooms, P. H. J., Nivard, R. J. F., *Synthesis* **1973**, 149.

(60)   Chen, Y. T., Jordan, F., *J. Org. Chem.* **1991**, *56*, 5029.

(61)   Barton, D. H. R., Jang, D. O., Jaszberenyi, J. C., *Tetrahedron* **1993**, *49*, 7193.

• Chapter Five •

Oxidative Addition of 2-Substituted Azoliums to Group-10 Metal Zero Complexes

5.1 Introduction

The recent discovery of a facile decomposition route for palladium alkyl carbene complexes[1-4] and subsequent theoretical work[4] led our group to investigate the accessibility of carbene complexes of group 10 metals through the reverse process of oxidative addition.[5,6] Not only does the investigation of oxidative addition provide us with information on how to prevent reductive elimination (Chapters 6–8), but it may also provide information on potential new synthetic pathways to carbene complexes that may not be accessible via other routes.

Utilization of oxidative addition for the formation of carbene complexes is not a new idea. In 1974, Stone and co-workers[7] formed a number of carbene complexes through the oxidative addition of a 2-halothiazolium salt to a number of low valent metals (Scheme 5.1). This has been extended recently to encompass an imidazolin-2-ylide palladium complex through a similar route.[8]

$M^0(PRPh_2)_4$ +

M=Pd,Ni R=Ph
M=Pt, R=Me
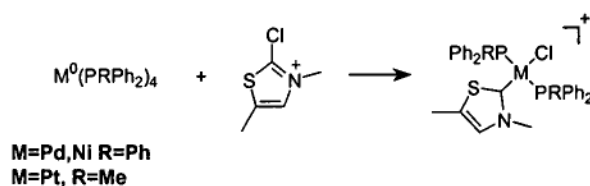
**Scheme 5.1** – Carbene complexes synthesised via oxidative addition

Our recent theoretical and experimental work highlighted the absence of a significant barrier to oxidative addition of 2-hydridoazoliums to group-10 metals, and resulted in the isolation of a number of platinum hydrido carbene complexes (Scheme 5.2).[5,6,9]   Similarly, Crabtree has proposed the existence of a palladium-hydride intermediate formed via oxidative addition of N-pyridylimidazolium to a palladium(0) precursor.[10]

R=Ph, n=4, X=N-CH₃, R'=H
R=Cy, n=2, X=S, R'=CH₃
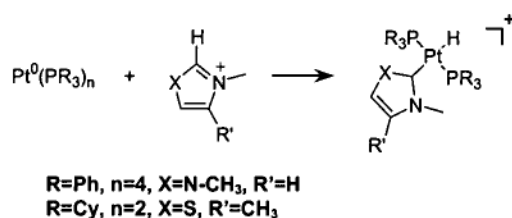
Scheme 5.2 – Recent oxidative addition reactions performed by our group that furnish platinum-hydrido carbene complexes

Theoretical research concerning the activation of carbon-hydrogen (C-H) bonds by metal complexes has been well covered and recently reviewed.[11]   However, information regarding activation of carbon-carbon (C-C) bonds by low valent metals has received comparatively less focus.[12]

Theoretical and experimental work has shown that the auxiliary ligands of low valent metals can influence oxidative-addition/reductive-elimination reaction chemistry significantly.[13-26] The use of a chelating basic phosphine provides a metal zero precursor amenable to oxidative addition.[5,6,22] The high reactivity of these chelated low-valent metal phosphine precursors to oxidative addition has been demonstrated experimentally with zerovalent analogues of nickel[14,27] and platinum[13,25,26] available through established synthetic routes (Scheme 5.3).
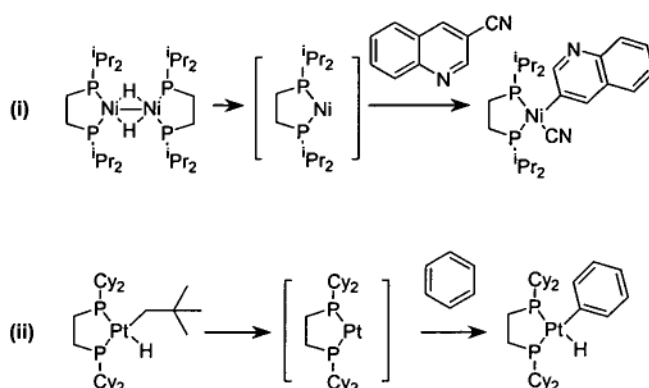
Scheme 5.3 – Reactivity of group 10 metals bearing chelating phosphine ligands

The high activity of these chelated phosphine complexes has been attributed to both a high energy d_π orbital extending generously into space and a low singlet-triplet splitting.[22] The departure from simple phosphines to a chelating basic phosphine has previously shown a benefit for the enthalpy of imidazolium salt oxidative addition (Figure 5.1).[6]
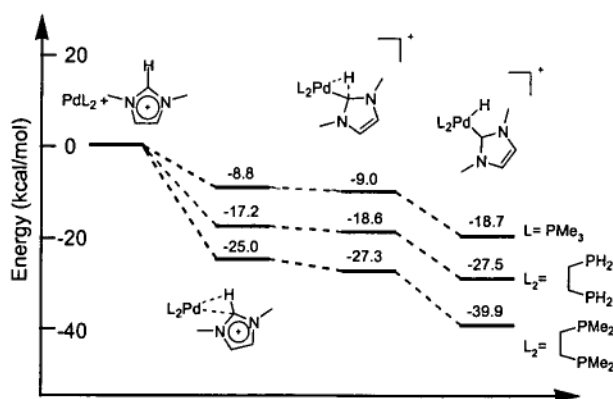
Figure 5.1. Influence of chelation on enthalpy of reaction

In this chapter the activation of C-H, C-C$_{alkyl}$ and C-C$_{aryl}$ bonds by oxidative addition across group 10 zerovalent 1,3-bis(dimethylphosphino)ethane (dmpe) complexes to afford carbene complexes is studied in detail (Scheme 5.4). The influence of sulphur and oxygen heteroatom substitutions for nitrogen in the imidazolium precursor has been surveyed with significant consequences for the barriers to oxidative addition being demonstrated. Where appropriate, reasoning for any trends is provided and the question on whether metal-hydrocarbyl carbene complexes may be accessed through C-C oxidative addition is addressed.

M = Ni, Pd, Pt
X = N-Me, O, S
R = H, Me, (Ph, X=N-Me)
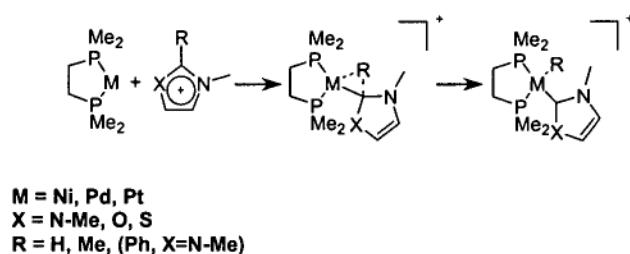
Scheme 5.4 – Reaction scheme that provides the focus of this chapter

5.2 Computational Methods

All geometry optimisations on metal complexes were initially carried out with the B3LYP[28-30] density functional employing a LANL2DZ[31,32] basis set and effective core potential (ECP). The azolium reactants were optimised at the B3LYP/6-31G(d) level and the zerovalent reactants optimized using a compound basis set B3LYP/LANL2DZ:6-31G(d), which showed a considerable improvement on the geometries previously obtained using a smaller basis set.[5,6] The compound basis set treatment involved LANL2DZ on the metal and 6-31G(d) on all other atoms. For optimised geometries harmonic vibrational frequencies were calculated to ascertain the nature of the stationary point and zero-point vibrational energy (ZPVE) and thermodynamic corrections were obtained using unscaled frequencies.

Single-point energies on metal containing systems were calculated at the B3LYP level with the 6-311+G(2d,p) basis set[33-35] on all atoms for the nickel system, a LANL2DZaugmented:6-311+G(2d,p) basis set for palladium complexes (incorporating the LANL2 ECP and the large f-polarized valence basis set of Bauschlicher and co-workers[36] on Pd and the 6-311+G(2d,p) basis set on all other atoms) and a LANL2DZaugmented:6-311+G(2d,p) basis set for platinum complexes (incorporating the LANL2TZ+(3f)[37] basis set of platinum and the 6-311+G(2d,p) basis set on all other atoms). Single point energies of organic molecules (azoliums) were calculated at the B3LYP/6-311+G(2d,p) level of theory. Calculations pertaining to homolytic bond

fission were performed at the ROB3LYP/6-311+G(2d,p)//UB3LYP/6-31G(d) level, which has shown to provide accurate results for such calculations.[38,39]

All energies mentioned throughout the text refer to these final levels of theory and include enthalpy and ZPVE corrections calculated at the optimisation level of theory. Calculations were carried out using the Gaussian 98 suite of programs.[40]

5.3 Results and Discussion

5.3.1 Geometries

The optimised geometries of the reactants (metal zero complexes (Figure 5.1) and

azoliums (Figure 5.2)), precursor complexes (**PC**) (Figure 5.3), transition structures (**TS**)

(Figure 5.4) and products (**PR**) (Figure 5.5) are shown over the following pages.
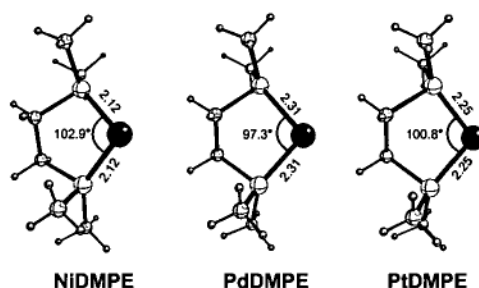
Figure 5.1 – Optimised geometries of metal zero reactants (b3lyp/lanl2dz:6-31G(d))
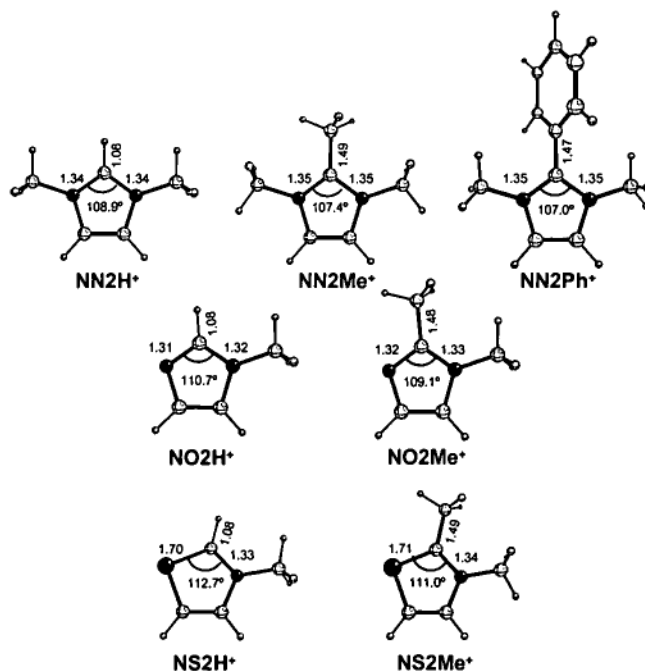
Figure 5.2 – Optimised geometries of azolium reactants (b3lyp/6-31G(d))

Ni_NN2Me⁺(PC)   **Ni_NN2Ph⁺(PC)**   **Ni_NO2Me⁺(PC)**

Ni_NS2H⁺(PC)   **Ni_NS2Me⁺(PC)**
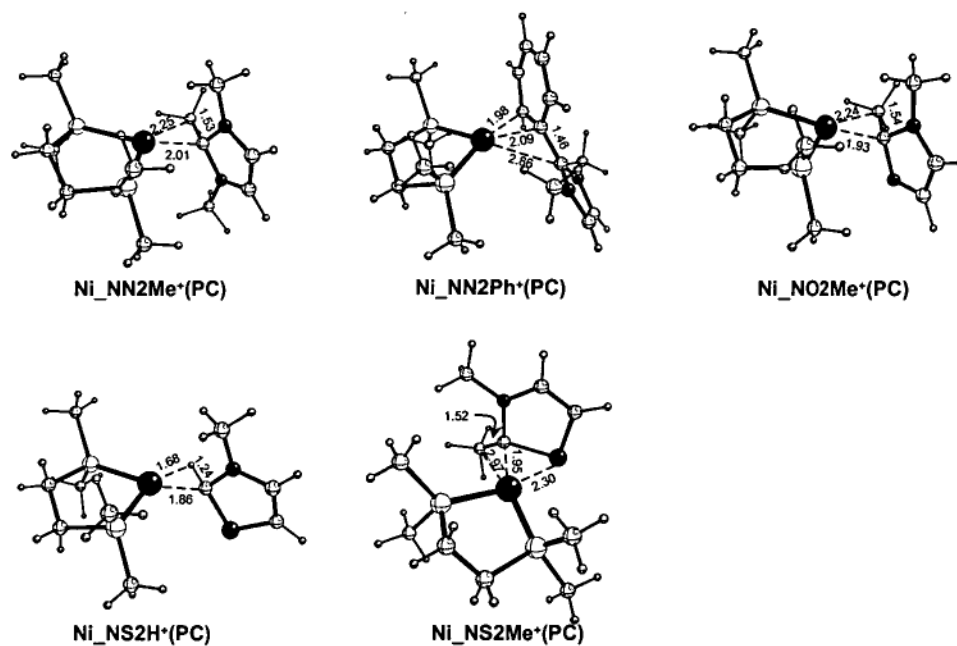
Figure 5.3a – Optimised geometries for nickel precursor complexes (**PC**) (b3lyp/lanl2dz)

Pd_NN2H⁺(PC)   **Pd_NN2Me⁺(PC)**   **Pd_NN2Ph⁺(PC)**

Pd_NO2H⁺(PC)   **Pd_NO2Me⁺(PC)**   **Pd_NS2H⁺(PC)**

Pd_NS2Me⁺(PC)
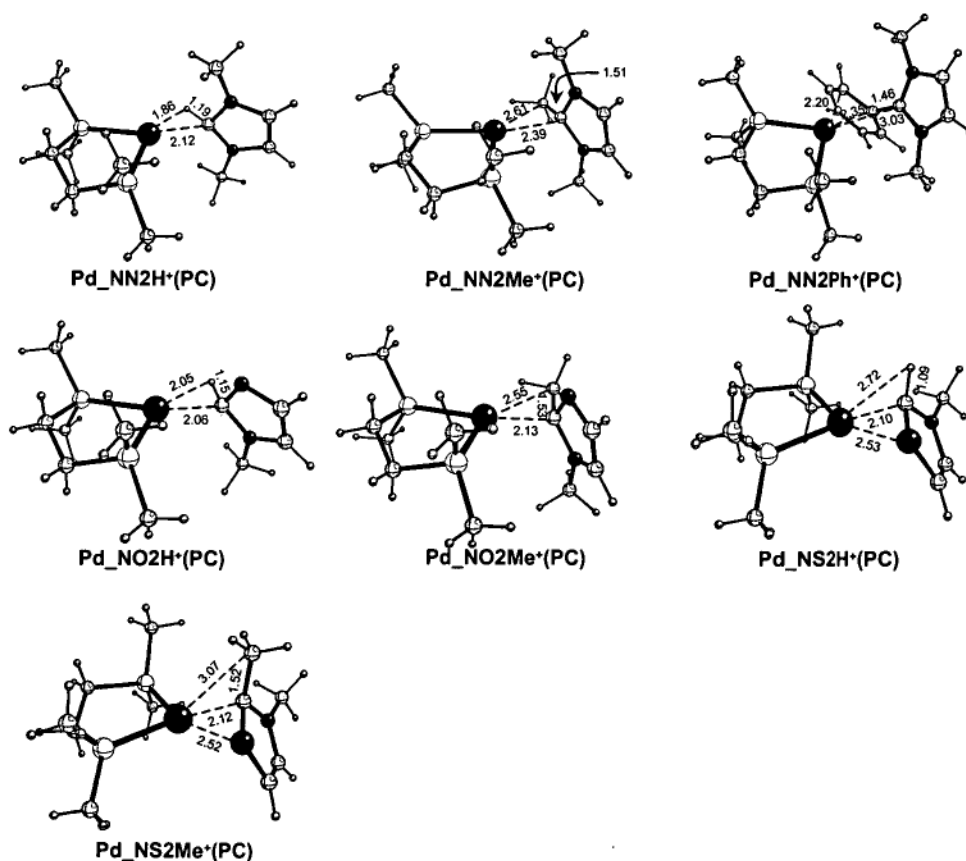
Figure 5.3b – Optimised geometries for palladium precursor complexes (**PC**) (b3lyp/lanl2dz)

Pt_NN2Me⁺(PC)   Pt_NN2Ph⁺(PC)   Pt_NS2Me⁺(PC)

Pt_NO2Me⁺(PC)
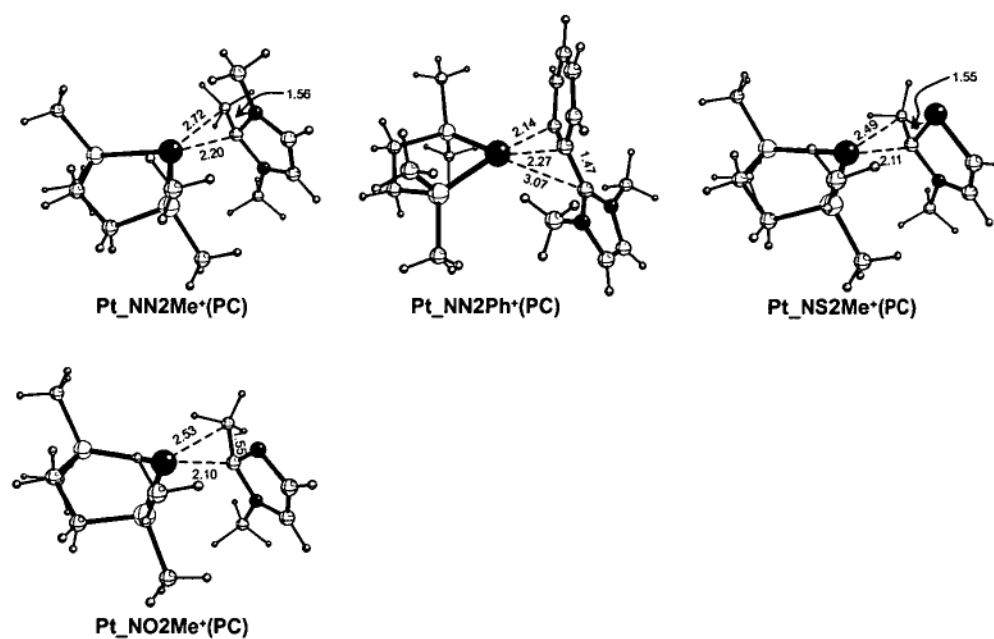
Figure 5.3c – Optimised geometries for platinum precursor complexes (**PC**) (b3lyp/lanl2dz)

Ni_NN2Me⁺(TS)   Ni_NN2Ph⁺(TS)   Ni_NS2H⁺(TS)

Ni_NS2Me⁺(TS)   Ni_NO2Me⁺(TS)

Figure 5.4a – Optimised geometries for nickel transition structures (**TS**) (b3lyp/lanl2dz)

Figure 5.4b – Optimised geometries for palladium transition structures (**TS**) (b3lyp/lanl2dz)

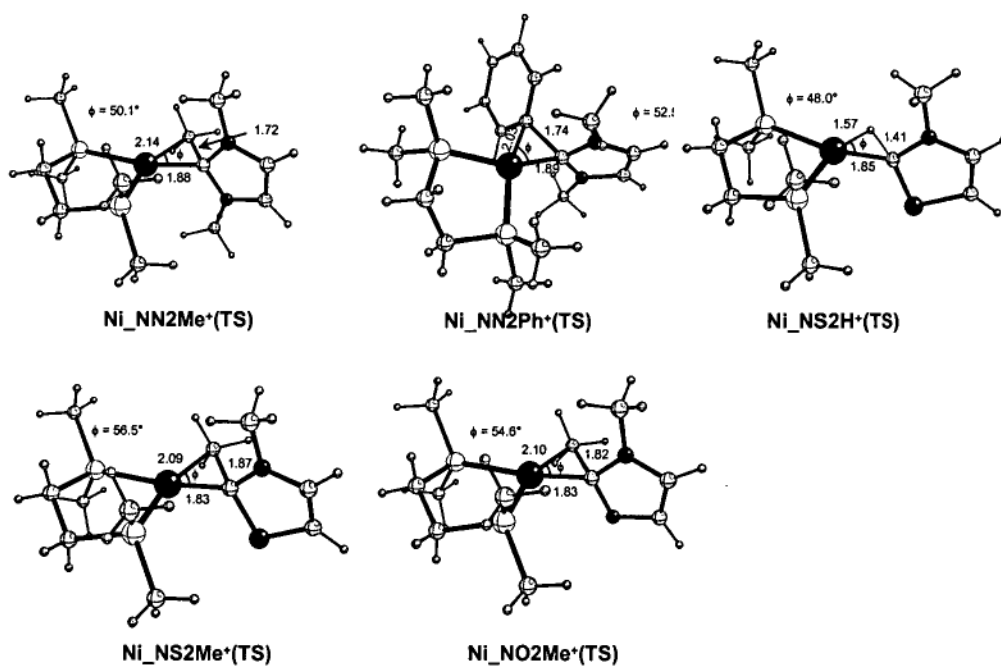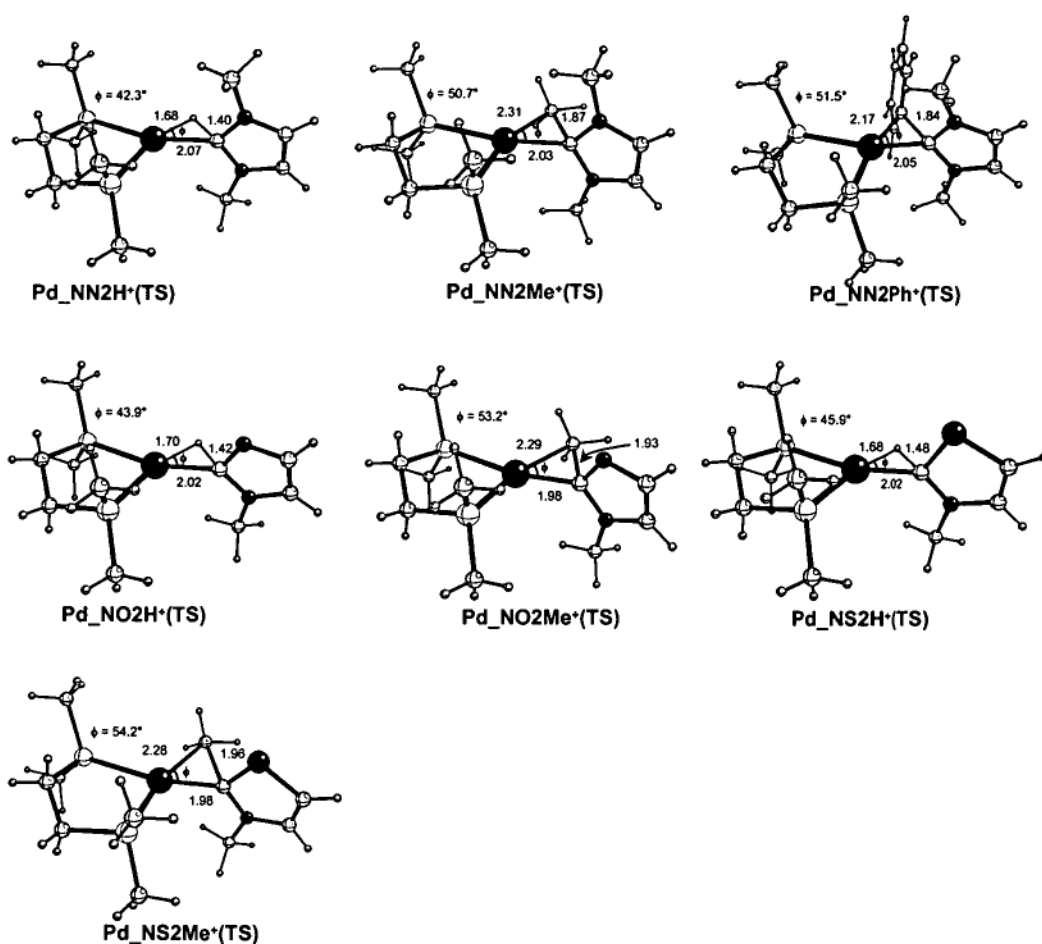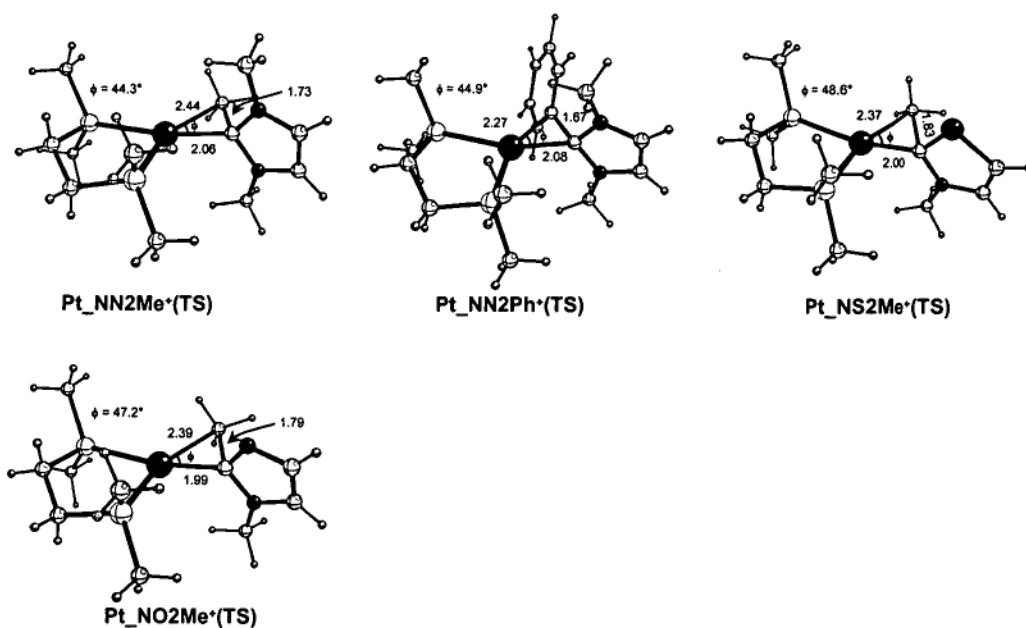**Figure 5.4c** – Optimised geometries for platinum transition structures (**TS**) (b3lyp/lanl2dz)
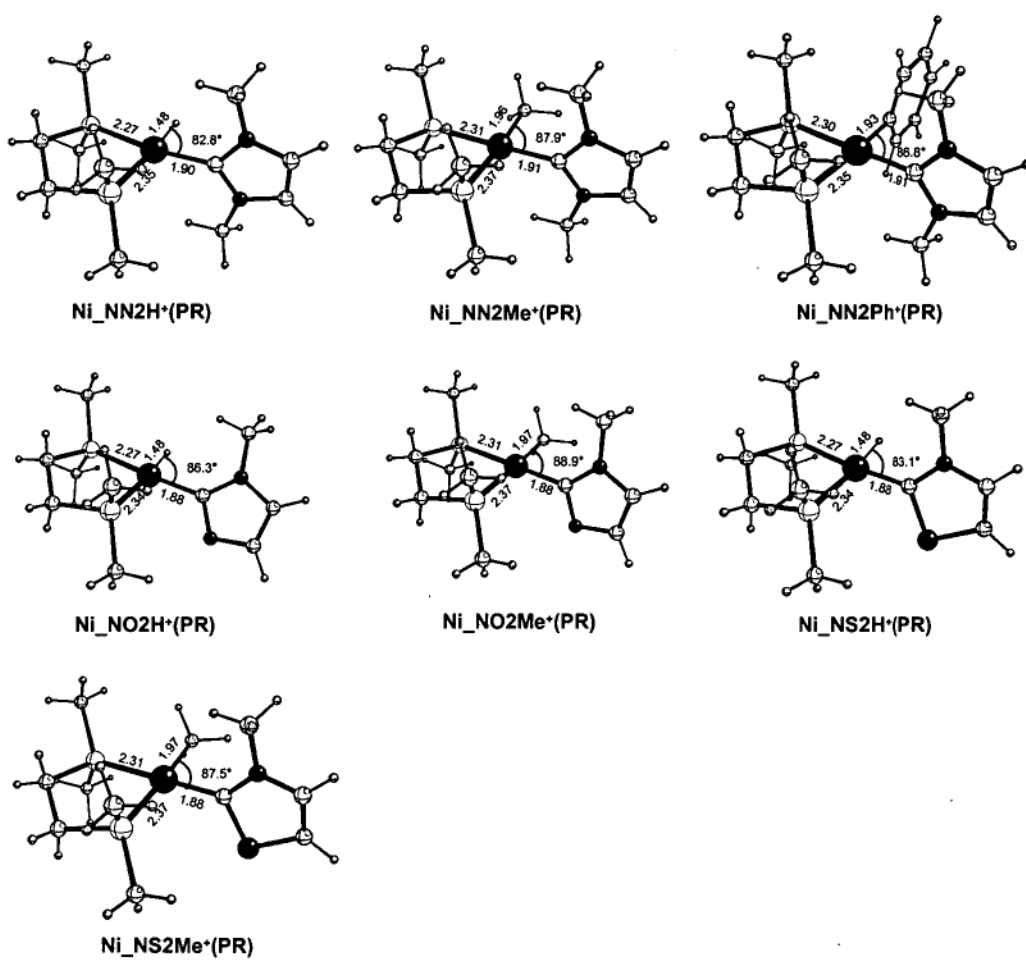
Figure 5.5a – Optimised geometries for nickel products (**PR**) (b3lyp/lanl2dz)
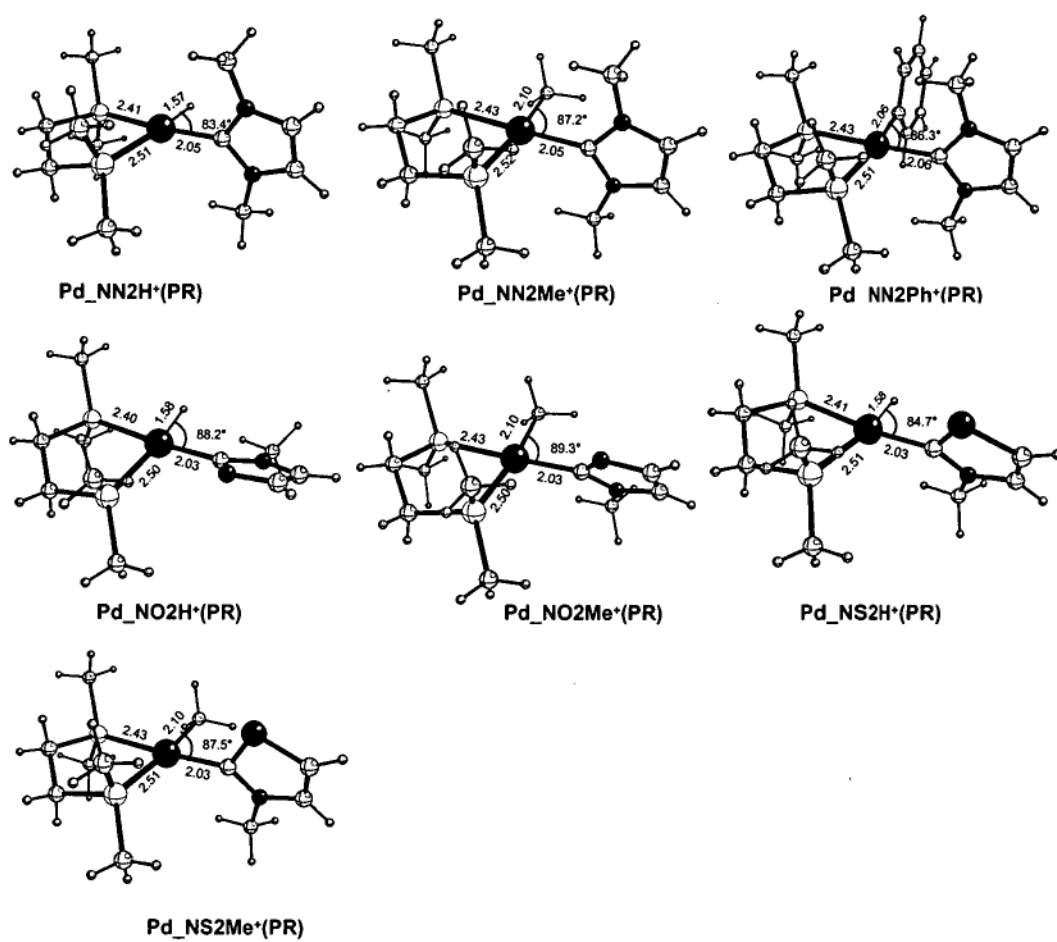
Figure 5.5b – Optimised geometries for palladium products (**PR**) (b3lyp/lanl2dz)

Pt_NN2H⁺(PR)   Pt_NN2Me⁺(PR)   Pt_NN2Ph⁺(PR)

Pt_NO2H⁺(PR)   Pt_NO2Me⁺(PR)   Pt_NS2H⁺(PR)

Pt_NS2Me⁺(PR)
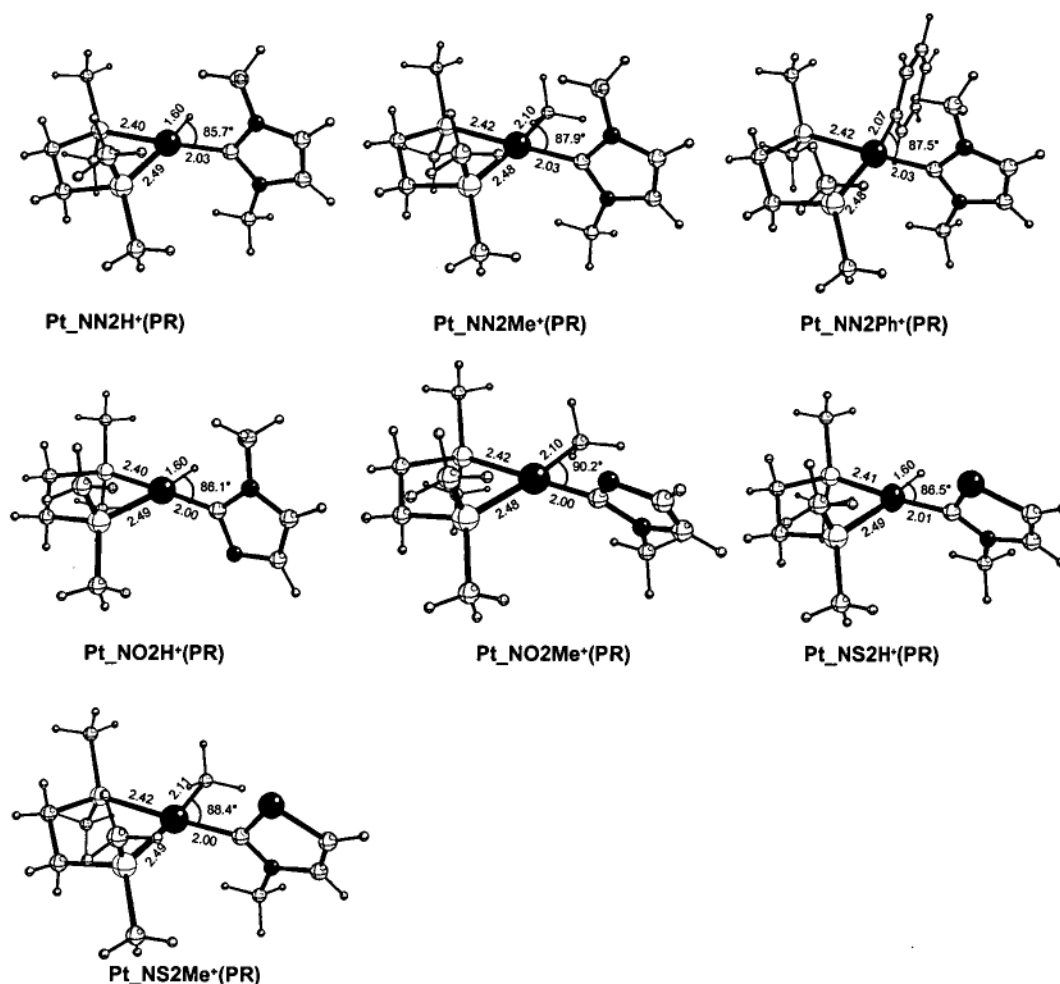
Figure 5.5c – Optimised geometries for platinum products (**PR**) (b3lyp/lanl2dz)

5.3.1.1 Effect of Heteroatom Exchange on Geometries. The steric and electronic differences of nitrogen, oxygen and sulphur have a number of consequences for the geometries on the potential energy surfaces investigated.

The azolium reactants (Figure 5.2) show similar structures despite their different heteroatoms, with the atoms in the five-membered core being co-planar. The length of the C(2)–R bond (R = H, Me, Ph) shows almost no variation upon heteroatom exchange.

Specifically, the length of the C(2)-H bond is constant across the series of azoliums (1.08 Å) and the C(2)-Me bond varies by only 0.01 Å (1.48-1.49 Å).

Precursor complexes for the addition of azolium salts to M^0(dmpe) are shown in Figure 5.3. There is little interaction between the imidazolium salts and the metal centre in the precursor complexes when compared with the corresponding oxazolium and thiazolium species and this will impact on the stabilisation energies (see section **5.3.2**). Taking the palladium-2-methyl system (**Pd_NN2Me$^+$**) as an example, the metal to C(2) azolium bonds are long in imidazole (2.39 Å, **Pd_NN2Me$^+$(PC)**) when compared to thiazole and oxazole (2.12 Å, **Pd_NS2Me$^+$(PC)** and 2.13 Å, **Pd_NO2Me$^+$(PC)**, respectively). This trend is echoed for all metal centres and R-substituents and is likely to be due to the higher steric bulk of imidazole when compared to thiazole and oxazole.

An additional interaction between sulphur and the metal centre is observed for a selection of those metals encountering thiazolium salts (i.e. **Ni_NS2Me$^+$(PC)**, **Pd_NS2H$^+$(PC)** and **Pd_NS2Me$^+$(PC)**). This interaction is facilitated by the lone pair on sulphur and consequently distances between the metal centre and sulphur are decreased (2.30–2.52 Å) relative to the M–S distances in the other precursor complexes (3.15–3.30 Å) with both C(2) and sulphur occupying positions coplanar with PdL$_2$.

The optimised geometries for the transition structures on the oxidative addition pathways are collected in Figure 5.4. Heteroatom exchange appears to have little influence on the geometry of the transition structure. All transition structures exhibit a three-centred interaction that occurs in the ML$_2$ plane conforming to the classical description of oxidative addition. The azolium salt is twisted perpendicular to the plane in all cases, eliminating any previous M–S interaction that may have occurred.

Product geometries (Figure 5.5) are similar despite the differences in the carbene heterocycles. Imidazol-2-ylidene shows slightly elongated M-C(2) bonds (*ca.* +0.03Å) when compared to oxazole and thiazole and the carbene lies almost perpendicular to the plane of the PdL_2 system. In comparison, the oxazole and thiazole carbenes are twisted from perpendicular by up to 58° (for **Pd_NO2H$^+$(PR)**), presumably as a consequence of possessing only one exocyclic ring substituent which results in lessened steric bulk.

5.3.1.2 Influence of 2-R Group Exchange on Geometries. Hydride, methyl and phenyl groups were all considered as 2-position substituents for the reactant azoliums.

The influence of the 2-R groups on the reactant azolium salt geometries is minimal (Figure 5.2). Exchange results in minimal disruption of the five-membered core with differences in bond lengths and angles restricted to 0.01 Å and 2.0° respectively. The phenyl ring in **NN2Ph$^+$** is calculated to twist out-of-plane to minimize steric repulsion.

The influence of the 2-R groups on the geometries of the precursor complexes (Figure 5.3) is much more profound. Increasing the size of the R-group increases the distance of the azolium C(2) from the metal centre significantly. Using the palladium-imidazole system as an example, altering the size of the R-group from H through Me to Ph increases the Pd-C(2) bond from 2.12 Å (**Pd_NN2H$^+$(PC)**) through 2.39 Å (**Pd_NN2Me$^+$(PC)**) to 3.03 Å (**Pd_NN2Ph$^+$(PC)**). This same trend is seen for all metals and for the three types of azolium, although the effect is reduced with thiazolium due to the additional sulphur interaction. Additionally, there exists an additional η^1 M–C$_{aryl}$

interaction with the metal centre in the precursor complexes of all metals with 2-phenylimidazolium (i.e. **Ni_NN2Ph$^+$(PC), Pd_NN2Ph$^+$(PC) and Pt_NN2Ph$^+$(PC)**).

There is little difference in the geometries of the transition structures and products bearing different R-groups (Figure 5.4 and 5.5). The only discernable change is the widening of the C(2)–M–R angle as we extend to larger R-groups to minimise steric repulsion.

5.3.1.3 Influence of Metal Exchange on Geometries. The geometries of reactant zerovalent metal complexes are very similar, with phosphine bite angles approximating 100° (Figure 5.1). Nickel shows significantly shorter metal-phosphorus bond lengths (2.12 Å) in comparison to palladium (2.31 Å) and platinum (2.25 Å).

None of the metals show significant electronic interaction with the incoming azolium at the precursor complex, with the exception of those interacting with sulphur (see previous). The phosphine bite angle reduces by approximately 10° to decrease steric interaction with the incoming azolium. The sterically demanding 2-phenylazoliums promote considerable closing of the phosphine bite angle in the encounter complexes which is reduced to 85.6° and 85.7° for palladium and platinum respectively, with the less flexible nickel bite angle reducing to 89.3°. In comparison to nickel and palladium, platinum shows little tendency to form additional stabilising M-S bonds with incoming thiazolium ligands.

Neither the transition structure nor the product geometries change significantly on the exchange of metal. The geometries are remarkably similar with the only difference

being the bond lengths to nickel, which are consistently shorter by approximately 0.1Å in all cases.

5.3.2 Reaction Energetics

Table 5.1 shows the reaction energetics for all modelled reactions, these values are expressed graphically in Figure 5.6.

Table 5.1. Energetics of Oxidative Addition[a]

	Nickel			Palladium			Platinum		
	S.E.[b]	E_{act}[c]	ΔH[d]	S.E.	E_{act}	ΔH	S.E.	E_{act}	ΔH
NN2H[+]	-	0.0	-45.5	18.5	-2.3	-33.2	-	0.0	-60.9
NO2H[+]	-	0.0	-58.9	29.6	-3.7	-45.2	-	0.0	-70.8
NS2H[+]	40.0	-3.3	-51.5	39.3	12.3	-38.2	-	0.0	-63.9
NN2Me[+]	12.6	3.0	-33.5	3.9	9.5	-21.3	2.2	0.5	-46.7
NO2Me[+]	28.7	3.2	-41.4	16.5	8.7	-28.4	21.4	2.5	-53.8
NS2Me[+]	48.0	26.3	-37.9	31.9	28.4	-25.3	20.8	4.0	-52.0
NN2Ph[+]	20.8	10.7	-31.6	10.5	16.0	-18.6	17.6	13.6	-44.6

[a]All energies are expressed in kcal/mol and are relative to reactants;
[b]Stabilisation Energy = -(energy of precursor complex); [c]E_{act} = (E_{ts} – E_{pc}); [d]ΔH = ($E_{product}$ – $E_{reactants}$)
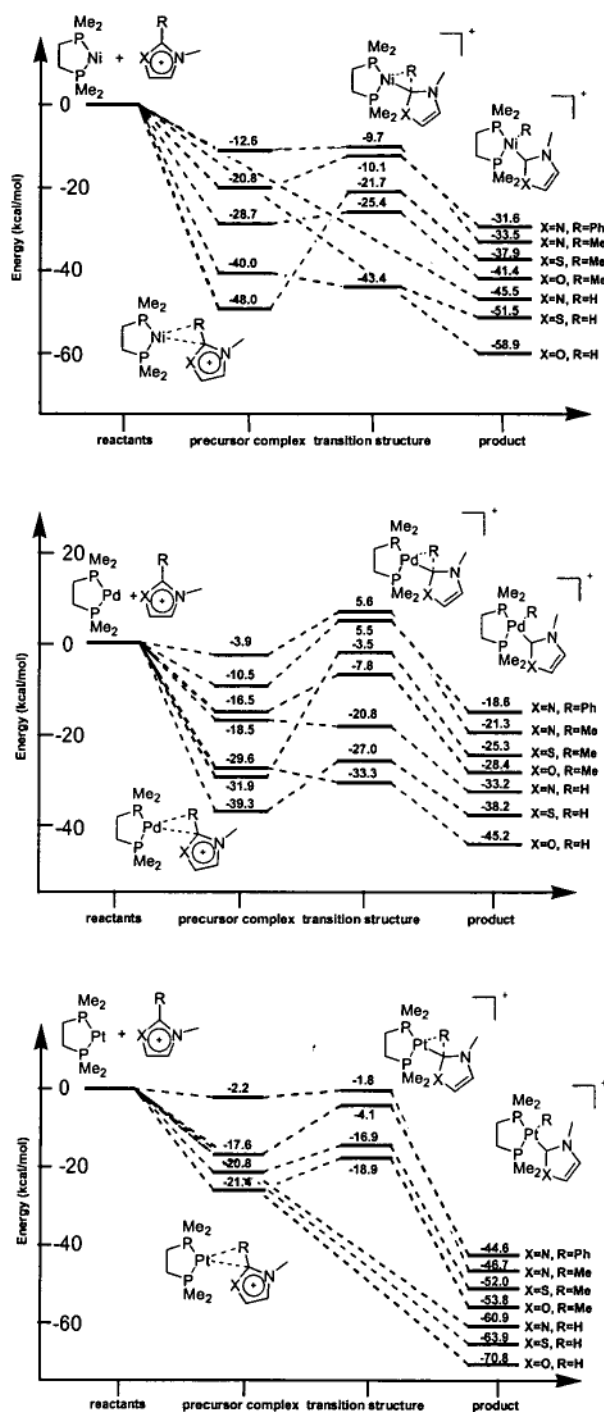
Figure 5.6 – Potential energy surfaces for oxidative addition reactions
(nickel (top), palladium (middle) and platinum (bottom))

5.3.2.1 Effect of Heteroatom Exchange on Potential Energy Surface. The activation energy (E_{act}) for the oxidative addition reaction is dependent on the energies of both the precursor complexes and the transition structures.

Through observing the precursor complexes, it can be seen that the greater steric bulk of the imidazole is likely to be responsible for the hesitant approach and as a consequence the stabilisation energies for imidazolium reactants are very low (Table 5.1, S.E. < 20 kcal/mol) compared to those of oxazolium and thiazolium, which show a more pronounced interaction with the metal centre.

The stabilization energy for the thiazolium reactants is very large due to an additional stabilizing interaction between the metal centre and the electron rich sulphur atom (see Figure 5.3). This energetically beneficial interaction is observed for the 2-methyl substituted thiazolium encountering nickel and palladium (**Ni_NS2Me$^+$(PC)** and **Pd_NS2Me$^+$(PC)**) and 2-hydrido thiazolium encountering nickel (**Ni_NS2H$^+$(PC)**). Consequently, significant stabilization energies of 48.0, 31.9 and 40.0 kcal/mol respectively are observed. Ultimately, these high stabilization energies lead to increased activation energies.

The high energy transition structures seen for imidazolium reactions are likely to be a result of the comparatively strong C(2)-R (C-H, C-C$_{methyl}$ and C-C$_{phenyl}$) bonds which require a greater energy input in order to break compared to the analogous oxazolium and thiazolium bonds (*vide infra*). The high transition structure energies observed for imidazolium are counteracted by the poorly stabilized encounter complex and hence we see activation barriers that, in general, follow the trend thiazolium > oxazolium ≥

imidazolium. Despite the trend for the activation energies, a dissimilar trend is observed

for the reaction enthalpies.

5.3.2.2 Energy of Azolium C(2)-R Bond. It can be seen that within each reaction group

oxazolium salts consistently show the most negative reaction enthalpy, followed by

thiazolium and imidazolium salts. This trend is independent of both the R-group and the

metal.

The oxidative addition of 2-R azoliums involves the breaking of the C(2)-R bond

and the formation of metal-carbene and metal-R bonds. Variation in reaction enthalpy

within each reaction group (for example differences between the enthalpy of oxidative

addition of **NN2Me$^+$** and **NO2Me$^+$**) must therefore be attributed to differences in either

the metal–carbene or azolium–R bond strengths.

Bond energies of the azoliums were evaluated through calculation of the C(2)–R

homolytic bond cleavage energy (Scheme **5.5a-c**).[38,39]
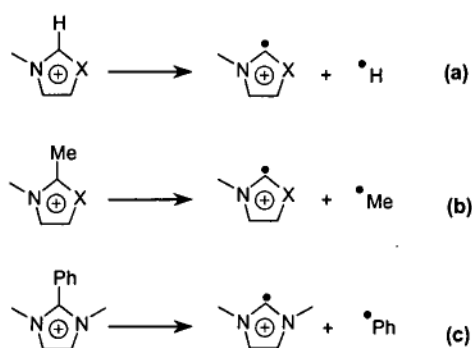
$$X = N-Me, O \text{ and } S$$

Scheme 5.5 – Homolytic bond cleavage of azoliums used to assess bond strength

The results (Table 5.2) show that the energy of cleavage of C–R bonds for the imidazolium-based reactants is high (148-160 kcal/mol) compared to the thiazolium and oxazolium reactants (121-134 kcal/mol).

Table 5.2. Homolytic Bond Cleavage Energies

system	bond broken	bond energy[a] (ROB3LYP//UB3LYP)
NN_2H$^+$	$E(H-C_{carb(NN)})$	158.1
NN_2Me$^+$	$E(CH_3-C_{carb(NN)})$	148.7
NN_2Ph$^+$	$E(Ph-C_{carb(NN)})$	159.7
NO_2H$^+$	$E(H-C_{carb(NO)})$	134.0
NO_2Me$^+$	$E(CH_3-C_{carb(NO)})$	129.9
NS_2H$^+$	$E(H-C_{carb(NS)})$	129.3
NS_2Me$^+$	$E(CH_3-C_{carb(NS)})$	121.1
CH$_4$	$E(H-CH_3)$	111.8
C$_6$H$_6$	$E(H-C_6H_5)$	118.0

[a]Energy in kcal/mol.

Palladium was chosen to investigate the bond strengths of different heterocyclic carbenes to the metal centre. The three-step sequence used to evaluate the palladium-carbene average bond energies (ABEs) is an adaptation of previously published work by Sakaki and co-workers (Figure 5.6).[41-43]
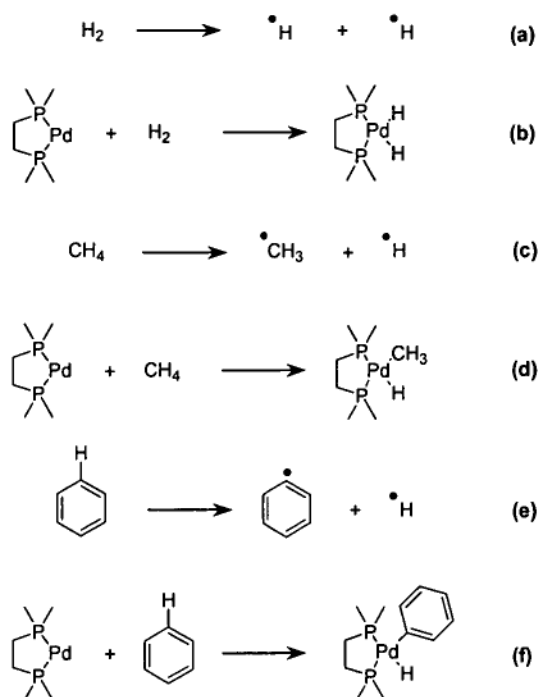
Scheme 5.6. Reaction schemes for calculation of palladium-carbene average bond energy

First, the Pd-H bond energy was evaluated using equations **5.6a** and **5.6b**.

Second, the sum of Pd-H and Pd-C$_{methyl}$ or Pd-C$_{phenyl}$ bond energies was estimated using

equations **5.6c-f**, with Pd-C$_{methyl}$ and Pd-C$_{phenyl}$ bond energies obtained by subtracting the

Pd-H bond energy evaluated in equation **5.6a-b**. Finally, the bond energies of the

palladium-carbene bonds were evaluated using the value of the combined Pd-C(2) and

Pd-R (R = H, CH$_3$ and Ph) (Scheme 5.1, M = Pd) and subtracting the energy of the

appropriate Pd-R bond evaluated previously. All bond-energy results are collected in

Table 5.3.
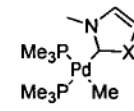
Table 5.3. Evaluation of palladium-carbene average bond energy (ABE)

system	bond broken	average bond energy[a]
PdH$_2$(dmpe)	E(Pd-H)	58.4
Pd(Me)(H)(dmpe)	E(Pd-Me)	38.6
Pd(Ph)(H)(dmpe)	E(Pd-Ph)	49.2
Pd_NN2H$^+$(PR)	E(Pd-C$_{carb(NN)}$)	132.8
Pd_NN2Me$^+$(PR)	E(Pd-C$_{carb(NN)}$)	132.3
Pd_NN2Ph$^+$(PR)	E(Pd-C$_{carb(NN)}$)	130.8
Pd_NO2H$^+$(PR)	E(Pd-C$_{carb(NO)}$)	120.7
Pd_NO2Me$^+$(PR)	E(Pd-C$_{carb(NO)}$)	120.5
Pd_NS2H$^+$(PR)	E(Pd-C$_{carb(NS)}$)	109.1
Pd_NS2Me$^+$(PR)	E(Pd-C$_{carb(NS)}$)	108.8

[a]Energy in kcal/mol.

The bond energies of Pd–H (58.4 kcal/mol), Pd–Me (38.6 kcal/mol) and Pd–Ph (49.2 kcal/mol) have been calculated previously[41] for a similar complex and the results presented here exhibit an identical trend (Pd–H > Pd–Ph > Pd–Me).

Imidazol-2-ylidene exhibits the greatest average bond strength to palladium (132.0 kcal/mol) followed by oxazol-2-ylidene (120.5 kcal/mol) and thiazol-2-ylidene (109.0 kcal/mol). CDA analysis on a model system revealed that the increased metal-carbene bond strength for imidazol-2-ylidene is attributed to enhanced electron donation from the carbene to the metal (**NN** 0.253e, **NO** 0.203e, **NS** 0.172e) (Figure 5.7). Donation is primarily from the carbene lone pair and is accepted by an appropriately aligned orbital on the metal.

system	q_d (donation)[a]	
CDA-MOD (X = N–Me)	0.253	
CDA-MOD (X = O)	0.203	
CDA-MOD (X = S)	0.172	

CDA-MOD
(X = N-Me, O and S)

[a]Values are in electrons and represent the sigma donation from the carbene sp_2 orbital to an appropriately aligned sd-hybrid on the metal

Figure 5.7 – Analysis of the electron donation from carbene to palladium

Although imidazol-2-ylidene was found to have the greatest bond energy to palladium, the exothermicity of the oxidative addition reaction between imidazoliums and palladium precursors is inhibited by their high C(2)–R bond dissociation energies (148-160 kcal/mol). In comparison, the lower cost of breaking the initial bond in oxazolium (**NO2H$^+$** 134 kcal/mol, **NO2Me$^+$** 130 kcal/mol) combined with a generous return on formation of the palladium-oxazolium bond (120.5 kcal/mol) gives oxazoliums the greatest reaction exothermicity. The reasoning applied here for palladium can presumably be transferred to nickel and platinum in order to explain the similar trends.

5.3.2.3 Effect of R-Group on Potential Energy Surface. Oxidative addition of 2-hydridoazoliums across the metal centre consistently gave larger reaction enthalpies in comparison to the methyl and phenyl substituents due to the superior binding energies of hydrides to the metal centre (Section 5.3.2.1).

Large stabilization energies are seen for R = H, where there is reduced steric demand allowing both the carbenic carbon and R group to come into close proximity to the metal centre to form a precursor complex. The energetic barrier of the approaching R = Ph group is reduced somewhat through a stabilizing π-interaction between an aryl carbon adjacent to the CH_3-C_{aryl} being activated in the oxidative addition (Section 5.3.1.2).

The energy of the transition structures is highly dependent on the type of bond being broken. For C-C_{alkyl} and C-C_{aryl} bond breaking, both carbon atoms must undergo a costly tilting process to correctly align themselves for a transition structure interaction.[44] Differences in transition structure energies of between 14 and 20 kcal/mol have been observed going from a C-H to a C-C bond breaking transition state[45] and a similar trend is observed here.

Activation energies were not observed (or were less than zero) in all but one case where R = H. In the remaining case (palladium + 2-hydridothiazolium) a large stabilisation energy attributed to the Pd-S interaction is observed (*vide supra*). This results in a significant barrier of 12 kcal/mol for the oxidative addition. Where transition states could not be found on the potential energy surface, a scan from reactants to products was performed and no energy barrier was observed.

In general the activation energy trend phenyl > methyl > hydrido is observed, with R = H having little or no barrier to oxidative addition. The oxidative addition of R = Ph is impeded by the stable formation of an encounter complex through an additional metal-C_{aryl} bond.

5.3.2.4 Effect of Metal Exchange on Potential Energy Surface. The substitution of metals down the group 10 period makes no difference to the order of enthalpies for each of the azolium salts. In each case the oxazolium salt shows the largest enthalpy of reaction with the 2-phenylimidazolium salt showing the least. Platinum shows the greatest reaction enthalpies followed by nickel, with palladium consistently showing the least negative enthalpies of reaction. A trend based purely on the strength of bonding resulting from the larger orbitals of heavier elements would suggest a Pt > Pd > Ni progression. The oxidative addition to zerovalent palladium is inhibited by its d^{10} ground state, which must be excited to a d^9s^1 configuration in order to fulfill the bonding requirements of the incoming ligands.[24] Platinum and nickel reside in the necessary d^9s^1 ground state and considerable energy must be expended for palladium to attain this state, thus the enthalpy of reaction is decreased proportionally. The average enthalpy difference between palladium and platinum reactions is 25 kcal/mol while the average difference between the enthalpies of nickel and platinum reactions is found to be 12 kcal/mol.

The shorter bond lengths exhibited by nickel in the transition structure (Figure 5.4) presumably results in stabilization of the transition structure through superior orbital overlap in comparison to palladium and platinum. This is indeed observed, and the barrier to oxidative addition is thereby reduced (e.g. E(TS) **X = N, R = Me** : – 9.7 kcal/mol (**M = Ni**), –1.8 kcal/mol (**M = Pt**), 5.6 kcal/mol (**M = Pd**)).

In general the activation energy (E_{act}) trend Pd > Pt = Ni is observed. In agreement with the findings of McGuinness[5,6] the influence of a chelating phosphine on the barrier to oxidative addition is profound for platinum with E_{act} reduced from 33.1 kcal/mol (for oxidative addition of 2-methylimidazolium to Pt(PH₃)₂) to just 0.5

kcal/mol (!) for the analogous chelated system studied here. The barriers for palladium

and nickel are likewise reduced by 22.3 kcal/mol and 13.8 kcal/mol, respectively.

5.4 Conclusions

Using the dmpe chelate provides a metal zero precursor which is significantly high in energy to enable the thermodynamics of the oxidative addition to be favourable, with each reaction pathway studied showing considerable exothermicity. Additionally, the chelate also results in a lowering of the barrier to oxidative addition in line with the results of McGuinness.[5,6]

Though platinum shows the greatest enthalpy of reaction, it is likely that nickel and even palladium will have little trouble proceeding to relatively stable products given the absence of a significant activation barrier. The electronic nature of palladium continues to provide a significant barrier to oxidative addition of carbon-carbon bonds even with this highly engineered system. Platinum appears to provide the best opportunity, with its more appropriate electronic ground state and large flexible orbitals conducive to stabilizing intermediates and products.

Thiazolium based reagents tend to form stable encounter complexes that present a stumbling block to oxidative addition by increasing the activation energy. The lack of a strong stabilising interaction between imidazolium reactants reduces the barrier to oxidative addition to such a degree that C-H bond activation is trivial making C-C bond activation for 2-methylazoliums across platinum an attractive prospect synthetically, with activation energies below 5 kcal/mol. The stable π-interaction in the precursor complex restricts the activation of C-C$_{aryl}$ bonds and additional engineering may be required to

prevent this ancillary interaction from occurring if oxidative addition of this system is to

be achieved synthetically.

5.5 References

(1)   McGuinness, D. S., Green, M. J., Cavell, K. J., Skelton, B. W., White, A. H., *J. Organomet. Chem.* **1998**, *565*, 165.

(2)   McGuinness, D. S., Cavell, K. J., Skelton, B. W., White, A. H., *Organometallics* **1999**, *18*, 1596.

(3)   Magill, A. M., McGuinness, D. S., Cavell, K. J., Britovsek, G. J. P., Gibson, V. C., White, A. J. P., Williams, D. J., White, A. H., Skelton, B. W., *J. Organomet. Chem.* **2001**, *617*, 546.

(4)   McGuinness, D. S., Saendig, N., Yates, B. F., Cavell, K. J., *J. Am. Chem. Soc.* **2001**, *123*, 4029.

(5)   McGuinness, D. S., Cavell, K. J., Yates, B. F., *Chem. Commun.* **2001**, 355.

(6)   McGuinness, D. S., Cavell, K. J., Yates, B. F., Skelton, B. W., White, A. H., *J. Am. Chem. Soc.* **2001**, *123*, 8317.

(7)   Fraser, P. J., Roper, W. R., Stone, F. G. A., *J. Chem. Soc., Dalton Trans.* **1974**, 102.

(8)   Furstner, A., Seidel, G., Kremzow, D., Lehmann, C. W., *Organometallics* **2003**, *22*, 907.

(9)   Duin, M. A., Clement, N., Cavell, K. J., Elsevier, C. J., *Chem. Commun.* **2003**, *3*, 400.

(10)   Grundemann, S., Albrecht, M., Kovacevic, A., Faller, J. W., Crabtree, R. H., *J. Chem. Soc., Dalton Trans.* **2002**, 2163.

(11)   Shilov, A. E., Shul'pin, G. B., *Chem. Rev.* **1997**, *97*, 2879.

(12)   Rybtchinski, B., Milstein, D., *Angew. Chem., Int. Ed. Engl.* **1999**, *38*, 870.

(13)   Hackett, M., Ibers, J. A., Jernakoff, P., Whitesides, G. M., *J. Am. Chem. Soc.* **1986**, *108*, 8094.

(14)   Garcia, J. J., Jones, W. D., *Organometallics* **2000**, *19*, 5544.

(15)   Abis, L., Sen, A., Halpern, J., *J. Am. Chem. Soc.* **1978**, *100*, 2915.

(16)   Ledford, J., Shultz, C. S., Gates, D. P., White, P. S., DeSimone, J. M., Brookhart, M., *Organometallics* **2001**, *20*, 5266.

(17)   Moravskiy, A., Stille, J. K., *J. Am. Chem. Soc.* **1981**, *103*, 4182.

(18)   Matsubara, T., Maseras, F., Koga, N., Morokuma, K., *J. Phys. Chem.* **1996**, *100*, 2573.

(19)   Marcone, J. E., Moloy, K. G., *J. Am. Chem. Soc.* **1998**, *120*, 8527.

(20)   Portnoy, M., Milstein, D., *Organometallics* **1993**, *12*, 1655.

(21)   van Leeuwen, P., Kamer, P. C. J., Reek, J. N. H., Dierkes, P., *Chem. Rev.* **2000**, *100*, 2741.

(22)   Su, M. D., Chu, S. Y., *Inorg. Chem.* **1998**, *37*, 3400.

(23)   Tatsumi, K., Hoffmann, R., Yamamoto, A., Stille, J. K., *Bull. Chem. Soc. Jpn.* **1981**, *54*, 1857.

(24)   Low, J. L., Goddard, W. A., III, *J. Am. Chem. Soc.* **1986**, *108*, 6115.

(25)   Hacket, M., Ibers, J. A., Whitesides, G. M., *J. Am. Chem. Soc.* **1988**, *110*, 1436.

(26)   Hacket, M., Whitesides, G. M., *J. Am. Chem. Soc.* **1988**, *110*, 1449.

(27)   Garcia, J. J., Brunkan, N. M., Jones, W. D., *J. Am. Chem. Soc.* **2002**, *124*, 9547.

(28)   Becke, A. D., *J. Chem. Phys.* **1993**, *98*, 5648.

(29)   Becke, A. D., *Phys. Rev. A.* **1988**, *38*, 3098.

(30)   Lee, C., Yang, W., Parr, R. G., *Phys. Rev. B.* **1988**, *37*, 785.

(31)   Hay, P. J., Wadt, W. R., *J. Chem. Phys.* **1985**, *82*, 299.

(32)   Dunning, T. H., Hay, P. J. *Modern Theoretical Chemistry*; Plenum: New York, 1976; Vol. 3.

(33)   Krishnan, R., Binkley, J. S., Seeger, R., Pople, J. A., *J. Chem. Phys.* **1980**, *72*, 650.

(34)   McLean, A. D., Chandler, G. S., *J. Chem. Phys.* **1980**, *72*, 5639.

(35)   Frisch, M. J., Pople, J. A., Binkley, J. S., *J. Chem. Phys.* **1984**, *80*, 3265.

(36)   Langhoff, S. R., Petterson, L. G., Bauschlicher, C. W., Partridge, H. J., *J. Chem. Phys.* **1987**, *86*, 268.

(37)   Yates, B. F., *J. Mol. Struct. (THEOCHEM)* **2000**, *506*, 223.

(38)   DiLabio, G. A., Pratt, D. A., Lofaro, A. D., Wright, J. S., *J. Phys. Chem. A* **1999**, *103*, 1653.

(39)   Chandra, A. K., Uchimaru, T., *J. Phys. Chem. A* **2000**, *104*, 9244.

(40)   Gaussian 98, Revision A.7, Frisch, M. J., Trucks, G. W., Schlegel, H. B., Scuseria, G. E., Robb, M. A., Cheeseman, J. R., Zakrzewski, V. G., Montgomery, J. A., Jr., Stratmann, R. E., Burant, J. C., Dapprich, S., Millam, J. M., Daniels, A. D., Kudin, K. N., Strain, M. C., Farkas, O., Tomasi, J., Barone, V., Cossi, M., Cammi, R., Mennucci,

B., Pomelli, C., Adamo, C., Clifford, S., Ochterski, J., Petersson, G. A., Ayala, P. Y., Cui,

Q., Morokuma, K., Malick, D. K., Rabuck, A. D., Raghavachari, K., Foresman, J. B.,

Cioslowski, J., Ortiz, J. V., Baboul, A. G., Stefanov, B. B., Liu, G., Liashenko, A.,

Piskorz, P., Komaromi, I., Gomperts, R., Martin, R. L., Fox, D. J., Keith, T., Al-Laham,

M. A., Peng, C. Y., Nanayakkara, A., Gonzalez, C., Challacombe, M., Gill, P. M. W.,

Johnson, B., Chen, W., Wong, M. W., Andres, J. L., Gonzalez, C., Head-Gordon, M.,

Replogle, E. S., Pople, J. A., Gaussian Inc, Pittsburgh, PA, 1998

(41)   Biswas, B., Sugimoto, M., Sakaki, S., *Organometallics* **2000**, *19*, 3895.

(42)   Sakaki, S., Kai, S., Sugimoto, M., *Organometallics* **1999**, *18*, 4825.

(43)   Sakaki, S., Biswas, B., Sugimoto, M., *Organometallics* **1998**, *17*, 1278.

(44)   Low, J. L., Goddard, W. A., III, *Organometallics* **1986**, *5*, 609.

(45)   Blomberg, M. R. A., Siegbahn, P. E. M., Nagashima, U., Wennerberg, J.,
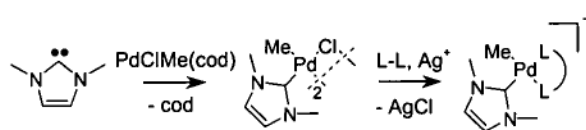
J. Am. Chem. Soc. **1991**, *113*, 424.

• Chapter Six •

Influence of Ring Heteroatoms on the Stability of Palladium Carbene Complexes

6.1 Introduction
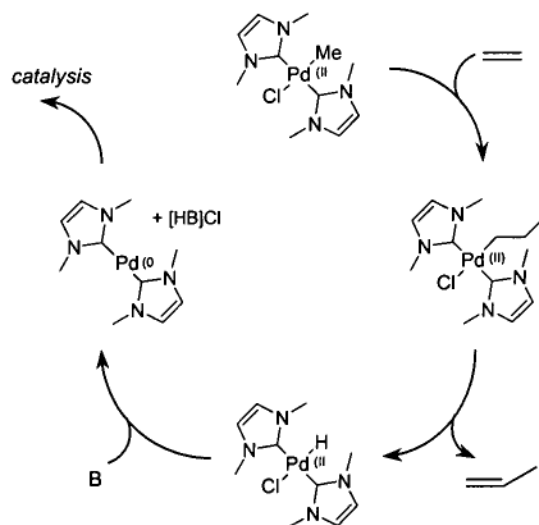
Our synthesis of the first palladium-methyl carbene complexes (e.g. Scheme 6.1)[1] provided fast access to the catalytically active species resulting in catalysts with little or no induction period (Scheme 6.2).[2]


Scheme 6.1 – Synthesis of the first palladium-methyl carbene complex

Scheme 6.2 – Reaction mechanism for active catalyst generation from a palladium-methyl complex

Recently, however, our discovery of a facile decomposition route for hydrocarbyl palladium carbene complexes[2-6] (Scheme 6.3) has instigated both synthetic and theoretical research with the aim of better understanding this unwanted decomposition reaction.
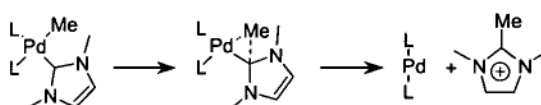
Scheme 6.3 – Unwanted decomposition of complexes via reductive elimination

Diversification of the original imidazol-2-ylidene based ligand has resulted in carbene ligands bearing both saturated backbone systems and heteroatoms other than nitrogen.[7-10]

The dependence of reductive-elimination on the nature of the heterocyclic ring has been recently highlighted. Caddick et al.[11] observed carbene-phenyl reductive-elimination coupling with a saturated NHC system, while an unsaturated system showed no tendency to decompose via this method (Scheme 6.4).
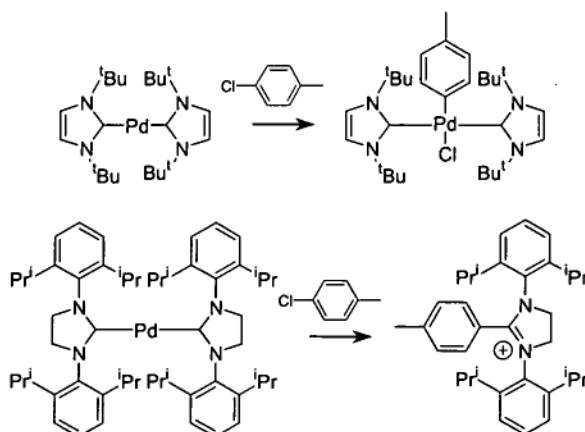
Scheme 6.4 – Decomposition variation based on the type of carbene ligand

The emerging area of heterocyclic carbenes containing heteroatoms other than nitrogen has been comparatively less well explored both synthetically and theoretically. Palladium-based catalysis utilising benzothiazol-2-ylidene ligands has recently exhibited excellent activity in ionic liquids.[12,13] Given the rapid expansion in this area it was of interest to extend our theoretical investigations on the decomposition on hydrocarbyl palladium carbene complexes to include thiazole and oxazole based heterocyclic carbene ligands.

Over the next three chapters research aimed at investigating the influence of various factors upon the decomposition of hydrocarbyl palladium carbene complexes is presented. The focus in this chapter is on the effect of changes to the five-membered core of the heterocyclic carbene on the aforementioned decomposition. The influence both saturation and heteroatom substitution have on the kinetic and thermodynamic nature of the decomposition reaction is investigated. Where appropriate factors that may help to impede this unwanted route are discussed.

6.2 Computational Methods

All geometry optimisations on palladium complexes were carried out with the B3LYP[14-16] density functional employing a LANL2DZ[17,18] basis set and effective core potential (ECP). The azolium reactants were optimised at the B3LYP/6-31G(d) level and the zerovalent product (Pd(dmpe)) optimised using the compound basis set B3LYP/LANL2DZ:6-31G(d), which showed considerable benefits over the basis set employed by McGuinness.[4] For optimised geometries harmonic vibrational frequencies were calculated to ascertain the nature of the stationary point and zero-point vibrational energy (ZPVE) and thermodynamic corrections were obtained using unscaled frequencies.

Single-point energies on palladium containing systems were calculated using a LANL2DZaugmented:6-311+G(2d,p) basis set for palladium (incorporating the LANL2 ECP and the large f-polarized valence bas set of Bauschlicher and co-workers[19] on Pd and the 6-311+G(2d,p) basis set[20-22] on all other atoms). Single point energies of organic molecules (azoliums) were calculated at the B3LYP/6-311+G(2d,p) level of theory. As the peripheral phosphine ligands are to represent pure spectator ligands, palladium–phosphine bond lengths are frozen at 2.48 Å in order to prevent their dissociation under sterically crowded conditions.

All energies mentioned throughout the text refer to these final levels of theory and include enthalpy and ZPVE corrections calculated at the optimisation level of theory. Calculations were carried out using the Gaussian 98 suite of programs.[23]

6.3 Results and Discussion

6.3.1 Free Carbenes

The decomposition route under investigation is shown in Scheme 6.5. As variation in the complexes under investigation is limited to the carbene ligand, any change in reductive elimination behaviour may be attributed to the nature of the carbene. Insight into the more complex process of reductive elimination is likely to be provided through investigation of the individual carbenes isolated from the environment of the complex.

(CX)   (TS)   (PR)

(1) X=N (unsaturated)
(2) X=N (saturated)
(3) X=S (unsaturated)
(4) X=O (unsaturated)
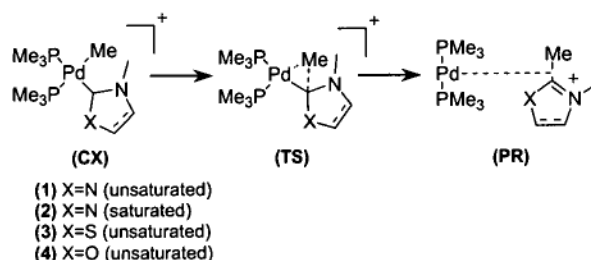
Scheme 6.5 – Decomposition route that provides the focus of this chapter

Despite the apparent differences, the four carbenes (Figure 6.1) show similar geometrical features. The unsaturated carbenes **1-CB** (1,3-dimethylimidazol-2-ylidene) **3-CB** (3-methylthiazol-2-ylidene) and **4-CB** (3-methyloxazol-2-ylidene)) are perfectly planar, while incorporation of the two sp^3 hybridised carbons in the backbone of the saturated imidazole **2-CB** creates a small twist in the ring. Experimental structures containing the imidazol-2-ylidene, imidazolin-2-ylidene and thiazol-2-ylidene cores are

available and compare well to the theoretical results obtained herein. An increase in the

N–C(2)–N valence angle going from imidazol-2-ylidene (**1-CB**, 101.5°) to imidazolin-2-

ylidene (**2-CB**, 105.2°) is associated with the lengthening of the opposing C–C bond

which increases from 1.357 to 1.539 Å due to the absence of double bond character.
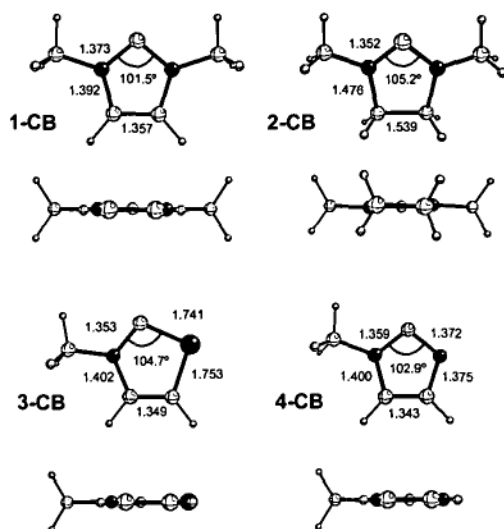
Figure 6.1 – Optimised geometries of azolium reactants (b3lyp/6-31G(d))

The charges observed at C(2) (Table 6.1) are a consequence of the 'push-pull'

characteristics of the adjacent heteroatoms (see Chapter 2). A near neutral charge is

evident at C(2) for **1-CB** (0.10 Mulliken, 0.12 NPA) associated with good σ-donation

from nitrogen to carbon coupled with appreciable π-backdonation from carbon to

nitrogen. Electron delocalisation is limited in the saturated carbene (**2-CB**) and therefore

the occupation of the p_π-orbital is reduced (0.55e) in comparison to its unsaturated

analogue (**1-CB**, 0.65e) where a more fully delocalised π-system exists. Poor π-donation

inherent with oxygen combined with significant electronegativity results in good σ-

withdrawal from C(2) and meagre p_π donation in return. Hence, a positive charge (0.16

Mulliken, 0.29 NPA) along with a reduced p_π-occupation (0.59e) is observed for oxazol-

2-ylidene (**3-CB**) in comparison to **1-CB**. The electropositive nature of sulphur confers a

negative charge on C(2) (–0.12 Mulliken, –0.19 NPA) via donation in both the σ and π

network in thiazol-2-ylidene (**4-CB**). As a result of the appreciable π-donation from

sulphur the C(2) p_π orbital is substantially occupied (0.67e).

Table 6.1. Charges and orbital occupation at C(2)

carbene	charges at C(2)		C(2)(Pπ)[a]
	Mulliken	**NPA**	
1-CB	0.10	0.12	0.65
2-CB	0.15	0.20	0.55
3-CB	0.16	0.29	0.59
4-CB	-0.12	-0.19	0.67

[a]Orbital occupation (electrons)

The variation in the σ and π properties at C(2) of the carbene are of paramount importance. The proposed decomposition transition state[4] (Figure 6.2) utilises both these orbitals and

Figure 6.2 – Three Centred Transition Structure

observed changes in the free carbene orbitals are likely to confer changes in the complex

and transition state.

The proton affinity (Scheme 6.6) may provide an indication of the σ-donating

capacity of the carbene lone pair. All the carbenes show significant tendency to form

their associated azolium salt (Table

6.2), which parallels the assertion that
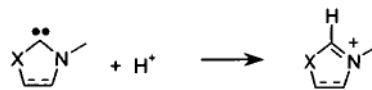
heterocyclic carbenes are among the   **Scheme 6.6** – Proton affinity

most powerful neutral Lewis bases known.[24] The imidazole-based carbenes (**1-CB** and

2-CB) exhibit the greatest proton affinities (–259.5 and –260.1 kcal/mol respectively)

with the heteroatom-substituted carbenes (**3-CB** and **4-CB**) showing a slightly reduced

tendency to form their corresponding salts (–248.8 and –243.7 kcal/mol).

Table 6.2. Proton Affinity[a]

Carbene	ΔH (P.A.)
1-CB	–259.5
2-CB	–260.1
3-CB	–248.8
4-CB	–243.7

[a]Energy in kcal/mol

6.3.2 Complexes

The geometries of the four carbene complexes under investigation (Scheme 6.5 -

CX) are shown in Figure 6.3. The calculated angles and bond lengths are remarkably

similar, with the only significant difference being the carbene twist angle (*i.e.* the angle

between the carbene and PdL$_2$ plane). The imidazol-2-ylidene (**1-CX**) and imidazolin-2-

ylidene (**2-CX**) based complexes show the carbene almost perpendicular to the PdL_2

plane (88.9° and 88.4° respectively). The remaining complexes have the carbene

adopting less perpendicular angles of 83.2° and 69.5° for the thiazol-2-ylidene (**3-CX**)

and the oxazol-2-ylidene (**4-CX**) based complexes respectively.
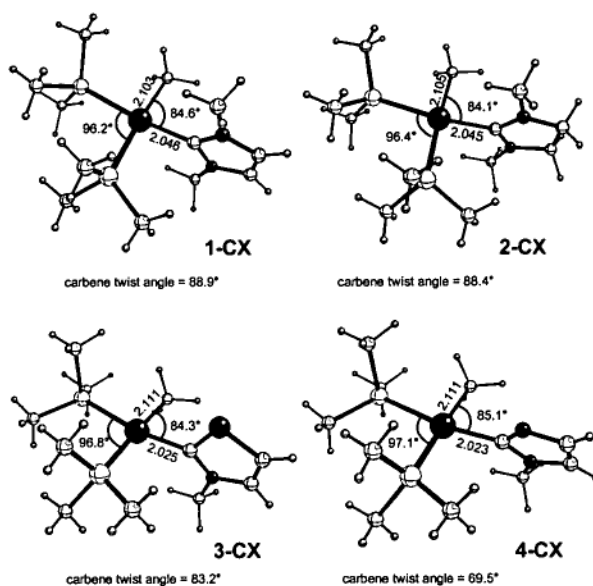
Figure 6.3 – Optimised complex geometries (b3lyp/lanl2dz)

Analysis of the bonding between the carbenic carbon and palladium in the

complexes was undertaken using Frenking and Dapprich's charge decomposition analysis

(CDA).[25] Observation of the value of q_s ($0 < q_s < -0.042$) (Table 6.3) indicates that the

Pd–C(2) bond is a donation-backdonation interaction and therefore CDA methods are

appropriate. Donation from the carbene to palladium (q_d) is significant, ranging from

0.545-0.578 electrons. Back-donation is less significant ($q_b < 0.15e$) and is in accordance

with previous literature accounts regarding carbene bonding behaviour.[26,27] Back-

donation increases slightly on going from the unsaturated system (**1-CX**, 0.127 e) to the

saturated system (**2-CX**, 0.147 e) and may be associated with the lower $C(2)p_\pi$ orbital

occupation for the free carbene **2-CB**. Despite this increase, no evidence of enhanced

back-bonding is observed on investigation of the Pd-C(2) bond lengths. By utilising

natural bond order (NBO) analysis it can be observed that the majority of the donation

(q_d) from the carbene to palladium occurs from the C(2) sp^2 lone pair to an appropriately

aligned sd-hybrid on palladium. The complexes based on imidazole (**1-CX** and **2-CX**)

exhibit the greatest donation to the metal centre (0.578 and 0.573 e) while the thiazole (**3-CX**) and oxazole (**4-CX**) based complexes show a reduction in donation tendency (0.545

and 0.549 e respectively). The donation results (q_d) are in qualitative agreement with the

calculated proton affinities of the individual carbenes.

Table 6.3. Results of charge decomposition analysis[a]

carbene	q_d[b]	q_b[c]	q_r	q_s
1-CB	0.578	0.127	-0.213	-0.042
2-CB	0.573	0.147	-0.215	-0.038
3-CB	0.545	0.137	-0.220	-0.032
4-CB	0.549	0.130	-0.231	-0.021

[a]All values are electrons; [b]Donation from carbene to palladium; [c]Back-donation from palladium to carbene

The difference in palladium-carbene bonding characteristics confers a variation in

charge on the palladium centre through an inductive effect. The calculated charges on

palladium (Mulliken and NPA) are shown in Table 6.4. Appreciable correlation is seen

between CDA(q_d) and the charge on palladium (Figure 6.4, $R^2 = 0.70$ (Mulliken), $R^2 =$

0.97 (NPA)) and similar trends are observed in Chapter 8. Thus the increase in negative

charge observed on palladium is related to the magnitude of the donation from the carbene to palladium calculated via CDA analysis.

Table 6.4. Calculated charges at Pd[a]

| Complex	Mulliken	NPA
1-CX	-0.43	0.30
2-CX	-0.41	0.31
3-CX	-0.37	0.33
4-CX	-0.31	0.33

[a]Units are electrons
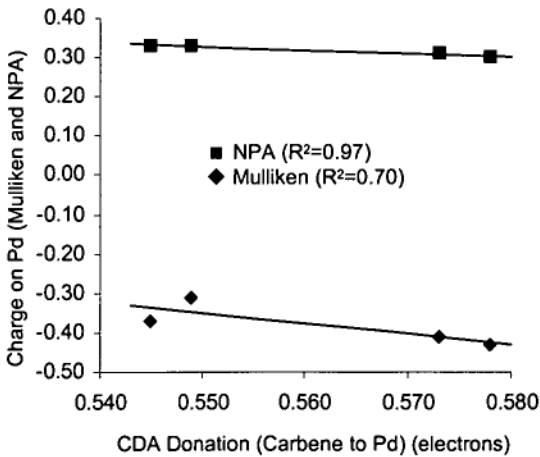
Figure 6.4 – Correlation between donation from carbene (q_d) and charge observed on palladium

6.3.3 Transition Structures

Calculated transition structure geometries (Scheme 6.5 - **TS**) are shown in Figure 6.5. In comparison to the complex geometries, the P(1)-Pd-P(2) angle has opened approximately 10° and the C(2)-Pd-CH$_3$ angle has closed by *ca.* 30°. Elongation of the Pd-CH$_3$ bond is coupled with the concerted formation of the new C(2)-CH$_3$ bond. The carbene twist angle for all transition structures is within 4° of perpendicular. The carbene ligands in the thiazol-2-ylidene (**3-TS**) and oxazole-2-ylidene (**4-TS**) based transition structures twist 3.2° and 26.7° respectively on going from the complex to the transition structure. This is likely to allow good orbital overlap in the proposed transition state (Figure 6.2). Any twist on the carbene away from the perpendicular in the transition structure may minimise overlap between its C(2) p$_\pi$ orbital and the methyl sp^3 orbital.
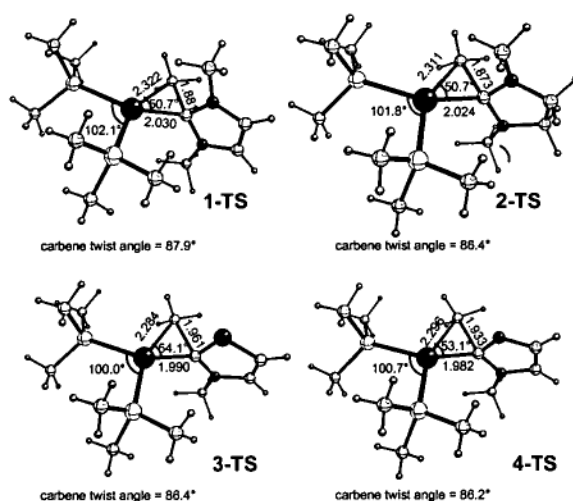

Figure 6.5 – Optimised transition structure geometries (b3lyp/lanl2dz)

The longer C(2)–CH$_3$ bonds observed in both the heteroatom substituted transition structures (**3-TS**, 1.961 Å and **4-TS**, 1.933 Å) identify them as early in

comparison to the imidazole transition states (**1-TS**, 1.881 Å and **2-TS** 1.873 Å) and are

expected to be associated with lower activation barriers in accordance with Hammond's

postulate.[28]

6.3.4 Potential Energy Surfaces

The potential energy surface for the reductive elimination (Scheme 6.5) is shown

in Figure 6.6.
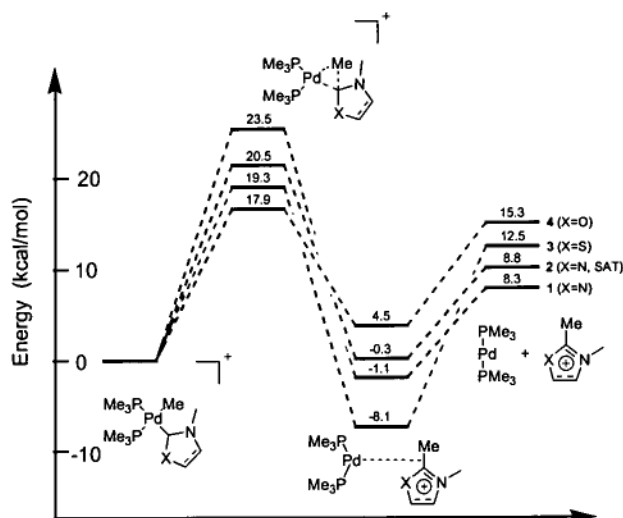
Figure 6.6 – Potential energy surface for reductive elimination (Scheme 6.5)

Imidazol-2-ylidene (**1**), imidazolin-2-ylidene (**2**) and thiazol-2-ylidene (**3**) all

show exothermic reactions for their products while the oxazol-2-ylidene pathway (**4**) is

endothermic by 4.5 kcal/mol. The considerable stability of the thiazol-2-ylidene based

product (**3-PR**) can be attributed to an additional stabilising interaction between

palladium and sulphur (Figure 6.7, see also Chapter 5). While the imidazole based

products (**1-PR** and **2-PR**) show the newly formed -olium salt to be planar and distant

(> 3 Å) from palladium, the leaving salts in **3-PR** and **4-PR** show considerable interaction with the palladium centre and are non-planar. Additionally, the existence of short Pd-C(2) bonds in **3-PR** and **4-PR** may suggest the reaction is better described as methyl-migration rather than reductive elimination for these two pathways.[29]
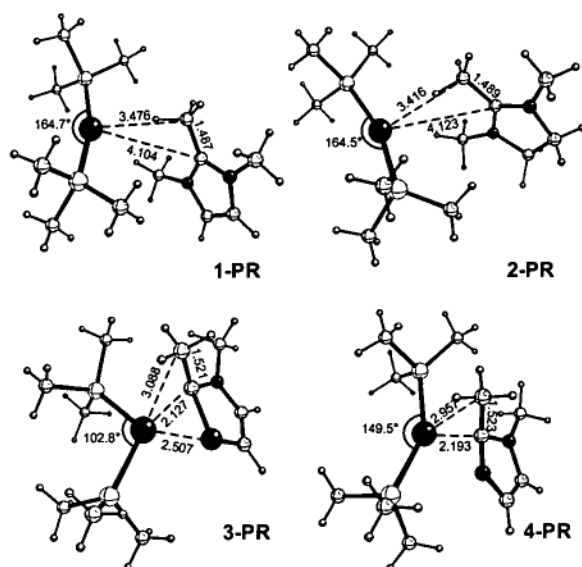
Figure 6.7 – Optimised product geometries (b3lyp/lanl2dz)

As a thermodynamic driving force exists for three out of four of the decomposition pathways, the kinetic barrier may be the sole factor preventing decomposition of the complexes. The imidazol-2-ylidene based complex (**1-CX**) shows the greatest barrier (E_{act}) to decomposition at 23.5 kcal/mol. The remaining complexes (**2-CX**, **3-CX** and **4-CX**) show reduced kinetic stability with barriers of 20.5, 19.3 and 17.9 kcal/mol respectively.

6.3.5 Influence of the Carbene Twist Angle

At first glance it may seem intuitive that the lower barriers observed for the substituted heteroatom pathways (**3** and **4**) are related to the twist angle exhibited by the carbene in the complex. To determine if this was the case, investigation of the same reaction was undertaken with the carbene twist angle fixed at 90° for the complex and transition structure. The results for the 'fixed' pathway are collected in Table 6.5. Those complexes that showed little deviation from the perpendicular in the relaxed case (*i.e.* **1-CX** and **2-CX**) showed little change in E_{act} (< 0.2 kcal/mol). The remaining complexes (**3-CX, 4-CX**) showed a small reduction in their activation barriers (0.9 and 0.7 kcal/mol respectively) primarily associated with the energy required to rotate the carbene twist angle in the complex to perpendicular.

Table 6.5. Fixed carbene twist angle energies[a]

Pathway	Rel E[b] (complex)	E_{act}	ΔE_{ac}
1	+0.1	23.3	-0.2
2	+0.0	20.7	+0.2
3	+0.8	18.4	-0.9
4	+0.6	17.2	-0.7

[a]Energy in kcal/mol; [b]Energy of fixed complex relative to relaxed complex

Utilising a model complex (Figure 6.8) the palladium-carbene bonding scheme was investigated for both thiazol-2-ylidene and oxazol-2-ylidene based complexes (**3-**

MOD and **4-MOD**).   Table 6.6 shows the variation in the donation (q_d) and back-donation (q_b) as a function of the carbene twist angle (45°-90°).
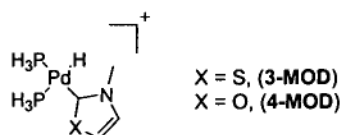
Figure 6.8 – Model complexes for CDA analysis

Table 6.6. CDA donation and back-donation *vs.* carbene twist angle (CTA)

Complex	CTA[a]	q_d[b]	q_b[c]
3-MOD	45	0.532	0.102
	60	0.536	0.105
	75	0.539	0.109
	90	0.541	0.110
4-MOD	45	0.544	0.101
	60	0.545	0.103
	75	0.546	0.106
	90	0.546	0.108

[a]CTA = Carbene twist angle; [b]CDA donation from carbene to palladium; [c]CDA backdonation from palladium to carbene

As the main bonding sp^2 orbital on the carbene is spherically symmetric about the Pd-C(2) axis, little bonding variation is observed as the bond is rotated. From the CDA data it is difficult to rationalise why thiazole and oxazole based carbene ligands adopt a

twist angle that is tilted toward the PdL_2 plane. Though the energy benefit is small ($\Delta H < 1$ kcal/mole), it still seems favourable in lieu of steric hindrance from exocyclic ring substituents for the carbene to adopt a non-perpendicular twist angle. Consequently, reduced carbene twist angles are observed as we move to the less bulky exocyclic ring substituents (oxazol-2-ylidene < thiazol-2-ylidene < imidazol-2-ylidene).

It is important to note from the previous section however, that the carbene twist angle appears to have little influence on the E_{act} of decomposition.

6.3.6 Origins of the Activation Energy (Decomposition)

A correlation between the activation energy (decomposition) and the charge observed on palladium is observed here (Figure 6.9). It is known that cationic palladium carbene complexes show increased rates of reductive elimination compared to neutral complexes[2,6] and the findings reported here parallel this.
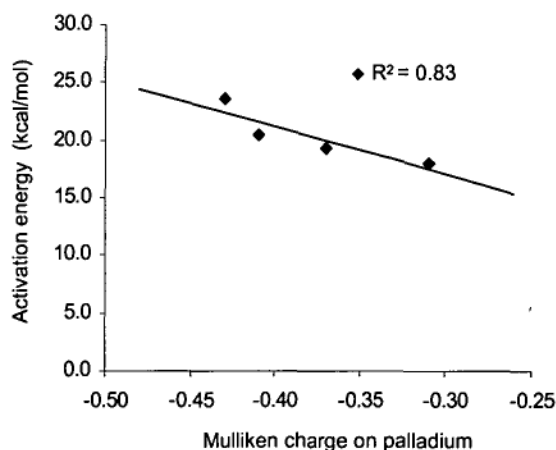
Figure 6.9 - Charge on palladium vs E_{act} (decomposition)

Given the proposed transition structure for the reductive elimination reaction (Figure 6.2) it is not surprising that the p_π orbital occupancy of the carbene has an effect on the activation energy. The relation between the p_π orbital and the nature of the transition state has been documented in previous literature.[4] The occupation of the p_π orbital in the complex and transition structure is shown in Table 6.7.

Table 6.7. Variation of carbene p_π occupation[a]

pathway	C(2) p_π(CX)	C(2) p_π(TS)
1 (NN)	0.82	0.89
2 (NN_SAT)	0.72	0.83
3 (NS)	0.82	0.89
4 (NO)	0.74	0.84

[a]Gaussian98 NBO orbital occupations

The occupations compare qualitatively to those in the free carbene, seemingly validating our initial premise that the estimation of the properties of the carbene in the complex can be achieved through observing the free carbene. The occupation of the p_π orbital increases slightly on going from the free carbene to the complexed carbene, which is as a result of an increase in ring aromaticity.[30,31] Reduced p_π occupation in **2-TS** (0.83e) appears to lead to a more stable transition structure and consequently a lower barrier to decomposition. This same relationship has been observed for NHCs and HCs with Ge and Si.[29] Although the p_π occupation in the thiazole-based transition structure (**3-TS**, 0.89 e) is identical to that of **1-TS** (0.89 e), the reduced activation barrier (19.3

kcal/mol) is likely to be associated with the inferior σ-donating ability of thiazol-2-ylidene. The oxazole based pathway (4) exhibits neither of the attributes believed to be associated with decomposition stability. It exhibits reduced p_π occupation in the transition state (0.84 e) accompanied with poorer σ-donation resulting in a barrier of just 17.9 kcal/mol. Despite this, 4-**CX** may have an additional benefit given that the product is mildly thermodynamically unstable.

6.4 Conclusions

Using DFT, an investigation into the relationship between the heteroatoms in the carbene ring to the decomposition behaviour of the corresponding hydrocarbyl-palladium complexes has been carried out. The proton affinity of the individual carbenes showed good qualitative correlation with the σ-donating ability of the carbene toward palladium.

The carbene twist angle in the thiazole- (83.2°) and oxazole-based (69.5°) complexes were twisted toward the PdL_2 plane in comparison to those of imidazole, which adopted an almost perpendicular arrangement. It is likely that the non-perpendicular geometry is associated with a balance between electronic preference for an acute carbene twist angle combined with a steric preference for the perpendicular arrangement. As the steric influence of the exocyclic ring substituents decreases, the carbene twist angle becomes more acute (*i.e.* less perpendicular). Despite the differences in the geometries of the complexes, the carbene twist angle was found to play little role in the activation energy.

The main contributors to the height of the activation barrier were found to be the σ-donation of the carbene and the occupation of the carbene carbon p_π orbital. Strong σ-donation and a filled π-orbital lead to a high barrier for reductive elimination (*i.e.* less facile decomposition). These stabilising attributes were observed in the imidazol-2-ylidene case, which possessed a barrier of 23.5 kcal/mol. The reduced σ-donation and a comparatively empty p_π orbital in the oxazol-2-ylidene case resulted in a reduced barrier

to decomposition (17.9 kcal/mol) but this pathway has the benefit of thermodynamic stability of the product (ΔH = +4.5 kcal/mol). Those complexes exhibiting only one of the attributes required for stabilization had activation energies lying mid-way between those previously described (imidazolin-2-ylidene 20.7 kcal/mol, thiazol-2-ylidene 18.4 kcal/mol). With respect to the enthalpies of reaction, the imidazol(in)e based carbene ligands show a slight exothermic reaction (ΔH = –1.1 kcal/mol and –0.3 kcal/mol for imidazole-2-ylidene and imidazolin-2-ylidene, respectively), with the thiazol-2-ylidene pathway show a greater reaction enthalpy (ΔH = –8.1 kcal/mol) as a result of a stabilising Pd–S interaction in the product.

The observed behaviour of the complexes toward reductive elimination can be correlated with the nature of the isolated carbene ligand. Occupancies and characteristics of the orbitals associated in the decomposition transition state can be extrapolated from observables derived from the free carbene. Therefore, monitoring of the free carbene can provide considerable insight in to its behaviour when it forms part of a complex.

6.5 References

(1)   Green, M. J., Cavell, K. J., Skelton, B. W., White, A. H., *J. Organomet. Chem.* **1998**, *554*, 175.

(2)   McGuinness, D. S., Green, M. J., Cavell, K. J., Skelton, B. W., White, A. H., *J. Organomet. Chem.* **1998**, *565*, 165.

(3)   McGuinness, D. S., Cavell, K. J., *Organometallics* **2000**, *19*, 4918.

(4)   McGuinness, D. S., Saendig, N., Yates, B. F., Cavell, K. J., *J. Am. Chem. Soc.* **2001**, *123*, 4029.

(5)   Magill, A. M., McGuinness, D. S., Cavell, K. J., Britovsek, G. J. P., Gibson, V. C., White, A. J. P., Williams, D. J., White, A. H., Skelton, B. W., *J. Organomet. Chem.* **2001**, *617*, 546.

(6)   McGuinness, D. S., Cavell, K. J., Skelton, B. W., White, A. H., *Organometallics* **1999**, *18*, 1596.

(7)   Arduengo, A. J., Goerlich, J. R., Marshall, W. J., *Liebigs Ann.-Recl.* **1997**, 365.

(8)   Alder, R. W., Butts, C. P., Orpen, A. G., *J. Am. Chem. Soc.* **1998**, *120*, 11526.

(9)   Merceron, N., Miqueu, K., Baceiredo, A., Bertrand, G., *J. Am. Chem. Soc.* **2002**, *124*, 6807.

(10)   Arduengo, A. J., Goerlich, J. R., Marshall, W. J., *J. Am. Chem. Soc.* **1995**, *117*, 11027.

(11)   Caddick, S., Hitchcock, P. B., *Organometallics* **2002**, *21*, 4318.

(12)   Calo, V., Del Sole, R., Nacci, A., Schingaro, E., Scordari, F., *Eur. J. Org. Chem.* **2000**, 869.

(13)   Calo, V., Nacci, A., Lopez, L., Mannarini, N., *Tetrahedron Lett.* **2000**, *41*, 8973.

(14)   Becke, A. D., *J. Chem. Phys.* **1993**, *98*, 5648.

(15)   Becke, A. D., *Phys. Rev. A.* **1988**, *38*, 3098.

(16)   Lee, C., Yang, W., Parr, R. G., *Phys. Rev. B.* **1988**, *37*, 785.

(17)   Hay, P. J., Wadt, W. R., *J. Chem. Phys.* **1985**, *82*, 299.

(18)   Dunning, T. H., Hay, P. J. *Modern Theoretical Chemistry*; Plenum: New York, 1976; Vol. 3.

(19)   Langhoff, S. R., Petterson, L. G., Bauschlicher, C. W., Partridge, H. J., *J. Chem. Phys.* **1987**, *86*, 268.

(20)   Krishnan, R., Binkley, J. S., Seeger, R., Pople, J. A., *J. Chem. Phys.* **1980**, *72*, 650.

(21)   McLean, A. D., Chandler, G. S., *J. Chem. Phys.* **1980**, *72*, 5639.

(22)   Frisch, M. J., Pople, J. A., Binkley, J. S., *J. Chem. Phys.* **1984**, *80*, 3265.

(23)   Gaussian 98, Revision A.7, Frisch, M. J., Trucks, G. W., Schlegel, H. B., Scuseria, G. E., Robb, M. A., Cheeseman, J. R., Zakrzewski, V. G., Montgomery, J. A., Jr., Stratmann, R. E., Burant, J. C., Dapprich, S., Millam, J. M., Daniels, A. D., Kudin, K. N., Strain, M. C., Farkas, O., Tomasi, J., Barone, V., Cossi, M., Cammi, R., Mennucci,

B., Pomelli, C., Adamo, C., Clifford, S., Ochterski, J., Petersson, G. A., Ayala, P. Y., Cui,

Q., Morokuma, K., Malick, D. K., Rabuck, A. D., Raghavachari, K., Foresman, J. B.,

Cioslowski, J., Ortiz, J. V., Baboul, A. G., Stefanov, B. B., Liu, G., Liashenko, A.,

Piskorz, P., Komaromi, I., Gomperts, R., Martin, R. L., Fox, D. J., Keith, T., Al-Laham,

M. A., Peng, C. Y., Nanayakkara, A., Gonzalez, C., Challacombe, M., Gill, P. M. W.,

Johnson, B., Chen, W., Wong, M. W., Andres, J. L., Gonzalez, C., Head-Gordon, M.,

Replogle, E. S., Pople, J. A., Gaussian Inc, Pittsburgh, PA, 1998

(24)   Herrmann, W. A., Kocher, C., *Angew. Chem., Int. Ed. Engl.* **1997**, *36*,

2163.

(25)   Dapprich, S., Frenking, G., *J. Phys. Chem.* **1995**, *99*, 9352.

(26)   Green, J. C., Scurr, R. G., Arnold, P. L., Cloke, F. G. N., *Chem. Commun.*

1997, 1963.

(27)   Herrmann, W. A., Runte, O., Artus, G., *J. Organomet. Chem.* **1995**, *501*,

C1.

(28)   Hammond, G. S., *J. Am. Chem. Soc.* **1955**, *77*, 334.

(29)   McGuinness, D. S., Yates, B. F., Cavell, K. J., *Organometallics* **2002**, *21*,

5408.

(30)   Boehme, C., Frenking, G., *Organometallics* **1998**, *17*, 5801.

(31)   Tafipolsky, M., Scherer, W., Ofele, K., Artus, G., Pedersen, B., Herrmann,

W. A., McGrady, G. S., *J. Am. Chem. Soc.* **2002**, *124*, 5865.

• Chapter Seven •

# Influence of Geometry on the Stability of Palladium Carbene Complexes

7.1 Introduction

Reductive elimination from d^8 square planar complexes is known to be sensitive to orientation of both the spectator ligands and leaving groups.[1,2] The influence of the spectator ligand bite-angle on reductive elimination has been the subject of both experimental and theoretical studies in recent times.[3-6] Widening of the spectator bite-angle conveys a dramatic increase in the rate of reductive elimination. Moloy identified a 10^4-fold increase in the rate of reductive elimination of alkyl cyanides on going from the chelating phosphine ligand diphos (bite-angle = 85°) to DIOP (bite-angle = 100°).[6] Similar trends have been identified for the decomposition of methyl-palladium carbene complexes, with those complexes bearing bulky phosphine ligands (and presumably large phosphine bite-angles) exhibiting more facile decomposition.[7]

An initial theoretical study by our group into the effect of chelation on oxidative addition of imidazolium salts to palladium also revealed associated reductive elimination information.[8,9] Constraining the phosphine bite angle to 82.4° via chelation (with diphosphinoethane) resulted in a small increase in the barrier to reductive elimination from 22.4 kcal/mol for the non-chelated case (bite angle = 97.6°) to 23.1 kcal/mol. Additionally, the exothermic reductive elimination in the bisphosphine case (ΔH = −3.7 kcal/mol) shifted to endothermic (ΔH = +15.8 kcal/mol) on the incorporation of the chelate.

The effect of re-orienting the leaving groups on reductive elimination is less well known. Incorporation of chelating side-arms as exocyclic ring substituents in

NHC complexes can have a significant effect on the orientation of the carbene with respect to the PdL$_2$ plane. Experimental observations have found carbene twist angles ranging from *ca.* 90° for those bearing considerable bulk on nitrogen to *ca.* 0° for those constrained in an inflexible chelate system (Figure 7.1).[10-13] The involvement of an essentially planar transition state for reductive elimination from four-membered palladium complexes is generally accepted (Figure 7.2), and only recently have alternatives been suggested based on theoretical results.[14] With chelation, and hemi-labile inclusions in NHC complexes being common, rarely would the orientation of the ideal transition state proposed by McGuinness *et al.*[7], where the carbene is perperdicular to the PdL$_2$ plane, be achieved in reality.
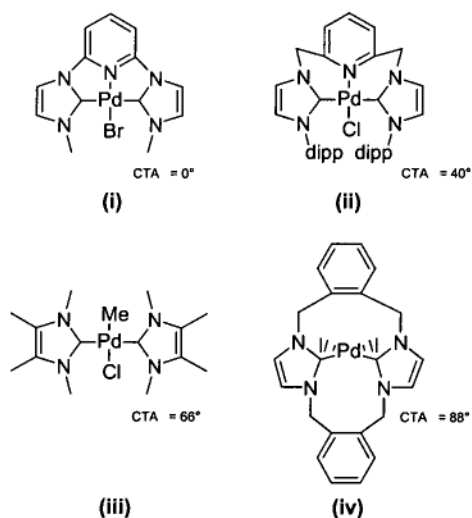
Figure 7.1 – Carbene twist-angles (CTA)
of experimentally isolated palladium-carbene complexes[10-13]
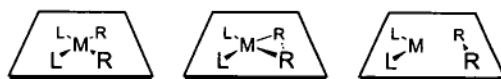
Figure 7.2. Classical in-plane reductive elimination

Palladium complexes where the carbene adopts a near-zero carbene twist angle have shown considerable experimental stability, and corresponding calculations have revealed a transition structure orientation that deviates considerably from what is considered ideal.[15]

In this chapter density functional theory is utilised to investigate the influence of both the spectator bite-angle and the carbene twist angle on the reductive elimination of 1,2,3-trimethylimidazolium from palladium bisphosphine complexes. Where appropriate, reasoning is provided for the trends observed and methods aimed at engineering hydrocarbyl-palladium carbene complexes for enhanced stability are suggested.

7.2 Computational Methods

All geometry optimisations of palladium complexes were carried out with the B3LYP[16-18] density functional employing a LANL2DZ[19,20] basis set and effective core potential (ECP). The azolium reactants were optimised at the B3LYP/6-31G(d) level and the zerovalent reactants (Pd(dmpe)) optimised at the compound basis set B3LYP/LANL2DZ:6-31G(d), which showed considerable benefits over the previous basis set employed by McGuinness.[7] For optimised geometries harmonic vibrational frequencies were calculated to ascertain the nature of the stationary point and zero-point vibrational energy (ZPVE) and thermodynamic corrections were obtained using unscaled frequencies.

Single-point energies on palladium containing systems were calculated using a LANL2DZaugmented:6-311+G(2d,p) basis set for palladium (incorporating the LANL2 ECP and the large f-polarized valence basis set of Bauschlicher and co-workers[21] on Pd and the 6-311+G(2d,p) basis set[22-24] on all other atoms). Single point energies of organic molecules (azoliums) were performed at the B3LYP/6-311+G(2d,p) level of theory. As the peripheral phosphine ligands are to represent pure spectator ligands, palladium–phosphine bond lengths are frozen at 2.48 Å in order to prevent their dissociation under sterically crowded conditions.

All energies mentioned throughout the text refer to these final levels of theory and include enthalpy and ZPVE corrections calculated at the optimisation level of theory. Calculations were carried out using the Gaussian 98 suite of programs.[25]

7.3 Results and Discussion

7.3.1 Bite-Angle Effects

The reaction scheme used to determine the effect of auxiliary bite-angle on methyl-palladium carbene complexes is shown in Scheme 7.1. The angles used (80°–130°) were chosen to span the range of commonly available chelating ligands.[3,4]

A = 80°, 90°, 100°, 110°, 120° and 130°
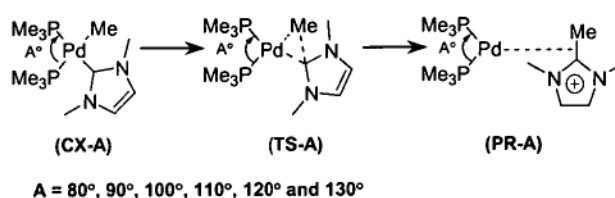
Scheme 7.1. Reductive elimination reaction with variation in the phosphine bite-angle

7.3.1.1 Complexes. Optimised geometries for the complexes (Scheme 7.1 **CX-A**) are shown in Figure 7.3. Despite the increase in auxiliary bite angle the four ligands remain coplanar with the central palladium atom with the sum of bond angles (SBA) around the metal centre close to 360° (Table 7.1).

Narrowing of the P-Pd-C(2) angle (Table 7.1) absorbs a significant proportion of the increase in bite-angle, while narrowing of the CH_3-Pd-C(2) angle absorbs less than 20% of the increase. On going from A = 80° to A = 130° the decrease in CH_3-Pd-C(2) angle is just 10°.
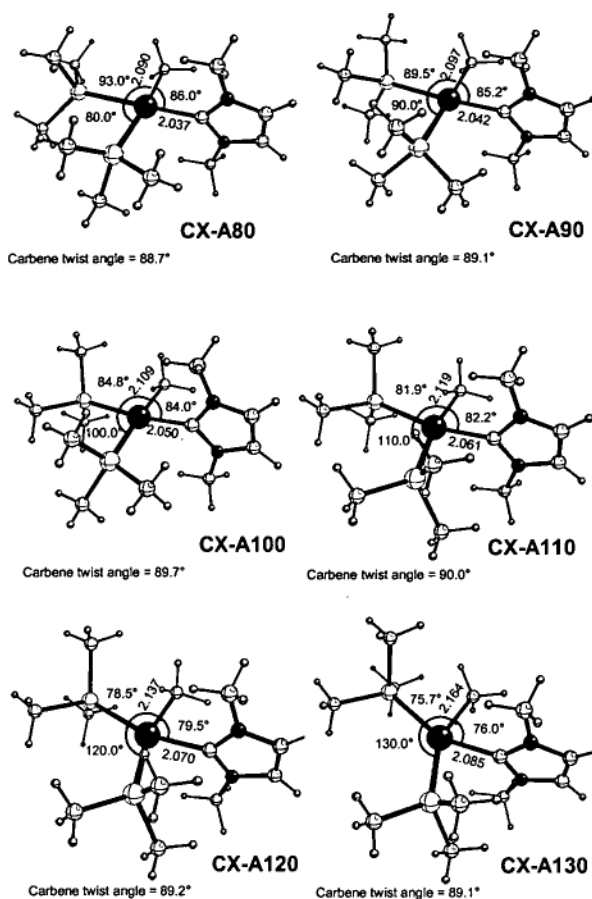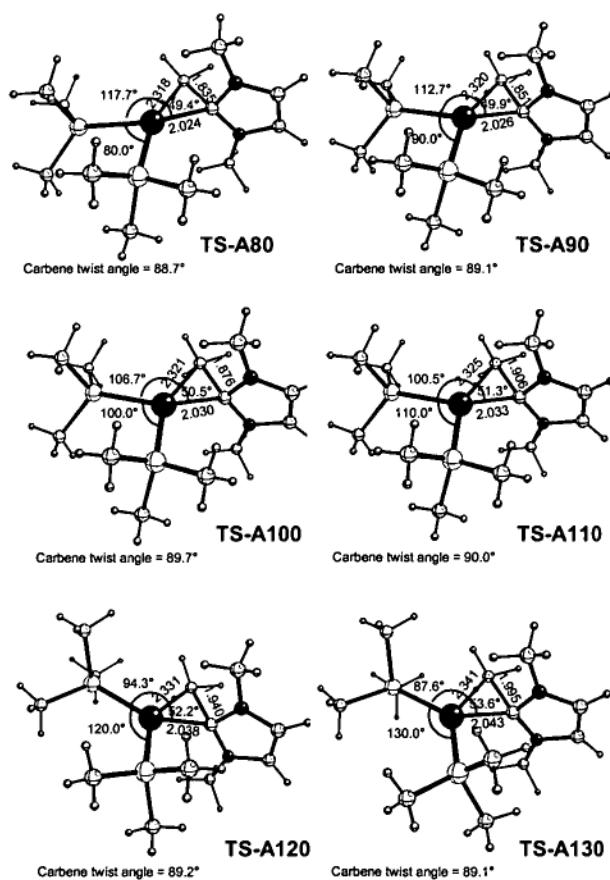
Figure 7.3. Optimised geometries of differing bite-angled complexes (**CX-A**)

Table 7.1. Absorption of increase in bite-angle[a]

Complex	SBA(Pd)[b]	%decrease in angle (w.r.t. CX-A80)		
		P-Pd-CH$_3$	CH$_3$-Pd-C$_2$	P-Pd-C$_2$
CX-A80	360.9	-	-	-
CX-A90	360.0	35%	10%	55%
CX-A100	360.0	40%	10%	50%
CX-A110	360.1	35%	10%	55%
CX-A120	360.0	35%	15%	50%
CX-A130	360.0	35%	20%	45%

[a]Shows the extent of opening of the other angles around palladium when the phosphine bite angle is increased;
[b]Sum of bond angles around palladium (360° indicates planar)

Further strain relief between the carbene and methyl group may be achieved via elongation of both the Pd-CH$_3$ and Pd-C(2) bonds. An increase in the Pd-CH$_3$ bond of 0.074 Å is observed between **CX-A80** (2.090 Å) and **CX-A130** (2.164 Å), while a similar increase (0.048 Å) is evident for the Pd-C(2) bond (**CX-A80** 2.037 Å, **CX-A130** 2.085 Å). In each case, the carbene twist angles are twisted approximately 90° with respect to the PdL$_2$ plane.

7.3.1.2 Transition Structures. Optimised geometries of the transition structures (Scheme 7.1 **TS-A**) are shown in Figure 7.4.

Figure 7.4. Optimised geometries of differing bite-angled transition structures (TS-A)

The coplanarity of the ligands and the central palladium in all structures indicate the classical in-plane form of reductive elimination from square-planar

complexes is observed (Figure 7.2). Increasing the auxiliary bite-angle results in no narrowing of the opposite CH_3-Pd-C(2) angle, in fact a slight increase of 4.2° is observed. Elongation of Pd-CH_3 (2.318 Å to 2.341 Å), Pd-C(2) (2.024 Å to 2.043 Å) and consequently, C(2)-CH_3 (1.835 Å to 1.995 Å) bonds, is observed on going from **TS-A80** to **TS-A130**.

The carbene twist angle remains essentially unchanged from that in the associated complexes, indicating the likelihood of a transition structure akin to that proposed by McGuinness *et al.*[7](see also Chapter 6).

7.3.1.3 Products. Optimised geometries calculated for the products (Scheme 7.1 **PR-A**) are collected in Figure 7.5.
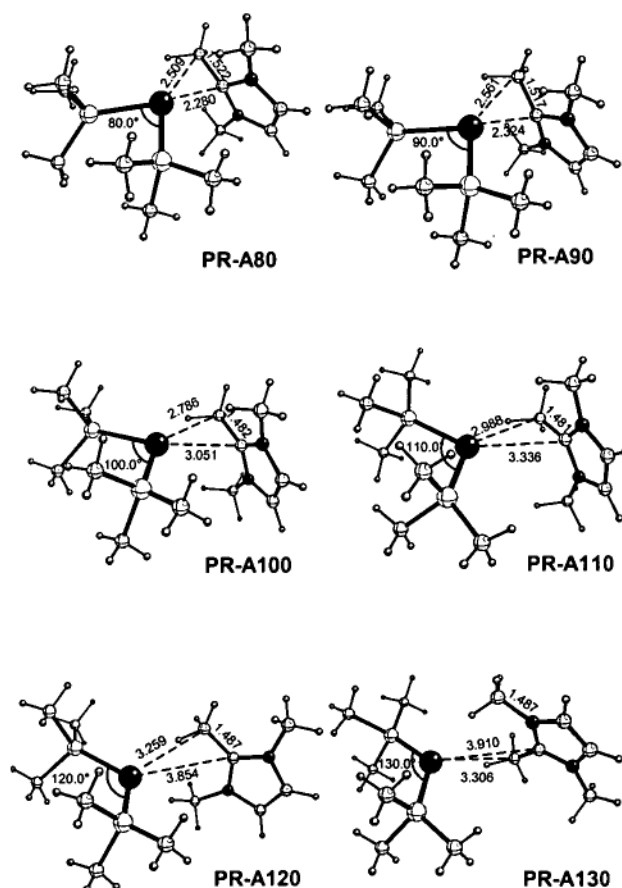
Figure 7.5. Optimised geometries of differing bite-angled products (**PR-A**)

As the auxiliary bite-angle is increased, the PdL_2 fragment shows a reduced interaction with the imidazolium salt. This is indicated through both a move toward sp^2 hybridisation of C(2) and the large Pd-C(2) distances observed for the larger bite-angles. The carbene carbon is essentially sp^2 hybridised when the auxiliary bite-angle is $\geq 100°$ (Table 7.2; SBA(C(2)) = 360.0) while **PR-A80** and **PR-A90** show distortion toward sp^3 hybridisation (SBA(C(2)) = 348.8 and SBA(C(2)) = 350.3 respectively) indicating that there is still a residual bonding interaction between palladium and the C(2) carbon.

Table 7.2. Sum of bond angles (SBA) about C(2) in **PR-A**

structure	SBA (C(2))
PR-A80	348.8°
PR-A90	350.3°
PR-A100	359.6°
PR-A110	360.0°
PR-A120	360.0°
PR-A130	360.0°

An elongation of the Pd-C(2) bond (2.280 Å to 3.910 Å), combined with a rotation of the bond out of the PdL_2 plane on going from **PR-A80** to **PR-A130** are likely to be strain reducing measures aimed at preventing interaction between the auxiliary ligands and the imidazolium ring.

Despite the interactions observed between palladium and C(2) in the products with smaller bite angles, these interactions appear to have little influence on the enthalpy of reaction. With reference to the separated fragments on the potential energy surface (Figure 7.6) the stabilisation energies observed for the products range from –11.8 kcal/mol (A = 130°) to –17.4 kcal/mol (A = 80°), which indicates enhanced interaction with the palladium centre for the smaller bite-angles.
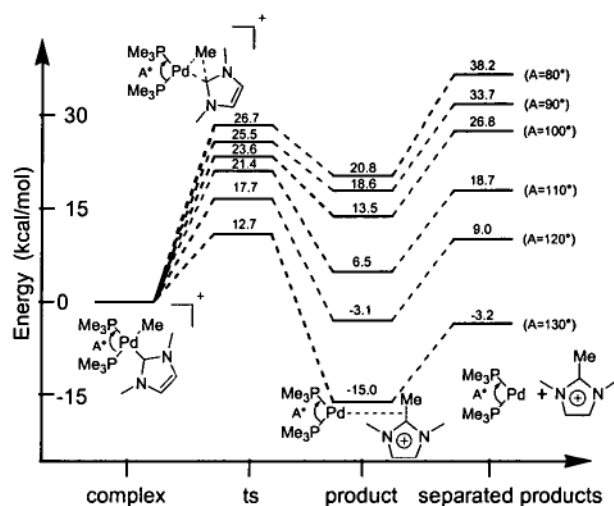

Figure 7.6. Potential energy surface for changes in phosphine bite-angle

This additional interaction is of little benefit in terms of stabilising the product as the enthalpy of the reaction is primarily controlled by the relative stabilities of the PdL$_2$ fragments. Constraining the bite angle from the ideal geometry (*ca.* 180°) results in an increase in energy of the d$_\pi$ orbital and hence an associated destabilisation of the PdL$_2$ fragment. Consequently, only the complexes with large auxiliary bite-angles show a thermodynamic preference for products (A = 120° ΔH = –3.1 kcal/mol, A = 130° ΔH = –15.0 kcal/mol). In contrast, A = 80° exhibits a very endothermic reaction (ΔH = +20.8 kcal/mol). In fact, the systems where the bite-

angle is less than 110° will prefer oxidative addition of imidazolium in preference to reductive elimination in the absence of a significantly high activation barrier.

7.3.1.4 Barriers to Reductive Elimination. The activation energies for the investigated pathways encompass a large range from the readily attainable 12.7 kcal/mol (A = 130°) to 26.7 kcal/mol (A = 80°) (Figure 7.6). By observing the relative energies of the complex and transition structure (Figure 7.7) it can be seen that the relative decrease in E_{act} as the auxiliary bite-angle increases is associated with a destabilisation of the initial complex with respect to the transition structure.
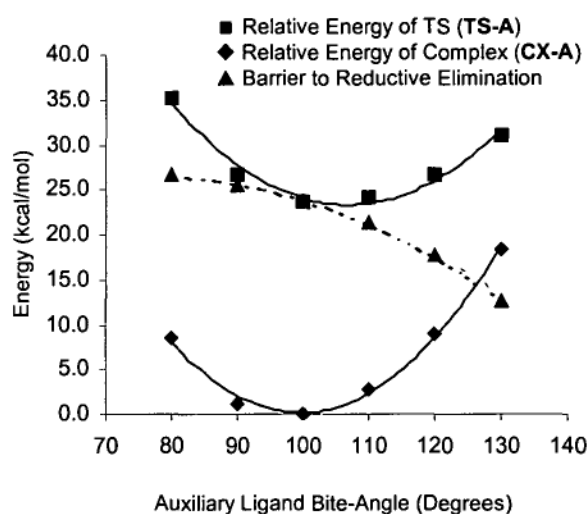
Figure 7.7. Relative complex and TS energies *vs.* bite-angle
(energies are relative to **CX-A100**)

It is likely that the compact nature of the CH_3-Pd-C(2) system in the transition structure is less affected by the encroaching auxiliary ligands as the bite angle increases, in comparison to the complex. The steric influence of the auxiliary ligands is reflected in the strain-relieving elongation of the Pd-CH_3 and Pd-C(2) bonds. Comparing the difference between **A80** and **A130,** this elongation is dramatic in the complex (0.074 Å and 0.048 Å respectively) but less profound in the transition

structure (0.023 Å and 0.019 Å respectively) suggesting the transition structure is not subjected to as much strain as the complex.

Morokuma[26] has recognised that the steric influence of widening the bite angle is primarily responsible for the increase in energy of the structures and the change in electronic structure is comparatively insignificant.

The most stable geometry of the complex and transition structure can be interpreted from Figure 7.7 to have approximate ligand bite angles of 100° and 107° respectively. Below 90° the closing of the auxiliary bite-angle appears to have similar influence on both the transition structure and complex energies and the E_{act} begins to plateau toward a value of approximately 27 kcal/mol.

7.3.2 Carbene Twist Angle Effects

The pathway used to ascertain the effect of the carbene twist angle on the reductive elimination of methyl-palladium carbene complexes is shown in Scheme 7.2. The carbene twist angle was set between 15° and 90° in an attempt to model the orientations that the carbene may adopt in free, hemi-labile and chelated complexes. Setting the angle at 0° in this system resulted in high-energy buckled structures that deviated considerably from planarity and were considered unlikely to exist in reality.

D = 15°, 30°, 45°, 60°, 75° and 90°
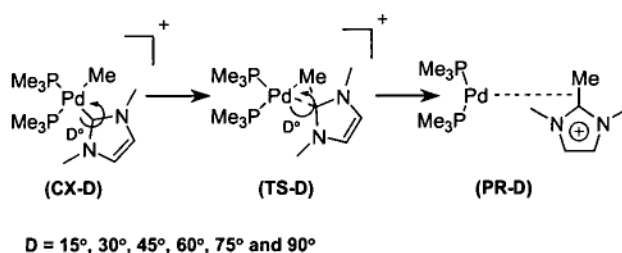
Scheme 7.2. Reductive elimination reaction for carbene twist angle deviation

7.3.2.1 Complexes. The optimised geometries calculated for the complexes (Scheme 7.2 **CX-D**) and transition structures (Scheme 7.2 **TS-D**) are collected in Figure 7.8. Twisting the carbene from perpendicular to the PdL_2 plane (**CX-D90**) toward almost in-plane (**CX-D15**) has only minor effects on the complex geometry. In general, all complexes exhibit an essentially square planar geometry with all ligands and the central palladium being coplanar. An exception is **CX-D15** where the steric strain imposed by the almost in-plane carbene results in a distortion where the methyl group on palladium is 'pushed' out of the plane.
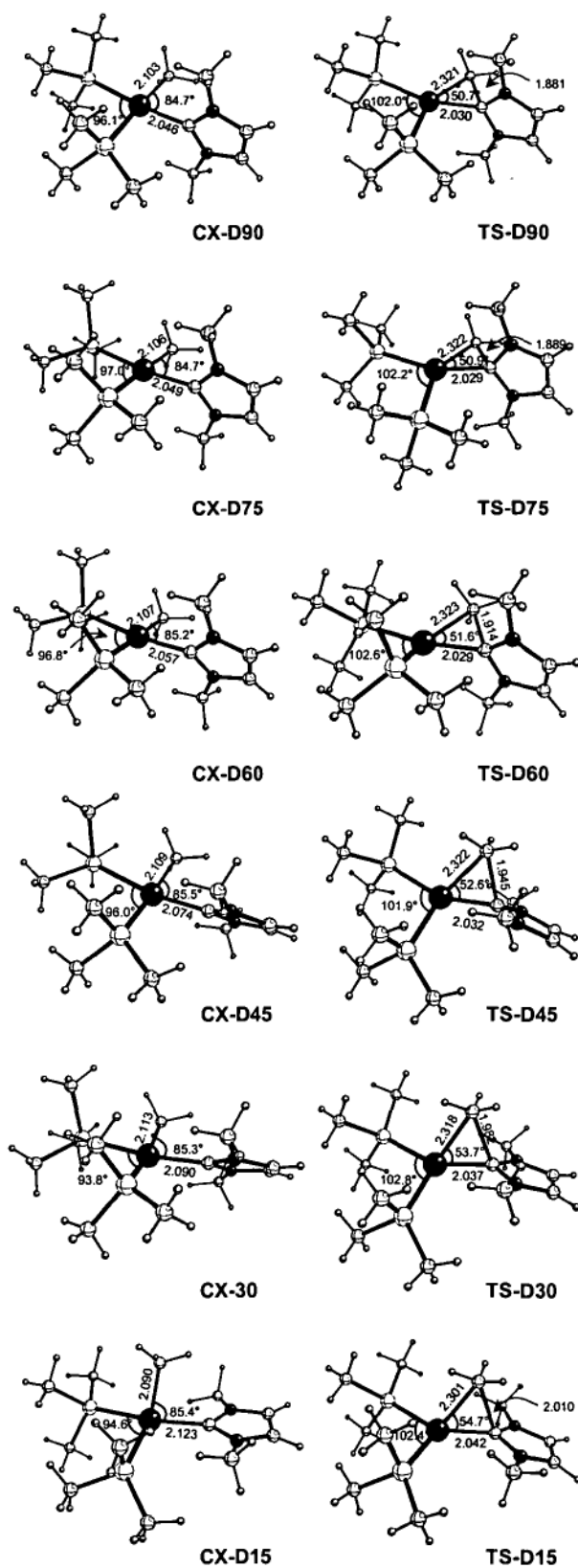
Figure 7.8. Product and transition structure geometries for **CX-D** and **TS-D**

The phosphine bite-angle closes by approximately 2° on twisting the carbene in to the plane while the CH$_3$–Pd–C(2) angle is relatively unaffected (84.7°-85.4°). Any congestion that is introduced by twisting the carbene in to the plane appears to be relieved to some degree via the elongation of the Pd-C(2) bond. An increase of 0.077 Å is observed on going from **CX-D90** (Pd–C(2) = 2.046 Å) to **CX-D15** (Pd–C(2) = 2.123 Å).

7.3.2.2 Transition Structures. Similarly, the transition structures show limited variation from **TS-D90** to **TS-D15**. The auxiliary bite-angle (P-Pd-P) remains approximately constant at 102°, while the Pd-C(2) bond shows a gentle elongation on moving from **TS-D90** (2.030 Å) to **TS-D15** (2.042 Å). There is an increase in the CH$_3$-Pd-C(2) angle as the carbene is twisted toward the plane (**TS-D90** 50.7°, **TS-D15** 54.7°) and an associated lengthening of the C(2)-CH$_3$ bond (**TS-D90** 1.881 Å, **TS-D15** 2.010 Å).

The main differences between the transition structures results from the location of the migrating methyl group in relation to the PdL$_2$ plane. Rather than stay in plane in accordance with the classical description of reductive elimination, the methyl group prefers an orientation highly dependent on that of the carbene. Specifically, the adopted position is that which allows maximum overlap between the carbene C(2) p$_\pi$ orbital and sp^3 orbital of the methyl group. As a result of this, the methyl group adopts a position in the plane orthogonal to the plane of the carbene ring (Figure 7.9). This suggests that in the proposed transition state, the bonding between carbene and methyl may be more important than that between the d-orbital on the metal and the methyl group, which can not occur in the cases other than D = 90°.
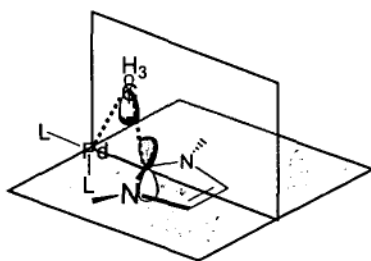
**Figure 7.9**. Location of methyl group with respect to carbene in **TS-D**.
Despite the carbene twist angle in **TS-D**, the methyl group is always located in the plane
perpendicular to that of the carbene, presumably in an attempt to maximize carbene-pπ and
methyl-sp$^3\sigma$ orbital overlap.

7.3.2.3 Energies.   Examination of the potential energy surface for the reductive

elimination reaction (Figure 7.10) shows that all pathways exhibit a thermodynamic

preference for the product. The steric strain imposed by the almost in-plane carbenes

result in the largest enthalpies of reductive elimination (e.g. D = 15° ΔH = –

22.7 kcal/mol), while those more perpendicular to the plane show a lessened

thermodynamic preference for the product (e.g. D = 90° ΔH = –1.1 kcal/mol).   As a

result of the exothermic behaviour of the reaction in all cases, the height of the barrier

to reductive elimination becomes the sole factor preventing decomposition.
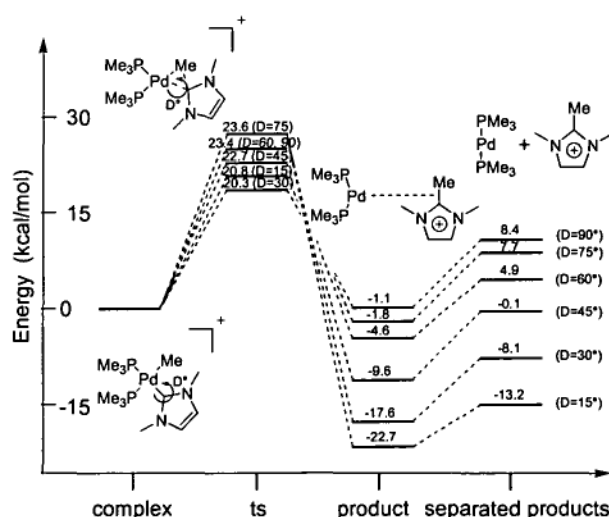
Figure 7.10. Potential energy surface for changes in carbene twist angle

The origin of the differences in barriers as the carbene twist angle is changed can be observed by comparing the relative energies of the complex and transition states as a function of twist angle (Figure 7.11). The activation energy changes by approximately 3 kcal/mol from the more in-plane pathways (*i.e.* D = 15° E_{act} = 20.8 kcal/mol, D = 30° E_{act} = 20.3 kcal/mol) to those twisted more perpendicular to the plane (*i.e.* D = 45° E_{act} = 22.7 kcal/mol, D = 60°, 90° E_{act} = 23.4 kcal/mol and D = 75° E_{act} = 23.6 kcal/mol).
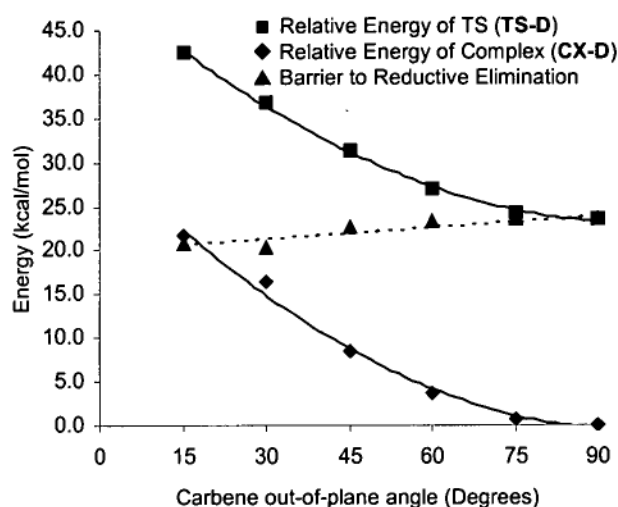
Figure 7.11. Complex and TS energies *vs* carbene twist angle.
(energies are relative to **CX-D90**)

The relative energy of the complex is found to increase as the carbene twist angle approaches zero. To ascertain if the origin of this increase was electronic in nature, charge decomposition analysis[27] (CDA) was performed on a model system (Figure 7.12). The results for the analysis are shown in Table 7.3. The low values of q_s ($q_s < -$
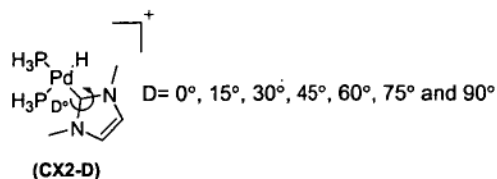
Figure 7.12. Model system for CDA Analysis

0.034) indicate that the Pd-C(2) bond is one of donation/back-donation type and therefore CDA analysis is applicable. The carbene to palladium donation changes little as a function of twist angle, staying reasonably constant at approximately 0.58 electrons. The back-donation is minimal (q_b < 0.1e), which is in accordance with previous theoretical and experimental findings,[28,29] with the change in back-donation confirming the directional nature of the d-orbital interaction. Taking these results into account, it is likely that the energy change in the complex as the carbene is rotated into the PdL_2 plane is a consequence of steric interactions between the N-substituents of the carbene and peripheral ligands on palladium rather than electronic in nature.

Table 7.3. Results of charge decomposition analysis (CDA) on a model system

Complex	q_d[a]	q_b[b]	q_r	q_s
CX2-D0	0.578	0.079	-0.193	-0.027
CX2-D15	0.576	0.080	-0.186	-0.027
CX2-D30	0.575	0.084	-0.180	-0.027
CX2-D45	0.575	0.092	-0.179	-0.029
CX2-D60	0.578	0.096	-0.172	-0.031
CX2-D75	0.580	0.101	-0.163	-0.033
CX2-D90	0.581	0.105	-0.159	-0.034

[a]Donation from carbene to palladium (electrons); [b]Back-donation from palladium to carbene (electrons)

Compact arrangement of the methyl-Pd-carbene system in the transition structure makes steric crowding between the carbene and auxiliary ligands less substantial than in the complex. Therefore the increase in the transition structure energy as the carbene is rotated toward the plane may be resultant from the divergence from the ideal transition state proposed by McGuinness et al.[7] The lack of

d_π-p_π overlap for carbene twist angles less than 90° is likely to result in a less energetically favourable transition state.

In the system studied here, the rate of increase in energy of the complex due to steric strain is similar to the rate of increase in energy of the transition structure believed to be a result of electronic factors. As a result of this, the activation energy remains essentially constant.

7.4 Conclusions

The influence of both auxiliary ligand bite-angle and carbene twist angle on the reductive elimination of methyl-palladium-carbene complexes has been investigated.

Changing the auxiliary ligand bite-angle from 80° to 130° has a profound effect on both the activation energy and the thermodynamic driving force for the decomposition reaction. The activation energy is small when the bite-angle is large (*e.g.* A = 130°, E_{act} = 12.7 kcal/mol) and large when the bite angle is small (*e.g.* A = 80°, E_{act} = 26.7 kcal/mol) (*i.e.* E_{act} is inversely proportional to the bite angle). This trend is primarily associated with the steric influence of the auxiliary ligands on the leaving groups in the complex.

The thermodynamic driving force for complexes with small bite angles is reduced due to the instability of the PdL_2 fragment.

Therefore we see a two-fold benefit in constraining the bite angle of the ligands opposing the carbene and methyl leaving groups. Not only is the decomposition reaction less thermodynamically favourable but also an increased barrier resulting in superior kinetic stability compared to the larger-bite-angled analogues is observed.

Rotation of the carbene toward the PdL_2 plane resulted in little change in the activation energy, but has significant effects on the thermodynamics of the decomposition reaction. The instability of the complexes where the carbene approaches coplanarity with PdL_2 can be attributed to steric strain rather than

electronic influences through the use of charge decomposition analysis. As a result of this steric strain, we see an increased thermodynamic driving force for decomposition in those complexes where the carbene approaches almost in-plane (*e.g.* D = 15° ΔH = –22.7 kcal/mol) in comparison to those which are closer to being perpendicular to the plane (*e.g.* D = 90° ΔH = –1.1 kcal/mol). The change in activation energy associated with rotating the carbene was found to be minimal for the system investigated here (20.3 kcal/mol (E_{act}(D = 30°)) to 23.6 kcal/mol (E_{act}(D = 75°)). The increase in energy of the complex associated with steric strain was balanced by the increase in energy of the transition structure attributed primarily to non-favourable orbital overlap as the carbene twist angle rotated toward coplanar with PdL_2.

Relieving strain in complexes where the carbene is approximately coplanar with the PdL_2 plane is likely to result in systems that are very stable to reductive elimination. This may be achieved by chelation of the carbene to a neighbouring ligand in combination with narrowing the bite angle of the opposing ligands to provide more room in the PdL_2 plane. Additionally, minimisation of the bulk on nitrogen in the heterocyclic carbene may result in a more planar complex.

7.5 References

(1)   Tatsumi, K., Hoffmann, R., Yamamoto, A., Stille, J. K., *Bull. Chem. Soc. Jpn.* **1981**, *54*, 1857.

(2)   Low, J. L., Goddard, W. A., III, *J. Am. Chem. Soc.* **1986**, *108*, 6115.

(3)   van Leeuwen, P., Kamer, P. C. J., Reek, J. N. H., Dierkes, P., *Chem. Rev.* **2000**, *100*, 2741.

(4)   Dierkes, P., van Leeuwen, P., *J. Chem. Soc., Dalton Trans.* **1999**, 1519.

(5)   Portnoy, M., Milstein, D., *Organometallics* **1993**, *12*, 1655.

(6)   Marcone, J. E., Moloy, K. G., *J. Am. Chem. Soc.* **1998**, *120*, 8527.

(7)   McGuinness, D. S., Saendig, N., Yates, B. F., Cavell, K. J., *J. Am. Chem. Soc.* **2001**, *123*, 4029.

(8)   McGuinness, D. S., Cavell, K. J., Yates, B. F., Skelton, B. W., White, A. H., *J. Am. Chem. Soc.* **2001**, *123*, 8317.

(9)   McGuinness, D. S., Cavell, K. J., Yates, B. F., *Chem. Commun.* **2001**, 355.

(10)   Peris, E., Loch, J. A., Mata, J., Crabtree, R. H., *Chem. Commun.* **2001**, 201.

(11)   Tulloch, A. A. D., Danopoulos, A. A., Tizzard, G. J., Coles, S. J., Hursthouse, M. B., Hay-Motherwell, R. S., Motherwell, W. B., *Chem. Commun.* **2001**, 1270.

(12)   McGuinness, D. S., Green, M. J., Cavell, K. J., Skelton, B. W., White, A. H., *J. Organomet. Chem.* **1998**, *565*, 165.

(13)   Baker, M. V., Skelton, B. W., White, A. H., Williams, C. C., *J. Chem. Soc., Dalton Trans.* **2001**, 111.

(14)   Matsubara, T., Hirao, K., *Organometallics* **2002**, *21*, 2662.

(15)   Nielsen, D. J., Magill, A. M., Yates, B. F., Cavell, K. J., Skelton, B. W., White, A. H., *Chem. Commun.* **2002**, 2500.

(16)   Becke, A. D., *J. Chem. Phys.* **1993**, *98*, 5648.

(17)   Becke, A. D., *Phys. Rev. A.* **1988**, *38*, 3098.

(18)   Lee, C., Yang, W., Parr, R. G., *Phys. Rev. B.* **1988**, *37*, 785.

(19)   Hay, P. J., Wadt, W. R., *J. Chem. Phys.* **1985**, *82*, 299.

(20)   Dunning, T. H., Hay, P. J. *Modern Theoretical Chemistry*; Plenum: New York, 1976; Vol. 3.

(21)   Langhoff, S. R., Petterson, L. G., Bauschlicher, C. W., Partridge, H. J., *J. Chem. Phys.* **1987**, *86*, 268.

(22)   Krishnan, R., Binkley, J. S., Seeger, R., Pople, J. A., *J. Chem. Phys.* **1980**, *72*, 650.

(23)   McLean, A. D., Chandler, G. S., *J. Chem. Phys.* **1980**, *72*, 5639.

(24)   Frisch, M. J., Pople, J. A., Binkley, J. S., *J. Chem. Phys.* **1984**, *80*, 3265.

(25)   Gaussian 98, Revision A.7, Frisch, M. J., Trucks, G. W., Schlegel, H. B., Scuseria, G. E., Robb, M. A., Cheeseman, J. R., Zakrzewski, V. G., Montgomery, J. A., Jr., Stratmann, R. E., Burant, J. C., Dapprich, S., Millam, J. M., Daniels, A. D., Kudin, K. N., Strain, M. C., Farkas, O., Tomasi, J., Barone, V., Cossi, M., Cammi, R., Mennucci, B., Pomelli, C., Adamo, C., Clifford, S., Ochterski, J., Petersson, G. A.,

Ayala, P. Y., Cui, Q., Morokuma, K., Malick, D. K., Rabuck, A. D., Raghavachari,

K., Foresman, J. B., Cioslowski, J., Ortiz, J. V., Baboul, A. G., Stefanov, B. B., Liu,

G., Liashenko, A., Piskorz, P., Komaromi, I., Gomperts, R., Martin, R. L., Fox, D. J.,

Keith, T., Al-Laham, M. A., Peng, C. Y., Nanayakkara, A., Gonzalez, C.,

Challacombe, M., Gill, P. M. W., Johnson, B., Chen, W., Wong, M. W., Andres, J. L.,

Gonzalez, C., Head-Gordon, M., Replogle, E. S., Pople, J. A., Gaussian Inc,

Pittsburgh, PA, 1998

(26)   Matsubara, T., Maseras, F., Koga, N., Morokuma, K., *J. Phys. Chem.*

1996, *100*, 2573.

(27)   Dapprich, S., Frenking, G., *J. Phys. Chem.* **1995**, *99*, 9352.

(28)   Green, J. C., Scurr, R. G., Arnold, P. L., Cloke, F. G. N., *Chem.*

Commun. **1997**, 1963.

(29)   Herrmann, W. A., Runte, O., Artus, G., *J. Organomet. Chem.* **1995**,

501, C1.

• Chapter Eight •

# Influence of *N*-Substituents on the Stability of Palladium Carbene Complexes

8.1 Introduction

The steric bulk of heterocyclic carbenes is said to be responsible for a number of observed properties of the carbene and its corresponding complex. Early studies[1,2] on the isolation of *N*-heterocyclic carbenes (NHCs) suggested that the bulk at nitrogen was the most significant reason for the observed remarkable stability. This postulate was later dispelled with the isolation of 1,3,4,5-tetramethylimidazol-2-ylidene (tmiy),[3] but steric bulk continues to be an integral stabilizing feature for other free carbenes such as thiazol-2-ylidenes and the group of acyclic carbenes isolated by Alder.[4,5]

The role of steric bulk in the stability and catalytic activity of complexes containing heterocyclic carbenes as ligands is less well known. Certainly bulk plays a role in catalysis, with many groups observing changes in catalytic activity associated with varying the R-group attached to nitrogen.[6-9] Specifically, Suzuki catalysis is believed to be enhanced by steric bulk on the carbene that aids in promoting the reductive elimination step of the catalytic cycle.[9] Douthwaite[10] has suggested that bulky substituents combined with a chelated carbene system may help to reduce the rate of catalyst deactivation via the pathway brought to light by McGuinness *et al.*[11-13]

Research on the role of steric bulk in the decomposition behaviour of NHC complexes is one of the continuing projects within our group. A rigorous computational study of the decomposition pathway has constituted a significant proportion of our research and continues to direct our synthetic efforts.

In this chapter, research is primarily concerned with the effect that exchanging *N*-substituents for groups that differ both sterically and electronically has on the barrier for reductive elimination (Scheme 8.1). The range of substituents was chosen to cover a suitable breadth of steric and electronic properties. A number of these substituents (Ph, Me, ^{i}Pr, Cy and ^{t}Bu) are common in both experimentally isolable carbenes and their complexes.[14-16] In all figures and tables the substituents are ordered according to their σ-donating ability (weakest to strongest).[17]
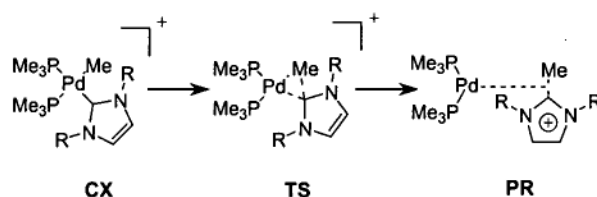
R = Cl, H, Ph, Me, ^{i}Pr, Cy, neopentyl and ^{t}Bu

Scheme 8.1. Reductive elimination reaction that is the focus of this chapter

8.2 Computational Methods

All geometry optimizations of palladium complexes were carried out with the B3LYP[18-20] density functional employing a LANL2DZ[21,22] basis set and effective core potential (ECP). The azolium reactants were optimized at the B3LYP/6-31G(d) level and the zerovalent reactants (Pd(dmpe)) optimised using the compound basis set B3LYP/LANL2DZ:6-31G(d), which showed considerable benefits over the previous basis set employed.[13] For optimized geometries harmonic vibrational frequencies were calculated to ascertain the nature of the stationary point and zero-point vibrational energy (ZPVE) and thermodynamic corrections were obtained using unscaled frequencies.

Single-point energies on palladium containing systems were calculated using a LANL2DZaugmented:6-311+G(2d,p) basis set for palladium (incorporating the LANL2 ECP and the large f-polarized valence bas set of Bauschlicher and co-workers[23] on Pd and the 6-311+G(2d,p) basis set[24-26] on all other atoms). Single point energies of organic molecules (azoliums) were performed at the B3LYP/6-311+G(2d,p) level of theory. As the peripheral phosphine ligands are to represent pure spectator ligands, palladium–phosphine bond lengths are frozen at 2.48 Å in order to prevent their dissociation under sterically crowded conditions.

All energies mentioned throughout the text refer to these final levels of theory and include enthalpy and ZPVE corrections calculated at the optimization level of theory. Calculations were carried out using the Gaussian 98 suite of programs.[27]

8.3 Results and Discussion

8.3.1. Free Carbenes

Complexes chosen for study are outlined in Scheme 8.1 (**CX**). As variation between the complexes is limited to the substituents at nitrogen, any change in
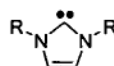

R = Cl, H, Ph, Me, ^{i}Pr, Cy, neopentyl and ^{t}Bu

Figure 8.1 Carbene ligands that are the focus of this chapter (**CB**)

reductive elimination behaviour is a result of the carbene. It follows then, that by observing both the structural and electronic properties of the individual carbene involved as a ligand in the reaction (Figure 8.1), one may gain insights into the more complex process of reductive elimination.

The optimised geometries of the various NHCs are presented in Figure 8.2. Each carbene exhibits a similar planar core with little deviation in the N-C(2)-N valence angle (98.5°-102.6°). The C(2)-N bond lengths are essentially constant (1.362-1.373Å) with the exception of the C(2)-N bonds in **CB**(Ph) which are slightly elongated (1.390Å). Additionally, the N-C$_{exocylic}$ bonds are shortened (1.430Å *vs* 1.452-1.491Å in the other *N*-alkyl-carbenes), while the N-C$_{4/5}$ bond is lengthened. These features suggest that the nitrogen lone pair is primarily involved in the N-C$_{phenyl}$ bond through interaction with the delocalised p$_\pi$ system of the phenyl ring. Consequently, the double bond nature of the N-C(2) and N-C$_{4/5}$ bonds is reduced in comparison to those carbenes incapable of forming a π-interaction between nitrogen and the exocyclic ring substituent. Appreciable

interaction between the carbene and phenyl π-system is facilitated by the small twist angle (18°) of the phenyl ring with respect to the carbene plane. Further rotation of the phenyl ring toward the perpendicular is likely to remove this additional bonding interaction. Elimination of this additional bonding interaction may play an important role in stabilising the complex (*vide infra*).
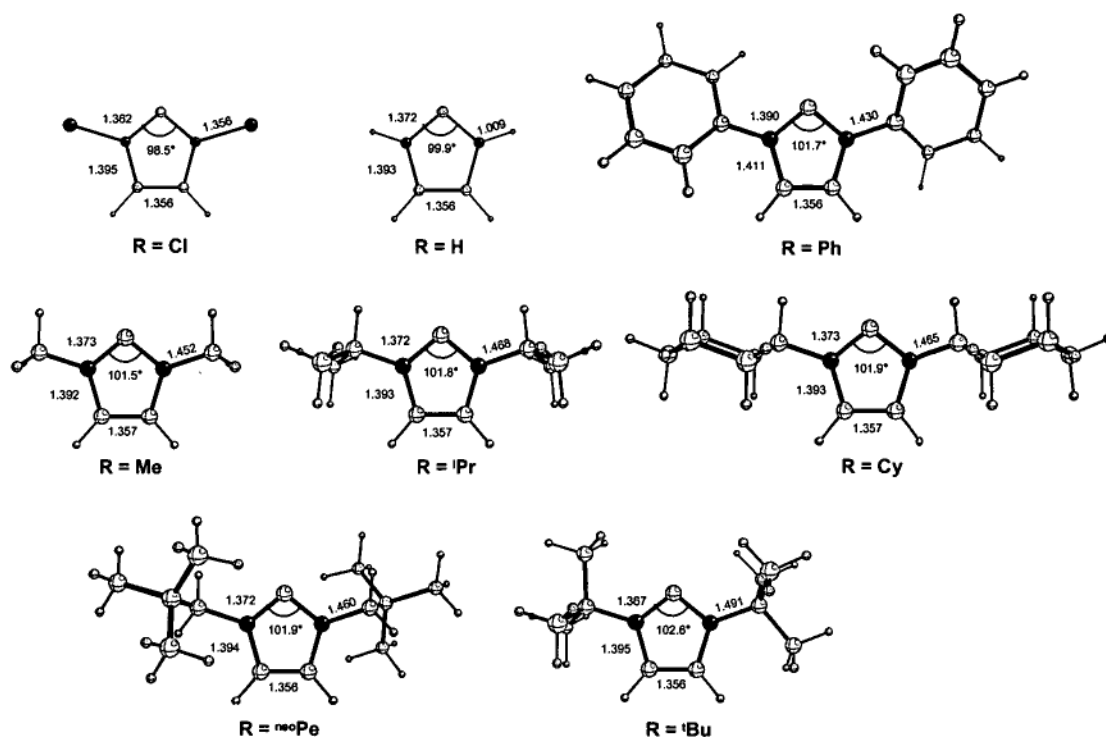
Figure 8.2 – Optimised geometries of *N*-substituted carbenes (**CB**)

8.3.1.1 Charges at C(2). It may be expected that the C(2) carbon will bear a near neutral charge due to the push-pull mechanism associated with the stabilisation of NHCs (Figure 8.3).
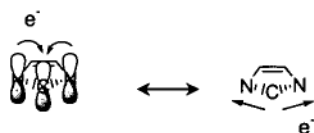
Figure 8.3. 'Push-pull' electronic stabilisation scheme of heterocyclic carbenes

With the exception of **CB**(Ph) and **CB**(Cl) the carbene carbon shows only a slight net depletion of electronic charge (Table 8.1). The further depletion shown by **CB**(Ph) results from the reduced $N(p_\pi) \rightarrow C_{carbene}(p_\pi)$ donation as discussed previously. Consequently, in comparison to *N*-substituents that are capable of σ-bonding only, a depletion of the $C(2)(p_\pi)$ orbital occupancy is observed for the phenyl substituent (0.635 e). Reduced $C(2)(p_\pi)$ occupation is also observed for **CB**(Cl) (0.625e) and is attributed to π involvement of the nitrogen lone pair with chlorine (similar to that described for **CB**(Ph)). In additional to this, charge depletion may occur as a result of the strong electron withdrawing effect of chlorine, resulting in an inductive effect which extends to deplete σ electron density from the carbene carbon, consequently increasing its charge (0.197 Mulliken, 0.176 NPA).

Table 8.1. Charges at C(2)

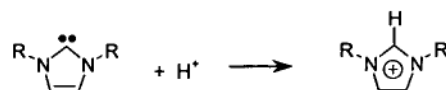| Carbene	Charges at C(2)		$C2(p_\pi)^a$
	Mulliken	NPA	
CB(Cl)	0.197	0.176	0.625
CB(H)	0.116	0.116	0.630
CB(Ph)	0.162	0.141	0.635
CB(Me)	0.098	0.117	0.652
CB(^{i}Pr)	0.091	0.114	0.660
CB(Cy)	0.093	0.113	0.660
CB(^{neo}Pe)	0.111	0.110	0.661
CB(^{t}Bu)	0.117	0.094	0.671

^{a}Gaussian98 NBO orbital occupancy

8.3.1.2 Carbene Proton Affinity. The calculated proton affinity (Scheme 8.2 and Table 8.2) provides an indication of the σ-lone pair availability. All the carbenes show very high

Scheme 8.2. Proton Affinity

affinity for protons, in alignment with previous literature findings, which suggest that NHCs are among the most powerful neutral Lewis bases known.[16] The general trend observed here shows a qualitative correlation between the σ-withdrawing nature of the *N*-substituents[17] and the basicity of the carbene (i.e. $R_{substituted\ alkyl} > R_{alkyl/aryl} > H > Cl$).
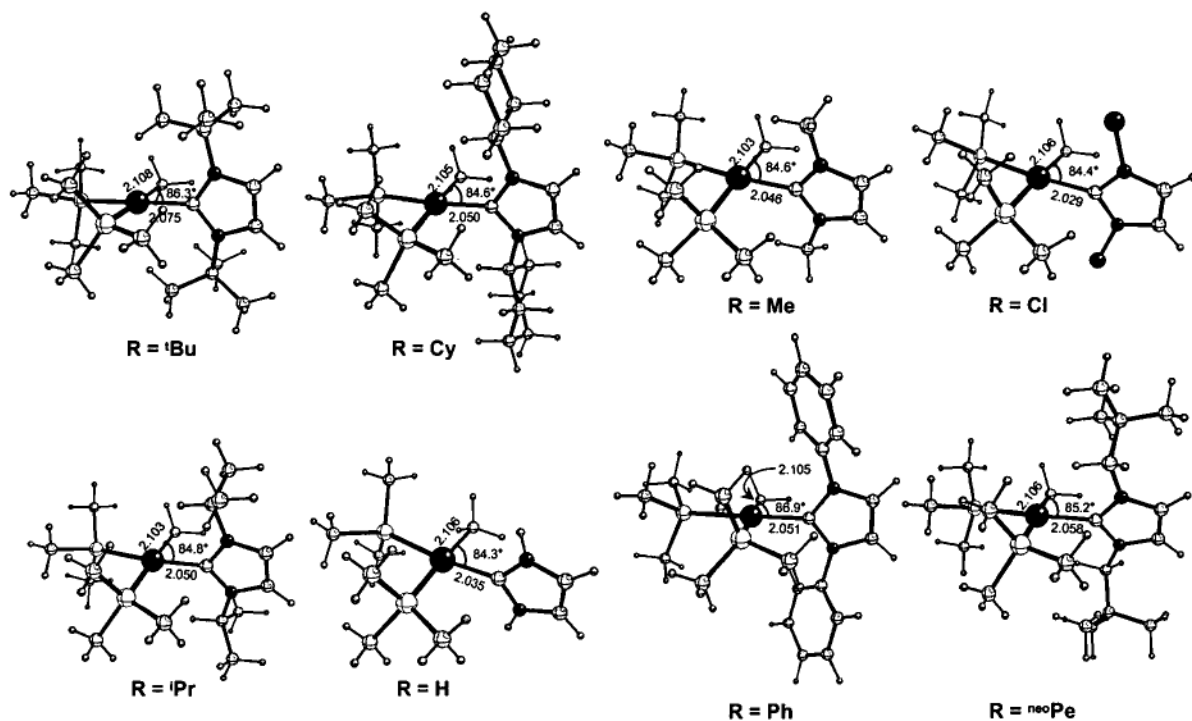
Table 8.2. Proton Affinity Results[a]

carbene[b]	ΔH (P.A.)
CB(Cl)	-238.6
CB(H)	-250.8
CB(Ph)	-262.6
CB(Me)	-259.5
CB(^{i}Pr)	-265.2
CB(Cy)	-268.3
CB(^{neo}Pe)	-266.6
CB(^{t}Bu)	-267.8

[a]Energies are in kcal/mol; [b]Ordered via σ-donation of group (low to high)

8.3.2 Complexes

Optimised geometries of the complexes (Scheme 8.1 **CX**) are shown in Figure 8.4.

Figure 8.4 – Optimised geometries of *N*-substituted complexes (**CX**)

All complexes exhibit the square planar geometry expected of Pd^{II} complexes bearing four substituents. The ancillary phosphine bite-angle ($\angle P(1)\text{-}Pd\text{-}P(2)$) shows little deviation (95-98°) between complexes. The dihedral angle of the carbene relative to the PdL_2 plane is essentially 90°, with little variation across the range of substituents. Consequently, it may be suggested that the steric nature of the *N*-substituents surveyed here will have little influence on reductive elimination rates as the bulk is distant to such an extent that it would be unlikely to interfere with the reaction. Additionally, the

perpendicular nature of the carbene rules out the involvement of the apical position proposed by Matsubara and Hirao in the current decomposition reaction.[28] There is little variation in the bonding between the leaving groups and Pd. Pd-CH$_3$ and Pd-C(2) bond lengths are essentially constant at 2.105 ± 0.003Å and 2.050 ± 0.025Å respectively.

8.3.2.1 CDA Analysis of Bonding. The charge decomposition analysis (CDA) partitioning scheme,[29] the results of which are shown in Table 8.3, was used to assess the nature of the palladium-carbene bond.

Table 8.3. CDA calculations on complexes (**CX**)

| complex	$q_d{}^a$	$q_b{}^b$	$q_r{}^c$	q_s
CX(Cl)	0.501	0.143	-0.214	-0.019
CX(H)	0.515	0.116	-0.204	-0.024
CX(Ph)	0.605	0.151	-0.246	-0.037
CX(Me)	0.570	0.139	-0.218	-0.039
CX(^{i}Pr)	0.613	0.159	-0.227	-0.044
CX(Cy)	0.631	0.158	-0.227	-0.045
CX(^{neo}Pe)	0.654	0.157	-0.265	-0.042
CX(^{t}Bu)	0.738	0.168	-0.349	-0.056

^{a}Donation from carbene to palladium; ^{b}Backdonation from palladium to carbene; ^{c}Repulsion

The small q_s values ($0 > q_s > -0.06$ e) imply that the palladium-carbene bond is a donation/back-donation interaction, and hence CDA partitioning is appropriate for its analysis. Donation from the carbene to the palladium centre ranges from 0.50-0.74 e.

NBO analysis reveals that this donation occurs primarily from the in-plane σ lone pair of the carbene to an appropriately aligned sd-hybrid on palladium. Back-donation from palladium to the carbene is negligible ($q_b < 0.17$ e), in accordance with previous experimental and theoretical findings.[30,31] Any relation between the amount of back-donation and the occupancy of the free carbene p_π orbital appears non-existent.

Increased electron donation from the carbene to palladium may be correlated with the σ-donating ability of the R-group (Cl < H < R). While **CX(H)** and **CX(Cl)** show modest σ-donation via CDA analysis (0.501 and 0.515e, respectively), the highly branched alkyl groups where appreciable σ-donation is expected (i.e. ^{neo}Pe, ^{t}Bu) show an increase of approximately 20% in sigma donation capacity to palladium. Additionally, the calculated sigma donation capacities are in qualitative agreement with the individual carbene's proton affinity.

In accordance with the additional donation provided by some carbenes, an increase in charge at the palladium centre is observed. The calculated Mulliken charges (Table 8.4) show a trend that correlates well ($R^2 = 0.96$) with the CDA donating ability of the carbene (Figure 8.5).
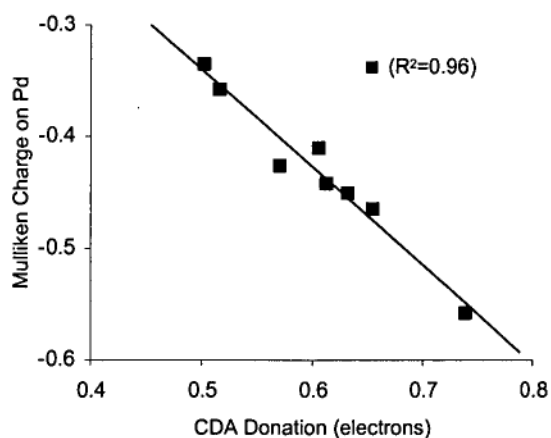
Figure 8.5. Mulliken / CDA Donation Correlation

An increase in the electron density around palladium occurs as we extend to the more efficient σ-donating carbenes. Despite the unreliability of Mulliken charges at predicting absolute charge, the trends provided are, in general, reliable.

Table 8.4. Mulliken charges at palladium[a]

Complex	Mulliken Charge
CX(Cl)	-0.33
CX(H)	-0.36
CX(Ph)	-0.41
CX(Me)	-0.43
CX(^{i}Pr)	-0.44
CX(Cy)	-0.45
CX(^{neo}Pe)	-0.47
CX(^{t}Bu)	-0.56

[a]Calculated with a split level LANL2DZ:6-31G(d) basis set (see computational details)

8.3.3 Transition Structures

The optimised geometries of the transition structures are shown in Figure 8.6. In accordance with previous literature results,[13] the P(1)–Pd–P(2) angle opens approximately five degrees (to 101.1°–102.3°) on going from the complex to the transition structure. Subsequently, the CH_3–Pd–C(2) angle also closes considerably (*ca.* 35°) in agreement with the concept of reductive elimination. Elongation of the Pd-CH_3 bond is combined with the concerted formation of the new CH_3-C(2) bond. The carbene twist angle remains comparable to that observed in the complexes at around 90°.
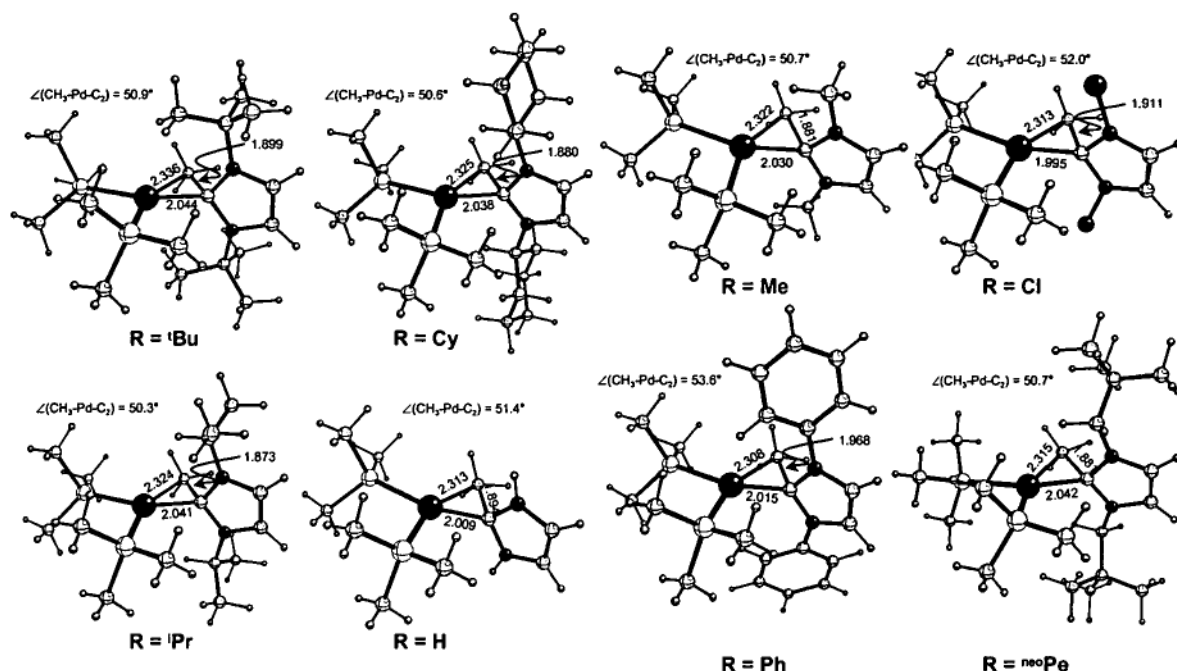
Figure 8.6 – Optimised geometries of *N*-substituted transition structures **(TS)**

8.3.4 Potential Energy Surfaces

The potential energy surfaces for the reductive elimination are shown in Figure 8.7. All complexes show exothermic product formation, with the exception of the R = H pathway (ΔH = +5.5 kcal/mol). Given the thermodynamic preference for product formation, the height of the activation barrier becomes the sole factor preventing decomposition of the complexes. No product could be located where R = Cl, with calculations where the two fragments were placed in close proximity to one another resulting in N–Cl bond scission. Therefore an accurate assessment of the reaction thermodynamics was not possible. As it was still possible to calculate the barrier to reductive elimination for R = Cl, some insights into the decomposition of NHCs

containing strong electron withdrawing groups may be obtained by studying this pathway, and for this reason it was not omitted.

The activation barriers (E_{act}) range from 20.2 kcal/mol (R = Cl) to 25.4 kcal/mol (R = ^{t}Bu, ^{neo}Pe). These barriers are quite high, although reactions involving palladium carbene catalysts are often carried out at high temperatures making these activation energies attainable. The reverse barriers (for oxidative addition) are very high also, with oxidative addition being considerably more difficult than reductive elimination in all cases except R = H.
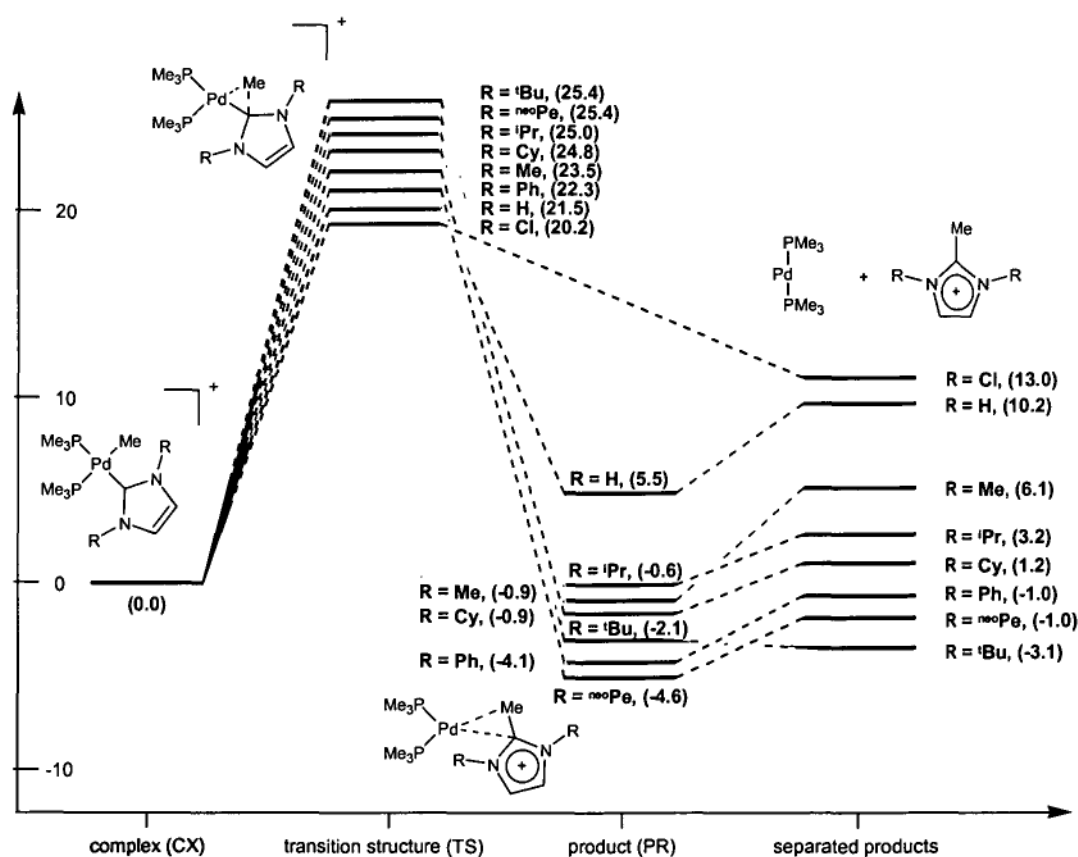

Figure 8.7 – Potential energy surface for reductive elimination (Scheme 8.1)

Carbenes that show a higher degree of σ-donating ability appear to stabilise complexes to reductive elimination (Figure 8.8). Accordingly, those complexes where significant electron density is localized on palladium (e.g. ^{t}Bu, ^{neo}Pe) show large barriers to decomposition, or stated alternatively *a more positive charge on the palladium centre will make the complex more susceptible to decomposition* (Figure 8.9).
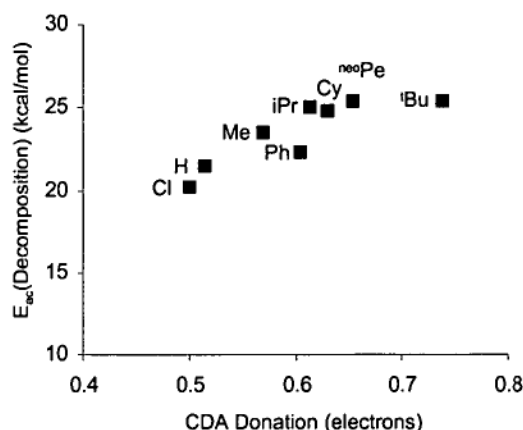
Figure 8.8. Correlation of CDA donation (carbene → palladium) and E_{act}
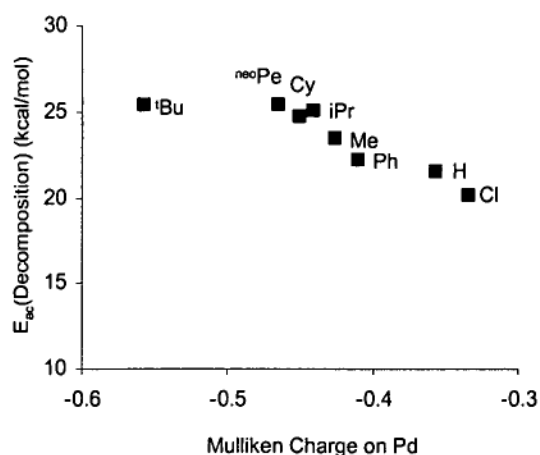

Figure 8.9. Correlation of Mulliken charge on Pd and E_{act}

This parallels experimental findings that cationic palladium complexes are more susceptible to decomposition via reductive elimination,[12,32] but is in disagreement with the conclusions of Hoffmann who suggests stronger σ-donors should *decrease* the barrier for reductive elimination.[33]   Hoffmann's conclusions were based on results from two simplified complexes, however, and may not extend well to the more complex systems studied here.

It may seem appropriate to propose that the greater donating ability of the carbene would equate to a stronger Pd-C(2) bond and it is for this reason we see an increase in the activation barrier for decomposition. Unfortunately, correlation of CDA donation results with the Pd-C(2) bond strengths showed no obvious trend.

Previous work[13] (see also Chapters 6 and 7) has detailed the orbital interaction of the proposed three centred transition structure in the decomposition process (Figure 8.10).
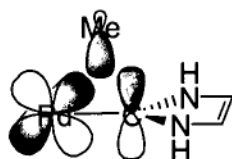
Figure 8.10. Three-centred transition
structure orbitals

Those carbenes that show decreased C(2) p_π orbital occupations (**CB(Ph)**, **CB(H)** and **CB(Cl)**) also show the lowest barriers to reductive elimination (22.3, 21.5 and 20.2 kcal/mol respectively).   The elongated C(2)–CH$_3$ bonds (1.968, 1.894 and 1.911Å respectively) in their associated transition structures indicate that the transition states are

comparatively early in nature and therefore associated with a lower barrier in accordance with Hammond's postulate.[34]

Excellent correlation (R^2 = 0.95) is observed between the occupation of the carbene p_π orbital and the activation energy for decomposition (Figure 8.11). This indicates that lower occupation of the $C(2)(p_\pi)$ orbital promotes a more energetically favourable transition state resulting in a more facile decomposition. This trend has also been identified for the reductive elimination of the higher Si and Ge carbene homologues.[35]
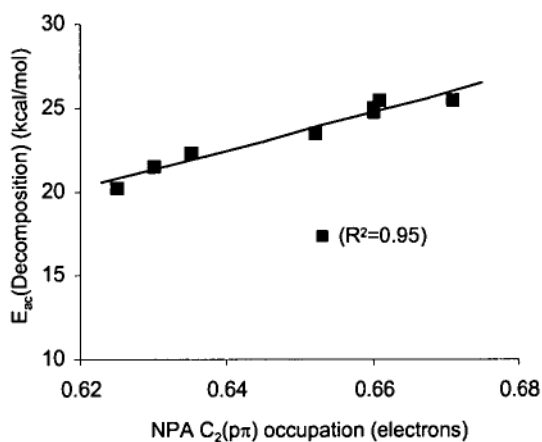
Figure 8.11. C(2) p_π occupation *vs.* E_{ac}

8.4 Conclusions

DFT methods have been employed to assess the effect of varying *N*-substituents on the stability of hydrocarbyl palladium carbene complexes to reductive elimination. The σ-donating ability of the carbene directly impacts the reductive elimination behaviour of complexes. *N*-substituents that possess appreciable σ-donating capability (e.g. branched alkyl) inductively confer a decreased positive charge on palladium providing a more stable system. The proton affinity has been identified as a reasonable qualitative assessment of the σ-donating ability of the carbene.

Additionally, the carbene p_{π} orbital appears to be intimately involved in determining the barrier to reductive elimination. A π-interaction between nitrogen and the exocyclic ring substituent (e.g. Cl and Ph) reduces electron density in the carbene p_{π} orbital allowing for a more energetically favourable three-centred transition structure and consequently, a more facile reductive elimination. Because of this, incorporation of groups in the 2 and 6 positions of *N*-substituted phenyl rings (e.g. 2,6-diisopropylphenyl, 2,4,6-trimethylphenyl) may be a synthetic advantage. The additional steric bulk of these groups is known to make the phenyl ring adopt an orientation perpendicular to the carbene plane. This eliminates any π-conjugation effects that may occur and thus the carbene p_{π} orbital electron depletion brought about by π interaction of the phenyl and imidazole rings.

Steric bulk associated with the *N*-substituents appears to play little role in the systems studied here. The orientation of the carbene perpendicular to the PdL_2 plane removes the bulk to a suitably distant location where it is unlikely to interfere with the reaction. In systems where steric crowding is more likely to play a significant role in the reaction (e.g. in chelated systems where the carbene out-of-plane angle is less than 90°) nitrogen substituents with reduced steric bulk may be required to produce stable complexes. The conformational flexibility of the *neo*-pentyl group, for example, distances the sterically demanding portion of the molecule from the metal centre, avoiding the congestion that may occur with the inflexible tertiary-butyl substituent.

It is hoped that this and the previous two chapters of theoretical information may aid the development of catalytic systems less prone to unwanted decomposition behaviour.

8.5 References

(1)   Arduengo, A. J., Harlow, R. L., Kline, M., *J. Am. Chem. Soc.* **1991**, *113*, 361.

(2)   Dixon, D. A., Arduengo, A. J., *J. Phys. Chem.* **1991**, *95*, 4180.

(3)   Kuhn, N., Kratz, T., *Synthesis* **1993**, 561.

(4)   Arduengo, A. J., Goerlich, J. R., Marshall, W. J., *Liebigs Ann.-Recl.* **1997**, 365.

(5)   Alder, R. W., Butts, C. P., Orpen, A. G., *J. Am. Chem. Soc.* **1998**, *120*, 11526.

(6)   Furstner, A., Leitner, A., *Synlett* **2001**, 290.

(7)   Herrmann, W. A., Bohm, V. P. W., Gstottmayr, C. W. K., Grosche, M., Reisinger, C. P., Weskamp, T., *J. Organomet. Chem.* **2001**, *617*, 616.

(8)   Lee, S., Hartwig, J. F., *J. Org. Chem.* **2001**, *66*, 3402.

(9)   Hillier, A. C., Grasa, G. A., Viciu, M. S., Lee, H. M., Yang, C. L., Nolan, S. P., *J. Organomet. Chem.* **2002**, *653*, 69.

(10)   Douthwaite, R. E., Green, M. L. H., Silcock, P. J., Gomes, P. T., *J. Chem. Soc., Dalton Trans.* **2002**, 1386.

(11)   McGuinness, D. S., Cavell, K. J., *Organometallics* **2000**, *19*, 741.

(12)   McGuinness, D. S., Cavell, K. J., Skelton, B. W., White, A. H., *Organometallics* **1999**, *18*, 1596.

(13)   McGuinness, D. S., Saendig, N., Yates, B. F., Cavell, K. J., *J. Am. Chem. Soc.* **2001**, *123*, 4029.

(14)   Herrmann, W. A., *Angew. Chem., Int. Ed. Engl.* **2002**, *41*, 1291.

(15)   Bourissou, D., Guerret, O., Gabbai, F. P., Bertrand, G., *Chem. Rev.* **2000**, *100*, 39.

(16)   Herrmann, W. A., Kocher, C., *Angew. Chem., Int. Ed. Engl.* **1997**, *36*, 2163.

(17)   March, J. *Advanced Organic Chemistry*; 4th ed.; John Wiley and Sons: New York, 1992.

(18)   Becke, A. D., *J. Chem. Phys.* **1993**, *98*, 5648.

(19)   Becke, A. D., *Phys. Rev. A.* **1988**, *38*, 3098.

(20)   Lee, C., Yang, W., Parr, R. G., *Phys. Rev. B.* **1988**, *37*, 785.

(21)   Hay, P. J., Wadt, W. R., *J. Chem. Phys.* **1985**, *82*, 299.

(22)   Dunning, T. H., Hay, P. J. *Modern Theoretical Chemistry*; Plenum: New York, 1976; Vol. 3.

(23)   Langhoff, S. R., Petterson, L. G., Bauschlicher, C. W., Partridge, H. J., *J. Chem. Phys.* **1987**, *86*, 268.

(24)   Krishnan, R., Binkley, J. S., Seeger, R., Pople, J. A., *J. Chem. Phys.* **1980**, *72*, 650.

(25)   McLean, A. D., Chandler, G. S., *J. Chem. Phys.* **1980**, *72*, 5639.

(26)   Frisch, M. J., Pople, J. A., Binkley, J. S., *J. Chem. Phys.* **1984**, *80*, 3265.

(27)   Gaussian 98, Revision A.7, Frisch, M. J., Trucks, G. W., Schlegel, H. B., Scuseria, G. E., Robb, M. A., Cheeseman, J. R., Zakrzewski, V. G., Montgomery, J. A.,

Jr., Stratmann, R. E., Burant, J. C., Dapprich, S., Millam, J. M., Daniels, A. D., Kudin, K. N., Strain, M. C., Farkas, O., Tomasi, J., Barone, V., Cossi, M., Cammi, R., Mennucci, B., Pomelli, C., Adamo, C., Clifford, S., Ochterski, J., Petersson, G. A., Ayala, P. Y., Cui, Q., Morokuma, K., Malick, D. K., Rabuck, A. D., Raghavachari, K., Foresman, J. B., Cioslowski, J., Ortiz, J. V., Baboul, A. G., Stefanov, B. B., Liu, G., Liashenko, A., Piskorz, P., Komaromi, I., Gomperts, R., Martin, R. L., Fox, D. J., Keith, T., Al-Laham, M. A., Peng, C. Y., Nanayakkara, A., Gonzalez, C., Challacombe, M., Gill, P. M. W., Johnson, B., Chen, W., Wong, M. W., Andres, J. L., Gonzalez, C., Head-Gordon, M., Replogle, E. S., Pople, J. A., Gaussian Inc, Pittsburgh, PA, 1998

(28)   Matsubara, T., Hirao, K., *Organometallics* **2002**, *21*, 2662.

(29)   Dapprich, S., Frenking, G., *J. Phys. Chem.* **1995**, *99*, 9352.

(30)   Green, J. C., Scurr, R. G., Arnold, P. L., Cloke, F. G. N., *Chem. Commun.* **1997**, 1963.

(31)   Herrmann, W. A., Runte, O., Artus, G., *J. Organomet. Chem.* **1995**, *501*, C1.

(32)   McGuinness, D. S., Green, M. J., Cavell, K. J., Skelton, B. W., White, A. H., *J. Organomet. Chem.* **1998**, *565*, 165.

(33)   Tatsumi, K., Hoffmann, R., Yamamoto, A., Stille, J. K., *Bull. Chem. Soc. Jpn.* **1981**, *54*, 1857.

(34)   Hammond, G. S., *J. Am. Chem. Soc.* **1955**, *77*, 334.

(35)   McGuinness, D. S., Yates, B. F., Cavell, K. J., *Organometallics* **2002**, *21*, 5408.